Organic matter characterization with 3D fluorescence spectroscopy for anaerobic digestion modeling of wastewater treatment sludge

Julie Jimenez

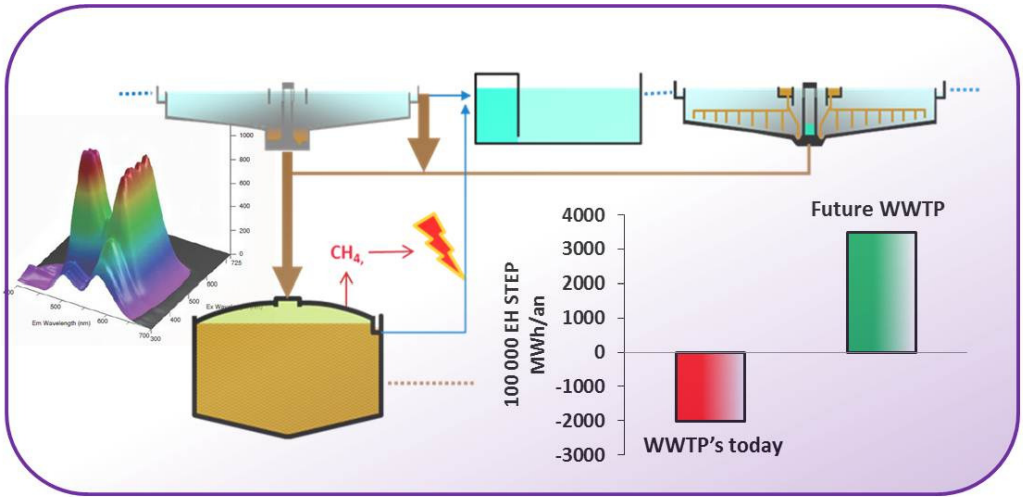

Organic matter characterization with 3D fluorescence spectroscopy for anaerobic digestion modeling of wastewater treatment sludge

Caractérisation de la matière organique par spectrofluorimétrie 3D pour la modélisation de la digestion anaérobie des boues issues de stations d'épuration

PhD thesis 2012

Julie JIMENEZ

ALIMENTATION
AGRICULTURE
ENVIRONNEMENT

UNIVERSITE MONTPELLIER II
SCIENCES ET TECHNIQUES DU LANGUEDOC

T H E S E

Pour obtenir le grade de

DOCTEUR DE L'UNIVERSITE MONTPELLIER II

Discipline : Génie des procédés.
Ecole Doctorale : Sciences et Procédés-Sciences des Aliments

devant être présentée et soutenue publiquement le 23 Novembre 2012

par

Julie JIMENEZ

Titre :

Caractérisation de la matière organique par spectrofluorimétrie 3D pour la modélisation de la digestion anaérobie des boues issues de stations d'épuration

-

Organic matter characterization with 3D fluorescence spectroscopy for anaerobic digestion modeling of wastewater treatment sludge

---

JURY

M**. Fabrice BELINE** Directeur de recherche, IRSTEA Rennes	Rapporteur
M**. Yves DUDAL** Président ENVOLURE Montpellier	Examinateur
M**. Alain GRASMICK** Professeur, Université de Montpellier II	Examinateur
M. **Jean-Philippe STEYER** Directeur de Recherche, INRA Narbonne	Directeur de Thèse
M**. Peter VANROLLEGHEM** Professeur, Université de Laval	Rapporteur
M**. Fabien VEDRENNE** Chercheur confirmé, VERI Maisons Laffitte	Co-directeur de Thèse

ABSTRACT

In an energetic crisis context, alternative sources of energy and saving costs has become of first importance. From this observation, the wastewater treatment plants of the future aim at a positive energetic balance and worldwide research on sludge treatment today focuses on energetic and material valorization through the optimization of anaerobic digestion processes. To this end, knowledge of the input organic matter is crucial to avoid suffering from these disturbances and to control, predict or drive the process through modeling. In the present study, a methodology of sludge characterization is investigated to describe biodegradability and bioaccessibility variables used in anaerobic digestion models. This method is based on the three dimensional fluorescence spectroscopy measurement performed on the chemical extraction of sludge simulating accessibility. Results obtained in 52 sludge samples (primary, secondary digested and thermally treated) show that the method can be successfully correlated with the sludge biodegradability and bioaccessibility within 5 days instead of the 30 days usually needed for the biochemical methane potential tests. Based on these results, input variables of dynamic models of biological processes occurring in anaerobic digestion have been characterized as well as recalcitrant fluorescent compounds. Validation has been performed with modeling of experimental data obtained from two different laboratory scale reactors. Scenarios analysis with the calibrated model have shown that using the measurements of sludge bioaccessibility and biodegradability, a minimal hydraulic retention time could be calculated with a linear correlation leading to the improvement of digesters design. Moreover, this approach has a high potential for applications such as instrumentation or decision support systems to improve both control and optimization of anaerobic digesters.

RESUME

Dans un contexte énergétique en crise, les sources alternatives d'énergie et d'économie d'énergie sont primordiales. Fort de ce constat, la station d'épuration de demain se doit d'atteindre un bilan énergétique positif. Dans cet objectif, de nombreux travaux de recherche se focalisent au niveau mondial sur la valorisation matière et énergétique à travers un procédé d'intérêt : la digestion anaérobie des boues. Afin d'optimiser ce procédé, la connaissance de la matière organique entrante est cruciale pour ne plus la subir mais la contrôler et en prédire les impacts sur les performances des digesteurs, notamment grâce à la modélisation. Une méthodologie de caractérisation de la matière organique des boues a donc été mise en place et testée afin de prédire les variables du modèle de digestion anaérobie basées sur la biodégradabilité et la bioaccessibilité. Cette méthode repose sur la mesure de la fluorescence en 3 dimensions réalisée sur les extractions chimiques de la boue, extractions simulant son accessibilité. Les résultats obtenus sur 52 échantillons de boues (primaires, secondaires, digérées, et traitées thermiquement) ont mis en évidence avec succès la corrélation entre cette méthode et la biodégradabilité anaérobie ainsi que la bioaccessibilité des boues. Le temps analytique classique de 30 jours pour les tests de potentiel méthane est par ailleurs réduit à 5 jours. Grâce à ces résultats, les variables d'entrée du modèle des processus biologiques ont pu être caractérisées ainsi que les composés réfractaires à la digestion. Une validation de la méthodologie a également été réalisée par le biais de la modélisation de 2 réacteurs pilotes expérimentaux. Une analyse de scenarios utilisant le modèle calibré a aussi montré que grâce à la prédiction de la bioaccessibilité et de la biodégradabilité, un temps de séjour minimum des digesteurs peut être calculé via une corrélation linéaire et ainsi optimiser le dimensionnement des digesteurs. De plus, cette approche s'est avérée être d'un grand potentiel en termes d'applications pour l'instrumentation et l'aide à la décision afin d'optimiser les performances des procédés de digestion anaérobie.

MOTS-CLES/KEYWORDS

Anaerobic digestion modeling, biodegradability, bioaccessibility, fluorescence, organic matter characterization, sludge

REMERCIEMENTS

Avant tout, je souhaiterais exprimer ma gratitude aux examinateurs et rapporteurs d'avoir accepté d'examiner mon travail.

Je souhaiterais exprimer toute ma reconnaissance aux personnes qui ont fait que cette thèse existe. Je remercie Alexis Mottet et Mathieu Muller d'avoir réalisé respectivement leur thèse et post-doctorat. Sans vos résultats prometteurs et réflexions, mon sujet n'aurait jamais vu le jour ! Merci pour votre sympathie, vos commentaires et vos participations à mes comités de thèse.

Je remercie également VERI et particulièrement Stephane Déléris et Emmanuel Trouvé qui ont cru en ce projet et m'ont permis de réaliser une thèse en tant que salarié. Stephane, tu as été d'un grand appui pour moi et je te remercie de m'avoir soutenu et encouragé !

Je voulais remercier une personne qui a fait basculer ma façon de penser quand j'étais en IUP mais aussi il y a 3 ans : Jean-Phillippe Steyer. Je pense que je n'aurai jamais pensé faire une thèse si tu ne m'avais pas motivé et si ce n'avait pas été toi mon directeur de thèse, sincèrement. En IUP, tu étais déjà un enseignant qui m'impressionnait et qui me donnait envie de me dépasser. Des années plus tard, pouvoir travailler avec toi a été très enrichissant. Ton enthousiasme et ta motivation dans les sujets de recherche innovants m'ont vraiment donné envie de réaliser ce travail. Je te remercie de m'avoir fait confiance et de m'avoir accueilli au sein du LBE lors de mes divers séjours. Yop Yop ☺

Ensuite j'aimerais remercier les gens qui ont travaillé et collaboré dans cette étude. En premier lieu, je souhaiterais exprimer ma sincère reconnaissance à Estelle Gonidec. Depuis ton apprentissage, la respirométrie, en passant par les effluents industriels et en terminant par les extractions, tu as été pour moi d'une aide précieuse. Rigoureuse, motivée, tu t'es adaptée à toutes mes manips, même si des fois ça ne marchait pas toujours. J'ai adoré travailler avec toi. J'espère pouvoir le faire à nouveau !

Je remercie également Xavier Lefebvre du LISBP INSA Toulouse d'avoir participé à certains comités de thèse et de m'avoir donné des conseils avisés. Je remercie Etienne Paul INSA de Toulouse qui m'a convaincu de rentrer à l'INSA et m'a poussé à postuler à Anjou Recherche. Moi qui ne voulais pas faire thèse…

J'exprime toute ma reconnaissance à Eric Latrille du LBE. Grâce à toi la PLS n'a plus de secret pour moi ! Tu as toujours été disponible, accueillant et de très bon conseil. Merci de ta sympathie et de ton aide.

A Jesus Cacho, gracias por tu apoyo, tu ayuda y tu implicacion en mi trabajo. Tus consejos y correcciones me han mucho ayudado. Aunque el modelado y tu no seais buenos amigos, espero que este trabajo te haya quitado las dudas que tenias. Pero estoy segura que en el fondo sueñas de poder utilisar ADM1!

Enfin, je tiens à remercier toutes les personnes de VERI qui m'ont encouragé et soutenu, surtout les équipes PAN, PAE, BIA. Tout particulièrement, merci à Rémi Lestienne, Nicolas Boudaud, Sandra Saussereau, Benoit Beraud et Pascal Boisson. Vous êtes bien plus que des collègues à mes yeux. Vous avez toujours été là, dans les bons et mauvais moments. Rémi, tu me supportes quotidiennement dans le bureau et rien que ça je te dis bravo ! Tu as été de très bons conseils et un super coach de course à pied ! Sandra, je t'adore, ton soutien et ta grande amitié ont été de précieuses sources de motivations pour moi. Tu vas me manquer ma belle !. Nico, pendant ces 3 ans tu as été d'un soutien sans failles, merci pour tout. Benoit et Pascal, malgré vos conversations de geeks vous m'avez été d'un grand soutien et d'une grande amitié…. Pascal, ne te fais pas d'illusions, tu restes toujours aussi insupportable !

En plus des collègues de VERI je tiens à remercier tous les thésards et les stagiaires que j'ai pu rencontrer au LBE, surtout dans la dernière ligne droite.

Je ne pourrais pas terminer ce paragraphe sans remercier quelqu'un que j'affectionne beaucoup, avec qui travailler est synonyme d'efficacité et bonne humeur : Fabien Vedrenne. Je n'aurai pas pu faire tout ce travail sans tes précieux conseils et ta disponibilité. Ton aide, ton soutien dans les moments de doute et ta bonne humeur ont beaucoup contribué à l'élaboration de cette thèse. Merci pour ces moments de fous rires au labo, les moments karaoké et surtout nos joutes verbales. Saches que j'arriverai à passer la barre des 1h au 10km et que je te trouverai un autre défi plus dur que la zumba… trop facile ! ;)

Enfin je terminerai ces remerciements en exprimant toute ma reconnaissance à mes amis de toujours : Seb, Elo, Ju, mon Phanou, Max vous avez toujours été là. Merci.

Quiero dedicar este trabajo a toda mi familia: mis padres, hermanos y sobrinos. Aunque estos últimos años he tenido momentos muy dificiles, siempre me habeis apoyado en todo. Me habeis permitido llegar a donde he podido llegar. Para todos vosotros, una sola palabra: gracias.

Ah! J'allais oublier le principal soutien que j'ai eu depuis 2 ans! Mon lapin Pinpin ! Je n'oublierai jamais les moments où tu m'as bouffé les fils d'alimentation de mon ordinateur, téléphone, frigo…mes feuilles volantes quand je travaillais à la maison… Merci pour ton affection et ton écoute ☺ !

Aux modélisateurs d' « Anjou »

« Mon modèle, c'est moi-même ! Je suis mon meilleur modèle
parce que je connais mes erreurs, mes qualités, mes victoires et mes défaites.
Si je passe mon temps à prendre un autre modèle comme modèle,
comment veux-tu que ce modèle puisse modeler dans la bonne ligne ? »

Jean-Claude Van Damme

TABLE OF CONTENTS

List of figures 1
List of tables 5
Abbreviations 7
Nomenclature 10
Introduction 15
I. BETTER INPUT CHARACTERIZATION FOR BETTER ANAEROBIC DIGESTION MODELS: TOWARDS NEW METHODOLOGIES FOR MUNICIPAL SLUDGE CHARACTERIZATION 19
I.1. Statement in methane production prediction from municipal wastewater sludge 23
I.1.1. Municipal wastewater treatment sludge: definition and composition 23
I.1.2. Predicting methane production: the analytical way 27
I.1.3. Predicting methane production: predicting tools 28
I.1.3.1. Static models 29
- Correlations between organic matter composition and anaerobic biodegradability 29
- Indirect correlations 32

I.1.3.2. Dynamic models and evolution of substrate complexity 33
- Dynamic models and substrate definition: 1969-2002 33
- Modified ADM1 and substrate definition: 2002-2012 37

I.1.3.3. ADM1 and influent characterization 39
- Variables lumped with practical analysis 40
- Interpretation of the methane production curve 42
- Plant-wide modelling technique and ASM-ADM mapping 44

I.2. Critical review 46
I.3. Advanced techniques for organic matter characterization 52
I.3.1. Near infrared reflectance spectroscopy (NIRS) 54
I.3.2. 3D Excitation Emission fluorescence spectroscopy 55
I.4. Conclusions and perspectives 59
I.5. Problematic definition and scientific strategy 60
II. MATERIAL AND METHODS 63
II.1. Sludge characterization: analytical methods 64
II.1.1. Total organic matter analysis 64
II.1.1.1. Total solids and volatile solids 64
II.1.1.2. Chemical Oxygen Demand 64
II.1.1.3. Total carbon analysis 65
II.1.1.4. Nitrogen analysis 65
II.1.2. Biochemical characterization 65
- Lipids 65
- Volatile fatty acids 66
- Colorimetric methods for protein and carbohydrate contents measurement 66
- Biochemical expression results 68

II.2. Biodegradability and bioaccessibility : definition of quantitative variables 68
II.2.1. Biochemical Methane Potential tests 69
II.2.2. Interpretation and calculation of BMP 70
II.2.3. Interpretation and calculation of X_{RC}/X_{SC} 70
II.3. Sludge samples 71
II.4. Chemical sequential extraction protocol 74
II.4.1. Definitions 74
II.4.2. Sequential extraction Protocol 75
II.4.2.1. Laboratory material 75

II.4.2.2. DOM 76
II.4.2.3. S-EPS 76
II.4.2.4. REPS 77
II.4.2.5. HSL 77
II.4.2.6. COD mass balance and organic matter extraction yield calculations 78
II.5. 3D-EEM fluorescence spectroscopy 80
II.5.1. Fluorescence Spectrometer 80
II.5.2. Fluorescence Spectra 82
II.5.3. Dilution and linearity for quantification 83
II.5.4. Spectra interpretation 84
II.6. Anaerobic digestion laboratory scale reactors 86
II.7. Mathematical modeling : modified ADM1 and statistical methods 89
II.7.1. Modified ADM1 89
II.7.2. Input variables modifications 89
II.7.3. Kinetic modifications 90
II.7.4. Liquid/Gas transfer modification 92
II.7.5. Modified ADM1 input implementation 93
II.8. Statistical tools 94
II.8.1. Partial Least Square Regression 94
II.8.1.1. Definition 94
II.8.1.2. Interpretation 96
II.8.2. Other statistical tests 97
II.9. Conclusion 97
III. BIOACCESSIBILITY AND CHEMICAL ACCESSIBILITY CORRELATION INVESTIGATION 99
III.1. Preliminary results : Biochemical methane potential (BMP) test and sequential extractions 100
III.1.1. Biochemical Methane Potential: S/X ratio investigation 100
III.1.2. Sequential extraction and sludge profile 102
III.1.2.1. Validation extractions number 102
III.1.2.2. Fractions extraction repartition and sludge type 104
III.1.2.3. Effect of size particle distribution on chemical extractions protocol 108
III.1.3. Biochemical nature of sludge and extracted organic matter 110
III.1.3.1. Non-fractionated sludge characterization 110
III.1.3.2. Fractionated sludge characterization 111
III.1.4. Sludge fractionation conclusion 114
III.2. Correlation between chemical and biochemical accessibility investigation 115
III.2.1. Material flow investigation : anaerobic stabilization test 115
III.2.2. Biodegradability and bioaccessibility investigation of sequential extraction fractions 121
III.2.3. Methane production curve and correlation of fractions extracted 126
III.3. Conclusions 129
IV. BIODEGRADABILITY AND BIOACCESSIBILITY INDICATORS INVESTIGATION FROM SEQUENTIAL EXTRACTIONS COUPLED WITH 3D-EEM FLUORESCENCE SPECTROSCOPY 133
IV.1.1. Fluorescence spectroscopy and organic matter complexity 134
IV.1.1.1. Sequential extractions fractions fluorescence 134
IV.1.1.2. Evolution of fractions during anaerobic treatment 139
IV.1.1.3. Thermally treated sludge 142

IV.2. Definition of indicators from sequential extractions coupled with 3D-EEM liquid phase fluorescence spectroscopy (3D-SE-LPF) results 145
IV.2.1. General complexity indicator 145
IV.2.2. Zone-specific biodegradability indicator 148
IV.3. Correlations between 3D-SE-LPF indicators and biodegradability 150
IV.3.1. Exploratory PLS regressions 150
IV.3.2. PLS regression model set up for biodegradability prediction 154
IV.3.2.1. Calibration and validation datasets 154
IV.3.2.2. Validation results of PLS regression 155
IV.4. Correlations between 3D-SE-LPF indicators and bioaccessibility 157
IV.4.1. Exploratory PLS regressions 157
IV.4.2. Validation PLS regression for X_{RC} prediction 162
IV.5. Identification of recalcitrant molecules to biodegradation: sensitivity analysis 163
IV.5.1. Sensitivity analysis of PLS models: definition 163
IV.5.1.1. Sensitivity analysis of PLS models: fractionation variables 164
IV.5.1.2. Sensitivity analysis of PLS models: fluorescence zones variables 164
IV.5.1.3. Sensitivity analysis of PLS models: scenario analysis 165
IV.6. Conclusions 169
V. METHODOLOGY GLOBAL VALIDATION : MODIFIED ADM1 MODELLING AND DIGESTERS DESIGN IMPACT 173
V.1. Continuous lab pilots performances 175
V.1.1. Reference period 176
V.1.2. Disturbing period 177
V.2. Modified ADM1 modeling 180
V.2.1. Modeling procedure 180
V.2.2. Input implementation and parameters 181
V.2.3. Model calibration 182
V.2.3.1. Steady state calibration 182
V.2.3.2. Dynamic state calibration 186
V.3. Model validation 192
V.3.1. Dynamic validation with disturbing data 192
V.3.1.1. Input data during both references and disturbing period 192
V.3.1.2. Dynamic validation 193
V.3.1.3. Sensitivity analysis 199
V.4. Bioaccessibility variables and impact on hydraulic retention time 199
V.4.1. Scenarii analysis 200
V.4.2. Correlations found between bioaccessibility variables and HRT 201
V.5. Conclusions and discussion 205
Conclusions 207
Perspectives 211
References 213
Annex 229
Annex 1 : A statistical comparison of protein and carbohydrate characterisation methodology applied on sewage sludge samples ..... 231_Toc346010032
Annex 2: ADM1 and modified ADM1 (Mottet, 2009) Petersen matrix 255
Annex 3: PLS regression results for BD prediction with X-variables containing VFA percent of total COD 259
Annex 4: Identification of fluorescence compounds in zones VI 263
Annex 5: Simulation results obtained for reactors P1 and P2 for all data 265

List of figures

Figure 1: Evolution through the years on AD topics of the published scientific papers..... 20
Figure 2: Biochemical and physical-chemical reactions in the ADM1 model (Batstone *et al.*, 2002)..... 37
Figure 3: Experimental methodology to assess the readily hydrolysed matter and the slowly hydrolysed matter in a BMP batch test: cumulated methane specific production for a waste activated sludge before and after thermal pre-treatment at 165°C and 220°C (Mottet, 2009) 42
Figure 4: FRI EEM regions obtained using consistent excitation and emission wavelength boundaries (He *et al.*, 2011 based on Chen *et al.*, 2003) 57
Figure 5 : Overview of the study framework 62
Figure 6 : (a) AMTPS from BIOPROCESS CONTROL and (b) glass bottle with stirring device 69
Figure 7 : Cumulated methane production curve (a) and methane production rate curve (b) for the same sludge degradation with a ratio S/X = 1gCOD.gVS^{-1} 71
Figure 8 : Schematic concept of sludge floc bioaccessibility decomposition and extractions definitions based on Muller *et al. (In press*) 75
Figure 9 : Shaker table used for chemical extractions 76
Figure 10 : Extraction profiles of three different sludge natures, in duplicate (primary BI, secondary BII and anaerobic digested BD)..... 78
Figure 11 : Modified protocol based on Muller *et al. (*in press) 79
Figure 12 : Fluorescence phenomena explanation with the Jablonski energetic diagram 80
Figure 13 : Fluorescence spectrometer Perkin Elmer LS 55..... 80
Figure 14 : Liquid phase fluorescence measurement (a) and solid phase fluorescence measurement (b)..... 81
Figure 15 : Solid phase module for fluorescence spectrometer Perkin Elmer LS 55 81
Figure 16 : 2D scan fluorescence spectroscopy spectra example 82
Figure 17 : 3D scan fluorescence spectroscopy spectra for Tryptophan..... 82
Figure 18 : Auto-quenching phenomenon problem for quantification and linearity 84
Figure 19 : FRI for spectra interpretation and quantification..... 84
Figure 20 : (a) Laboratory reactors description and (b) closed trap cell from biogas circuit... 87
Figure 21 : Modified ADM1 model by Mottet (2009)..... 90
Figure 22 : Methane production rate curves from a secondary sludge BMP test with (a) S/X=0.5 gCOD.gVS^{-1} and (b) S/X=1 gCOD.gVS^{-1} 100
Figure 23 : methane production rates for several S/X ratios..... 101
Figure 24 : Extracted sludge COD concentration depletion for (a) S-EPS, (b) RE-EPS and (c) HSL for six different sludge..... 103
Figure 25 : Extracted sludge CODs profiles for several sludge studied 104
Figure 26 : Boxplot representation of the COD fractions from sequential extractions of all the sludge 105
Figure 27 : Boxplot representation of COD fractions from sequential extractions for (a) primary sludge, (b) secondary sludge, (c) anaerobic digested sludge and (d) thermally treated sludge 106
Figure 28 : COD total extraction versus median size particle for several kinds of sludge 109

Figure 29 : Biochemical fractionation of primary (a), secondary (b), anaerobic digested (c) and thermally treated (d) sludge 111
Figure 30 : Organic matter repartition in S-EPS (a), RE-EPS (b) and HSL(c) fractions 113
Figure 31 : Cumulated methane production obtained during the anaerobic digestion of SII_F_1 and sampled recovered for sequential extraction analysis 116
Figure 32 : Evolution of VFA in both anaerobic digestion of SII_F1 and SII_F2 117
Figure 33 : Evolution of extracted fractions during anaerobic digestion of SII_C_2 and SII_C_3 117
Figure 34 : Biochemical fractionation evolution during stabilization test: (a) proteins and (b) carbohydrates 119
Figure 35 : Cumulated methane produced obtained for total sludge deprived of successive fractions (the highest to the least accessible) by BMP tests 123
Figure 36 : Zoom [0-2] days of cumulated methane produced obtained for total sludge deprived of successive fractions (the highest accessible to the least one) 124
Figure 37 : Methane production curves of fraction extracted from thermally treated sludge for Total, DOM and S-EPS fractions (a) and for Total, RE-EPS, HSL and NE fractions 125
Figure 38 : Biogas production rate comparison between total sludge and total sludge without DOM (S/X=0.13 gCOD.gVS^{-1}) 127
Figure 39 : (a) Superposition of biogas production rate comparison between total sludge and total sludge without (DOM+SEPS+RE-EPS) at S/X=0.08 gCOD.gCOD^{-1}); (b) Methane production rate at S/X=0.24 gCOD.gCOD^{-1} (Yasui et al., 2006) 128
Figure 40 : PLS regression correlation circles obtained for BD (a) and X_{RC} (b) prediction .. 129
Figure 41 : Schematic overview of the next chapter issue 131
Figure 42 : 3D-LPF spectra obtained for SII_F_2 sludge chemical fractionation 135
Figure 43 : DOM 3D-LPF spectra obtained for SI_H (a), SII_H (b) and SD_H (c) 137
Figure 44 : S-EPS 3D-LPF spectra obtained for SI_A (a), SII_A (b) and SD_A (c) 137
Figure 45 : RE-EPS 3D-LPF spectra obtained for SI_A (a), SII_A (b) and SD_A (c) 138
Figure 46 : HSL 3D-LPF spectra obtained for SI_A (a), SII_A (b) and SD_A (c) 138
Figure 47 : NE 3D-SPF spectra obtained for SI_A (a), SI_D (b), SII_D (c) and SD_D (d) .. 139
Figure 48 : 3D-LPF spectra obtained for sequential extractions of SII_F_2 before anaerobic stabilization 140
Figure 49 : 3D-LPF spectra obtained for sequential extractions after anaerobic stabilization test of SII_F_2 named SII_F_2_3 141
Figure 50 : Evolution of the ratio of fluorescence percentage between complex zones (IV-VII) and protein-like zones (I-III) 142
Figure 51 : 3D-LPF spectra obtained at 3 sampling points from a sludge treatment unit: raw sludge, thermally treated sludge and anaerobically digested sludge 144
Figure 52 : Approach used for biodegradability and bioaccessibility prediction of sludge ... 145
Figure 53 : Boxplots of the “complexity indicator” relative to each fraction for primary, secondary, anaerobically digested and thermally treated sludge 146
Figure 54 : Correlation circle obtained in PLS regression of BD with the complexity indicators calculated for each fraction, considering all the sludge (a) and not considering the thermally treated sludge (b) 147

Figure 55 : BD versus complexity indicators for primary sludge (a) and secondary sludge (b) 148
Figure 56 : Hierarchical Cluster Analysis performed on all indicators data from the 52 sludge studied 149
Figure 57 : Correlation circle obtained for the two first components in PLS regression of 28 variables (a) and 28 variables and VFA (b) 151
Figure 58 : Correlation circle of sludge samples repartition obtained in PLS regression 152
Figure 59 : Observed versus predicted values of biodegradability in PLS regression 153
Figure 60 : Boxplot of biodegradability repartition in calibration (a) and validation (b) samples 154
Figure 61 : Observed versus predicted biodegradability 155
Figure 62 : BD PLS regression coefficients scaled and centered and error bars obtained with a confidence interval of 95% 156
Figure 63 : Correlation circle obtained for the two first components in PLS regression of 28 variables (a) and 28 variables and VFA (b) for X_{RC} prediction 158
Figure 64 : Scaled and centered coefficient values from X_{RC} PLS regression of 28 variables (a) and 28 variables with VFA (b) obtained with a confidence interval of 95% 159
Figure 65 : Correlation circle obtained for sample sludge in PLS regression for 28 variables and VFA 160
Figure 66 : Observed versus predicted X_{RC} obtained in PLS regression of all sludge in 28 variables and VFA case 161
Figure 67 : Observed X_{RC} versus predicted X_{RC} from PLS regression 162
Figure 68 : Matrix representation of the indicators contribution to BD and X_{RC} prediction . 170
Figure 69 : Detailed scheme representation of sludge bioaccessibility and biodegradability according to fractionation and fluorescence results 171
Figure 70 : Strategy used for characterization methodology validation 175
Figure 71 : Evolution of total solids and volatile concentration of output reactors 176
Figure 72 : Reference period performances comparison in P1 and P2 reactors in terms of (a) organic loads and HRT, methane production rate (b) and output COD concentration (c) 177
Figure 73 : Disturbing period performances comparison in P1 and P2 reactors in terms of (a) organic loads and HRT, methane production rate (b) and output COD concentration (c) 179
Figure 74 : Modeling procedure 181
Figure 75 : Particulate COD repartition on ADM1 state variables obtained by steady-state simulation without calibration 184
Figure 76 : Particulate COD repartition on ADM1 state variables obtained by steady-state simulation after calibration 186
Figure 77 : COD output prediction before (a) and after (b) calibration P2 187
Figure 78 : pH output prediction before (a) and after (b) calibration 188
Figure 79 : Methane and carbon dioxide proportion in biogas prediction before (a) and after (b) calibration 189
Figure 80 : Total biogas flowrate output prediction before (a) and after (b) calibration for P2 190
Figure 81 : Acetate and propionate concentrations output prediction before (a) and after (b) calibration 191

Figure 82 : Ammonium concentration output prediction before (a) and after (b) calibration 192
Figure 83 : Validation of input state variables X_I and X_{SC} obtained from PLS (respectively 1-BD and BD-X_{RC}) 193
Figure 84 : Methane flow rate simulated during disturbing period 194
Figure 85 : Observed methane versus predicted methane in P2 195
Figure 86 : Particulate COD simulated in reactors P1 and P2 during the disturbing period . 196
Figure 87 : pH evolution in P1 and P2 during the reference and the disturbing periods 196
Figure 88 : Output ammonium concentration in P1 and P2 during the reference and the disturbing periods 197
Figure 89 : Output acetate concentration in P1 and P2 during the disturbing period 197
Figure 90 : Methane flow rate kinetic simulation on DOM, S-EPS and RE-EPS removal in P2 198
Figure 91 : Total biogas versus HRT for several R=X_{SC}/X_{RC} ratios obtained by simulations 201
Figure 92 : Methodology definition for minimal HRT assessment 202
Figure 93 : Correlation obtained between minimal HRT and X_{SC}/X_{RC} ratio (a) Observed HRT versus predicted HRT (b) minimal liquid volume of reactor versus X_{SC}/X_{RC} (c) 203
Figure 94 : Repartition of X_{SC}/X_{RC} ratio and minimal HRTobtained by model prediction for primary sludge (a), secondary sludge (b), anaerobic digested sludge (c) and thermally treated sludge (d) 204

List of tables

Table 1: Literature data on organic composition of sewage sludges 24
Table 2: Analytical protocols for biochemical compounds determination 26
Table 3: Dynamic models evolution: hydrolysis and substrate variables 35
Table 4: Stoichiometric parameters calculation from literature data 43
Table 5: Summary of the different methodologies used in integrative tools found in the litterature 51
Table 6: Different advanced methods to characterize the EPS of sludge 53
Table 7 : Conversion ratios for COD equivalent concentration assessment 68
Table 8 : Primary sludge samples characterized 72
Table 9 : Secondary sludge samples characterized 72
Table 10 : Sludge samples after thermal treatment characterized 73
Table 11 : Anaerobic digested sludge samples characterized 73
Table 12 : Definition of FRI zones 86
Table 13 : Operating conditions of the continuous lab pilots from the test bench 88
Table 14 : Analysis performed on lab pilots in continuous tests for model calibration and validation. 88
Table 15 : New parameters introduced in modified ADM1 91
Table 16 : Soluble variables of modified ADM1 definition and measurement 93
Table 17 : Particulate variables of modified ADM1 definition and measurement 94
Table 18 : Results obtained in the comparison test of S/X ratios: impact of DOM in X_{RC} assessment 101
Table 19 : COD extraction comparison before and after grinding for primary, secondary and anaerobic sludge 108
Table 20 : Organic matter repartition in DOM fraction for each kind of sludge 114
Table 21 : Mass balance calculated between samples A-B and B-D 118
Table 22 : COD mass balance and recovery of X_{RC} and X_{SC} 120
Table 23 : PLS regression performances parameters 150
Table 24 : Validation samples used for PLS regression 154
Table 25 : PLS regressions performances parameters for X_{RC} prediction 157
Table 26 : Validation samples used for X_{RC} regression 162
Table 27 : Relative sensitive function calculated for COD fractions on BD and X_{RC} variables obtained in PLS 164
Table 28 : Relative sensitive function calculated for fluorescence zones on BD variable obtained in PLS 165
Table 29 : Relative sensitive function calculated for fluorescence zones on X_{RC} variable obtained in PLS 165
Table 30 : Predicted BD and X_{RC} by PLS models for several scenarios where zone I and VI are removed from RE-EPS and HSL in digested sludge SD_E 167
Table 31 : Literature survey of fluorescent molecules location in 3D spectra 169
Table 32 : COD mass balance on P1 and P2 180
Table 33 : New parameters from modified ADM1 values used in this study before calibration step. 182
Table 34 : Steady-state values of state variables from ADM1 with default values parameters 183
Table 35 : Steady-state values of state variables from ADM1 with calibrated values parameters 185
Table 36 : Steady-state values of state variables from ADM1 with calibrated values parameters 186
Table 37 : PLS results for disturbed sludge 193
Table 38 : RSF analysis on input characterization of ADM1 obtained by biochemical measurement and PLS 199
Table 39 : Composition of the « Whey Creatine Complex by EAFIT®" used as certified reference. 239

Table 40 : Accuracy and rightness tests: comparison of the characterisation methods with a reference value of protein concentration. 242
Table 41 : Accuracy and rightness tests: comparison of the characterisation methods with a reference value of carbohydrate concentration. 243
Table 42 : Protein concentration of sludge sample obtained by two methods: calibration curve and dosed addition of BSA and reference regression model..... 244
Table 43 : Fisher and Student tests results for the comparison of proteins determination methods: Lowry and BCA 245
Table 44 : Carbohydrates concentration of sludge sample obtained by two methods: calibration curve and dosed addition of glucose and cellulose regression model 246
Table 45 : Fisher and Student tests results for the comparison of carbohydrates determination methods: Anthrone and Dubois..... 246
Table 46 : Comparison summary of protein and carbohydrates dosage protocols 250

Abbreviations

Abbreviation	Definition	Units
A	Ash content	g.gTS-1
ABP	Anaerobic Biogas Potential	$NL.gTS^{-1}$
AD	Anaerobic Digestion	
ADF	Acid Detergent fibers content	g.gTS-1
ADM1	Anaerobic Digestion Model N°1	
AFM	Atomic Force Microscopy	
AMPTS	Automated Methane Potential Test System	
ASM1	Activated Sludge Model N°1	
BCA	BiCinchonic Acid	
BD	Anaerobic BioDegradability	%
BMP	Biochemical Methane Potential	$NmlCH4.gCOD^{-1}$
BOD	Biological Oxygen Demand	$mgO2.L^{-1}$
BSA	Bovine Serum Albumin	
Cel	Cellulose	$g.gTS^{-1}$
Ch	Carbohydrates	g eqCOD.$gCOD^{-1}$ or $g.gTS^{-1}$
CLSM	Confocal Laser Scanning Microscopy	
COD	Chemical Oxygen Demand	$gO2.L^{-1}$ or $gCOD.L^{-1}$
D50	Median particles diameters	µm
DOM	Dissolved Organic Matter	
DOM_fluo	Fluorescent DOM	
DRI	Dynamic Respiration Index	$mgO_2.gTS^{-1}.h^{-1}$
EPS	Extracellular Polymeric Substances	
FRI	Fluorescence Regionalization Integration	
FTIR	Fourier Transformed Infra-Red	
GASDM	General Activated Sludge and Digestion Model	
GB21	Biogas produced in 21 days	$NL.kgTS^{-1}$

GC/MS	Gas Chromatography/Mass Spectrometry	
HA	Humic Acid	g eqCOD.gCOD^{-1} or g.gTS^{-1}
HEM	Hexane Extractible Matter	g eqCOD.gCOD^{-1} or g.gTS^{-1}
HIM	Hydrophilic Matter	
HPLC	High Performance Liquid Chromatography	
HRT	Hydraulic Retention Time	d
HSL	Humic Substances Like	
IC	Inorganic Carbon	gC.L^{-1}
IWA	International Water Association	
LCFA	Long Chain Fatty Acids	
LC-MS/MS	Liquid Chromatography coupled with tandem Mass Spectroscopy	
Li	Lipid	g eqCOD.gCOD^{-1} or g.gTS^{-1}
LIF	Laser Induced Fluorescence	
LPF	Liquid Phase Fluorescence	
MPR	Methane Production Curve	
NE	Non Extracted matter	
NIRS	Near Infra-Red Spectroscopy	
NMR	Nuclear Magnetic Resonance spectroscopy	
Ox	Oxidation degree	gCOD.gTOC^{-1}
PLS	Partial Least Square	
POM	Particular Organic Matter	
Pr	Proteins	g eqCOD.gCOD^{-1} or g.gTS^{-1}
PRESS	Predicted Residual Sums of Squares	
RI4	Respiration Index 4 days	mgO_2.gTS^{-1}
RMSE	Root Mean Square Error	
RMSEP	Root Mean Square Error of Prediction	
RSF	Relative Sensitive Function	

RE-EPS	Readily Extractible EPS	
SDS-PAGE	Sodium Dodecyl Sulfate Polyacrylamide Gel Electrophoresis	
SEM	Scanning Electron Microscopy	
S-EPS	Soluble EPS	
SI	Primary Sludge	
SPF	Solid Phase Fluorescence	
SII	Secondary Sludge	
SD	Digested Sludge	
STT	Thermally Treated Sludge	
S/X	Substrate on biomass ratio	$COD.gCOD^{-1}$
SolOC	Soluble Organic Carbon	$g.gVS^{-1}$
T	Temperature	°C
TC	Total Carbon content	$gC.L^{-1}$
TEM	Transmission Electron Microscopy	
TKN	Total Kjedhal Nitrogen content	$gN.L^{-1}$
TN	Total Nitrogen content	$gN.L^{-1}$
TOC	Total Organic Carbon content	$gC.L^{-1}$
TS	Total Solids	$gTS.L^{-1}$
VFA	Volatile Fatty Acids	
VS	Volatile Solids content	$gVS.L^{-1}$
WWTP	WasteWater Treatment Plant	
X_l	Lignin content	$g.gTS^{-1}$
XPS	X-ray Photoelectron Spectroscopy	
3D-EEM	3 Dimension Excitation Emission Matrix (3D-EEM) fluorescence spectroscopy	

Nomenclature

Stoichiometric coefficients in ADM1

Symbol	Description	Units
$\nu_{i,j}$	Stoichiometric coefficients for component I on process j	$kgCOD.m^{-3}$
fproduct,substrate	Yield (catabolism) of product on substrate	$kgCOD.kgCOD^{-1}$
$f\_X_C\_X_{PR,CH,LI,I}$	Protein, carbohydrates, lipids or inert compound fraction in X_C	$kgCOD.kgCOD^{-1}$
$f\_X_{RC}\_X_{PR,CH,LI,I}$	Protein, carbohydrates, lipids or inert compound fraction in X_{RC}	$kgCOD.kgCOD^{-1}$
$f\_X_{SC}\_X_{PR,CH,LI,I}$	Protein, carbohydrates, lipids or inert compound fraction in X_{SC}	$kgCOD.kgCOD^{-1}$

Equilibrium coefficients and constants in ADM1

Symbol	Description	Units
$K_{H,i}$	Henry's law coefficient of gas i	$M.bar^{-1}$
K_La_i	the transfer coefficient multiplied by specific transfer area of gas i	d^{-1}
$P_{gas,i}$	partial pressure of gas i	bar
D_i	diffusivity of gas i	$m^2.s^{-1}$

Kinetic parameters in ADM1

Symbol	Description	Units
K_{dec},process	First order decay constant	d^{-1}
kprocess	First order parameter (classical ADM1 hydrolysis)	d^{-1}
K_m,process	partial pressure of gas i	d^{-1}
K_S,process	Half saturation constant	$kgCOD\_S.m^{-3}$
ρj	Kinetic rate of process j	$kgCOD\_S.m^{-3}.d^{-1}$
$Y_{substrate}$	Yield of substrate S on biomass X	$kgCOD\_X.kgCOD\_S^{-1}$

Algebraic Variables

Symbol	Description	Units
pH	$-\log[H^+]$	
V_i	Methane volume produced at time i	$NmlCH_4$
V_{CH4}	Methane volume obtained in BMP test	$NmlCH_4$
Q_BG	Total biogas flowrate	$m^3.d^{-1}$
Q_CH4	Methane biogas flowrate	$m^3.d^{-1}$
S_i	Soluble component i	$kgCOD.m^{-3}$
V_R	Reactor Volume	m^3
V_H	Gas volume	m^3
X_i	Particulate component i	$kgCOD.m^{-3}$
X_{RC}	Readily biodegradable particulate COD	$kgCOD.m^{-3}$
X_{SC}	Slowly biodegradable particulate COD	$kgCOD.m^{-3}$

Dynamic State Variables in ADM1

Symbol	Description	Units
X_C	Classical ADM1 particulate COD	$kgCOD.m^{-3}$
X_{RC}	Readily biodegradable particulate COD	$kgCOD.m^{-3}$
X_{SC}	Slowly biodegradable particulate COD	$kgCOD.m^{-3}$
X_{CH}	Particulate Carbohydrates COD	$kgCOD.m^{-3}$
X_{PR}	Particulate Proteins COD	$kgCOD.m^{-3}$
X_{LI}	Particulate Lipids COD	$kgCOD.m^{-3}$
X_I	Non biodegradable particulate COD	$kgCOD.m^{-3}$
S_I	Non biodegradable soluble COD	$kgCOD.m^{-3}$

Ssu	Monosaccharides	kgCOD.m^{-3}
Saa	Amino acids	kgCOD.m^{-3}
Sfa	Long chain fatty acids	kgCOD.m^{-3}
Sva	Valerate	kgCOD.m^{-3}
Sbu	Butyrate	kgCOD.m^{-3}
Spro	Propionate	kgCOD.m^{-3}
Sac	Acetate	kgCOD.m^{-3}
Sh2	Soluble hydrogen	kgCOD.m^{-3}
S_{CH4}	Soluble methane	kgCOD.m^{-3}
SIC	Soluble inorganic carbon	M
SIN	Soluble inorganic nitrogen	M
Xsu….Xh2	ADM1 Biomass	kgCOD.m^{-3}
Scat	Cations	M
San	Anions	M
X_bio_X_{RC}	Modified ADM1 hydrolytic biomass	kgCOD.m^{-3}
X_bio_X_{SC}		kgCOD.m^{-3}
X_bio_X_{PR}		kgCOD.m^{-3}
X_bio_X_{CH}		kgCOD.m^{-3}
X_bio_X_{LI}		kgCOD.m^{-3}

Dynamic State Variables in ASM1

Symbol	Description	Units
X_S	Slowly biodegradable fraction	gCOD.L^{-1}
X_H	Heterotrophic biomass	gCOD.L^{-1}
X_P	Inert produced fraction of particulate COD	gCOD.L^{-1}

Fluorescence parameters

Symbol	Description	Units
λ_{ex}	Excitation wavelength	nm
λ_{em}	Emission wavelength	nm
Φ	Quantic yield	
I_f	number of photons emitted	
I_a	number of photons absorbed	
A	Absorbance	
ε	molar absorptivity	$L.mol^{-1}.cm^{-1}$
l	optic path length crossed by light	cm
I_0	incident light intensity	U.A.
h	Planck constant	j.s
c	Light speed	$m.s^{-1}$
E	Energy lost in Stockes law	J
$V_{imageJ}(i)$	raw volume obtained in IMAGE J	U.A
S(i)	Area of a zone i	nm^2
$V_f(i)$	Fluorescence volume of a fluorescence zone i	$U.A.mgCOD^{-1}.L^{-1}$
$P_f(i)$	Fluorescence percentage of a zone i	%

Extractions mass balance and PLS parameters

Symbol	Description	Units
COD_s	COD mass extracted	mg COD
COD_5	the COD mass obtained after one extraction with 5g of pellet	mg COD
m_p	pellet mass obtained for the initial centrifugation	Mg
m_{ext}	pellet mass used for sequential extractions	mg
V_s	raw sludge volume considered	L
V_p	raw sludge volume used for initial centrifugation	L
COD_{total}	COD concentration of total raw sludge	$mgCOD.L^{-1}$
$CODs_{ample}$	COD concentration of the sample analyzed	$mgCOD.L^{-1}$
R^2X	Cumulated variance on X variables	
R^2Y	Cumulated variance for Y variable/Correlation coefficient	
Q^2	Percent of variation of Y predicted by model in cross-validation	

Introduction

In an energetic crisis context, alternative sources of energy and the reduction of costs have become of the most importance. In France, wastewater treatment plant (WWTP) energy consumption is about 20 kWh per year per person equivalent (plant of 100 000 person equivalent, VEOLIA 2012). From this observation and knowing that wastewater contains a potentially high amount of energy that can be recovered (e.g. by converting COD in methane through anaerobic digestion), it is clear that WWTP of the future should aim at a positive energy balance. For that purpose, several worldwide research studies focus on energetic and material valorization in particular through anaerobic digestion (AD) of sludge.

Nowadays, pretreated wastewater flux undergoes a biological treatment based on carbon, nitrogen and phosphorus removal. Sludge produced during pretreatment and secondary treatment is treated by anaerobic digestion. However, several aspects of the today WWTP strategy make impossible energy savings:

- aeration during secondary treatment is highly energy consuming,
- current energetic valorization from anaerobic treatment of sludge does not achieve a net or positive energy balance in the WWTP,
- an accurate and detailed characterization of the wastewater organic matter would avoid digesters to suffer from its variation and would largely enhance process performance,
- anaerobic digested sludge still contains a high methane potential since as much as 50% of the non-bioaccessible organic matter still remains after digestion.

In order to improve energetic performance and to place WWTP within a “biorefinery” concept, it is essential to better characterize the raw material, to use it properly and to optimize the processes while avoiding being subject to wastewater hazard and variations of sludge characteristics. To tackle these general objectives, mathematical models are key aspects to be developed. This is specifically the case of anaerobic digestion models which will be studied in the present thesis.

The first target for AD modeling is the fate of the biodegradable part of the organic matter. Significant progress has been made on this topic going from simple stoichiometric equations to dynamic models that require a highly detailed organic matter characterization. Ten years ago, the International Water Association (IWA) specialist group on anaerobic digestion

developed the Anaerobic Digestion Model N°1 (ADM1). During this last decade, the ADM1 model appeared to be a standard for a large range of applications but has been also modified on several occasions, depending upon the application and the substrate considered. Focusing on urban wastewater sludge, a particulate and complex substrate, hydrolysis of macromolecules has been identified as the limiting step. In order to be biodegraded, a macromolecule present in a digester has to be both bioaccessible and bioavailable (possibility of access into the microorganisms). Bioaccessibility is becoming a key concept to characterize the anaerobic digestion of complex wastes representing another important target for anaerobic digestion modeling. This refers to the ability for macromolecules to be biodegraded more or less rapidly and accessibility to enzymes, extracellular enzymes in particular, is important. It is intimately linked to hydraulic residence time of the process and consequently to reactor design. Other variables such as rapidly and slowly hydrolysable fractions, and more adapted kinetic equations, the Contois equation for example, are included in recent models, making them increasingly performing. But, how to precisely characterize these input variables?

Organic matter characterization has progressed enormously in the last decades. New promising techniques used in others domains are being successfully transposed to environmental engineering. However, in the literature, only few methodologies to "feed" anaerobic digestion models exist with precise waste characterization. And they present limitations, such as the time required for the determination of the biodegradability and bioaccessibility from long and tedious batch tests.

The knowledge of waste bioaccessibility and biodegradability is still today an issue and remains an important challenge. In this context, the present work focuses on the process optimization using an innovative methodology to measure these two key aspects. The characterization method is based on 3D fluorescence spectroscopy of liquid samples obtained from specific chemical extractions. The interest of such a methodology will be demonstrated from results obtained using a modified ADM1 model.

From the state of art presented in chapter I, a promising advanced methodology, fluorescence spectroscopy coupled with sequential chemical extractions, is described. Material and Methods are detailed in Chapter II before highlighting the three main sub-objectives: first, Chapter III focuses on the ability of optimized chemical extractions to simulate the biological accessibility of the sludge. Second, the fluorescence and sequential chemical extractions based methodology is applied on a large panel of wastewater sludge (52) in chapter IV.

Correlations between the variables obtained from the characterization methodology and biodegradability and bioaccessibility are also investigated. Third, the studied characterization methodology is used in chapter V to improve modeling of anaerobic digesters. The model is confronted to experimental data from laboratory scale reactors in order to validate the overall approach.

I. BETTER INPUT CHARACTERIZATION FOR BETTER ANAEROBIC DIGESTION MODELS: TOWARDS NEW METHODOLOGIES FOR MUNICIPAL SLUDGE CHARACTERIZATION

I.1. Statement in methane production prediction from municipal wastewater sludge 23
I.1.1. Municipal wastewater treatment sludge: definition and composition 23
I.1.2. Predicting methane production: the analytical way 27
I.1.3. Predicting methane production: predicting tools 28
I.1.3.1. Static models 29
- Correlations between organic matter composition and anaerobic biodegradability 29
- Indirect correlations 32

I.1.3.2. Dynamic models and evolution of substrate complexity 33
- Dynamic models and substrate definition: 1969-2002 33
- Modified ADM1 and substrate definition: 2002-2012 37

I.1.3.3. ADM1 and influent characterization 39
- Variables lumped with practical analysis 40
- Interpretation of the methane production curve 42
- Plant-wide modelling technique and ASM-ADM mapping 44

I.2. Critical review 46
I.3. Advanced techniques for organic matter characterization 52
I.3.1. Near infrared reflectance spectroscopy (NIRS) 54
I.3.2. 3D Excitation Emission fluorescence spectroscopy 55
I.4. Conclusions and perspectives 59
I.5. Problematic definition and scientific strategy 60

Note for the reader:

Chapter I includes a literature review focused on WWTP sludge characterization methods used to obtain input parameter on anaerobic digestion models. It summarizes the methodologies and their evolution with models complexity. A critical review is also included in order to highlight the lack of precise characterization tools for wastewater sludge and to propose new promising advanced techniques. The chapter defines of main issue of the study.

Anaerobic Digestion (AD) is a biological conversion process with no external electron acceptor. Organic carbon is converted through oxidation-reduction reactions to both its most oxidised state (CO_2) and its most reduced form (CH_4). The methane produced is an energy source which can be valorised as electricity, heat, biofuel or can be injected in the natural gas grid. In an energetic and climatic crisis context, this process has become a very interesting alternative for organic waste treatment. Through the years, and until recent interest for the topic, publications about AD process, modelling and characterization have increased constantly as shown by Figure 1. The graph presents the percentage of papers published with the keywords “anaerobic digestion AND modelling” and “anaerobic digestion AND organic matter characterization”. Additionally the figure 1 shows the total number of paper published on AD and the number of these two specific subjects.

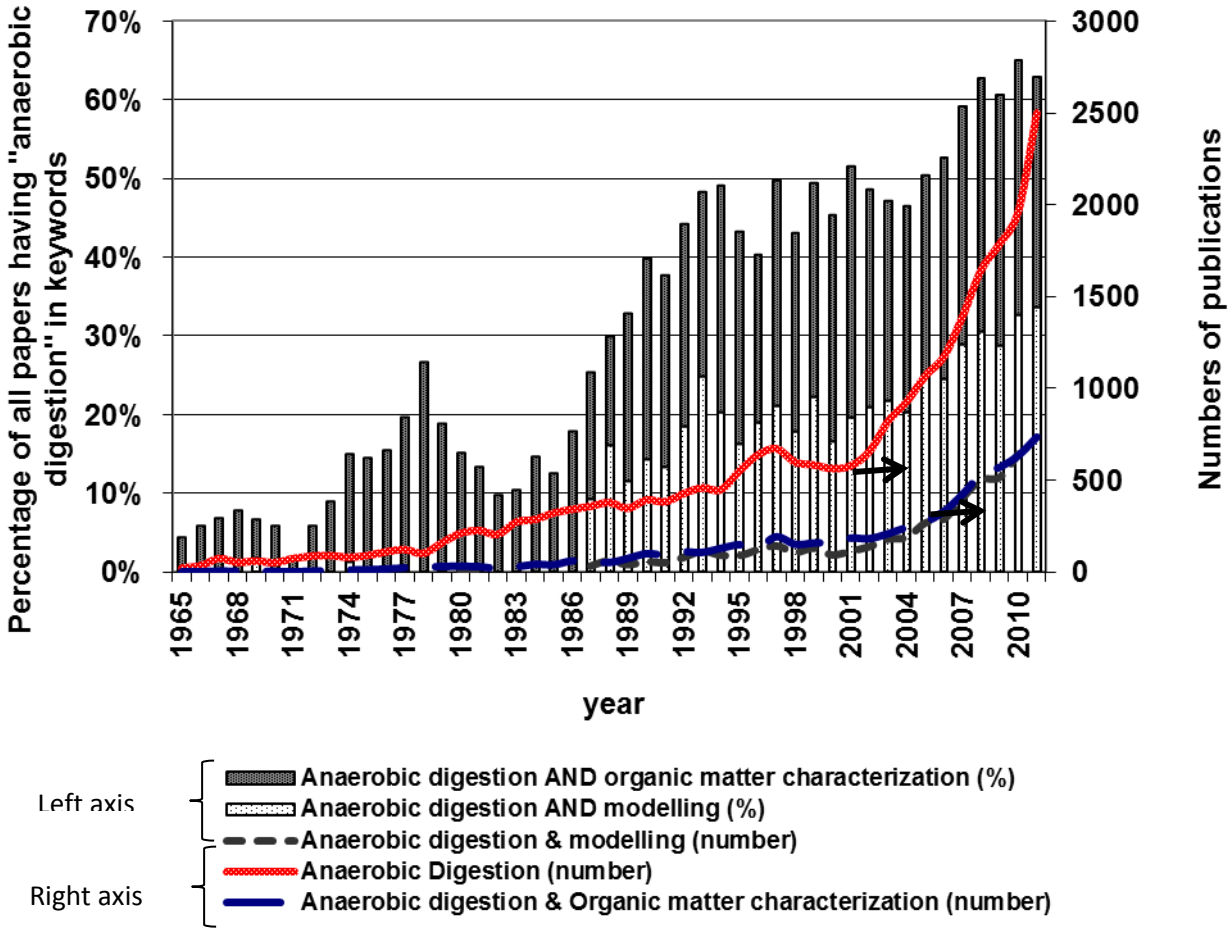

Figure 1: Evolution through the years on AD topics of the published scientific papers
Source: www.ScienceDirect.com

Reflecting the increasing knowledge on the process, models were developed through the years, in parallel with the characterization of substrates. In the sixties, fossil combustible was cheap, and there was a lack of interest on the process that changed drastically during the oil crisis in the seventies. The main objectives for research were to optimise the stabilisation and control of the process. And for that, knowledge on methane production prediction, reaction kinetics, and substrate nature was necessary (Tomei *et al.*, 2009). Fulfilment of these objectives led to the development of dedicated models. These models, static or dynamic, allow the estimation of hydraulic retention time (HRT), reactor volume, gas production and composition. Sensitivity of the system performance to various parameters was investigated and provided simulation results that can be cross-checked with the plant performance (Appels *et al.*, 2008). Before and during the first half of the eighties, very few papers on AD modelling appeared, and only 10% (baseline) of the publications were about organic matter characterization on AD. At the end of the eighties, the willing for energetic independence promoted the development of alternative solutions. Moreover, landfill disposal of sludge (considered as waste) was banned by legislations in the late nineties in Europe. This explains the increase of percentage of papers that can be noticed during the late eighties and nineties.

The last 10 years, the overall number of papers on AD increases rapidly due to a favourable environment policy: the Kyoto protocol (2005), legislation promoting AD, special rates for selling electricity produced from biogas. Concomitantly, farmers have been increasingly interested in the AD process as an energy producing process without greenhouse gas emission. The case of Germany with more than 7000 plants generating more than 2.3 GW of electricity is an example (Bywater, 2011). Moreover, AD is one of the technologies that meet European criteria for second generation biofuel production (fuels manufactured from various types of complex organic carbon sources such as lignocellulose biomass or agricultural residues and waste).

In parallel of these developments, the evolution of the market led to the complexity of the substrates considered for AD valorisation. In the sixties, a fixed biomass reactor concept was set up and applied to liquid industrial wastewater (Coulter *et al.*, 1957). In the eighties, industrial wastewater was the main substrate treated by AD (Van Lier, 2008). In this case, substrates were in liquid phase and hydrolysis was not the limiting step. Therefore, the main discussion on AD modelling was about kinetics of soluble substrate considering acetogenesis and methanogenesis (Mata-Alvarez *et al.*, 2000). At the same time, the Upflow Anaerobic Sludge Blanket (UASB) was born (Lettinga, 1980) and was applied on high organic load

industrial wastewaters (15-50 kg COD/m^3.j^{-1}) containing few solids. The use of AD process exploded on industrial wastewater treatment. Several years after its creation, the number of UASB in the world reached 930 (Bafing Consulting, 2007). The overall number of anaerobic reactors treating industrial wastewater reached 2266 references in 2007 (Van Lier *et al.*, 2008).

At the end of the eighties, AD focused also on solid waste as a substrate. The increasing production of solid waste combined with waste management policies aiming at reducing long-term environmental impacts of landfill disposal have created a need for alternative treatments. The use of AD to treat the organic fraction of municipal solid waste became a reality (De Baere, 2000 and 2008): from 3 plants in 1990 to 55 plants referenced in 2010 in Europe. From a process standpoint, hydrolysis became the limiting step for solid waste (Mata-Alvarez *et al.*, 2000). Hydrolysis of complex substrates was identified as an important issue for AD modelling (Vavilin *et al.*, 1997), through substrate characterization and hydrolysis kinetics. Sewage sludge, considered as solid waste by legislation, is also concerned by the hydrolysis as limiting step.

Indeed, sewage sludge is a complex substrate mainly composed by particulate material. Although initially the objective of anaerobic digestion of municipal sludge was to reduce solids disposal, the interest in energy recovery from sewage sludge is increasing nowadays as the modern wastewater treatment plant should present a positive energy balance (Cao *et al.*, 2012). To achieve this purpose, optimization through modelling of municipal sludge anaerobic digestion could be used. However, knowledge of WWTP sludge characterization is one of the modelling first step.

Therefore, the main objective of this review is to investigate the parallelism between the evolution of organic matter (OM) characterization and the integrative tools that are static and dynamic models. The focus is made on complex substrates such as municipal sludges (primary, secondary or anaerobically digested sludge). Methodologies, analytical techniques and models are reported and evaluated. An analysis of the interactions between OM characterization and modelling is also made in order to highlight the additional studies still required to improve these relationships.

I.1. Statement in methane production prediction from municipal wastewater sludge

I.1.1. Municipal wastewater treatment sludge: definition and composition

The review is focused on municipal wastewater by-products as main substrates. Sludge stand for the main by-products produced through the wastewater treatment plant, at different locations: primary, secondary or biological and sometimes tertiary sludge (post-treatment). Primary sludge consists of organic solids, inorganic fines and settleable particles of variable sizes (Yasui *et al.*, 2008). Its composition varies widely from plant to plant. Total solids vary depending on the sludge collection and removal system operation (Vesilind, 2003). Therefore, the characteristics of the primary sludge depend on both separation unit and wastewater quality.

Secondary sludge is mainly composed of biological solids resulting from the conversion of soluble and colloidal substrate in microorganisms or biomass (Yasui *et al.*, 2008). It also includes some of the particulate matter not removed by primary sedimentation. These solids are produced by treatments as activated sludge, membrane bioreactors, biological nutrient removal, trickling filters and other attached-growth systems. The quantity of sludge produced depends on many factors such as efficiency of primary treatment, ratio of suspended solids to biological oxygen demand (BOD), amount and quality of soluble organic matter and design parameters. For activated sludge systems, the sludge age (average time that solids remain in the tank) has a significant effect on the amount of secondary solids produced: the longer the sludge age is, the more particulate biodegradable organic matter is uptaken and the more endogenous decay of biomass occurs leading to non-biodegradable products accumulation in the reactor (Vesilind, 2003). Activated sludge is a heterogeneous mixture of particles, microorganisms, colloids, organic polymers and cations (Jorand *et al.*, 1995). The composition depends on the quality/composition of the wastewater leaving the primary treatment and on the origin of the sample. Apart from the bacterial cells, in average 80–95% of the organic matter in the activated sludge floc, it consists of various types of organic material. Among them, the exopolymeric substances (EPS) are the largest fraction (Nielsen *et al.*, 2004). EPS come from microbial metabolism, cell lysis and organic matter adsorbed from influent wastewater (Park *et al.*, 2008). EPS are present outside of cells and inside of microbial aggregates and represent different types of macromolecules: carbohydrates, proteins, nucleic acids, lipids and others polymeric compounds such as humic acids and fibers.

Carbohydrates and proteins are usually found as the major EPS components having a protein to carbohydrate ratio between 0.2 and 5 (w/w) (Frølund *et al.*, 1996). Indeed, wastewater organic fractionation is mainly composed of protein, carbohydrate, lipid and minor groups such as VFA and amino acids (Raunjkaer *et al.*, 1994).

Data about organic matter characterization of municipal sludge based on the main biochemical families (carbohydrates, lipids and proteins) can be found in the literature (Table 1).

Table 1: Literature data on organic composition of sewage sludges

Sludge type (number)	Compounds	Methods	Average value g compound/g VS or g eq COD/gCOD*	Standard deviation (%)	References
Municipal wastewater * (12)	Pr	GC/MS/Lowry	0.188	47%	*Raunjkaer et al., 1994, (4 references) Sophonsiri and Morgenroth (2004) (7 references) Huang et al., 2010 (1 reference)*
	HA	GC/MS	0.057	-	
	Ch	GC/MS/Anthrone	0.196	51%	
	VFA	GC/MS	0.051	-	
	Fibers	GC/MS	0.155	-	
	Li	GC/MS/IR	0.213	85%	
Primary sludge (13)	Pr	Lowry/ N-content	0.234	44%	*Elefsiniotis 1994, Wilson et Novak, 2009, Barret et al., 2010, Ji et al. (2010)*
	Ch	Anthrone/Dubois/ASTM(1)	0.246	51%	
	Li	Soxlet ether	0.123	43%	
	VFA	GC	0.069	47%	
Secondary sludge (10)	Pr	Lowry/ N-content	0.496	23%	*Frolund et al. 1996, Wilson et Novak, 2009, Mottet et al. 2010, Barret et al., 2010, Ji et al. (2010)*
	Ch	Anthrone/Dubois	0.245	59%	
	Li	Soxlet ether	0.048	73%	
	HA	Modified Lowry	0.203	19%	
	VFA	GC	0.024	88%	
Anaerobic Digested sludges (9)	Pr	Lowry	0.643	11%	*Mottet et al. 2010 Barret et al., 2010*
	Ch	Anthrone	0.138	8%	
	Li	Soxlet ether	0.038	56%	
	VFA	GC	0.009	6%	

Pr: proteins; Ch: carbohydrates, Li: lipids, VFA: volatile fatty acids; HA: humic acids

(1): ASTM: American Society for Testing Materials, Standard method for chromatographic analysis of chemically refined cellulose (1989)

Municipal wastewater is mainly composed of carbohydrates (19.6% carbohydrates and 15.5% fibres). They are mainly similar in primary sludge where carbohydrates content represents 24.6% of VS and protein content is 23.4% of VS. Concerning secondary sludge and digested sludge, proteins are the major component (49.6% and 64.3% of VS respectively), followed by carbohydrates (24.5% and 13.8% of VS respectively) and lipids (4.8% and 3.8% respectively). Concerning lipids content, high variation can be noticed with a standard deviation of 85% in the average wastewater composition.

The content of this fraction may depend on industrial wastewater rejection in municipal network (Sophonsiri and Morgenroth, 2004). As mentioned before, the organic composition of sludge varies significantly depending on two major elements: the wastewater composition depending on the sources (household and industrial) and the kind and degree of treatment used in the wastewater treatment plant. High deviations can also come from the different analytical protocols used to measure composition. Colorimetric methods exist for decades. Initially conceived to analyse proteins, lipids and carbohydrates in serum samples, they have been applied in environmental engineering. They are now coupled with analytical improvements such as organic matter extraction techniques (Comte *et al.*, 2006; Park and Novak, 2007; Ras *et al.*, 2008 and Sheng *et al.*, 2010). Standard methods for analysis of proteins and carbohydrates in wastewater do not exist. Only the measurement of lipids is standardized according to Standards Methods (APHA, 1985). Table 2 synthesizes, based on D'Abzac *et al.*, (2010), some of the available methods used to determine the main components of municipal sludge. Generally, carbohydrates content is measured using the Anthrone method (Dreywood, 1946) or the Phenol–sulfuric acid method (Dubois *et al.*, 1956). Proteins concentration is measured with the following colorimetric methods: Biuret (Gornall *et al.*, 1949), Lowry (Lowry *et al.*, 1951), Bradford (Bradford *et al.*, 1976) and BCA (Smith *et al.*, 1985) or with the N-content determination using the TKN determination (Kjehdahl *et al.*, 1883). Recently, several works used a more advanced methodology, the Gas Chromatography with Mass Spectroscopy determination (GC/MS), in order to determine the detailed composition of carbohydrates, proteins and lipids present in the sample. Huang *et al.* (2010) used such technology on wastewater characterization.

Pros and cons of the different colorimetric methods were evaluated in several articles (Raunjkaer *et al.*, 1994; Frølund *et al.*, 1996 and Ras *et al.*, 2008) leading to different conclusions. According to Raunjkaer *et al.* (1994), the Lowry method and the Anthrone method are suitable for proteins and carbohydrates assessments in wastewater. Frølund *et al.* (1996) modified the Lowry method for proteins measurement in order to take into account the humic acids interference and to quantify them. On the contrary, Ras *et al.* (2008) based all their data on the BCA method for proteins and on the Anthrone method for carbohydrates. Depending on the nature of the substrate (total sludge or EPS solubilised in an extractant) the methods are more or less adequate.

Organic matter characterization evolves with time, revealing the increasing complexity of both municipal wastewater and sludge.

Table 2: Analytical protocols for biochemical compounds determination

Organic fraction	Method type	Concentration (mg/L)	Reagent used	Standard	Reference
Proteins	Colorimetric	0-200	Folin reagent Copper sulfate 0.5% (w/w)	Bovine albumin serum	Lowry et al., 1951 Frølund et al., 1995
	Colorimetric	0-200	Bicinchonic acid		Smith et al., 1985
	Colorimetric	0-100	Gornall biuret reagent and NaCl		Gornall et al., 1949
	Colorimetric	2-120	Coomassie brilliant blue G-250 reagent		Bradford 1976
	Standard method for TKN assessement	N content x 6.25 g proteins/gN	Mineralisation and ammonia dosage	None	Kjeldahl 1883
Humic acids like	Colorimetric	0-200	Folin Reagent	Humic acids (Aldrich)	Frølund et al., 1995
Polysaccharides	Colorimetric	0-100	Phenol 5% (w/w) Sulfuric acid 95%	Glucose	Dubois et al., 1956
	Colorimetric	0-100	Anthrone 0.125% (w/v) Sulfuric acid 95%		Dreywood et al. 1946 Raunkjaer et al., 1994
Nucleic acids	Colorimetric	0-50	Diphenylamine 0.6% (w/w) Sulfuric acid 95%	Calf thymus DNA (10 mg/mL, Aldrich)	Burton, 1956
Uronic acids	Colorimetric	0-250	m-hydroxidiphenil sulphiric acid	glucuronic acid	Blumenkrantz et al., 1973
Fibers	Extractions	-	Weende method Van Soest	None	Henneberg and Stohmann (1860) Van Soest (1963)
Lipids	Colorimetric	0-1000	Vanillin 0.6% (w/w) Phosphoric acid 85% Sulfuric acid 95%	Commercial olive oil	Frings and Dunn 1970
	Extraction Infrared spectroscopy	-	CCl_4, Uvasol, Al_2O_3, Na_2SO_4, HCL 6M	cornoil	APHA 1985
	Extraction Gravimetry		Organic solvent	-	APHA 1995

Nielsen *et al.* (1992) characterized organic matter in order to measure and predict changes in wastewater composition through sewers. Raunjkaer *et al.* (1994) had the same interest but the authors also proposed to improve the knowledge of the specific fractions from wastewater for hydrolysis prediction during biological treatment. Sophonsiri and Morgenroth (2004) characterized effluent from primary and secondary treatments in order to improve solid-liquid separation and biological processes design. They showed, with a particle size distribution study, that municipal wastewater is composed of large particles which require extracellular hydrolysis. Moreover, Huang *et al.* (2010) performed a detailed characterization of municipal wastewater in order to establish links with Activated Sludge Models (ASM) for process performance prediction. Concerning sewage sludge, the main purposes of Elefsiniotis *et al.* (1994), Wilson and Novak (2009) and Ji *et al.* (2010) were to characterize and optimize the hydrolysis and solubilisation of macromolecules present in primary and secondary sludge during AD. Ramirez *et al.* (2009) and Mottet *et al.* (2010) focused on the link between organic matter characterization and anaerobic biodegradability of sludge and modelling. All the previous references cited aimed at better predicting and understanding mechanisms of biological process of macromolecules hydrolysis and solubilisation. Thus, the role of organic matter characterization in process modelling and prediction is obviously important.

I.1.2. Predicting methane production: the analytical way

The main aim of AD modelling is to predict methane production from an organic matter source defined by its own characterization.

Traditionally the performance of AD in wastewater treatment was evaluated using parameters such as chemical oxygen demand (COD), total organic carbon (TOC) and biological oxygen demand (BOD). In order to optimize plant design and operation, Raunjkaer *et al.* (1994) proposed to link COD fractions and biodegradability (useful for modelling purposes). Kayhanian *et al.* (1995) showed that the content of biodegradable volatile solids (VS) impacted the prediction of biogas production rate, the computation of the organic loading rate and the Carbon/Nitrogen (C/N) ratio. However, since the seventies, the most widely used indicator to assess the performance of the digesters is the amount of methane produced per unit of Total Solid (TS) or Volatile Solids (VS) of any given substrate (Chynoweth *et al.*, 1993). The most commonly used method to measure anaerobic biodegradability is the biochemical methane potential (BMP) (ISO EN 11734, 1995).

The BMP assay is a procedure developed to determine the methane yield of an organic material during its anaerobic decomposition by a mixed microbial flora in a defined medium. The procedure was developed for a serum-bottle technique by Owen *et al.* (1979). Angelidaki *et al.* (2004) described the procedure and the calculations. The test ends when the cumulative biogas curve reaches an asymptote, usually after 30 days of incubation but it may be much longer for non-easily degradable material such as fibers e.g. 200 days for cardboard (Abassi-Guendouz et al., 2012). Therefore, the main inconvenient of the test is the time consumed. Chynoweth and Isaacson (1987) wrote that maximum theoretical methane yield determination was useful to evaluate digester performance and to provide basis for experimental work. However, the literature reports different analytical conditions for the test and many factors may influence the anaerobic biodegradability of organic matter. Enhancements of this method led to different parameters studies: substrate/biomass from inoculum ratio (S/X), pressure biogas measurement, macro and micronutrients additions, etc. (Owen *et al.*, 1979; Gledhill *et al.*, 1979; Shelton *et al.*, 1984; Battersby *et al.*, 1989; Kameya *et al.*, 1995). More recently, a specific group from IWA (i.e. the specialist Group on Anaerobic Biodegradation, Activity and Inhibition Assays) has been set up in order to discuss about BMP methodologies and to propose a standard protocol (Angelidaki *et al.*, 2009). Thus, first guidelines for a definition of a new international standard protocol were defined.

In the same way, an international interlaboratory study has been conducted in order to compare the BMP test with substrates such as starch, cellulose, gelatine and biomass material (Raposo *et al.*, 2011). Nineteen laboratories participated in the study, using different protocols. Except for the gelatine, a small number of outliers were obtained. The relative standard deviation ranged between 15% and 24% and decrease to 10% when the outliers were not considered. The influence of inoculum, temperatures, volume, and headspace gas appeared to be insignificant. However, kinetic rates were widely different (standard deviations ranged from 57% to 68%) and they were impacted by substrate/inoculum ratio.

In order to reduce time consumption, other ways to determine an equivalent of the BMP value have been investigated using several kinds of organic matter characterization techniques.

I.1.3. Predicting methane production: predicting tools

According to Buffiere *et al.*, (2006), "*methane productivity not only depends on the amount of degraded volatile solids, but also on the nature of the solid: carbohydrates, proteins or fats have different methane potential.*

Consequently, the biochemical composition has become an important descriptor for anaerobic digestion, both for production prediction and for kinetics assessment". In other words, biochemical composition is required for the use of integrative tools such as models (static or dynamic) and to achieve an accurate prediction of digester performance. As Angelidaki *et al.* (2004) concluded, methane yield depends strongly on the nature of each biochemical family in addition of the COD content. Integrative tools, in this review, are the implementation of different relationships between the organic matter composition and the methane production or the anaerobic biodegradability. Static models are correlations (obtained by linear regression or partial least square regression) where the variable of interest is explained by one or more variables based on some analytical composition of the given substrate. Static implies neither kinetic equation nor variation over time. Dynamic models include these variations and are usually more complex: biological reactions are explained by kinetic equations such as the Monod type and included in differential equations representing mass balance in the process. In the following paragraphs, an overview of the different integrative tools found in literature is presented.

I.1.3.1. Static models

- Correlations between organic matter composition and anaerobic biodegradability

Theoretical BMP has been calculated since 1930 with the Buswell formula (Buswell, 1930). The stoichiometric equation is based on elemental composition ($C_nH_aO_b$) where organic matter is reduced to methane and oxidised to carbon dioxide (equation 2.1), with the assumption of total conversion.

$$C_nH_aO_b + (n - \frac{a}{4} - \frac{b}{2})H_2O \rightarrow (\frac{n}{2} - \frac{a}{8} + \frac{b}{4})CO_2 + (\frac{n}{2} + \frac{a}{8} - \frac{b}{4})CH_4 \qquad \text{Equation 2.1}$$

Derived from the Buswell formula, another existing relationship (equation 2.2) is based on the knowledge of the main biochemical composition of a substrate, carbohydrate, protein and lipids, and based on the stoichiometric conversion of model compounds in COD (Raposo *et al.*, 2011).

$$B_{th} = 415 \times \%\text{Carbohydrates} + 496 \times \%\text{Proteins} + 1014 \times \%\text{Lipids} \qquad \text{Equation 2.2}$$

However, these relationships remain theoretical and they assume that organic matter is fully converted.

Shanmugan *et al.* (2009) calculated the empirical formula for each waste based on the results of the chemical analysis. The formula was used to estimate the COD equivalent and the stoichiometric methane potential with the Buswell equation (Buswell, 1930). The measurement of elemental composition (carbon, hydrogen, nitrogen and sulphur) was used to characterize different types of sludge and municipal solid waste. The methane production potential calculated overestimated the experimental one. Lesteur *et al.* (2010) explained that measuring elemental composition is very fast but the obtained value takes into account all the organic matter, without any differentiation between biodegradable and non-biodegradable organic matter. Moreover, part of the biodegradable organic matter used for bacterial growth is not taken into account by the Buswell formula. Additionally, when applied on municipal solid wastes, Davidsson *et al.* (2007) showed that theoretical methane potential is more realistic when calculation is based on biochemical composition (lipids, carbohydrates, proteins) rather than on elemental composition analysis.

During the last two decades, several authors tried to build other static integrative tools based on organic matter characterization but they are mainly applied to municipal solid waste (Buffiere *et al.* 2006), kitchen, fruits and vegetables wastes (Gunaseelan, 2007 and 2009). Few studies dealt with municipal sludge although the methodologies used on solid waste can be transposed to sludge. The most recent publication has been made by Mottet *et al.* (2010) and Appels *et al.* (2011).

Seeking an indicator of biodegradability, Mottet *et al.* (2010) proposed to link Van Sœst fractionation with biodegradability of sludge, using partial least square regression. Extraction mainly occurs with the first neutral detergent (50% to 80% of TS). Following detergents, targeting hemicelluloses, cellulose and lignin, extract little material (5-20% of TS). Thus, this method, adapted for vegetable wastes, was not suitable for municipal sludge (mainly proteinaceous). Previously to Mottet et al. (2010), Chandler *et al.* (1980) showed that the anaerobic biodegradability was inversely proportional to the lignin content (equation 2.3). Buffiere *et al.* (2006) found an interesting relationship between the sum of cellulose and lignin percentage of VS to the biodegradability of kitchen waste. In the same way, Gunaseelaan *et al.* (2009) showed that there was a correlation between biodegradability and carbohydrate, proteins, lipids, acid detergent fibres, cellulose and ash concentrations obtained with Van Soest method. An accuracy of 94% was obtained when applied to fruit and vegetables. That approach was validated on real scale plants (equation 2.4)

$$BD = 0.83 - (0.028) \times X_1$$ Equation 2.3

Where: BD is the biodegradable fraction of VS (0<BD<1)

and X_l (0<X_l<20%) is the initial lignin content.

$$BD = 0.045 + 1.23 \times \text{Carbohydrates} + 0.24 \times \text{Proteins} + 1.51 \times \text{Lipids} - 0.68 \times \text{ADF} - 0.81 \times \text{Cel} - 6.1 \times A$$

Equation 2.4

Where: Proteins is proteins concentration

Carbohydrates is carbohydrates concentration

Lipids is lipids concentration

ADF is the acid detergent fibers content

Cel is the cellulose content

and A is the ash in ADF

Contrary to previous studies, Mottet *et al.* (2010) observed that the Van Sœst fractionation cannot be used as a tool for biodegradability prediction. Applied on municipal sludge, the error for the validation model is about 35%. These authors highlighted that it would be interesting to develop a new method based on successive extractions more adapted to this substrate.

In the second part of their work, the authors found a better correlation between anaerobic biodegradability and specific fractions of organic matter (equation 2.5).

$$BD = 0.043 - 0.106 \times \text{Proteins} + 0.661 \times \text{Carbohydrates} + 0.836 \times \text{Lipids} + 0.074 \times \text{Ox} + 0.349 \times 0.074$$

Equation 2.5

Where: Ox is the ratio COD/TOC and SolOC is the dissolved organic carbon (g.gVsoluble^{-1})

The oxidation degree (i.e. COD/TOC), the proteins, carbohydrates, lipids and soluble organic carbon percentages of VS were input variables of a PLS model. The validation step gave an error of 11% and the model regression coefficient was 0.938. However, the number of used secondary sludge used was small (6 sludge used for calibration and 4 substrates used for validation, including cellulose) and the biodegradability range was narrow (35% to 66%).

In the same way, Appels *et al.* (2011) developed a PLS model to predict the BMP of waste activated sludge with 19 characterization parameters (soluble and total COD, soluble and total carbohydrates, soluble and total proteins, TS, VS, pH, heavy metals, detailed VFA). They showed a strong positive correlation is established with VFA, carbohydrates and proteins whereas soluble organic matter is not influential for this kind of sludge.

- Indirect correlations

Correlations between aerobic activity tests and anaerobic tests such as BMP are often proposed. Aerobic tests are less time consuming than anaerobic ones and they are easier from a practical point of view (e.g. no need of anaerobic conditions).

Cossu *et al.* (2008) showed a good correlation ($r^2 = 0.80$) between respiration index (RI_4) (mgO_2/gTS), which represents the oxygen consumption cumulated in 4 days (Sapromat® apparatus used), and the biogas produced in 21 days GB_{21} (Nl/kgTS) on municipal solid waste from landfills. Scaglia *et al.* (2010) found similar results with a correlation between dynamic respiration index (DRI) and anaerobic biogas potential (equation 2.6) with a regression coefficient of 0.89.

$$ABP = (34.4 \pm 2.5) + (0.109 \pm 0.003) \cdot DRI \qquad \text{Equation 2.6}$$

Where the ABP is expressed in NL.kg^{-1} dry matter and the DRI in kg O_2.kg^{-1} dry matter.h

Another kind of commonly established correlations is between the initial reaction rate of the BMP assay and the final production value. Donoso *et al.* (2010) developed an experimental procedure to estimate kinetic parameters from sewage sludge based on the initial reaction rate method. Batch experiments were performed for 3 to 4 days and methane production was monitored. The maximal slope (linear regression) represents the initial reaction rate. S/X ratio is also investigated in order to evaluate the specific effect of the substrate. The optimum ratio went from 0.51 to 1.11 gVS_{Fed} $gVS_{Inoculum}^{-1}$. The set of data of initial methane production rate at different initial substrate concentrations was used to estimate the maximal production rate of methane and the affinity constant. An optimization of the experimental data with the simulated data was performed. Authors succeeded in predicting methane production with Monod kinetics. However, the simplified model did not allow accounting for overloads, temperature, inhibitions on continuous digesters modelling and the model underestimated CH_4 production by 20% with the parameters obtained in batch tests. Moreover, the inoculum adaptation to the substrate is crucial for this kind of analysis.

Predicting methane potential and biodegradability is possible using the mentioned statistic correlations. The BMP test gives some kinetics information, even though attention had to be paid to the S/X ratio (Raposo *et al.*, 2011). However, it is not sufficient to predict hydrolysis rates, optimal retention time and to get an overview of the multiple biological reactions occurring in AD.

I.1.3.2. Dynamic models and evolution of substrate complexity

- Dynamic models and substrate definition: 1969-2002

The first objective for dynamic modelling AD is to describe the limiting steps causing digesters failures under stress conditions (Lyberatos *et al.*, 1999). These limiting steps depend on wastewater characterization (complex, liquid or soluble and particulate), hydraulic loading rate and/or temperature. These models are simple and readily usable but are limited for the description of the digestion behaviour. Table 3 presents the chronologic evolution of dynamic models with respect to substrate characteristics, limiting steps and hydrolysis kinetics. Over time, substrates used in the models have become more complex. For that reason and depending on the considered substrate, the limiting step evolved and hydrolysis of complex substrate appeared as a crucial issue. At first, methanogenesis or acetogenesis had been widely considered as the limiting step due to their high sensitivity to overloading, VFA accumulation or pH break down. The first dynamic model was developed by Andrews *et al.* (1969) to describe biological processes in AD. Studies were conducted, using this model, to determine the effects of VFA concentrations and pH values on the efficiency of AD process. But the model only took into account the degradation rate of acetate to describe the overall rate of organic matter digestion. Hill and Barth (1977) included in their model both the hydrolysis and acidogenesis processes to consider organic overload caused by VFA accumulation. Initially, the organic matter of the substrates was characterized in models using lumped variables such as COD (Eastman et Ferguson, 1981), BOD (Pavlostathis et Gosset, 1986) or glucose equivalent (Andrews, 1969; Graef and Andrews, 1974; Mosey *et al.*, 1983; Moletta *et al.*, 1986; Costello *et al.*, 1991; Pullammanappalil *et al.*, 1991; Kiely *et al.*, 1997 and Cecchi and Mata-Alvarez, 1991).

From 1986 to 1990, Moletta *et al.* initiated the complete modelling of the anaerobic reactor taking into account the three phases: liquid, solid and gaseous. However, the organic composition of complex effluents was expressed as glucose or acetic acid equivalent COD.

Since the work of Eastman and Ferguson (1981) on the prediction of AD of primary sludge, hydrolysis (first order) was not considered as the limiting step until the study of Pavlostathis and Gosset (1986). In Eastman and Ferguson (1981), the substrate variable was expressed as degradable $COD_{particulate}$. In Pavlostathis and Gosset (1986), the substrate was a secondary sludge composed of about 80% of particulate matter and showed that the limiting step was hydrolysis, stating the difference between soluble and particulate phases. In the same way, Smith *et al.* (1988) defined the organic particulate substrates by two fractions: the rapidly and the slowly degradable.

Representation of waste activated sludge digestion was improved considering intermediate levels of polymeric cell components (Shimizu, 1993; Siegrist *et al.*, 1993) such as proteins, nucleic acids, lipids and polysaccharides with first order hydrolysis kinetics. Indeed, a more accurate representation of the process requires the pathway description of the main analytical groups of organic matter, such as polysaccharides, proteins, amino acids and lipids (Van Haandel *et al.*, 1998). Proteins, lipids and carbohydrates have different hydrolysis constants (first order) depending on the hydraulic retention time (HRT): 0.015-0.075 d^{-1} for proteins, 0.005-0.010d^{-1} for lipids and 0.025-0.020 d^{-1} for carbohydrates (Mata-Alvarez *et al.*, 2000). Siegrist *et al.* (1993) developed a model on sewage sludge able to simulate the hydrolysis of solid waste, with constants for the hydrolysis of lipids, proteins and carbohydrates.

More complicated models appeared as the complexity of the considered substrate (manure or sludge) increased. Models of the hydrolysis of particulate compounds were developed (first order), but acetogenesis was still considered as the limiting step (Angelidaki *et al.*, 1993; Siegrist *et al.*, 1993). Biochemical characterization of organic matter was also introduced by the <METHANE> model (Vavilin and Vasiliev (1993, 1994)) and by Shimizu *et al.* (1993). Input variable standing for the total organic matter of the substrate was decomposed on protein, carbohydrates and lipids. Thus, hydrolysis was considered as the limiting step in order to predict the methane production (of waste activated sludge, manure and sorted household waste). An interesting comparison between several hydrolysis kinetics descriptions was made by Vavilin *et al.* (1996). First-order kinetic Monod equation, Contois function (surface limitation) and a two-phase model (colonization and hydrolysis) were tested on sewage sludge, manure and swine waste. The worst model was the Monod equation, proving that hydrolysis is not a traditional enzymatic reaction. The Contois function and the two-phase model fitted well with the experimental data.

Table 3: Dynamic models evolution: hydrolysis and substrate variables

References	Limiting step of the model	Hydrolysis kinetic	Substrate characteristics	Suitable for digestion of
Andrews et al. (1969)	Acetogenic Methanogenesis	-	Glucose	Soluble organic matter
Graef and Andrews (1974)	Methanogenesis	-	Glucose	Soluble organic matter
Hill and Barth (1977)	Methanogenesis	Andrews	Insoluble organics	Manure
Eastman and Ferguson (1981)	**Hydrolysis**	First order	COD degradable particulates	Primary sludge
Hill (1982)	Acetogenesis	-	Glucose	Animal waste
Kleinstreuer and Powegha (1982)	Methanogenesis	-	Lipids, carbohydrates, proteins	Various substrates
Mosey et al. (1983)	Acetogenesis	-	Glucose	Glucose
Bryers et al. (1985)	Acetogenesis	First order	Insoluble organic matter	Biodegradable organic particulate
Pavlosthatis and Gosset (1986)	**Hydrolysis**	First order	BOD particular and soluble	Biological sludge
Moletta (1986)	Methanogenesis	-	Glucose equivalent	Easily fermentable
Smith et al. (1988)	Methanogenesis	First order	Rapidly and slowly degradable biomass	Biodegradable organic particular
Pullammanappallil et al. (1991)	Acetogenesis and/or Methanogenesis	-	Glucose	Glucose
Costello et al. (1991)	Acetogenesis	-	Glucose	Soluble carbohydrates
Angelidaki et al. (1993)	Acetogenesis	Enzymatic hydrolys first order	Insoluble carbohydrates	Manure
Siegrist et al. (1993)	Acetogenesis	First order	Biopolymers	Sludge
Shimizu et al. (1993)	**Hydrolysis** of intracellular biopolymers	First order	Proteins, lipids, nucleic acids, carbohydrates	Waste activated sludge
Vavilin et al. (1993, 1994)	**Hydrolysis**	Two-step kinetics	Lipids, carbohydrates, proteins	Slaughterhouse waste and sorted household solids
Vavilin et al. (1996)	**Hydrolysis**	Surface colonization Contois model and two-phase model	Lipids, carbohydrates, proteins	Sewage sludge, manure, swine waste
Kiely et al. (1997)	Methanogenesis	Andrews	Equivalent glucose of each co-substrate	Co-digestion of municipal solid waste and primary sludge
Angelidaki et al. (1997)	**Hydrolysis**	First order	Lipids, carbohydrates, proteins	Co-digestion of different wastes including sewage sludges
Sanders et al. (2001)	**Hydrolysis**	Surface related hydrolysis	Starch	Particulate substrates
Batstone et al. (2000)	**Hydrolysis**	Enzyme production and adsorption (Langmuir and first order)	Lipids, carbohydrates, proteins	Slaughterhouse
Batstone et al. (2002)	**Hydrolysis**	First order	Lipids, carbohydrates, proteins	Various substrates

Sanders *et al.* (2001) introduced a mathematical description of the surface related hydrolysis kinetics for spherical particles (using starch in the experiment). The model fitted with experimental data concerning particle size distribution and the authors underlined that the surface of the particle is the key aspect of the hydrolysis process.

In parallel, Batstone *et al.* (2000) proposed a hydrolysis description based on the enzyme production and adsorption applied on AD of slaughterhouse waste. Concerning co-digestion, Kiely *et al.* (1997) developed a two-stage model (hydrolysis/acidogenesis and methanogenesis) in order to predict the co-digestion of the organic fraction of municipal solid waste and primary sludge. Acetogenesis remained the limiting step and the substrate variable was a glucose equivalent of each substrate. Similarly, Angelidaki *et al.* (1997) developed a dynamic model with a substrate characterization based on the biochemical groups previously mentioned to characterize organic waste. The bioconversion process of six substrates was considered, taking into account the difference between particulate and soluble compounds. The particulate solid variable, expressed as COD, was hydrolysed into amino acids, sugars, inert and fatty acids.

More recently, a formal IWA task group (Batstone *et al.*, 2002) proposed a new model resulting of the collaboration between international experts. The Anaerobic Digestion Model n°1 (ADM1) was set up in order to provide a tool to simulate a broad category of processes and a common platform of simulation. In the model, the three phases, gas-solid-liquid, are represented and chemical-physical reactions are considered (calculation of inhibiting factors such as NH_4^+/NH_3, VFA/VFA^-). ADM1 assumes that anaerobic degradation of organic compounds proceeds in the following order: (1) disintegration, (2) hydrolysis, (3) acidogenesis, (4) acetogenesis and (5) methanogenesis. It takes into account seven bacterial groups considered as particulate matter suitable for modelling. The biological degradation pathways are described using Monod kinetics, except the extracellular steps (disintegration and hydrolysis) and the biomass decay processes that are described using first-order kinetics (Silva *et al.*, 2009). A schematic overview of the model is presented in Figure 2. Considering the two extracellular solubilisation steps, in the first, a physical breakdown of the particulate material X_C (total particulate COD) is first translated during the disintegration step into the following particulate variables: X_{pr} (biodegradable particular proteins), X_{ch} (biodegradable particular carbohydrates), X_{li} (biodegradable particular lipids), and X_I and S_I (particular and soluble inert fractions respectively). Inert fractions are represented by (1-BD), where BD is the ultimate biodegradability factor (Batstone *et al.*, 2002).

The fractions X_{pr}, X_{ch} and X_{li} are then hydrolysed into soluble compounds (respectively amino acids, sugars and LCFA). These products will follow the acidogenesis, acetogenesis and methanogenesis steps.

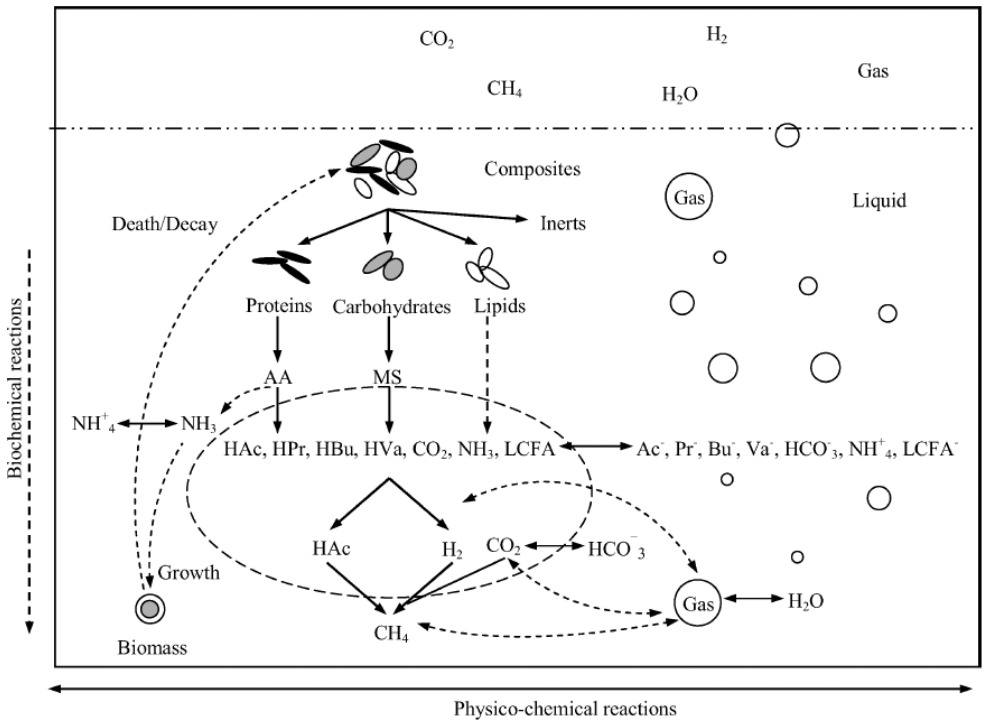

Figure 2: Biochemical and physical-chemical reactions in the ADM1 model (Batstone *et al.*, 2002)

From 1969 to 2002, researchers made important efforts to better understand and represent AD. The historical evolution showed a "complexification" of the models, searching to detail more the metabolic pathways, and closer to the reality. The increasing substrate complexity led to a more detailed model input, taking into account the main biochemical families: lipids, proteins and carbohydrates and considering hydrolysis as the limiting step.

- Modified ADM1 and substrate definition: 2002-2012

After 2002, ADM1 has been considered as a unified model, widely used. The model can predict the trends of experimental data of several scenarii (Parker *et al.*, 2005). Using sludge, with short sludge retention time (SRT), the model overestimated the VFA experimental data and underestimated solids hydrolysis. Authors highlighted that for an accurate model simulation, characterization in terms of biodegradable and recalcitrant COD, TKN and ammonium should be done. They proposed lines of research to standardize a protocol for the determination of the biodegradable fraction.

ADM1 has also been applied to co-digestion. Zaher *et al.* (2009) modified ADM1 by modelling the hydrolysis of each waste separately in order to optimise co-digestion parameters (i.e. HRT). Derbal *et al.* (2009) used the ADM1 model to show that, although trends were well predicted, there were still limitations in the simulation of complex processes.

Recently, several authors have continued to work on the improvement of the definition of hydrolysis, the rate-limiting step in AD of sewage sludge (Batstone *et al.*, 2005; Vavilin *et al.*, 2008; Yasui *et al.*, 2008; Jones *et al.*, 2008). In all cases, hydrolysis was linked to both substrate characterization and bioaccessibility.

Three major concepts to consider have been defined: bioavailability, bioaccessibility and biodegradability.

Aquino *et al.* (2008) defined bioavailability as the direct access to the molecule to be degraded. Molecules with a weight below 1000 Da can pass through the cell wall. Due to the complex organisation of sludge, bioaccessibility is defined as the possible access to the molecule depending on the digestion time, the hydrolytic activity and the pre-treatment applied to the sludge (a molecule bioaccessible becomes bioavailable with a sufficient HRT). The biodegradable fraction is the organic matter bioavailable consumed by the biomass.

In order to eliminate the prediction limitations, ADM1 has been modified including the definition of new variables For sewage sludge and municipal solid waste co-digestion, Esposito *et al.* (2011) upgraded the mathematical model including the possibility to separate each product of disintegration (carbohydrates, proteins, lipids) into readily and slowly biodegradable fractions (introduction of a higher hydrolysis rate constant for readily biodegradable fraction). Indeed, protein hydrolysis rate depends on the nature of the polymer, globular or fibrous, on the surface area and on the solubility of the protein. Protein-based complex can have different proteins being readily or slowly biodegradable (Batstone *et al.*, 2000). Hydrolysis rate of lipids depends on the length of the chain of fatty acid, on the physical state (solid or liquid) and on the specific surface area.

Yasui *et al.* (2008), working under batch conditions, focused on modelling primary sludge biodegradation in order to refine ADM1. Three biodegradable fractions were identified: readily biodegradable, slowly biodegradable and large-sized biodegradable particles. The last two fractions represented the main part of the different primary sludge studied (on average 33% and 40% respectively).

A simplified particle break-up model was introduced with a number of individual stages for disintegration of the three fractions. As disintegration and hydrolysis were the main rate-limiting steps, soluble organic fractions were simplified by defining one variable. Soluble substrate consumption was also simplified (biomass state variables of acetate and methane producers were lumped into two variables respectively). Hydrolysis and disintegration were described as first order kinetics. Authors found a large variation in the hydrolysis rates due to differences in primary sludge composition from one plant to another. They highlighted that the major limitation was the determination of the number of disintegration steps, requiring a complex implementation.

For a better representation of the concept of bioaccessibility, Mottet (2009) proposed a new fractionation of the particulate organic matter in waste activated sludge in order to use it as input variable of ADM1: a readily hydrolysable fraction *Xrc* and a slowly hydrolysable fraction *Xsc* hydrolysed with the Contois model. This new calibrated model was tested and successfully validated at pilot scale showing better simulation performance than the standard ADM1.

Since its development, in 2002, the ADM1 model has been applied to increasingly complex substrates and to co-digestion of different waste mix. The complexity of these substrates conditioned modifications of the model with the definitions of new variables and more appropriate kinetics, both substrate dependants. In the case of sewage sludge, the model has evolved towards the concept of bioaccessibility considering that biodegradability was insufficient.

I.1.3.3. ADM1 and influent characterization

ADM1 model requires a detailed characterization of the organic matter. Soluble and particulate carbohydrates, protein, lipids and individual volatile fatty acids concentrations are required (Kleerebezem, 2006). In terms of predicting treatment performance, biomass composition and chemical characteristics, ADM1 indeed strongly depends on the influent characteristics (Kleerebezem, 2006).

An interesting remark by Mottet *et al.* (2010) is that the proposed static model (equation 2.5) highlighted the main organic fractions used in dynamic models such as ADM1: proteins, carbohydrates and lipids. Depending on the composition of the sludge, some pathways in AD

biological reactions could be preferential and consequently impact hydrolysis products, kinetic reactions, biomass involved and methane production kinetics.

Several authors have made such analysis on ADM1 (Jeong *et al.*, 2005; Lee *et al.*, 2009; Silva *et al.*, 2009). In general, a sensitivity analysis identifies the most important parameters on the dynamic behaviour of the process (Silva *et al.*, 2009). Jeong *et al.* (2005) performed a sensitivity analysis on ADM1 model using glucose as a substrate. The substrate fractionation highly impacted the model components, such as methane content.

The following section gives an overview of different organic matter characterisation methodologies found in the literature and coupled with model developments.

- Variables lumped with practical analysis

A key-point for a successful description of a bioprocess using a mathematical model is a good influent characterisation (Huete *et al.*, 2006).

Kleerebezem *et al.* (2006) admitted that identification of individual substrate concentrations from ADM1 requires specific and not easily available analytical techniques. These authors proposed a calculation method in which the elemental composition of organic substrates, required in ADM1, was lumped with general analysis, such as COD, TOC, alkalinity and TKN.

In the same way and to simulate the co-digestion process, Zaher *et al.*, (2009) proposed the GISCOD (General Integrated Solid Waste Co-Digestion) model. A transformer model was developed to generate detailed input for ADM1, estimating the carbohydrates, proteins, lipids and inert concentrations in the particulate waste fraction. The model was based on the mass balance of elemental composition: it maintained the continuity of COD and elemental mass and interfaced the ADM1 input to practical characteristics of each waste stream (Vanrolleghem *et al.* 2005).

Huete *et al.* (2006) proposed an enhanced characterization methodology for sludge to improve the ADM1 classical model. They also separated the biomass lysis and the disintegration process, and introduced the continuity of mass balance of C, O, N, H, P elements. However, some assumptions were taken such as the composition of monosaccharides and total polysaccharides (stoichiometric formula of glucose), fatty acids, lipids (palmitic acid and palmitate triglyceride stoichiometric formula respectively), proteins and amino acids.

The authors also assumed the elemental mass characterization (C, N, H, O, P content) for the variables X_C (particulate organic compound) and the non-biodegradable soluble (S_I) and particulate (X_I) using an optimization algorithm in order to respect the mass balance continuity. In order to estimate S_I and X_I input variables values, the biodegradability obtained from the BMP of filtered sewage sludge (for non-biodegradable soluble organic matter) and total sewage sludge (for non-biodegradable particulate organic matter) is used. By adjusting the output soluble COD with the COD variable S_I, the value of X_I is the difference between the non-total biodegradability proportion and the S_I proportion.

The amino-acids variable is calculated with the concentration of organic nitrogen obtained from the measure of TKN on filtered samples. The biodegradable fractions of X_C were chosen based on the ADM1 parameters values obtained by Siegrist *et al.* (2002). Simulation results showed a good fit for both nitrogen and COD contents but biogas concentration was not accurate, whatever model used (classical or modified ADM1). Huete *et al.* (2006) suggested that a more appropriate definition of the model components is required.

Many authors also wanted to experimentally measure the main input variables of ADM1: lipids, proteins and carbohydrates concentrations, which are the products of the disintegration of the X_C. They are the result of a first-order equation with a stoichiometry representing the part of each biochemical group. The conclusion remains the same: a good fit of the experimental data needs an accurate substrate characterization (Parker *et al.*, 2005 and Huete *et al.*, 2006). Girault *et al.* (2012) proposed to measure the percentages of protein and lipids contained in total COD by respectively organic nitrogen method from TKN and hexane extraction method. Remaining COD obtained by mass balance was attributed to carbohydrates. Authors used these ratios to split as well particulate and soluble fractions of COD. Mottet (2009) and Ramirez *et al.* (2009) proposed a method to calculate the biochemical disintegration stoichiometry of particular COD. Stoichiometric parameters of disintegration were calculated from protein, polysaccharides and lipids contents and depending on the biodegradability of sludge (equation 2.7). For a given compound $X_{compound}$, its disintegration fraction is the ratio between its biodegradable fraction and the sum of the biochemical fractions of X_C.

$$f\_Xc\_Xcomp\ ound = \frac{X\_compound \times BD(\%)}{X\_li + X\_pr + X\_ch} \qquad \text{Equation 2.7}$$

Variables X_{li}, X_{pr} and X_{ch} are obtained by analysis of the particulate fraction of the substrate. Lipids are measured by hexane extraction in a Soxhlet, and both proteins and carbohydrates are measured with colorimetric methods, such as Lowry for proteins (Lowry *et al.*, 1951) and Anthrone for carbohydrates (Dreywood *et al.*, 1946). In all cases, results are expressed in COD equivalent. The inert particulate fraction, X_I represents the particulate unbiodegradable COD. It is calculated from the biodegradability (BD): $X_I = COD_{particulate}$ x (1-BD(%)), (Batstone *et al.*, 2002).

Table 4 presents the stoichiometric parameters used as default in ADM1 and those calculated for waste activated sludge obtained from several sources (Mottet *et al.*, 2010). A great variation (21% for the carbohydrates and 68% for the lipids) was observed for the same type of sludge. Differences on the process, on the sludge age and on the organic load also impact significantly the values obtained. Consequently, hydrolysis and other biological reactions such as methane production estimation will be impacted.

- Interpretation of the methane production curve

In the model proposed by Mottet (2009), particulate organic matter variable, X_C, is composed of two fractions, the readily and the slowly hydrolysable fractions. Concentrations of the organic matter present in each fraction were determined from the cumulate methane production curves (figure 3) obtained from BMP tests.

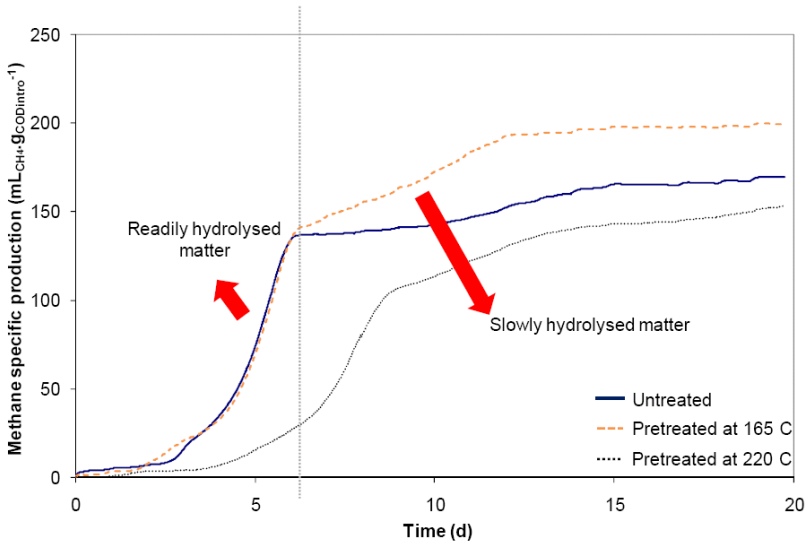

Figure 3: Experimental methodology to assess the readily hydrolysed matter and the slowly hydrolysed matter in a BMP batch test: cumulated methane specific production for a waste activated sludge before and after thermal pre-treatment at 165°C and 220°C (Mottet, 2009)

Table 4: Stoichiometric parameters calculation from literature data

Authors	**Batstone et al. (2002)**	**Siegrist (2002)**	**Mottet et al. 2009**								
Yield of product on substrate kgCOD/kgCOD	ADM1 default	Activated sludge	Activated sludge	Highly loaded urban	Highly loaded urban and industrial (30%)	Urban Very highly loaded	Urban Very high load	Urban extended aeration	Urban extended aeration	Mean	SD (%)
fxi_xc	0.25	0.44	0.61	0.46	0.34	0.48	0.25	0.65	0.54	0.45	31%
fch_xc	0.2	0.11	0.09	0.15	0.21	0.21	0.13	0.16	0.10	0.16	21%
fpr_xc	0.2	0.17	0.16	0.33	0.33	0.26	0.46	0.27	0.37	0.34	28%
fli_xc	0.25	0.26	0.13	0.12	0.15	0.16	0.13	0.00	0.03	0.10	68%

The readily hydrolysable fraction is calculated by dividing the volume of methane produced during the first phase and the total volume of methane produced. The remaining proportion corresponds to the slowly biodegradable fraction. A good fitting was obtained when applied into successive batch tests using the same parameters.

Yasui *et al.* (2008) modelled AD of primary sludge using the double-peak of the methane production rate (MPR) curves. MPR curve represents the evolution of the production rate of methane with time (derivative of cumulated methane traditionally obtained in BMP). The substrate was defined as several COD fractions according to the regions of the curves. This technique is comparable to the tests of aerobic respirometry performed to assess readily and slowly biodegradable fractions of activated sludge models (Ekama *et al.*, 1986). The variables are defined depending on the considered substrate. The inert fraction is assumed to be the difference between total COD and the sum of the area of three regions. Girault *et al.* (2012) used the MPR curves under anaerobic batch tests of waste activated sludge and pig slurry for process optimisation with ADM1. They identified two input variables on the MPR curves: (1) biodegradable fractions calles S_fractions for which hydrolysis is not rate limiting, VFA and (S_{aa}+S_{su}+S_{fa}) representing respectively amino acids, monosaccharides and long chain fatty acids, (2) biodegradable fractions for which hydrolysis is rate limiting (Xpr+Xch+Xli) called X_fractions. Particulate inert fraction X_I is obtained by a COD mass balance. With their optimization methodology, they identified also the hydrolysis rate associated to particulate variables. Authors tested several substrates on biomass ratios and advised a range between 0.37 and 1.3 g $COD_{biodegradable}/gCOD_{biomass}$ to avoid inhibition and discrepancies. They highlighted that the origin of inoculum is also important: it can influence fractionation results even if a continuous stirred reactor simulation did not show significant differences. Finally, authors made an interesting sensitivity analysis of their fractionation depending on HRT. As expected, the fractionation of the S_fractions and X_fractions had an impact on HRT of the continuous reactor simulated.

- Plant-wide modelling technique and ASM-ADM mapping

In order to simplify input characterization, some authors considered modelling AD by modelling the whole wastewater treatment plant. Activated sludge is modelled with Activated Sludge Model (ASM) and AD of primary and secondary sludge is modelled with ADM1. Two techniques exist.

The first one, known as the "supermodel", considers the entire wastewater treatment plant with a single model where all the variables from ADM1 and ASM are present in all the process units. The second one, the interface ASM/ADM technique, aims at lumping the ASM variables, generated during the activated sludge modelling, into ADM variables.

Concerning the first technique, Jones *et al.* (2008) used a plant-wide modelling to reduce the input characterization of the AD model to the characterization of the wastewater, more systematic and simple. Using the continuity based interfacing models described in Vanrolleghem *et al.* (2005), Grau *et al.* (2007) proposed an integrated plant-wide modelling considering all the components and transformations present in both aerobic and anaerobic models. Mass balances are closed from an elemental point of view and biomass lysis is decoupled from the disintegration step, as proposed by Huete *et al.* (2006).

Using the General Activated Sludge and Digestion model (GASDM) from BIOWIN®, Yasui *et al.* (2006) proposed, for waste activated sludge, a mapping between the ASM1 variables, the heterotrophic (X_H) biomass and slowly hydrolysable fraction of COD (X_S) and the biodegradable fractions of ADM1. Using both anaerobic and aerobic respirometry tests, authors showed that part of readily biodegradable fraction came from the biodegradation of X_H and part of the slowly biodegradable from the biodegradation of X_S. The inert fractions in the ASM1 model are assumed to remain inert during AD (Ekama *et al.*, 2007) until a SRT of 30 days (Jimenez *et al.*, 2010). In anaerobic model, the first fraction identified as X_H, was assumed to be hydrolyzed through a decay reaction (first-order hydrolysis equation) while the second one X_S was assumed to be hydrolyzed through a Contois equation by Yasui *et al*. (2006).

In the GASDM model, particulate COD, represented by heterotrophic biomass in the ASM, is transformed into slowly biodegradable COD in the ADM and it is responsible for the methane production during the first 60 days. Authors proposed to link methane yield with the proportion of heterotrophic biomass. Moreover, the main difference between primary and secondary sludge composition is that primary sludge is rich in X_S and waste activated sludge is rich in X_H. Additionally, the nature of X_S is different. For primary sludge, X_S represents settled particles of variable sizes. While for secondary sludge, X_S is mainly composed of colloidal particles.

Considering the interface ASM/ADM technique, Nopens *et al.* (2009) based on Copp *et al.* (2003) proposed a mapping of ASM variables into ADM1 variables.

The defined interface and characterisation model converts degradable components directly into carbohydrates, proteins and lipids (and their soluble analogues) as well as organic acids. X_C was not considered. The inert particulate fractions X_I and X_P of the ASM1 model are lumped into X_I (inert particulate in ADM1). X_S and the organic particulate nitrogen are lumped into protein content. The remaining fraction of X_S is converted into carbohydrates and lipids with 30 and 70 % ratios respectively for primary sludge and 60 and 40 % respectively for waste activated sludge. Authors highlighted that these changes brought more realism and better agreement with literature values (in terms of biodegradability and methane production).

Techniques, using plant-wide modelling, lead to a simplification of the detailed characterization of the ADM1 model. However, the requirement of some hypotheses for the mapping and others limitations such as the modelling of all the process units of the selected configuration have to be considered. These aspects will be discussed in the following section.

I.2. Critical review

"The need of a simple, quick and accurate method to estimate biomethane yield and biodegradability is apparent" (Labatut *et al.*, 2011).

Table 5 reports a comparative analysis, including benefits and drawbacks, of the different characterization methodologies involved in the integrative tools previously presented.

- BMP: experimental test

According to Labatut *et al.* (2011), the BMP test is not suitable to predict the methane production kinetics because it is made under diluted conditions preventing inhibitions. The results obtained with this test should be limited to determine the maximum methane production potential of any given substrate and the feasibility of anaerobic treatment and not to estimate daily biomethane yield or large scale digesters performance. Moreover, Donoso *et al.* (2010) warn that using kinetics parameters obtained in batch tests could underestimate the methane production performance in continuous reactor modelling.

- BMP: theoretical determination

The experimental biogas yield obtained in an anaerobic reactor is systematically lower than the theoretical potential due to the following factors: (i) the fraction of substrate used for bacterial growth is not taken into account, (ii) at any given hydraulic retention time a fraction of the organic matter is lost in the effluent, (iii) the refractory organic matter (such as lignin) contained in the substrate and considered in the elemental formula is not degraded, (iv) a

fraction of the organic matter remains inaccessible due to binding within particles and limitation of other nutrients (Angelidaki *et al.*, 2004). Labatut *et al.* (2011) found the same overestimation of the BMP using the Buswell formula. When the equation was corrected with the introduction of the parameter related to the biodegradable fraction, the BMP prediction was more accurate. However, this method does not account for substrate biodegradability and assumes that all the electrons from the donors are available for the electron acceptors. This problem remains since the adequate use of this empirical formula requires the knowledge of the biodegradable fraction, which is obtained by the BMP test.

- Interpretation of the cumulated methane production and MPR curves

The determination of the bioaccessibility fraction and the non-biodegradable part of COD, to characterize input variables of the Mottet (2009) and the ADM1 model (Batstone *et al.*, 2002) respectively, are obtained with successive BMP tests. Nevertheless the problem of time consuming test remains and is even amplified. Moreover, depending on the S/X ratio used in the batch tests, profile of the cumulated curve will be more or less easy to explain. A too low S/X ratio would imply a less visible inflexion point in the curve, and therefore a more difficult two-substrate differentiation, compared to a higher ratio, where substrate would not be limiting.

The MPR curve identification method, as described by Yasui *et al.* (2008), is an interesting tool for the characterization of the bioaccessibility that solves the previously mentioned problems. Test was carried out in 4 days and methane production rate was measured on line. However, for each kind of sludge the model had to be modified based on identified variables and it required specific implementation.

The respirometric method used for the assessment of the ASM input variables requires high S/X ratios. Sperandio *et al.* (2000) developed a methodology with two ratios: a high ratio to assess the readily biodegradable fraction, and a low ratio to estimate both the slowly biodegradable and the hydrolysable fractions. Yasui *et al.* (2008) used low ratios from 0 (blanks) to 0.214 $gCOD.gCOD^{-1}$ introducing a risk of underestimation of the first readily hydrolysable fraction in the curve interpretation. However, higher ratios could generate inhibitions and impact the identification of fractions. Girault *et al.* (2012) estimated that S/X ratios did not impact significantly fractions estimation from MPR curve. But they found that errors are more important in the case of a low ratio ($0.37gCOD_{biodegradable}.gCOD_{biomass}^{-1}$) and recommended a ratio below 1.3 $COD_{biodegradable}.gCOD_{biomass}^{-1}$.

In this work, ratios were calculated using biodegradable COD of the substrate and the specific biomass expressed in COD from ADM1 simulation of the anaerobic digester providing the inoculum. Therefore, the first limitation of the technique used by Girault *et al.* (2012) is the ability to simulate the composition of the anaerobic sludge used as inoculum.

Moreover, compared to Yasui *et al.* (2006), Girault *et al.* (2012) present two main differences, concerning waste activated sludge:

1. the first bioaccessible fraction is composed of biodegradable "soluble fractions" of ADM1 (VFA, Saa, Ssu and Sfa) following a Monod model for Girault *et al.* (2012), whereas for Yasui *et al.* (2006), it is mainly composed of the slowly particulate COD from ASM1 Xs following a Contois model.
2. the less available fraction is composed of particulate biodegradable fraction of ADM1 for Girault *et al.* (2012), whereas this fraction is mainly composed of heterotrophic biomass X_H from ASM1 for Yasui *et al.* (2006).

Thus, this definition is not consistent with the results obtained by Yasui *et al.* (2006) considering waste activated sludge. The variables identified are mainly in the particulate phase in Yasui *et al.* (2006). In Buendia *et al.* (2008) work, anaerobic fractions and aerobic fractions were determined and compared using longer batch tests. Identification of a model for several substrates as waste sludge was then performed. They showed that about 74% of VS was composed of anaerobic readily biodegradable fraction, mainly particular fraction.

ADM1 defined Saa, Ssu and Sfa as soluble bioavailable organic matter, following a Monod equation, not appropriate for particulate matter (Vavilin *et al.*, 1996).

However, for both Yasui *et al.* (2006, 2008) and Girault *et al.* (2012), the particulate organic fraction X_I is obtained by mass balance between total COD and biodegradable COD obtained in batch tests run for between 4 and 10 days. This assumption could, depending on the substrate, lead to an overestimation of X_I fraction since 10 days might not sufficient to have a complete degradation of the total biodegradable COD. Another drawback is the use of the hydrolysis rate obtained in batch to simulate a continuous reactor. Other studies have shown erronous this assumption (Donoso *et al*., 2011).

- ASM-ADM mapping

The ASM-ADM mapping methodology requires the knowledge of the wastewater treatment plant including the ASM model outcomes (wastewater fractionation, aeration technologies,

retention times, etc…) as well as the settling and the thickening modelling. Usually, these data are difficult to obtain. Additionally, many assumptions and hypothesis are made in the mapping: assumptions on X_I, X_S and X_H mapping depending on the nature of the sludge. Nevertheless, static models could be used to determine the biodegradable and the recalcitrant fractions to be implemented in the dynamic models.

- Aerobic tests for BMP determination

Although the respirometric test is shorter in time than the BMP test, there are some limitations for using it to determine the BMP. First, only the readily available organic matter is considered (more complex organic matter, such as cellulose, is not taken into account) (Lesteur *et al.*, 2010). The second limitation is the assumption, also made in the ASM-ADM mapping, that the organic matter of sludge presents the same biodegradability under aerobic and anaerobic conditions. Buendia *et al.* (2008) used long anaerobic and aerobic batch test in order to estimate readily and slowly biodegradable fractions. The authors found that there was a good correlation between the anaerobic and the aerobic readily fraction, whereas the slower fraction was underestimated by the aerobic batch. The inert fraction is then overestimated by the mass balance.

Park *et al.* (2006; 2008) showed that cations bound to proteins from EPS in the floc in the secondary sludge play a significant role in the determination of the biodegradability. Proteins bounded to divalent cations show biodegradability only under aerobic conditions but are not bioaccessible under anaerobic conditions while iron associated proteins are more bioaccessible under AD. Higher volatile solids removal was observed under aerobic conditions (48%) compared to AD (39%).

- Biochemical fractionation: input for static and dynamic models

A faster approach could be the use of biochemical fractionation in order to feed both static models correlated with anaerobic biodegradability (Mottet, 2009) and ADM1-like models. The use of the organic matter characterisation of sludge based on proteins, lipids and carbohydrates concentrations in static models has been developed for secondary sludge for only a small range of biodegradability and based on a small numbers of observations (Mottet *et al.*, 2010). Appels *et al.* (2011) based also BMP prediction on the characterization of organic matter through 19 variables such as proteins, carbohydrates, VFA, heavy metals, etc…..

They showed that soluble COD does not influence the BMP of waste activated sludge and, for that reason, authors concluded that pre-treatments inducing solubilization are irrelevant.

Although it seems promising, the validation of these models is not robust enough. Neither complexity nor accessibility were indeed described. Applied on digested sludge, obviously with low biodegradability, the models cannot predict methane production.

Additionally, attention must be paid to the choice of the analytical method used (i.e. colorimetric ones) for biochemical characterization. Table 2 already reported the different methodologies used for biochemical characterization of sludge. The models based on biochemical characterisation include in their prediction the errors coming from the analytical methods. Underestimation of some sugars (galactose, mannose, xylose and arabinose) by the Anthrone method (Lesteur *et al.*, 2010) or overestimation and underestimation of proteins concentrations by the BCA and the Lowry methods respectively (Ras *et al.*, 2008) are some examples. Critical comparison of colorimetric methods is found in the literature (Raunjkaer *et al.*, 1994; Frølund *et al.*, 1996 and Ras *et al.*, 2008) leading to different conclusions depending on the considered substrate. However, colorimetric methods are practical, fast and give a good idea of protein or carbohydrates contents.

Also questioned, the N-content method was developed by Frølund *et al.* (1996) and used among others by Huete *et al.* (2006) and Girault *et al.* (2012) to determine protein concentration. The concentration of proteins is calculated from the measure of the N content and the assumption that proteins in sludge contain on average 16.5% of N. However, the variation of the amino-acids content in the sludge implies changes in the reference value (Raunjkaer *et al.*, 1994). Using a GC/MS, Huang *et al.* (2010) studied the detailed composition of amino-acids on a municipal wastewater. The ratio was calculated from the amino-acids composition and the nitrogen content. The theoretical ratio of 6.25 g proteins.g N^{-1}, corresponding to 16.5% of N in proteins, varied in some cases up to 7.5 g proteins.g N^{-1} (or 13% of N in proteins).

Table 5: Summary of the different methodologies used in integrative tools found in the litterature

Integrative tools	Characterization methods	Benefits	Drawbacks	References
Static model PLS, correlations, Stoechiometric reaction	Biochemical characterization Proteins, carbohydrates, lipids, COD/TOC, TOC soluble	Analytical simple and rapid methods	Model validation not yet achieved Based on one type of sludge (secondary) Care to be taken of the accuracy of methods used Not take into account complexity and accessibility	*Mottet et al. (2010)*
	CHNOS elemental analysis	Fastand practical method	Consideration of the whole organic matter degradation: the biodegradable fraction is not used Over-estimation of BMP tests	*Davidsson et al. (2009)* *Shanmugan et al. (2009)*
	Van Soest and fibers analysis	Faster and practical method Validation on several solids wastes Accessibility taking into account with growing extraction power	Not suitable for sewage sludge in terms of protocol (porosity) Model validation not conclusive	*Chandler et al. (1980)* *Gunsaeelaan et al. (2009)* *Mottet et al. (2010)*
	Aerobic respiration rate	Faster than a BMP test (4 days instead of 21-30 days) Promising on solid wastes	Only readily substrate taken into account No accessibility taken into account Assumption on the same biodegradability under aerobic and AD	*Cossu et al. (2008)* *Scaglia et al. (2010)*
	Initial rate technique	Used on sewage sludge Maximum production rate and affinity constant determined	Extrapolation in continuous digester underestimate methane production Not information on substrate bioaccessibility	*Donoso et al. (2010)*
	Elemental composition general analysis	Elemental mass balance achieved Maintain of the COD continuity	Assumptions on C and N inert content Assomptions on biochemical fractionation and non biodegradable variable (Huete et al. 2006)	*Kleerebezem et al. (2006)* *Zaher et al. (2009)* *Huete et al. (2006)*
Dynamic and kinetic models ADM1 or simplified models	ASM-ADM mapping	General analysis are sufficient	Knowledge of wastewater treatment plant Predictions sensitivity relative to the settler modelling Assumptions made on ASM (XI+XP) and ADM (XI) and on biochemical fractions	*Jones et al. (2008)* *Copp et al. (2003)* *Nopens et al. (2009)*
	MPR curve interpretation	Analytical time consuming lower (4-10 days) Methane response optimisation for fraction identification	Low ratios S/X used: underestimation possible of entire biodegradable fractions Batch test duration: 4-10 days, overestimation possible of non-biodegradable fraction Model (Yasui et al., 2008) has to be adapt for each type of substrate	*Yasui et al. (2008)* *Girault et al. (2012)*
	Biochemical characterization bioaccessibility compartiment	Bioaccessibility taken into account Biochmical fractions calculated from practical analysis	Necessity of BMP for X_I fraction Necessity of long batch test for fractions assessment	*Mottet et al. (2010)*

The main conclusion, withdrawn from the mentioned above, is the lack of a rapid and pertinent tool to determine, in municipal sludge, both anaerobic biodegradability and bioaccessibility for hydrolysis prediction and dynamic models implementation

Secondary sludge description based on the EPS two-layer model (Nielsen and Jahn, 1999 and Sheng et *al.*, 2010) would be used to model the EPS degradation as a function of location and accessibility in the sludge floc. Because of the anionic nature of the EPS and the cell surfaces, cations become an important structural component as binding agent (Park *et al.*, 2008). Several studies focusing on EPS characterization have shown that changes in the kind of captions on the influent wastewater led to changes in the characteristics of the activated sludge as well as in the effluent quality (Wang *et al.*, 2005 & 2007; Park *et al.,* 2007 & 2008).

It is also important to notice that the introduction of advanced characterization methodologies in environmental engineering could be the answer to the required description of the different compartments of the sludge.

I.3. Advanced techniques for organic matter characterization

Progress in analytical chemistry led to the development of new instruments and techniques to characterize organic matter. As previously mentioned, increasing the knowledge of substrate composition implies a new definition of model inputs and consequently an improvement of the model itself. An exhaustive list of the promising novel techniques used to characterize in depth the composition of organic matter and the location of EPS on sludge is presented in Table 6.

Scanning Electron Microscopy (SEM) and Transmission Electron Microscopy (TEM) aim at visualising surface features at a molecular scale (Beech *et al.*, 1997). They are mainly used on sludge and biofilm characterization to observe microbial aggregates, their shapes and structures, spatial distribution of some biochemical compounds, to measure floc volume or to identify the microbial population in a floc.

Gas Chromatography coupled with Mass Spectroscopy (GC/MS) (Réveillé *et al.,* 2003; Jarde *et al.,* 2003, Amir *et al.*, 2006, Huang et al., 2010), Pyrolysis GC/MS (Dignac *et al.,* 1998; Parnaudeau *et al.,* 2007) and High Performance Liquid Chromatography (HPLC) aim at measuring the detailed biochemical composition such as amino-acids for proteins, mono-saccharides for carbohydrates, humic acids extracted and long chain fatty acid for lipids.

X-ray Photoelectron Spectroscopy (XPS) provides a direct chemical analysis of the outermost cell surface.

Nuclear Magnetic Resonance spectroscopy (NMR) allows the observation of specific quantum mechanical magnetic properties of the atomic nucleus. The most commonly studied nuclei are ^{1}H (the most NMR-sensitive isotope after the radioactive ^{3}H) and ^{13}C. The peaks of the nuclear magnetic resonance spectra are used to identify the structure of many compounds.

Table 6: Different advanced methods to characterize the EPS of sludge

Type of method	Method	Purpose	*References*
Electronic microscopy	SEM TEM AFM (atomic force microscopy) CLSM (confocal laser-scanning microscopy)	Microbial aggregates observations: original shapes and EPS structures Spatial distribution of carbohydrates, proteins and nucleic acid Determination of the floc volume, heterogeneity factors and the population structure of activated sludge flocs.	*Beech et al., 1996* *Li and Logan, 2004* *Staudt et al., 2004* *Shmid et al., 2002 ; 2005*
Electrophoresis technique coupled to mass chromatographic	SDS-PAGE LS-MS/MS	Proteomics : isolation of protein, molecular weight characterization and hydrophobicity Coupled with LC-MS/MS, characterization of protein nature and source	*Park et al. (2008)*
Spectrometry, Mass chromatography	GC/MS Pyrolysis GC/MS THM-GC/MS HPLC	Qualitative and quantitative analyses of the mono-saccharides and amino acids of EPS after hydrolysis. Identification of molecular markers: fingerprint of sample	*Dignac et al., 1998* *Parnaudeau et al., 2007* *Réveillé et al. 2003* *Jarde et al. 2003* *Amir et al. 2006*
Spectroscopy	XPS FTIR NIRS 3D-EEM NMR	Study of the surface functional groups of EPS, the interactions between EPS and metals, and the roleof EPS in microbial adhesion to substrates. Elucidation of functional groups and element composition in EPS or microbial aggregates Fingerprint of organic matter	*Dufrene and Rouxhet, 1996* *Ortega-Morales et al., 2007* *Allen et al., 2004* *Lesteur et al., 2010* *Tartotvsky et al. 1996* *Reynolds et al. 1997* *Sheng et al., 2006* *Esparza-Soto and Westerhoff, 2001* *Chen et al. 2003* *Wang et al. 2009 and 2010* *He et al. 2011* *Wan et al. 2012* *Muller et al. 2011* *Manca et al., 1996; Lattner et al., 2003*

These techniques have not been applied to characterize the complexity and bioaccessibility of organic matter. GC/MS technique seems promising to analyze the biochemical composition of sludge (Huang *et al.*, 2010).

Park *et al.* (2008) applied for the first time proteomics for EPS characterization on waste activated sludge and digested sludge. The Sodium Dodecyl Sulfate Polyacrylamide Gel Electrophoresis (SDS-PAGE) revealed, using the cation-targeted extraction method, the impact of the biological treatment on the proteins based on their molecular weight and degree of hydrophobicity. Isolated proteins were characterized by Liquid Chromatography coupled with tandem Mass Spectroscopy (LC-MS/MS) and not biodegraded proteins could be identified. Extraction method followed by protein identification technique on extracted samples would be pertinent to determine anaerobic biodegradability and to characterize recalcitrant protein. However, both techniques are only adequate for protein characterization, which are the main components of biological sludge. However they are not adequate for primary sludge, which is as well composed of carbohydrates. Moreover, both techniques are highly specialized and require a complex sample preparation.

Spectral techniques, Near InfraRed Spectroscopy (NIRS) and 3 Dimension Excitation Emission Matrix (3D-EEM) fluorescence spectroscopy, are beginning to provide more information about the complexity of organic matter.

The following sections present a state of art of the use of both spectral techniques on sewage sludge characterization.

I.3.1. Near infrared reflectance spectroscopy (NIRS)

The NIRS is a spectroscopic method using the near-infrared region of the electromagnetic spectrum (from 800 to 2500 nm). It is a non-destructive analytical technique based on the principle of absorption of electromagnetic radiation by organic matter. The main advantage of NIRS is the higher capacity of penetration compare to mid infrared radiation. The NIRS is able to analyse all the organic matter without restrictions of accessibility (Lesteur *et al.*, 2011). It has been applied to a wide panel of molecules to classify or predict their characteristics. Sampling is not required since the measurement can be carried out directly on the substrate by reflectance using fiber probes.

The NIRS is used for BMP assessment following two different approaches, the first is to determine the composition of the input material using the NIRS and to calculate the BMP value by regression using static models. The second approach to predict the biodegradability is using directly the spectra through a dedicated calibration.

Lesteur *et al.* (2011) found a direct correlation between the NIRS analysis and the biodegradability provided by the BMP tests for municipal solid waste. The prediction presented a good accuracy (standard deviation of 28 $mLCH_4/gVS$). Doublet *et al.* (2011) applied the technique to a wide range of organic matter, such as agro-food industries effluents, sewage sludge, etc., and found good relative error (13%) when compared to the experimental error of the BMP test (20%).

NIRS presents a great potential for monitoring the AD process. Nielsen *et al.* (2008) evaluated the use of NIRS technology on-line (Transflexive Embedded Near Infra-Red Sensor or TENIRS) to follow-up a thermophilic digester treating manure and organic food industrial waste. A good correlation was obtained between on-line NIRS measurement of glycerol and VFA content in the anaerobic digester. Zhang *et al.* (2009) succeeded in building PLS models between NIRS and ethanol, acetate, propionate and butyrate concentrations in a H_2 producing reactor fed by synthetic wastewater. The prediction ranges were 90 to 580 mg/L, 491 to 1274 mg/L, 321 to 2020 mg/L and 122 to 2230 mg/L respectively. Lignin concentration has also been correlated to NIRS measurement by Brinkmann *et al.* (2002).

The technique is really promising to determine the biodegradability of a substrate. However, NIRS is not enough sensitive for structural interpretation of complex molecules and bioaccessibility aspect is still missing. NIRS measurement for biodegradability assessment is still performed on dried-frozen samples not considering accessibility of sludge.

I.3.2. 3D Excitation Emission fluorescence spectroscopy

Fluorescence is the emission of photons by aromatic or polyaromatic molecules that have been excited by photons in the visible and the ultraviolet range. It is the energy lost by the molecules to come back to their elementary state, following the Stockes law. Fluorescence allows the characterization of the analysed organic material on both liquid and solid phase. The technique can be either used in 2 dimensions, with one excitation wavelength, or in 3 dimensions where several excitation wavelengths are scanned and the fluorescence intensity is represented in a topographic map as a function of the emission wavelength (Figure 4). Identification of molecular-like groups is possible based on the excitation and emission wavelength coordinates. Sludge contain aromatic structures and unsaturated fatty chains that present fluorescence properties. Therefore, 3D-EEM Fluorescence Spectroscopy might be a useful tool to study physicochemical properties of the EPS of the sludge.

It is a selective and sensitive method since fluorescence characteristics are related to the structure and the functional groups in the molecules (Sheng *et al.*, 2010).

The main components of solid waste and sewage sludge are naturally fluorescent:

- Proteins and melanoïdin are present mainly on secondary and digested sludge
- Chlorophyll, lignin-like, lignocellulose-like, fulvic acid and humic acid present on primary sludge,
- Green waste and organic fraction of municipal solid waste.

Some studies have revealed the fluorescence spectroscopy potential to link the complexity of a substrate with its biodegradability.
Tartakovsky *et al.* (1996) proposed correlations between multiple excitation emission fluorescence analysis and process parameters such as COD or biomass activity on wastewater treatment (aerobic and anoxic). Promising results were obtained when the correlations were tested on a synthetic medium. Authors proposed the use of the technology off-line (detailed study of the degradation rates) and on-line (sensors) combined with the appropriate numerical treatment and the identification of the excitation/emission pairs. Reynolds *et al.* (1997) found, in wastewater, a linear relationship between the 5-day biological oxygen demand and the corresponding fluorescence intensities at 340nm using an excitation wavelength of 280 nm (protein-like molecules).

In the last decade, the 3D technique has mainly been used for the qualitative characterization of EPS. Esparza-Soto *et al.* (2001) used 3D-EEM fluorescence spectroscopy to study the fluorescence spectra of EPS fractions (after extractions) to identify the characteristic fluorophore signature of an EPS tracer in treated wastewater. Similarly, Sheng *et al.* (2006) worked on EPS characterization in aerobic and anaerobic sludge using a fluorescence tool. Sheng *et al.* (2006) found similar peaks than Esparza-Soto (2001), Wang *et al.* (2009) and Li *et al.* (2008) on sequential batch reactor (SBR) sludge. The differences in the chemical structure of the EPS were defined by the peaks locations, the fluorescence intensities and the ratios between the intensities of the fluorescence peaks. Wang *et al.* (2010) managed a membrane reactor varying the solids retention time in order to link the molecular nature of the dissolved organic matter and bound EPS with membrane fouling.

Fluorescence spectroscopy was used to show that longer solid retention times implied higher complexity of both dissolved organic matter and bound EPS.

A ratio between the fluorescence intensity of the humic acid peak and the proteins peak was defined. This ratio increased with solid retention time. It increased, as well, between the extracted fractions (dissolved organic matter after centrifugation and bound EPS after extraction on pellet). Results were encouraging to establish the link between complexity, sludge stabilisation degree and accessibility (i.e.: the complexity of the EPS found in dissolved matter is different compared to the bound EPS). The inconvenient of using fluorescence intensities for the interpretation is not considering completely the massif of fluorescence: low intensity fluorescence could be coupled with the large volume of a peak. Chen *et al.* (2003) used a new quantitative analytical approach, the fluorescence regional integration (FRI) on dissolved organic matter from water and soil. Based on the literature, the 3D spectrum is divided into five molecule-like fluorescence regions using horizontal and vertical lines. He *et al.* (2011) applied this technique on leachates to investigate the characteristics of dissolved organic matter at different landfill ages and to evaluate the transformation during landfilling. Based on the FRI approach (Chen *et al.*, 2003), regions corresponding to each molecular-like fluorescence (Figure 4) were defined.

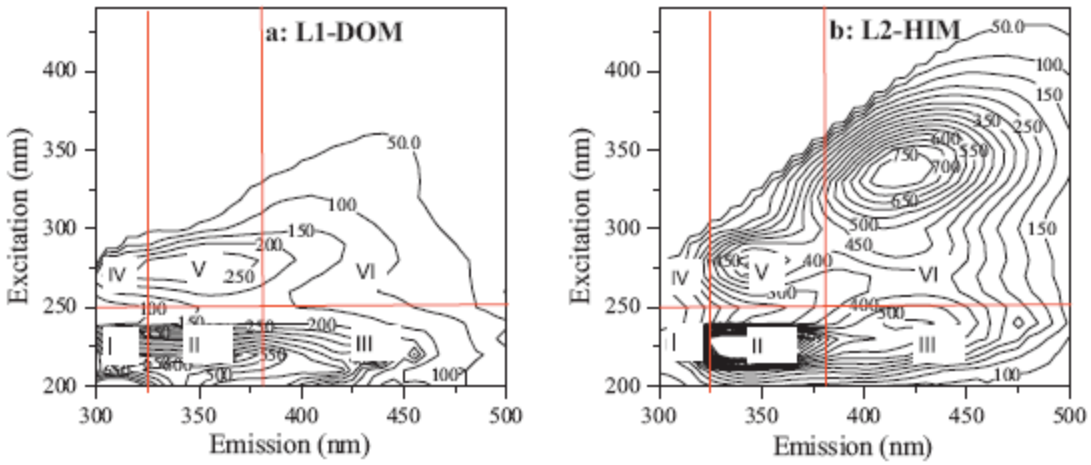

Figure 4: FRI EEM regions obtained using consistent excitation and emission wavelength boundaries (He *et al.*, 2011 based on Chen *et al.*, 2003)

Regions:

- *I and II: simple aromatic proteins as tyrosine-like*
- *III: fulvic-acid-like*
- *IV and V: soluble microbial products-like, correlated with tryptophan-like*
- *VI: humic-acid-like substance*

Samples:

- *L1-DOM: landfill leachates (age 3 years) sample 1, dissolved organic matter*
- *L2-HIM: sample 2; hydrophilic matter fraction from landfill leachates (age: 3-10 years)*

To make possible quantification, regions volume was calculated. The nature and the type of molecules and the complexity of the substrate are obtained using this approach. Highly complex dissolved organic matter was divided into several fractions depending on their hydrophobic and their hydrophilic character. The main result obtained was that the older is the leachate, the most predominant fractions in the spectra were the humic acid-like and the fulvic-like. Both fractions also increased with the hydrophobicity of the organic fraction. On the contrary, the hydrophilic organic matter and protein-like materials decreased with time of landfilling. The ratio between the percentage of the humic and fulvic-like fluorescence regions (III, VI) and the percentage of the protein-like materials (I, II, IV and V) was used to predict the adequate wastewater treatment. A low ratio indicates that biological treatment is more appropriate (protein-like matter more readily removed) and a high ratio suggests the use of a physicochemical treatment such as reverse osmosis.

Concerning AD, Wan *et al.* (2012) showed the potential of the fluorescence spectroscopy to be linked with anaerobic biodegradation of cattle and duck manure. They compared digestion and co-digestion of both substrates. Using 3D-EEM analysis of dissolved organic matter with digestion time, the authors identified molecules remaining after digestion. Based on the different fluorescence intensity peak ratios (protein-like on fulvic acid-like, protein-like on humic acid-like and fulvic acid-like on humic acid-like), they showed that fulvic acid-like and humic acid-like remained stable during both separated and co-digestion whereas the aromatic proteins tyrosine-like decreased, suggesting hydrolysis of these molecules into non-fluorescent structures. 3D-EEM spectroscopy is thus a proven tool to quantify both substrate degradation degree and organic matter transformation. The study of the complexity of fractionated organic matter could give more precise information on the location of molecule-like materials in the substrate.

Muller *et al.* (2011) characterized solid waste and sewage sludge using both the 3D solid phase fluorescence (SPF) spectroscopy and the 2D laser induced fluorescence (LIF). The SPF showed good results on the characterisation of several organic matter sources but reached its limits when sample was dark-coloured. The LIF was preferred for the characterization of sewage sludge using 2 excitation wavelengths. However further research is required in order to make the appropriate selection of the excitation wavelengths. To overcome 3D-SPF limitations, Muller *et al. (in press*) recently proposed an alternative for sludge characterization: a sequential extraction simulating the bioavailability of sludge organic matter according to its chemical accessibility.

These extractions were then coupled with 3D-EEM fluorescence spectroscopy in liquid phase for complexity assessment of the extracts. Based on the literature, they built a protocol to extract the organic matter from three secondary sludge. Four extractions were performed dissolved organic matter, EPS (soluble and bound) and humic substances. Spectra from 3D-EEM fluorescence spectroscopy were treated in order to calculate the volume of each zone, based on the FRI approach (Chen *et al.,* 2003). The sequential extractions results showed that each fraction had a well-defined and different availability. Concerning fluorescence footprint, there was also a hierarchy of complexity with the decreasing chemical accessibility. Dissolved organic matter contained easily bioavailable compartments mainly composed of protein-like compounds. Soluble EPS contained similar protein-like as dissolved organic matter, but it also included glycated protein or melanoidins-like compounds (excitation wavelength 340nm and emission wavelength 420 nm). Bound EPS seemed alike soluble EPS but with a higher percentage of complexity in fluorescence (40% instead of 20-30% previously) and the humic substance fraction was composed mainly of complex structures (40 to 50% of total fluorescence). Non-extractible fraction was also analysed in the SPF, the only visible peak was linked with lignocellulosic-like compounds, very slowly biodegradable in AD. Results from this study showed the high potential of fluorescence spectroscopy to predict complexity linked with biodegradability and the promising potential of extraction protocol to describe the accessibility of sludge.

As described 3D-EEM fluorescence spectroscopy has been used for qualitative characterization of EPS extracted from sludge. Complexity and maturity of organic matter can also be qualitatively assessed. Coupled with sequential sludge extractions, the technique also reveals information on bioaccessibility (Wang *et al.*, 2010 and He *et al.*, 2011, Muller *et al., in press*). Further research is thus needed concerning the biodegradability prediction with fluorescence spectroscopy (from a quantitative point of view) and bioaccessibility prediction with organic matter extractions. This is among the key objectives of the present thesis.

I.4. Conclusions and perspectives

Due to the increasing interest on AD, researchers have tried to increase the knowledge on the biological process by building/using models proven to be useful tools. The characterization based models, called in this paper integrative tools, have evolved rapidly in the last decades.

After 2002, with the creation of ADM1, they became more detailed and more complex studying different pathways occurring in AD.

Consequently, detailed substrate characterization became necessary since it is the key input data for precise simulations and predictions. Several characterisation methodologies are found in the literature. Initially biodegradability assessment was done using the BMP test with a major drawback due to time consumption. Static models have been proposed as an alternative solution to predict biodegradability with several kind of organic matter characterization as explicative variables.

Another evolution of the models, due to the increasing complexity of the substrates, was to consider hydrolysis as the limiting step introducing the notion of bioaccessibility. However, static model were not able to predict simultaneously the bioaccessibility and the biodegradability. The new variables that appeared by taking into account the bioaccessibility of the substrate were used to correct the kinetic equations. A better knowledge of the sludge composition indeed leads to more realistic although more complex models.

Advanced analytical techniques could provide a higher degree of information on the composition of any given substrate. Promising new tools can be used for direct measurement, such as NIRS, 3D-EEM SPF and LIF probes. Further investigations need to be performed in order to find a relevant and rapid tool for organic matter characterization of sludge in order to obtain reliable parameters for the biological processes models.

I.5. Problematic definition and scientific strategy

AD is becoming increasingly attractive to treat waste, such as municipal sludge. In order to control and optimize this process, biological processes modelling of anaerobic digestion has been used. From the first stoichiometric model, the research on AD modelling has significantly evolved. The need of a more accurate prediction tool of the performances, such as methane production and organic matter biodegradation yields, has driven the complexity of models. AD is indeed a complex process that cannot be oversimplified in “basic” models. In parallel, considered substrates had also evolved in complexity, from industrial wastewater to solid waste and municipal sludge. Models had also evolved by considering a more detailed OM characterization, such as using the biochemical families: protein, lipids and carbohydrates. Complexity consideration led to take into account the accessibility of substrates. Solid waste and sludge are mainly composed of particulate matter and the limiting step of the AD has become the hydrolysis, whereas the first models considered acetogenesis or the methanogenesis as limiting steps.

The first principal objective of AD modelling is the prediction of the substrate biodegradability. Considering complex substrates, another principal objective is nowadays considered: the assessment of the bioaccessibility. In the literature, several methodologies have been set up to relate biodegradability with organic matter characterization. However, only few references include either bioaccessibility assessment or both biodegradability and bioaccessibility assessments.

This review highlighted the evolution of the models, static or dynamic, and discussed about the experimental characterization methodologies found to feed these models. Due to the lack of a rapid and relevant characterization tools, an overview of advanced techniques applied in environmental sciences was conducted and some techniques like the fluorescence spectroscopy and sequential extractions of organic matter are today very promising.

On one hand, it appeared that biodegradability could be correlated with complexity by using the 3D spectra fluorescence spectroscopy results (Reynolds *et al.* (1997), Wan *et al.* (2012) and Muller *et al.* (In press). On the other hand, based on Muller *et al.* (In press), the alternative sludge characterization by sequential extractions, simulating chemical accessibility of the organic matter contained in the sludge, could be correlated with bioaccessibility. The key challenge is to find appropriate indicators from fluorescence spectra information and sequential extraction in order to predict accurately both biodegradability and bioaccessibility. The chemical accessibility could be linked to biological accessibility, but this hypothesis has to be proven. Fluorescence spectroscopy provides complexity cartography of a substrate. The main components contained in sludge (protein and lignocellulose-like compounds) are naturally fluorescent but others are not (monosaccharide, lipid and VFA). Complexity from fluorescence spectra and biodegradability seems to be linked, but is it sufficient to predict anaerobic biodegradability? It has to be studied.

Based on these observations, our main objective aims at identifying tools and methodologies to feed innovative and complex models for better representation and simulation of anaerobic digestion of municipal sludge. The methodologies are based on (1) the ability of fluorescence spectroscopy to provide complexity information and (2) on the organic matter fractionation by chemical sequential extractions simulating accessibility to give bioaccessibility information. Once the characterization methodology will be built up, a global validation with experimental results and a modelling exercise on an anaerobic digestion pilot plant will be performed. Figure 5 gives an overview of the framework of the study.

To conclude, questions to be answered in the following sections are:

- Bioaccessibility: is the chemical accessibility provided by sequential extractions correlated with biological accessibility or bioaccessibility?
- Determination of biodegradability and bioaccessibility indicators: are the information provided by fluorescence spectra coupled with the accessibility aspect provided by sequential extractions relevant to predict both anaerobic biodegradability and bioaccessibility?
- Validation of the overall methodology: is the characterization methodology able to improve available anaerobic digestion models?

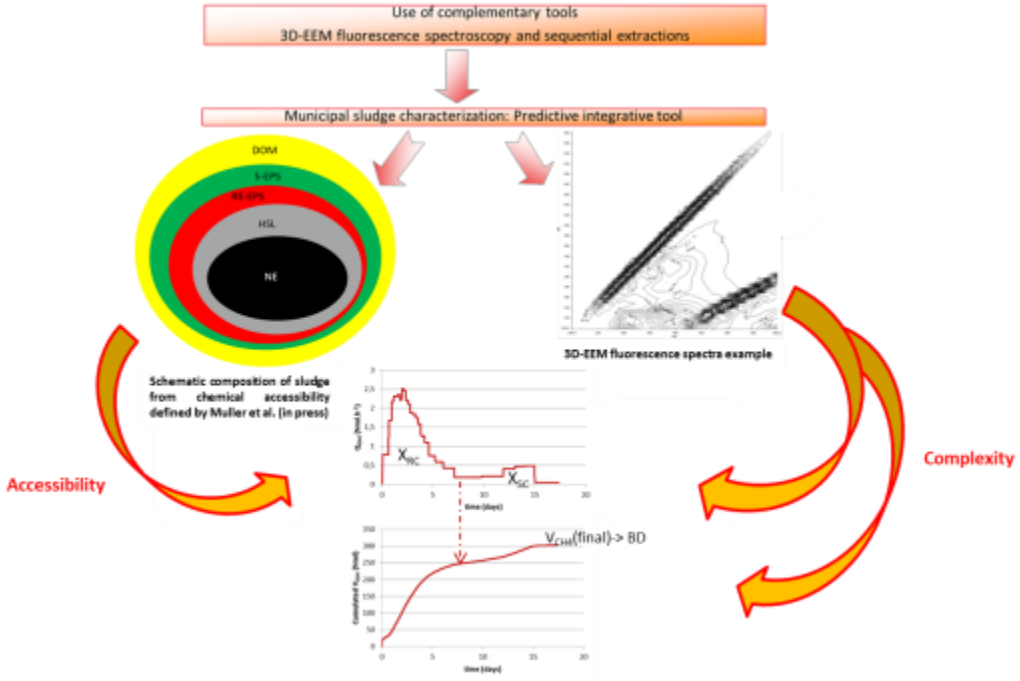

Figure 5 : Overview of the study framework

II. MATERIAL AND METHODS

II.1. Sludge characterization: analytical methods 64
II.2. Biodegradability and bioaccessibility : definition of quantitative variables 68
II.2.1. Biochemical Methane Potential tests 69
II.2.2. Interpretation and calculation of BMP 70
II.2.3. Interpretation and calculation of X_{RC}/X_{SC} 70
II.3. Sludge samples 71
II.4. Chemical sequential extraction protocol 74
II.4.1. Definitions 74
II.4.2. Sequential extraction Protocol 75
II.5. 3D-EEM fluorescence spectroscopy 80
II.5.1. Fluorescence Spectrometer 80
II.5.2. Fluorescence Spectra 82
II.5.3. Dilution and linearity for quantification 83
II.5.4. Spectra interpretation 84
II.6. Anaerobic digestion laboratory scale reactors 86
II.7. Mathematical modeling : modified ADM1 and statistical methods 89
II.7.1. Modified ADM1 89
II.7.2. Input variables modifications 89
II.7.3. Kinetic modifications 90
II.7.4. Liquid/Gas transfer modification 92
II.7.5. Modified ADM1 input implementation 93
II.8. Statistical tools 94
II.8.1. Partial Least Square Regression 94
II.8.2. Others statistical tests 97
II.9. Conclusion 97

Note for the reader:

Chapter II aims at presenting the methodologies carried out during the thesis for sludge organic matter characterization and model validation. Basic total characterization methods together with innovative approaches such as sequential extractions or 3D fluorescence spectroscopy are also described. A reader familiar with AD process could skip the 3 first sections but should read the section II.4 for a better understanding of the next chapters. Moreover, the modified model and the quantification of the input variables are also described and Chapter V requires the reading of this part to understand the modeling methodology.

In order to investigate the issues highlighted in the previous chapter from the literature review, several methodologies have been used. First, analytical methods are described starting from the classical ones and then focusing on the more specific methods.

Sludge samples and laboratory reactors used for experimental assays are also introduced. Finally, the modified ADM1 model used for the validation and the statistical methods are outlined such as Partial Least Square (PLS) regression method.

II.1.Sludge characterization: analytical methods

The procedure followed for a complete sludge characterization begins by a homogenization and 2 mm grinding using an Ultrathurax at 12000rpm during 8 min. The process is conducted on ice to prevent heating. Mass dilution is then performed in order to be in the adequate range of concentration of the performed analyses. Measurements are usually performed in duplicate.

II.1.1. Total organic matter analysis

II.1.1.1. Total solids and volatile solids

Different solid fractions are measured by weighing and drying the sludge according to the normalized method 2540G (APHA, 1999). Total solids (TS) represent the residual matter obtained after drying at 105°C (equation 3.1). Mineral matter is the remained mass after organic matter volatilization at 550°C. Volatile solids (VS) content is calculated as the difference between TS and mineral matter (equation 3.2). The average error of this measure ranges from 1 to 5%.

$$\boldsymbol{TS(g.L^{-1}) = \frac{mass_{105°C}}{mass_{raw\ sludge}} \times 1000} \qquad \textbf{Equation 3.1}$$

$$\boldsymbol{VS(g.L^{-1}) = \frac{mass_{105°C} - mass_{550°C}}{mass_{raw\ sludge}} \times 1000} \qquad \textbf{Equation 3.2}$$

II.1.1.2. Chemical Oxygen Demand

COD represents the oxidable organic matter. The oxidation reaction is performed by potassium dichromate ($K_2Cr_2O_7$) under acidic conditions at high temperature (170°C). Soluble and total COD was measured using a micro-method HACH LANGE kits (measurement range: 0 to 2000 $mgO_2.L^{-1}$) with an optical density measurement (HACH

LANGE DR5000 spectrophotometer) following the Beer-Lambert law. Measurement error is between 5 and 15%.

II.1.1.3. Total carbon analysis

Total Carbon (TC), Total Organic Carbon (TOC) and Inorganic Carbon (IC) are measured on soluble and total fraction with a Shimadzu® analyser including a Carbone TOC-VCSN module.

TC is dosed by infrared measurement of CO_2 emission after catalytic oxidation at 720°C. IC also dosed by infrared measurement of CO2 emission after acidification with hydrochloric acid (HCl, 2N). TOC is finally determined by subtracting the IC to the TC.

The concentration ranges are 0-250, 0-100 and 0-250 $mgC.L^{-1}$ for TC, IC and TOC respectively. Measurement error is about 5 to 10%.

II.1.1.4. Nitrogen analysis

Total Nitrogen (TN) measurement, on soluble and total fractions, is performed with a Shimadzu® analyser by chimioluminescence using a TOC-VCSN module. N is converted to NO by catalytic oxidation at 720°C. The ozone generated in the TN unit is used to convert NO into NO_2 (instable state). NO decomposition emits photons detected by a photoluminescence cell. Concentration range from 0 to 200 $mgN.L^{-1}$. Measurement error is between 5 and 10%.

Ammonium concentrations (NH_4^+) are measured with a HACH LANGE kit. Previously, this method was validated with the standard method using a Buchi® AutoKjehdahl Unit K-370. Measurement error is about 5 to 10%.

II.1.2. Biochemical characterization

Biochemical characterization of organic matter is becoming of key importance in wastewater treatment. Standardized methods exist for some organic molecules, such as volatile fatty acids or lipids. However there are no standard methods to measure proteins and carbohydrates content, which are the main components of sewage sludge.

- Lipids

Lipids are measured on freeze-dried samples by gravimetric method (APHA, 1995) using the SoxtecTM, 2050, FOSS with hexane (98%) extraction at 180°C.

Lipid content is assimilated to Hexane Extractable Material (HEM) and it is calculated using Equation 3.3. As the sample has been freeze-dried, solids content is expressed as TS ($g.L^{-1}$) (equation 3.4).

$$\%\mathbf{HEM} = \frac{p_3 - p_2}{p_1} \times 100 \qquad \textbf{Equation 3.3}$$

$$\mathbf{HEM} = \%\mathbf{HEM} \times \mathbf{TS_{sample}} \qquad \textbf{Equation 3.4}$$

where: p_1 is the sample mass (g),
p_2 is the empty beaker mass,
and p_3 is the final beaker mass.

- Volatile fatty acids

Volatile fatty acids (VFA), including acetate, propionate, isobutyrate, butyrate, isovalerate, and valerate, are determined on the soluble fraction using a gas chromatograph apparatus (Agilent Technologies 7890A).

Injector is heated at 250°C. Sample is injected in an Agilent capillary column (30meters, internal diameter 0.53mm). Oven temperature ramp is from 80°C to 240°C at 2.3mL.min^{-1} H_2 gas carrier flow. Flame ionization detector is heated at 250°C. H_2 and air flows are 30ml.min^{-1} and 300 ml.min^{-1} respectively. Calibration curves are set for each compound from 0.01 to 2.0 $g.L^{-1}$.

- Colorimetric methods for protein and carbohydrate contents measurement

A comparison study has been conducted to investigate the efficiency of several colorimetric methods used to determine proteins and carbohydrate contents in sludge matrices. Annex 1 presents the paper submitted to Water Research (Jimenez *et al.*, in press). The different methods were evaluated based on statistical criteria such as sensitivity, linearity, accuracy, rightness, and specificity using standard molecules such as Bovine Serum Albumin (BSA), glucose, cellulose and a certified reference product. Sewage sludge samples obtained from different locations in a wastewater treatment plant have been tested. The Lowry and the Dubois methods have been shown to be the best compromise for the considered criteria, respectively for protein and carbohydrates contents.

Protein content: the chosen colorimetric method is the Lowry method (Lowry *et al.*, 1951). The Lowry is described with a linearity range from 0 to 100 $mg_{BSA}.L^{-1}$.

The standard calibration used was the BSA set from Thermo Scientific Sigma P0914, made from 0 to 100 $mg_{BSA}.L^{-1}$.

A sample volume of 0.5 mL is introduced in a hemolysis tube with 2.5 mL of a mix solution (50mL of sodium bicarbonate $NaCO_3$ at 2% with NaOH (0,1N), 1mL of copper sulfate $CuSO_4$ solution at 1% and sodium and potassium tartrate $C_4H_4KNaO_6$) and let in ambient temperature during 10 minutes. Then 0.25 mL of Folin solution (commercial solution) is added.

After vortex homogenisation, reaction tubes are conserved at ambient temperature, in the dark during 30 minutes. In alkaline condition, proteins react with Cu^{2+} ions. A complexation between Cu^{2+} and nitrogen atoms contained in peptidic liaisons is formed.

Oxidation of amino acids and reduction of Cu^{2+} into Cu^{+} occur. Ions reduce the ions contained in Folin reactant, providing a blue coloration proportional to the protein concentration. The reaction time is about 2h in the dark. Absorbance of samples is then measured at 750nm with the HACH LANGE DR5000 spectrophotometer. Results are expressed in BSA equivalent ($mg_{BSA}.L^{-1}$). Measurement error is about 3% for soluble phase and about 6% for total phase (between 1 and 18%).

Carbohydrate content: the colorimetric method chosen is the Dubois method (Dubois *et al.*, 1956). The method is described with a linearity range from 0 to 100 $mg_{Glu}.L^{-1}$. The standard calibration was made with glucose (Merck 1.08337.1000). Colorimetric methods for carbohydrates assessment are based on the formation of strong acid hydrolysis product formation. Furfurals derived are then condensed with phenol to provide chromophores. During the Dubois method, carbohydrates are hydrolysed by sulphuric acid and monosaccharides are dehydrated by phenol. Orange coloration absorbing at 490 nm is developed with addition of phenol. Coloration intensity is proportional to the glucose equivalent concentration.

A sample volume of 1mL is added in a hemolysis tube with 1 mL of phenol at 5%. After vortex homogenisation, 5 mL of sulphuric acid at 98% is added. Two coloured phases appear and reaction tubes are let at ambient temperature during 10 minutes. Then, the tubes are closed and vortex homogenised before 30 minutes at ambient temperature rest. Absorbance of samples is then measured at 490 nm with the HACH LANGE DR5000 spectrophotometer. Results are expressed in glucose equivalent ($mg_{Glu}.L^{-1}$). Measurement error is about 4% for soluble phase and about 9% for total phase (between 2 and 23%).

- Biochemical expression results

Carbohydrates, proteins, HEM and VFA concentrations are then converted into COD equivalent in order to make mass balance and to feed ADM1 model (table 7).
From Annex 1, results show that, in average, the measured volatile fatty acids, lipids, proteins and carbohydrates contents represented 80 ± 7% (% volatile solids) of the organic matter from several sludge natures. Proteins and carbohydrates represented on average 69 ± 3%.

Table 7 : Conversion ratios for COD equivalent concentration assessment

Compounds	Ratio $g_{COD}.g_{compound}^{-1}$ (Batstone *et al.*, 2002)
Carbohydrates (g Glu.L^{-1})	1.0667
Proteins (g BSA.L^{-1})	1.5304
Lipids (gHEM.L^{-1})	2.8609
Acetate (g.L^{-1})	1.0667
Propionate (g.L^{-1})	1.5135
Butyrate and iso-butyrate (g.L^{-1})	1.8182
Valerate and iso-valerate (g.L^{-1})	2.0392

II.2.Biodegradability and bioaccessibility : definition of quantitative variables

The main objective of this study is to predict both biodegradability and bioaccessibility of a municipal sludge in order to quantify input variables of dynamic models.

Thus, indicators have to be defined. Previously mentioned in the literature review chapter, biodegradability (BD) is experimentally determined by the BMP test. Thanks to the biodegradability assessment, inert content in sludge could be calculated as equation 3.5.

$$\boldsymbol{X_I(\%COD) = 100\% - BD(\%)} \qquad \textbf{Equation 3.5}$$

Concerning bioaccessibility, definition of such a variable is not so easy. However, in the modified ADM1 model from Mottet (2009) particulate COD is composed of the variable X_{RC} (particulate readily hydrolysable COD fraction) and X_{SC} (particulate slowly hydrolysable COD fraction). This model will be used in this study for validation (described later).

Thus, bioaccessibility indicator chosen is based on X_{RC} variable translating the ability of a compound to be easily or not biodegraded.

Following sections present the experimental assessment of BD and X_{RC}, based on BMP tests.

II.2.1. Biochemical Methane Potential tests

Biochemical Methane Potential measurement tests are performed in serum bottles in the Automated Methane Potential Test System (AMTPS) from BIOPROCESS CONTROL (figure 6 a). The main advantage of this technique is the automatized continuous measurement of methane with dedicated gas counter for each serum bottle.

Glass bottles are not under pressure. Biogas produced goes to a soda bottle (NaOH, 4N) in order to trap the carbon dioxide. Then, biogas (methane) is conduced to a gas counter based on liquid displacement measurement. AMTPS software saves each impulsion and cumulates methane productions as methane production rate are drawn. A first blank test with inoculum and distilled water is performed in order to assess the inoculum remaining activity and a second blank test is performed with an addition of easily biodegradable substrate (glucose) in order to validate the inoculum viability.

(a)  (b) 

Figure 6 : (a) AMTPS from BIOPROCESS CONTROL and (b) glass bottle with stirring device

Concerning the glass bottle, anaerobic degradation of the sample occurs in batch mesophilic (35-37°C) condition thanks to a thermo regulated water bath. Reaction volume of 0.5 L is used with not limiting nutriment, in order to prevent deficiencies and with a favorable S/X ratio to optimize the degradation (usually $0.5 gCOD.gVS^{-1}$). Bottle is in contact with atmospheric pressure, gaseous volume of bottle is thus minimized as BMP calculation errors. Diluted conditions are applied in order to prevent any inhibitions: VS concentration in the serum bottle is about 3 to 5 $g.L^{-1}$. A stirring system with a rotating shaft is used (figure 6b).

Inoculum used is an adapted one from all the wastewater treatment plants which provide sludge samples for characterization in this study. This aspect is important in order to have an acclimated biomass and a more accuracy on kinetics results.

II.2.2. Interpretation and calculation of BMP

When cumulated curve of methane reached an asymptote (25-40 days), the test is stopped. Composition of biogas in the headspace of the glass bottle is then performed thanks to a portative gas analyzer GA-2000 PLUS from GEOTECH.

COD, VFA and pH analysis are performed. Cumulated volume of methane V_{CH4} is then calculated and normalized in standards conditions of temperature and pressure (equation 3.6). Then, BMP is calculated by normalizing V_{CH4} with the COD mass of the substrate introduced COD_0 (equation 3.7). From the Buswell formula and the organic matter oxidation reaction, the theoretical BMP is 350 $NmL_{CH4}.COD^{-1}$ (Angelidaki *et al.*, 2004). Biodegradability BD (equation 3.9) can be calculated from BMP (equation 3.8).

$$\boldsymbol{V_{CH4}(Nml_{CH4}) = V_h \times (y_{fin} - y_0) \times \frac{273.15}{273.15+T} + \sum_{i=0}^{fin} V_i} \qquad \textbf{Equation 3.7}$$

where

V_h (mL) is the gaseous volume in glass bottle

y_i (%) is the methane proportion in gaseous phase of glass bottle at time i

V_i (mL_{CH4})is the volume of methane produced at time i

$$\boldsymbol{BMP\left(Nml_{CH4}.g_{COD0}^{-1}\right) = \frac{V_{CH4}}{COD_0}} \qquad \textbf{Equation 3.8}$$

$$\boldsymbol{BD(\%) = \frac{BMP}{350} \times 100} \qquad \textbf{Equation 3.9}$$

II.2.3. Interpretation and calculation of X_{RC}/X_{SC}

From the methane production rate curve, X_{RC} and X_{SC} can be visualized (figure 7a). Then, reporting the time when X_{RC} is completely degraded to the cumulated production curve (figure 7b), the ratio cumulated $V_{CH4}(X_{RC})$ on V_{CH4}(final) correspond to $\%X_{RC}$ of biodegradable COD. To normalize this value, this ratio is multiplied by BD (equation 3.10). The remaining biodegradable COD composed of slowly biodegradable organic matter through the variable X_{SC} is then deduced from BD and X_{RC} (equation 3.11).

$$X_{RC}(\%COD) = \frac{V_{CH4}(X_{RC})}{V_{CH4}(final)} \times BD(\%)$$ **Equation 3.10**

$$X_{SC}(\%COD) = BD(\%) - X_{RC}(\%COD)$$ **Equation 3.11**

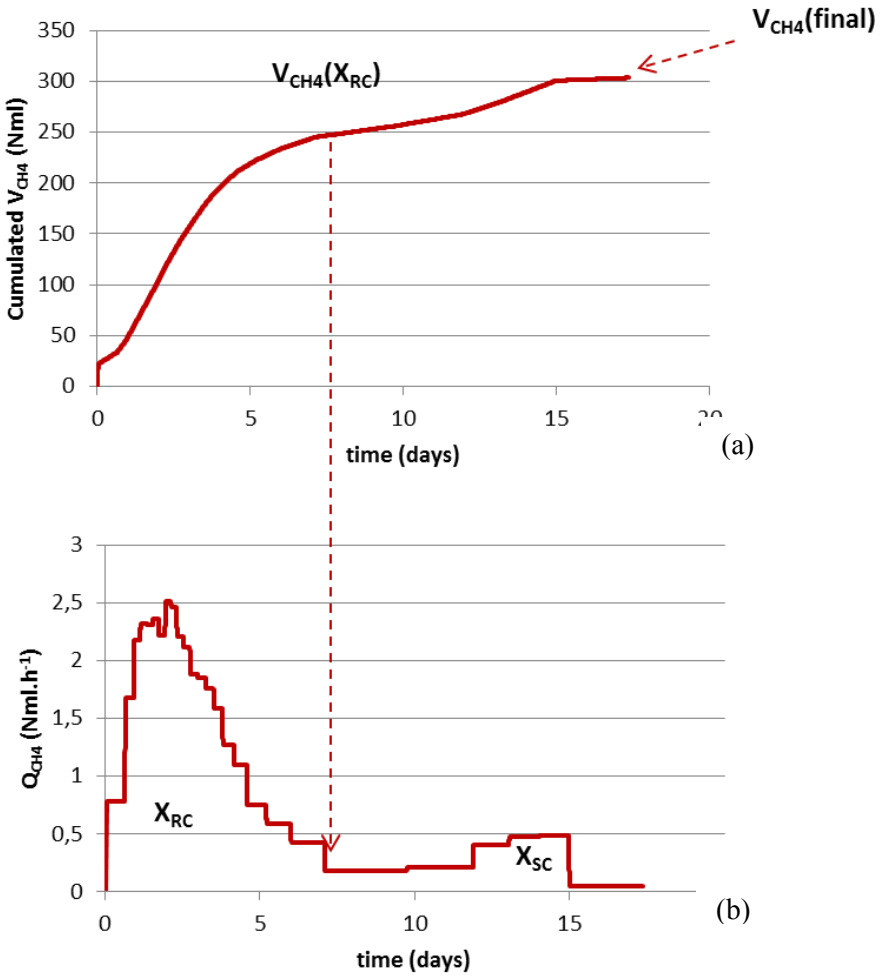

Figure 7 : Cumulated methane production curve (a) and methane production rate curve (b) for the same sludge degradation with a ratio S/X = 1gCOD.gVS^{-1}

II.3.Sludge samples

Fifty two municipal sludge samples have been recovered through a large measurement campaign in wastewater treatment plants around Europe. Based on their nature, municipals sludge samples can be divided in:

- 6 primary sludge (table 8),
- 23 secondary sludge,
- 15 anaerobic sludge (table 10)
- 8 thermally treated secondary sludge (table 11).

Nomenclature has been defined as follows:

- "S" for sludge and "R" for refusal (from screeners for example)
- "I", "II", "D" or TTtemperature for primary, secondary, digested and thermally treated sludge respectively
- Alphabetical letter from the wastewater treatment plant name

Table 8 : Primary sludge samples characterized

Sludge	Load	Process	Sludge age	BD (%COD)	X_{RC} (% COD)
SI_A	Primary sludge: sludge thickened after primary settler (after screen and greases treatments)			51.1	38.6
SI_C				61.0	51.6
SI_D_1				47.5	40.0
SI_D_2				49.0	21.0
RI_B		Screen pre-treatment		46.0	24.0
RG_B		Grease treatment		52.3	11.0

Table 9 : Secondary sludge samples characterized

Sludge	Load	Process	Sludge age	BD (%COD)	X_{RC} (% COD)
SII_A	Low	Activated sludge	19 days	43.5	31.3
SII_B	low		15 days	49.0	16.2
SII_B_i (i= 1to 13 corresponding to the sample date)	low		15 days	39.4-50.1	18.0-39.7
SII_C	Low		11 days	46.0	n.a.
SII_D	Low		11 days	47.0	15.0
SII_E	High		0.6 days	46.0	35.8
SII_F_1	Low		11 days	35.0	10.8
SII_F_2	low		11 days	35.0	10.8
SII_G	low	Membrane Bioreactor	8 days/35°C	36.0	29.0
SII_H	low	Activated sludge	15 days	46.3	n.a.

* *: sludge used for feeding continuous laboratory reactors.*

Table 10 : Sludge samples after thermal treatment characterized

Sludge	Process	BD (%COD)	X_{RC} (% COD)
S_TT165_B	CAMBI® treatment (165°C, 8 bar)	46.0	37.2
S_TT165_B_i (i=1 to 3)	CAMBI® treatment (165°C, 8 bar)	43.5-50.1	36.0-36.9
S_TT60_1	Batch test 60°C thermal treatment t=1 day	58.2	46.2
S_TT60_2	Batch test 60°C thermal treatment t=2 days	59.0	49.6
S_TT60_3	Batch test 60°C thermal treatment t=3 days	45.6	36.0
S_TT60_4	Batch test 60°C thermal treatment t=4 days	46.5	36.9

Table 11 : Anaerobic digested sludge samples characterized

Sludge	Process	Sludge age	BD (%COD)	X_{RC} (%COD)
SD_A	Mesophilic one reactor	15 days	16.5	7.1
SD_B_i (i=1 to 4)	Mesophilic one reactor	18 days	22.9-28.8	n.a.
SD_C	Thermophilic two stage reactor	16-20 days	15.0	13.3
SD_C_end	End of Batch test	50 days	0	0
SD_D	Thermophilic two steps reactor	15 days	8.2	7.65
SD_E	Thermophilic one reactor	8 days	10.0	2.5
SD_F_1_1	Batch test sample t1 from SII_F_1	12 days	33.9	33.9
SD_F_1_2	Batch test sample t2 from SII_F_1	25 days	10.5	0
SD_F_1_3	Batch test sample t3 from SII_ F_1	35 days	0	0
SD_F_2_1	Batch test sample t1 from SII_ F_2	10 days	19.0	19.0
SD_F_2_2	Batch test sample t2 from SII_ F_2	25 days	10.0	0
SD_F_2_3	Batch test sample t3 from SII_ F_2	35 days	0	0

For some sludge samples (SD_B, SII_H, and SII_C), methane production rate curve had not allowed the identification of X_{RC} (too low S/X ratios), so the notation “n.a.” is added in the corresponding table.

II.4. Chemical sequential extraction protocol

II.4.1. Definitions

Model floc defined by Nielsen *et al.*, (2004) can be translated into a floc schematic decomposition based on concepts such as bioavailability and bioaccessibility.

Based on this floc definition, Muller *et al. (in press*) proposed an alternative methodology for sludge characterization: a sequential extraction simulating the bioavailability of the organic matter of sludge according to the chemical accessibility (figure 8). Muller *et al. (in press*) proposed a chemical extraction of each compartment composing the sludge floc:

- Dissolved organic matter (DOM) is obtained after physical separation by centrifugation. In terms of bioaccessibility, DOM is considered as bioavailable.
- ExoPolySaccharide (EPS) from particulate extracellular organic matter is composed of two types, based on Esparza-Soto *et al.* (2001):
    - Soluble EPS (S-EPS) is considered as an extern layer of EPS. It is obtained by washing the centrifugation pellet with a saline solution. S-EPS simulates the extracellular particulate organic matter bioaccessible.
    - Readily Extractible EPS (RE-EPS) is considered as the bound EPS. Using an alkaline solution, the carboxylic groups from proteins and carbohydrates are ionised and then solubilized. RE-EPS extraction is performed after S-EPS. This fraction is considered as the extracellular particulate organic matter less bioaccessible.
- Not bioaccessible particulate organic matter (POM) is the remaining fraction. One part is extractible, assimilated to humic substance-like (HSL). The last one is named No Extractible (NE) fraction assimilated to cytoplasmic compounds. Concerning the extractible fraction, in order to follow the growing power of extractant, Muller *et al.* have been inspired by extraction of HSL soil and sediments found on Swift *et al.* (1996) and Giovanella *et al.* (2004).

  HLS were extracted after a hydrochloric acid pre-treatment. Then, after centrifugation and filtration, a strong alkaline solution is added in a N_2 saturated atmosphere. The residual pellet, NE fraction, is freeze-dried.

At the end of each extraction, COD, protein and carbohydrate content are measured.

COD measurement is used to calculate the extraction yield based on the sludge total COD concentration. These extractions are then coupled with 3D-EEM fluorescence spectroscopy in liquid phase for complexity assessment of the extracts (reference section). In order to extract the whole compartment, Muller *et al.* performed from 20 to 30 extractions for each fraction until the organic matter extracted reached a COD concentration near zero.

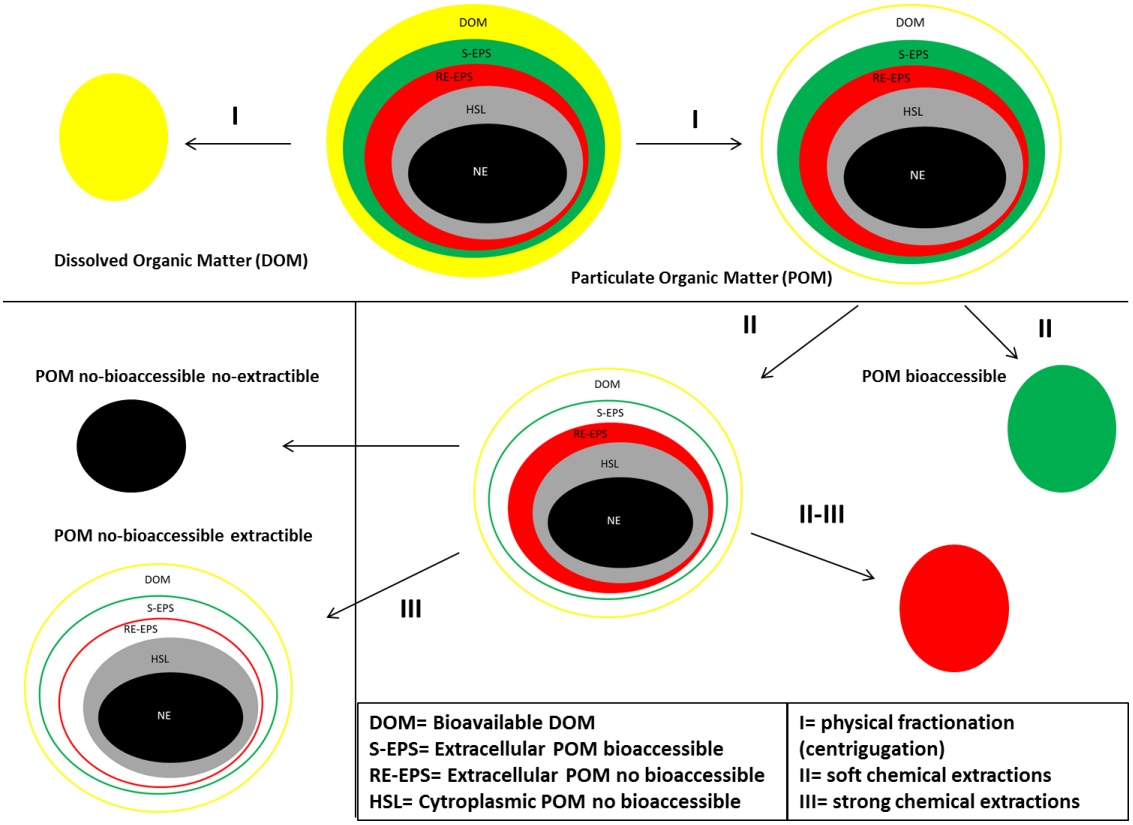

Figure 8 : Schematic concept of sludge floc bioaccessibility decomposition and extractions definitions based on Muller *et al.* *(In press)*

II.4.2. Sequential extraction Protocol

II.4.2.1. Laboratory material

- Shaker table

The extraction phase with each extractant (in solution) is optimised by using a shaker table THERMO SCIENTIFIC MAXQ 4000 at 200 rpm and 30°C (figure 9). Time contact depends on extraction type. Extractions are made in duplicate in order to recuperate the extracted fraction (supernatant) and use the remaining pellet for the next extraction step.

Figure 9 : Shaker table used for chemical extractions

- Centrifugation and filtration

Centrifugation is performed in a Thermo Scientific SORVALL RC6 PLUS centrifuge at a speed of 18,600 g, during 30 minutes and a temperature of 4°C. After each centrifugation, in order to recover only the soluble from supernatant, a filtration step is performed. Filters Minisart plus of 0.45µm porosity are used. Some tests have been performed in order to evaluate the organic matter lost by filtration in secondary and primary sludge. Mean value is about 5.4% of DOM not filtered i.e. 0.53% of total COD which is negligible. Concerning digested sludge, the lost is higher with a mean value of 40% of not filtered DOM i.e. 4% of total COD.

II.4.2.2. DOM

Dissolved organic matter is obtained after centrifugation of total sludge at the defined conditions. Total sludge introduced in the centrifugation glass is weighted, before and after removing supernatant for COD mass balance. Obtained supernatant is then filtered and DOM is conserved at -20°C for further analysis. Five grams of remaining pellet homogenised are taken for sequential extractions. Duplicate jars are used.

II.4.2.3. S-EPS

S-EPS are obtained after extraction step with 40mL of a buffer saline solution at pH 8, NaCl (10mM) and NaHCO3 (4mM). Shaker table is programmed for a contact time of 15 minutes.

After extraction, centrifugation and filtration are performed. Supernatant obtained is conserved at -20°C for further analysis.

S-EPS fraction is finally obtained by mixing equal part of volume of supernatant from each extraction step. As the extraction number performed by Muller *et al. (in press*) is too high for a practical use, this number has been reduced to N= 4. Results later presented will show that this number is sufficient to extract the main part of compartment. Remaining pellet is used for RE-EPS extractions.

II.4.2.4. REPS

RE-EPS are obtained after extraction step with 40mL of a saline and alkaline solution at pH 11, NaCl (10mM) and NaOH (10mM). Shaker table is programmed for a contact time of 15 minutes. After extraction, centrifugation and filtration are performed. Supernatant obtained is conserved at -20°C for further analysis. RE-EPS fraction is finally obtained by mixing equal part of volume of supernatant from each extraction step. As for S-EPS, number of extractions has been reduced to N= 4. Remaining pellet is used for HSL extractions.

II.4.2.5. HSL

HSL extraction is composed of two steps: an acid pre-treatment and an alkaline extraction.

- Pre-treatment

Pre-treatment consists in adding 40mL of HCl solution (0.1M) in the jar containing the remaining pellet. Shaker table is programmed for a contact time of 60 minutes. Then, centrifugation and filtration are performed. A washing step with ultrapure water is made. pH is then adjusted to 7 (pHmeter WTW) with drops of NaOH solution (1M). Centrifugation and filtration are finally performed. Remaining pellet is used for HSL extractions. Pre-treatment allows desorption of humic substances.

- Alkaline extraction

HSL is obtained after extraction step with 40mL of an alkaline solution at pH 12, NaOH (0.1M). Centrifugation jar used is then saturated with N_2 injection (30 to 60 seconds) in order to prevent oxidation of the organic matter. Shaker table is programmed for a contact time of 4 hours.

After extraction, centrifugation and filtration are performed. Supernatant obtained is conserved at -20°C for further analysis.

HSL fraction is finally obtained by mixing equal part of volume of supernatant from each extraction step. As for S-EPS and RE-EPS, number extraction has been reduced to N= 4. Remaining pellet is then freeze-dried and represents the Non Extractible fraction (NE).

Four liquid fractions are thus obtained. 3D-EEM fluorescence spectroscopy in liquid phase is then performed for each one. The not extractible fraction (NE) is then analysed by 3D-EEM fluorescence spectroscopy in solid phase.

II.4.2.6. COD mass balance and organic matter extraction yield calculations

Profiles extractions made in duplicates are represented by cumulated COD_s for primary (SI), secondary (SII) and digested (SD) sludge (figure 10).

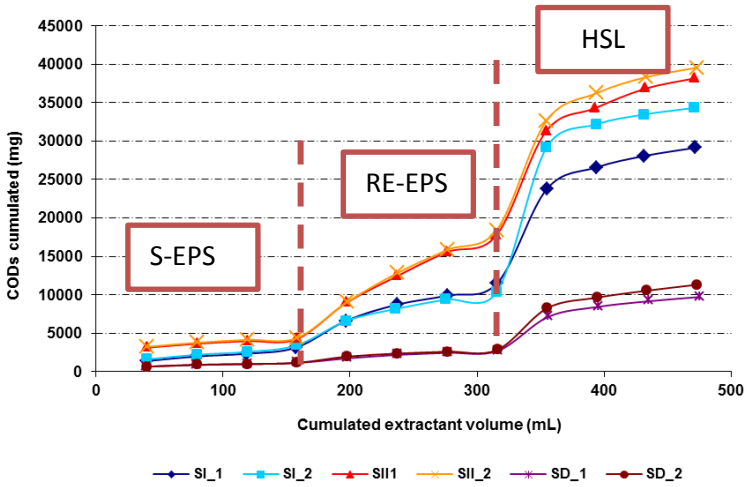

Figure 10 : Extraction profiles of three different sludge natures, in duplicate (primary BI, secondary BII and anaerobic digested BD)

In each extraction step, mass of extractant through the weighing of centrifugation pot before and after extractant addition has to be noted down. Then, COD concentration, representing a global organic matter measurement, is measured for the fourth extractions of each extraction compartment. COD_s extracted for an equivalent of 1liter of raw sludge is expressed in equation 3.12. Equation 3.13 presents the COD extraction yield.

$$\boldsymbol{COD_s = \frac{COD_5 \times m_p}{m_{ext}} \times \frac{V_s}{V_p}} \quad \textbf{(mg)} \qquad \textbf{Equation 3.12}$$

$$\boldsymbol{R(COD_s) = \frac{COD_s}{COD_{total}} \times 100} \quad \textbf{(mg/mg)} \qquad \textbf{Equation 3.1}$$

Where

COD_5 (mg) is the COD mass obtained after one extraction with 5g of pellet (COD concentration measured after filtration multiplied by the volume of extractant used)

m_p (mg) is the pellet mass obtained for the initial centrifugation (for DOM fraction)

m_{ext} (g)is the pellet mass used for sequential extractions (5 g)

V_s (L) is the raw sludge volume considered (1 liter)

V_p (L) is the raw sludge volume used for initial centrifugation (for DOM fraction)

COD_{total} ($mg.L^{-1}$) is the COD concentration of total raw sludge

Figure 11 synthesizes the operational conditions of the sequential extraction protocol.

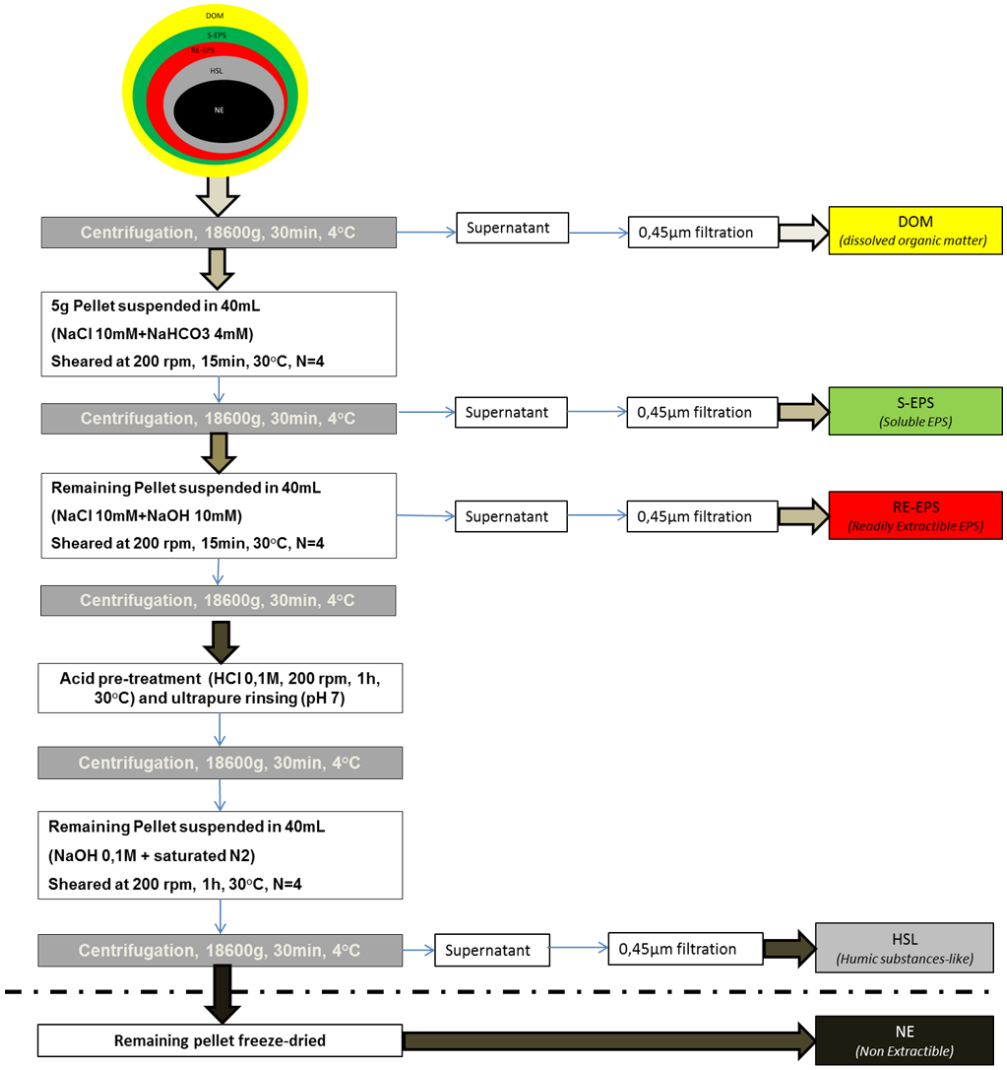

Figure 11 : Modified protocol based on Muller *et al.* (in press)

II.5. 3D-EEM fluorescence spectroscopy

Fluorescence is a light emitted by molecule excitation, usually due to the absorption of a photon and followed by a spontaneous emission. Organic and inorganic compounds (mainly aromatic or polyaromatic) in solution or solids emit light, when they are excited by photons, in order to come back to their fundamental state following the Stockes law.

Molecules at rest in the vibrational level of fundamental state electronic state S_0 are excited to the state S_1 under the effect of light radiation absorption (excitation wavelength) as shown by the energetic diagram of Jablonski (figure 12).

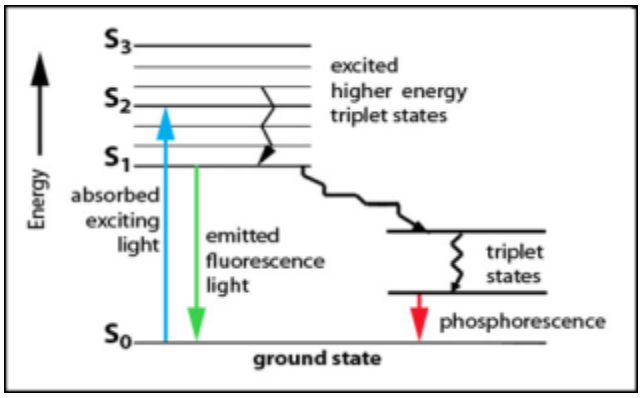

Figure 12 : Fluorescence phenomena explanation with the Jablonski energetic diagram

II.5.1. Fluorescence Spectrometer

The fluorescence spectrometer used is a Perkin Elmer LS55 (figure 13). It contains a xenon lamp producing a pulsed radiation between 200 and 600 nm. The monochromators presence in excitation and emission allows the acquisition of excitation emission spectra and 3D spectra.

Figure 13 : Fluorescence spectrometer Perkin Elmer LS 55

The measurement can be made for liquid and solid samples (powder or freeze-dried and grinded). For that, two measurement modules are available (figure 14).

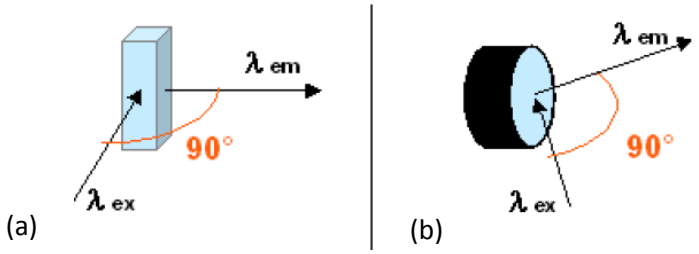

Figure 14 : Liquid phase fluorescence measurement (a) and solid phase fluorescence measurement (b)

Liquid phase fluorescence (LPF) is performed with a SUPRASIL quartz cell from HELLMA type 101-Q5. Solid phase fluorescence (SPF) module is constituted of an orientation support allowing the excitation radiation on the measurement cell angle variation. Measurement cell is composed of metal with a transparent window in silicon dioxide. Sample is introduced in the superior part of the cell (on window part) and is pressed against the window with the inferior part of the cell (figure 15). The fluorescence measurement is performed at the surface of the module.

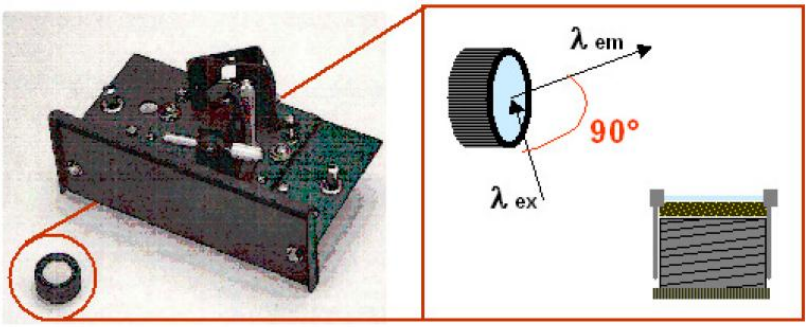

Figure 15 : Solid phase module for fluorescence spectrometer Perkin Elmer LS 55

For both liquid and solid phases, fluorescence emitted is recovered with an angle of 90°C. In case of 3D spectra, excitation wavelengths vary from 200 to 600 nm with increments of 10nm. The slit width of emission and excitation monochromators is fixed at 10nm. Scanning monochromator speed is about 1200 $nm.s^{-1}$. Fluorescence values are recorded every 0.5nm between 200 and 600 nm. Signals saved by the detector are treated by a micro-computer with the PerkinElmer FL Winlab software.

For all the tests in LPF, temperature is thermo regulated at 20°C with a water bath LAUDA device.

II.5.2. Fluorescence Spectra

Fluorescence spectra can be obtained in 2D with one excitation wavelength scan (figure 16) or 3D scan (200 to 600nm with an increment of 10nm) obtained for tryptophan amino acid (figure 17).

In 3D scan, excitation wavelength (λ_{ex}) constitutes the Y-axis, emission wavelength (λ_{em}) the X-axis and fluorescence intensity the Z-axis. The peak represented in the spectra represents the tryptophan fluorescence at λ_{ex}=280 nm and λ_{em}=330 nm.

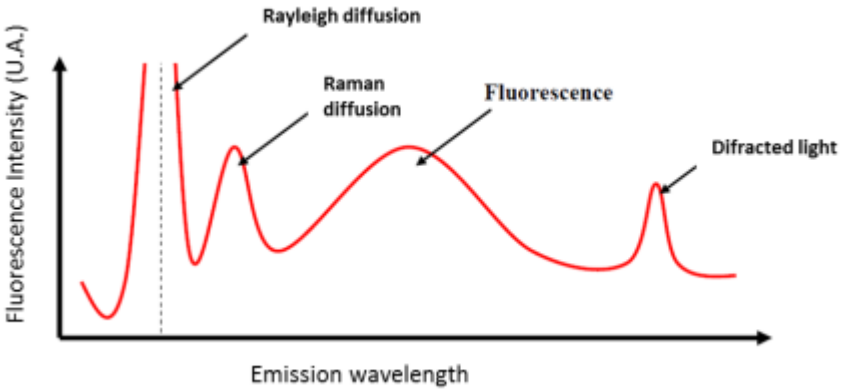

Figure 16 : 2D scan fluorescence spectroscopy spectra example

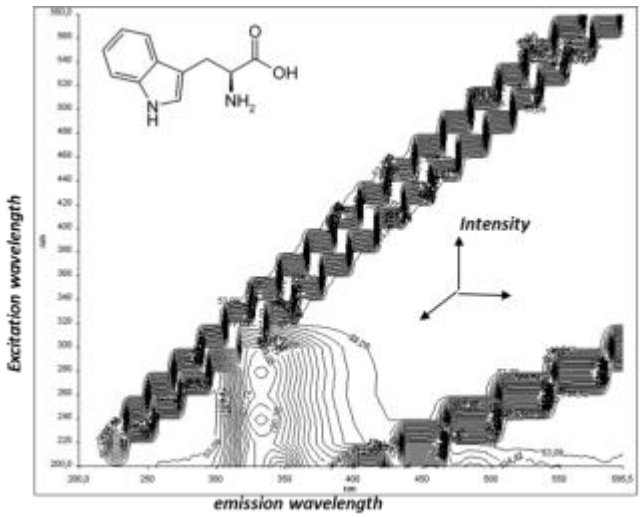

Figure 17 : 3D scan fluorescence spectroscopy spectra for Tryptophan

Extracted fractions from sequential extraction previously described are measured by LPF. In Muller *et al.* (in press), they measured LPF at the beginning of the extraction and at the end. Results showed different patterns (footprint) of fluorescence between the first and the last extraction of a given extracted fraction.

The methodology consisting in measuring by LPF the extracted fractions from sequential extractions (SE) is named SE-3D-LPF.

II.5.3. Dilution and linearity for quantification

Applied on solutions, the quantic yield is defined by the equation 3.2. The higher this yield, the more fluorescent is the compound. The quantic yield is not used directly for quantification. The number of photons absorbed is described as the difference between the incident light intensity I_0 and the transmitted light intensity I_t (equation 3.15).

For diluted solution, absorbance A is weak and equation 3.16 can be written. In this case, concentration is proportional to the fluorescence intensity.

$$\mathbf{\Phi = \frac{I_f}{I_a}} \qquad \textbf{Equation 3.2}$$

$$\mathbf{I_f = \Phi \times (I_0 - I_t) = \Phi \times I_0 \times \left(1 - \left({I_t}/{I_0}\right)\right) = \Phi \times I_0 \times (1 - e^{-A})} \qquad \textbf{Equation 3.3}$$

$$\mathbf{I_f = \Phi \times I_0 \times A = \Phi \times I_0 \times \varepsilon \times l \times C = K \times C} \qquad \textbf{Equation 3.4}$$

where

Φ is the quantic yield

I_f is the number of photons emitted

I_a is the number of photons absorbed

A the absorbance $A = \ln\left({I_0}/{I_t}\right)$ and $A = \varepsilon \times l \times C$ (Beer Lambert law)

ε ($L.mol^{-1}.cm^{-1}$) is the molar absorptivity

l (cm) is the optic path length crossed by light

C ($L.mol^{-1}$) is the concentration of the compound

I_0 is the incident light intensity

K is a factor representing $\Phi \times I_0 \times \varepsilon \times l$

If the absorbance is too important, there is a loss of linearity linked to equation 15 and due to the auto-quenching phenomenon in which molecules absorb the fluorescence radiation emitted by others molecules.

In order to avoid this phenomenon, for each sample analysis, a linearity test has to be performed for several dilutions (case A from figure 18), and for the λ_{ex} where a peak appears.

If the sample is not enough diluted, problem of concentration quantification appeared (case B).

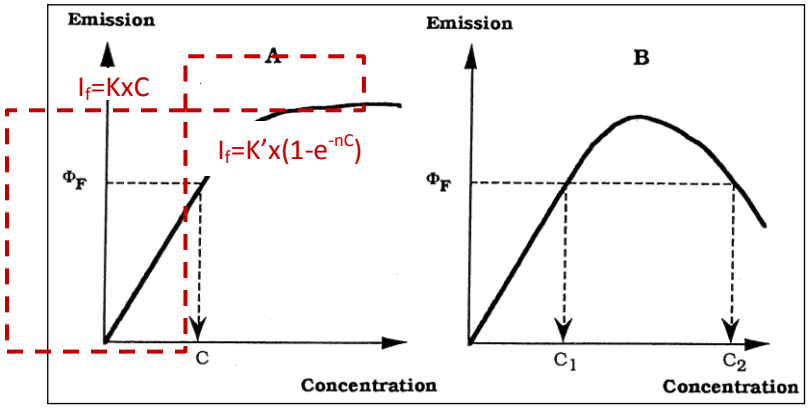

$K' = \Phi \times I_0$ and $n = \varepsilon \times l$

Figure 18 : Auto-quenching phenomenon problem for quantification and linearity

II.5.4. Spectra interpretation

Once the dilution is found for a sample, the spectra interpretation can be performed.

Based on Muller *et al. (in press*) and in Chen *et al*. (2003) studies, spectra is decomposed on seven zones corresponding on each molecule families-like fluorescence. Fluorescence regionalization integration (FRI) is thus done (figure 19). Table 12 sums up the pairs ($\lambda_{ex,}$ λ_{em}) for each zone of the spectra.

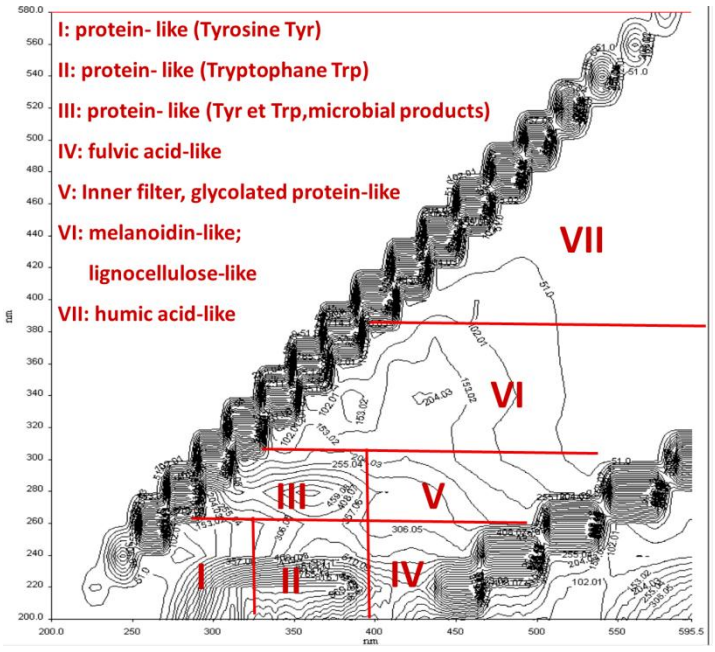

Figure 19 : FRI for spectra interpretation and quantification

Then, in order to have quantitative information of fluorescence, the main idea is to calculate the volume of each one. The procedure is the following:

- 3D spectra is obtained from λ_{ex}=200-600 nm with increments of 10nm, generating 40 2D spectra.
- . Coordinates values are found in table 12. Several spectra can be treated at the same time.

Results obtained are:

- "Intensity" which represents the volume of each zone: it is the most important result in this work because it translates the quantity of whole peak fluorescence.
- Area of each zone: this parameter is used to normalize the final volume used.
- The coordinates of barycenter of each zones (which have to be converted into nm).
- The distance between barycenter of a same zone from spectra to another. This result can be used to make comparison between two spectra (pre-treatment performances, digestion impact on molecules, etc...) through the calculation of energy lost (E) by Stokes law:

  $$\boldsymbol{E = h \times c / \Delta\lambda}\ \textbf{(j)}$$

  where

  h (j.s)is the Planck constant (6.63E^{-34} j.s),

  c (m.s^{-1}) is the light speed (3E^{+08} m.s^{-1})

  $\Delta\lambda$ (m) is the wavelength delta between emission and excitation.

Concerning fluorescence zone volume of a zone "i" $V_f(i)$, calculation based on the IMAGE J result is described by equation 3.17. COD sample and area zones normalization is performed. Area zone normalization is made in order to reduce dominance effect by shoulders in EEM regions (Chen *et al.*, 2003). The proportion of fluorescence of a zone "i" $\mathrm{P_f(i)}$ is also calculated from the fluorescence zone volume (equation 3.18).

$$\boldsymbol{V_f(i)}(\mathrm{U.A./mg.COD.L-1}) = \frac{\boldsymbol{V_{image\,J}(i)}}{\boldsymbol{COD_{sample}}} \times \boldsymbol{1} \Big/ \frac{\boldsymbol{S(i)}}{\sum_{i=1}^{7} \boldsymbol{S(i)}} \qquad \textbf{Equation 3.5}$$

$$\mathbf{P_f(i)}(\%) = \frac{\mathbf{V_f(i)}}{\sum_{i=1}^{7} \mathbf{V_f(i)}} \times \mathbf{100} \qquad \textbf{Equation 3.6}$$

where

$V_{image\,J}(i)$ (U.A./mg.COD.L^{-1}) is the raw volume obtained in IMAGE J (U.A)

COD_{sample} (mg.L^{-1}) is the COD concentration of the sample analyzed

$S(i)$ (nm²)is the area of a zone i

$P_f(i)$ (%) is the fluorescence proportion of a zone i

Table 12 : Definition of FRI zones

Zones	Definition	λ_{ex}, λ_{em} peak peak location	Coordinates x,y (pixel) of polygone under IMAGE J
I	Aromatic protein-like (Tyrosine-like)	220,300-310	50/395.5-50/375.5-80/345.5-30/345.5-130/395.5
II	Aromatic protein-like (Tryptophan)	220,360	130.5/395.5-130.5/345.5-190/345.5-190/395.5
III	Protein-like (Trp, Tyr, microbial products)	280,350-360	80-345/131.5/295.5-190/295.5-190/345
IV	Fulvic acid-like	230,400-420	190.5/390.5-190.5/335.5-288/335.5
V	Intern filter (glycolated protein-like)	280,440-450	190.5/335-190.5/295.5-360/295.5-288/335
VI	Glycolated protein-like (melanoidin), lignocellulose-like	340,420-450	131.5/295-213/215.5-395.5/215.5-395.5/275.5-360/295
VII	Lipofuscin-like (condensed protein), lignine-like humic acid-like	400,480-500	213/215-395.5/35.5-395.5-215

II.6.Anaerobic digestion laboratory scale reactors

A test bench of two anaerobic digestion laboratory scale reactors has been used for both batch tests and continuous tests (figure 21 a). They consist of 4 L glass reactors cylinder round-bottom-shaped (1), stirred by an impeller with seascape (rotor) blades, and Maxon DC motor (2).

A thermo regulated water batch (LAUDA E300) maintained the temperature of the reactors at 35°C through a double wrapping. Feeding is performed manually at the top of the reactor, and output samples are performed at the bottom (thanks to a gate). Biogas circuit consists of a pipe bringing biogas from reactor to a trap cell (figure 21 b) closed (in order to eventually trap foam from sludge). Then, biogas is sent to the milligascounter Ritter MGC-1V3.0 (measuring chamber of 3.15 mL and flowrate of 600 $mL.h^{-1}$) for total biogas flowrate measurement (4). Flow gas reaches a cell equipped with Bluesens (3) sensors for methane composition on-line assessment.

As this equipment is highly sensitive to under and over pressure, cell is at atmospheric pressure. Bluesense gives instant methane content. Gas is finally stored in sampling gas bags SKC (capacity 10L) for further analysis.

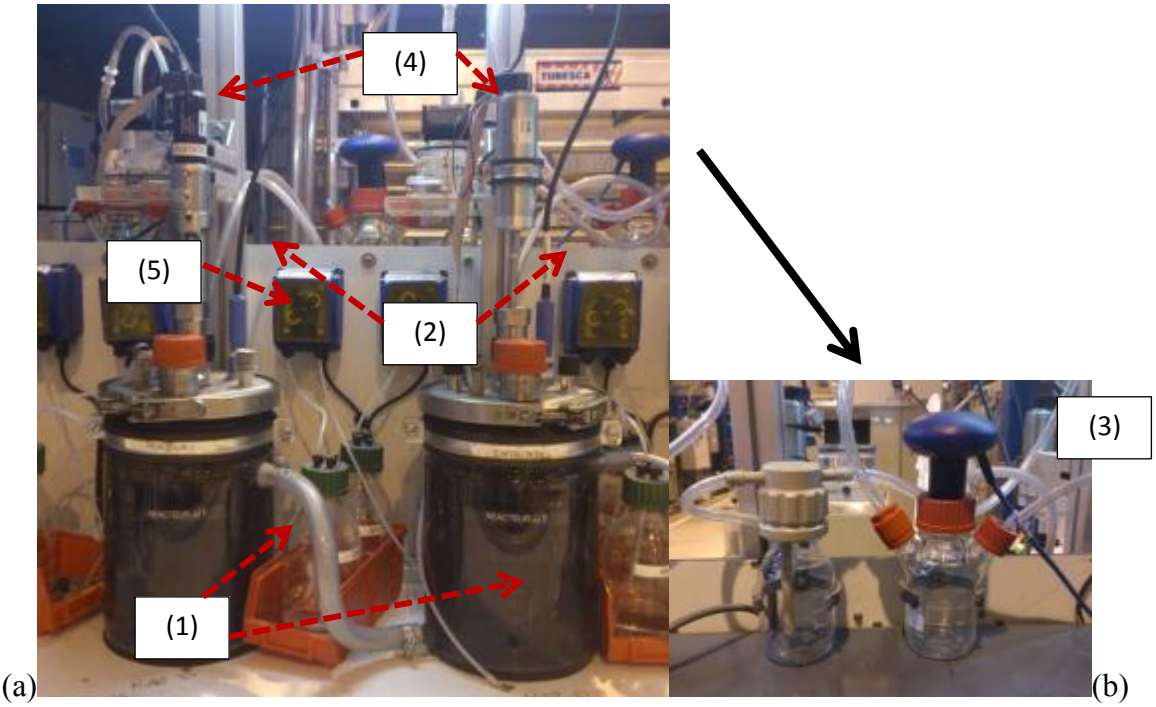

(a) (b)

Figure 20 : (a) Laboratory reactors description and (b) closed trap cell from biogas circuit

(1) Glass reactors of 4L
(2) Stirring system
(3) Methane measurement: Bluesense
(4) Biogas flowrate measurement (Ritter)
(5) pHmeter

In order to measure average biogas composition, daily cumulated biogas is analyzed with the portative GA-2000 PLUS from GEOTECH. Signals from Ritter and Bluesense are then sent to counter box BACCOM 12 with integrated temperature and pressure sensors. Signals are then treated by the software BACVis data acquisition. Each biogas impulsion is recorded and cumulated volume is visible on the microcomputer. Not regulated pH is measured with a pHmeter Endress Hauser immersed in the reactors (5).

Concerning the continuous tests, Table 13 describes the operating conditions performed on two pilots named P1 and P2. From an European wastewater treatment plant, secondary sludge named SII_B (described in section 7 of this chapter) is used to feed the continuous laboratory scale reactors.

Sludge samples are sampled once a week and stored at 4°C. Manual feeding is performed. Output sludge is first sampled and weighted to have an accurate measurement. Then, input sludge feeding is weighted in order to obtain the output weight.

Table 13 : Operating conditions of the continuous lab pilots from the test bench

	Definition	Inoculum	Substrate	Temperature	Reactor volume	TSH	Load
Units	-	-	-	*°C*	*liters*	*days*	$gCOD.gVS_{reactor}^{-1}.j^{-1}$
P1	Lab pilot used as reference	Digested sludge SD_B	Thickened Mixed sludge SII_B	35	3.8	18	0.13
P2	Disturbing added	Digested sludge SD_B	Thickened Mixed sludge SII_B	35	3.8	18	0.13

Table 14 sums up the analysis performed in input and output laboratory scale reactors for model calibration and validation purpose. Complete sludge characterization is performed once a week.

Table 14 : Analysis performed on lab pilots in continuous tests for model calibration and validation

Analysis	Phases	Frequency	Input flow	Output flow
SE-3D-LPF	Total		X	X
COD	Soluble+total	1/day	X	X
TC/TOC/IC/TN	Soluble+total	1/day	X	X
TS/VS	Total	1/day	X	X
Carbohydrates	Soluble+total	1/week	X	X
Proteins	Soluble+total	1/week	X	X
Lipids	total	1/week	X	X
VFA	Soluble	1/day	X	X
Ammonium	Soluble	1/day	X	X
Flow rate	-	1/day	X	X
Composition biogaz	-	On-line		X
Production biogaz	-	On-line		X
pH	Liquid			X

II.7.Mathematical modeling : modified ADM1 and statistical methods

II.7.1. Modified ADM1

Bioaccessibility is one of the main objectives of anaerobic digestion modeling as biodegradability. Thus, the choice of the model is crucial. ADM1 from Batstone *et al.* (2002) (described in Chapter I, figure 3) does not sufficiently describe the bioaccessibility concept and the kinetic limiting step for complex substrate.

For these reasons, ADM1 model modified by Mottet (2009) has been chosen because modifications respect our objectives and because these modifications are in line with our objectives. Additionally, Mottet (2009) showed that these new model applied on batch and continuous digesters at 55°C gave more representative results in terms of particular COD and biogas production prediction than classical ADM1.

Annex 2 presents the Petersen Matrix of ADM1 and ADM1 modified. Model implementation is made on WEST software from DHI.

As suggested in the ADM1 report (Batstone *et al*., 2002), inorganic carbon and nitrogen balances in stoichiometry have been completed for disintegration, hydrolysis, uptake of LCFA, valerate, butyrate and decay process (completed yet for uptake of sugars, amino acids, propionate, acetate and hydrogen in classical ADM1).

II.7.2. Input variables modifications

Several studies from literature have shown that methane production profile is composed of two main parts: a first gas production from readily degradable compounds and a second one from a slowly degradable one (Yasui *et al.* (2006; 2008); Mottet (2009); Girault *et al.* (2012)). Mottet (2009) replaced X_C fraction (total particulate COD fraction) by two fractions representing readily X_{RC} and slowly hydrolysable particle X_{SC} in ADM1 (figure 21). Both variables can be assessed from BMP tests as already described in this chapter.

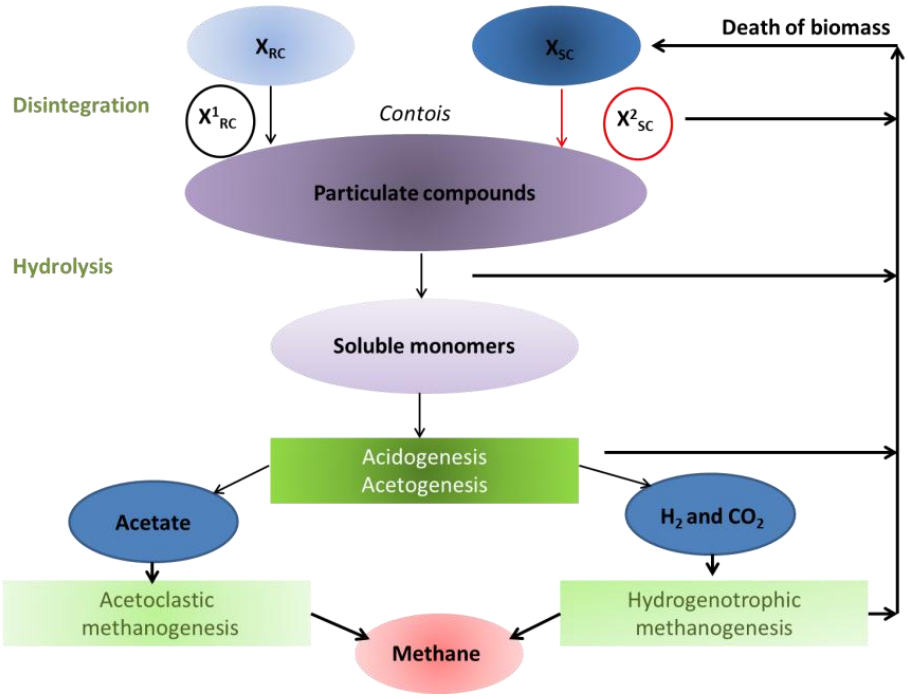

[1]Hydrolytic biomass associated to the disintegration step of readily hydrolysable fraction

[2]Hydrolytic biomass associated to the disintegration step of slowly hydrolysable fraction

Figure 21 : Modified ADM1 model by Mottet (2009)

II.7.3. Kinetic modifications

Reactions such as acidogenesis, acetogenesis and methanogenesis are identical to those from ADM1. However, in order to better represent the limiting effect of sludge anaerobic digestion, Vavilin *et al.* (1996), Yasui *et al.* (2008) and Mottet (2009) introduced Contois model (equation 3.18) instead of the first-order model.

This model represents the disintegration of X_{RC} and X_{SC} into macromolecules (X_{PR}, X_{CH}, X_{LI}, X_I and S_I) and hydrolysis steps (figure 23) associated to hydrolytic biomass colonization (surface limitation).

Five hydrolytic biomass variables are thus introduced: X_bio_X_{RC}, X_bio_X_{SC}, X_bio_X_{pr}, X_bio_X_{ch}, X_bio_X_{li} for respectively X_{RC}, X_{SC}, X_{PR}, X_{CH} and X_{LI} compounds. Decay model for each hydrolytic biomass is a first-order equation (equation 3.19).

Decayed biomass follows the death-regeneration concept of ADM1 and goes to the X_{SC} variable.

$$\rho_{process} = k_{m,process} \times \frac{S}{K_{S,process} X + S} = k_{m,process} \times \frac{S/X}{K_{S,process} + S/X}$$ **Equation 3.7**

Where

$\rho_{process}$ (kgCOD.m^{-3}.d^{-1}) is the process rate

$k_{m,process}$ (d^{-1}) is the maximum specific uptake rate of the process

$K_{S,process}$ (kgCOD.m^{-3}) is the half-saturation coefficient for the ratio S/X

X (kgCOD.m^{-3}) is the hydrolytic/disintegration biomass concentration

S (kgCOD.m^{-3}) is the particulate compound concentration

N.B: When S/X <<<$K_{S,process}$, $\rho_{process=k_{m,process}\times \frac{S}{K_{S,process}}}$, a first-order kinetic for substrate as in classical ADM1.

$$\boldsymbol{decay(Xbio\_X) = k_{dec,Xbio\_X} \times Xbio\_X} \qquad \textbf{Equation 3.8}$$

Where

Xbio_X (kgCOD.m^{-3}) is the hydrolytic biomass of X compound

$k_{dec,Xbio\_X}$ (d^{-1}) is the decay rate of the biomass Xbio_X degrading X compound

According to the Contois and decay models, new parameters are introduced in ADM1 for the hydrolysis equations: fifteen biochemical parameters as the maximum specific uptake rate, the decay rate and the half-saturation coefficient and five stoichiometric parameters Y representing the yield of biomass on substrate. Yield of particulate from disintegration of X_{RC} and X_{SC} are also introduced with the assumption that the yield for each compound is the same for X_{RC} and X_{SC}. Table 15 sums up the nomenclature of these parameters.

Table 15 : New parameters introduced in modified ADM1

Compound	Growth rate hydrolytic biomass (d^{-1})	Decay rate hydrolytic biomass (d^{-1})	Half-saturation constant (kgCOD.m^{-3})	Stoichiometric parameters	Yield of particulate disintegration
X_{RC}	$k_{m\_}X_{RC}$	$k_{dec\_}X_{RC}$	$K_{S\_}X_{RC}$	Y_{RC}	-
X_{SC}	$k_{m\_}X_{SC}$	$k_{dec\_}X_{SC}$	$K_{S\_}X_{SC}$	Y_{SC}	-
X_{PR}	$k_{m\_}X_{PR}$	$k_{dec\_}X_{PR}$	$K_{S\_}X_{PR}$	Y_{PR}	$f\_X_{RC}\_X_{PR}/f\_X_{SC}\_X_{PR}$
X_{CH}	$k_{m\_}X_{CH}$	$k_{dec\_}X_{CH}$	$K_{S\_}X_{CH}$	Y_{CH}	$f\_X_{RC}\_X_{CH}/f\_X_{SC}\_X_{CH}$
X_{LI}	$k_{m\_}X_{LI}$	$k_{dec\_}X_{LI}$	$K_{S\_}X_{LI}$	Y_{LI}	$f\_X_{RC}\_X_{LI}/f\_X_{SC}\_X_{LI}$
X_I	-	-	-	-	$f\_X_{RC}\_X_I/f\_X_{SC}\_X_I$

II.7.4. Liquid/Gas transfer modification

As Ramirez et al. (2009), the modified ADM1 model considers three coefficients liquid/gas transfer for each gas in Henry's law (equation 20) describing equilibrium between liquid and gas phases for CH_4, CO_2 and H_2: K_La_{CH4}, K_La_{CO2}, K_La_{H2}. In classical ADM1, this coefficient is assumed to be the same for the three gases. However K_La depends on reactor size, hydrodynamic conditions and diffusivity values. Ramirez *et al.* (2009) and Mottet (2009), based on Pauss *et al*. (1990) recommendations, proposed that K_La_{CH4} and K_La_{H2} can be estimated from the carbon dioxide transfer coefficient and diffusivity coefficients using the equation 21.

$$\boldsymbol{r_i = K_L a_i \times (S_{liq,i} - K_{H,i} P_{gas,i})} \qquad \textbf{Equation 9}$$

where

K_La_i (d^{-1}) is the transfer coefficient multiplied by specific transfer area of gas i

$S_{liq,i}$ ($kgCOD.m^{-3}$) is the liquid concentration of gas i

$K_{H,i}$ ($M.bar^{-1}$) is the Henry's law coefficient of gas i

$P_{gas,i}$ (bar) is the partial pressure of gas i

$$\boldsymbol{K_L a_i(d^{-1}) = K_L a_{CO2} \times \sqrt{\frac{D_i}{D_{CO2}}}} \qquad \textbf{Equation 10}$$

where

D_i ($m^2.s^{-1}$) is the diffusivity of gas i

II.7.5. Modified ADM1 input implementation

Table 16 and 17 sum up the analytical methods to feed ADM1 modified model.

Table 16 : Soluble variables of modified ADM1 definition and measurement

Variables	Units	Compounds	Analysis method
S_I	kg COD.m^{-3}	Inert soluble COD	Soluble COD obtained at the end of BMP tests/or soluble COD of output digester $COD_{soluble}$ biodegradable = $COD_{soluble}$-S_I
S_{Su}	kg COD.m^{-3}	Monosaccharides	Dubois et al. (1956) on soluble phase COD soluble proportion obtained is applied to $COD_{soluble}$ biodegradable
S_{aa}	kg COD.m^{-3}	Amino acids	Lowry et al. (1951) on soluble phase COD soluble proportion obtained is applied to $COD_{soluble}$ biodegradable
S_{fa}	kg COD.m^{-3}	Fatty acid long chain	Soluble COD mass balance
S_{pro}	kg COD.m^{-3}	Propionate	VFA measurement by gas chromatography
S_{bu}	kg COD.m^{-3}	Butyrate	
S_{va}	kg COD.m^{-3}	Valerate	
S_{ac}	kg COD.m^{-3}	Acetate	
S_{IN}	kmol N.m^{-3}	Inorganic nitrogen	Ammonium measurement: HACH LANGE kit
S_{IC}	kmol C.m^{-3}	Inorganic soluble carbon	IC measurement on soluble phase (Shimadzu)
S_{cat}	kmol.m^{-3}	Cations	Assumed to be at the same concentration than S_{IC}, used for pH calibration
S_{an}	kmol.m^{-3}	anions	Assumed to be at the same concentration than S_{IN} used for pH calibration

Table 17 : Particulate variables of modified ADM1 definition and measurement

Variables	Units	Compounds	Analysis method
X_{I*}	kg COD.m^{-3}	Inert particulate COD	BMP test (equation 14): f_$X_{R,S}$_$X_{I=}$1-BD(%COD) $X_{I\ (t=0)}$=0 Yield disintegration calculation
X_{RC}	kg COD.m^{-3}	Readily hydrolysable particulate fraction	BMP test at S/X ratio 1gCOD.gVS^{-1}: methane production curves interpretation (equation 15) $X_{RC}(\%COD_{biodegradable})=(X_{RC}(\%COD)/BD(\%))xCOD_{particulate}$
X_{SC}	kg COD.m^{-3}	Slowly hydrolysable particulate fraction	BMP test at S/X ratio 1gCOD.gVS^{-1} (equation 16) $X_{SC}(\%COD_{biodegradable})=(X_{SC}(\%COD)/BD(\%))xCOD_{particulate}$
X_{PR*}	kg COD.m^{-3}	Particulate protein	Lowry et al. (1951) on total and soluble phase to obtain the particulate phase $X_{PR\ (t=0)}$=0 Yield disintegration calculation
X_{CH*}	kg COD.m^{-3}	Particulate carbohydrates	Dubois et al. (196) on total and soluble phase to obtain the particulate phase $X_{CH\ (t=0)}$=0 Yield disintegration calculation
X_{LI*}	kg COD.m^{-3}	Particulate lipids	SOXTEC on particulate phase $X_{LI\ (t=0)}$=0 Yield disintegration calculation
Biomass	kg COD.m^{-3}		Input implementation =0

*: *Disintegration compounds are distributed with the following yield from X_{RC} and X_{SC} disintegration, depending on the biodegradable fraction of each one, and with the assumption that yields are the same for X_{RC} than for X_{SC}* as following:

$$f\_X_{RC}\_X_{compound} = f\_X_{SC}\_X_{compound} = f\_X_{R,SC}\_X_{compound} = \frac{X_{compound} \times (1 - f\_X_{R,SC}\_X_I)}{X_{LI} + X_{PR} + X_{CH}}$$

II.8.Statistical tools

II.8.1. Partial Least Square Regression

II.8.1.1. Definition

In order to find correlations between BD, X_{RC} and indicators from SE-3D-LPF, partial least square (PLS) regressions are performed. The software used SIMCA from UMETRICS.

Partial least squares regression is an extension of the multiple linear regression. In its simplest form, a linear model specifies the (linear) relationship between a dependent (response) variable *Y*, and a set of predictor variables, the *X*'s, so that

$Y = b_0 + b_1X_1 + b_2X_2 + ... + b_pX_p$, with b_i the regression coefficients.

The PLS regression interest is that this method combines explorative and explicative data analysis methods. Indeed, it is an explorative method because PLS realizes a data reduction in correlating variables X (maximizing the variances between predictors) through the definition of new variables. These variables are lower in number and are named components. They are orthogonal and independent. This step avoids the limitation obtained by multiple regressions where the explicative variables X have to be not correlated and independent.

PLS is also an explicative method because, as the multiple regressions, these components are also correlated with the variable to explain Y (BD or X_{RC}) by maximizing the variance explained between the new components and Y. The component number is usually chosen to have the lowest prediction error and the maximum of variance explained for both X variables and Y variable (SIMCA from UMETRICS). Finally, a linear combination of the explicative variables function of the variable to explain is created. The number of X variables can be higher than observations number (not the case in multiple regressions).

The parameters from PLS models used to assess the model robustness are the following ones:

- Correlation coefficient R^2: the closer R^2 to 1, the better is the model. It is obtained from the linear regression of the straight line obtained by plotted observed Y versus predicted Y.
- The Predicted Residual Sums of Squares (PRESS) is used in regression analysis to provide a summary measurement of the fit of a model to a sample of observations. These observations are not themselves used to estimate the model. PRESS is calculated as the sums of squares of the prediction residuals for these observations.

  When the PLS model is set up, each predictor is removed and model is refitted to the remaining points (cross-validation).

  The predicted value is calculated at the excluded point and PRESS is calculated as the sum of all the resulting errors as following:

$$PRESS = \sum_{i=1}^{n} (y_i - \hat{y}_i)^2$$

- Root Mean Square Error (RMSE) is used as an accuracy measurement of differences between values predicted and model values observed. The RMSE of an estimator $\hat{\theta}$ with respect to the estimated parameter θ is defined as the following expression:

$$RMSE(\hat{\theta}, \theta) = \sqrt{MSE(\hat{\theta}, \theta)} = \sqrt{E\left(\left(\hat{\theta} - \theta\right)^2\right)} = \sqrt{\frac{\sum_{i=1}^{n}(x_{1,i} - x_{2,i})^2}{n}}$$

For $\hat{\theta} = \begin{bmatrix} x_{11} \\ \vdots \\ x_{1n} \end{bmatrix}$ and $\theta = \begin{bmatrix} x_{21} \\ \vdots \\ x_{2n} \end{bmatrix}$

- RMSEP is the RMSE for the prediction of validation samples (not included in calibration PLS model)
- Q^2 is the percentage of variation of Y predicted by model according to cross-validation. This parameter indicates how well the model predicts the data. A large Q^2 (>0.5) indicates good predictivity. Moreover, it is a compromise between mean square error and R^2. Q^2 represents also the criteria of component number choice. When cumulated Q^2 reach its maximum value, the corresponding component is chosen.
- Variance X cumulated is translated by cumulated R^2X: it is the mean squared error allowing the values to average dispersion characterization. In PLS, component number has to be optimized in order to describe the maximum of the X variance. The higher R^2X, the better X variables are described by components.
- Variance Y cumulated is translated by cumulated R^2Y: as for R^2X, the higher R^2Y, the better Y variable is described by components from X and the more accurate is the PLS model.

II.8.1.2. Interpretation

In order to go further in the PLS regression interpretation, some graphical results could be plotted. The correlation circles are one of these graphs. By studying the correlation strength between X-variables and Y-variables following the component number, the impact of one X-variable on Y-variable could be explained. Usually, this study is made on the two first components which are those that explain the most the X-variables. The most an X-variable is on the same circle than Y-variable, the most strength is the correlation between both. At the same time, another correlation graph is needed: the impact of the observations on Y-variable answer. By analyzing both graphs, the impact of an observation on the prediction and how much each observation is linked with the X-variables could bring information to validate the relevance of the model.

The VIP coefficient graph is also important to study. This graph is composed of the scaled centered regression coefficients in order to point out the most important and significant variables to predict the Y-variables. The error bars are drawn with a confidence interval of 95% in order to show how much a variable is significant.

II.8.2. Other statistical tests

Box plot or box and whisker diagram plot (Tukey, 1977) is a convenient way of graphically depicting groups of numerical data. Values distribution simplified representation is made with the median (thickened line), a box extended from the quartile 0.25 to the quartile 0.75 and whiskers extended until the maximum value equal to 1.5 times the interquartile distance. The box itself contains the middle 50% of the data. If the median line in the box is not equidistant from edges, the set of data is skewed. Whiskers boundaries indicate the minimum and maximum data values, unless outliers are present. In this case, points outside of the ends of whiskers are suspected outliers. The software R (http://www.r-project.org/) is used for this graphical methodology.

II.9.Conclusion

Methodologies used in this study have been described. Some of them are innovative in sludge characterization domain such as bioaccessibility fraction determination, sequential extraction, and fluorescence spectroscopy. They need preliminary studies in order to validate some assumptions and to optimize the results. BMP tests are usually carried out with S/X ratio of 0.5 gCOD.gVS^{-1} in order to estimate X_{RC} and X_{SC} fractions. Nevertheless, preliminary tests have been set up to check if this ratio could be improved.

Sequential extractions from Muller *et al. (*in press) have been also modified by decreasing the extraction number. Indeed, the number of extractions recommended by Muller *et al.* (in press) i.e. 20 makes the protocol long and tedious. Investigation of a lower number of extractions has thus been performed looking for a compromise between convenience and representativeness of organic matter extracted in each compartment.

These two preliminary tests are summarized at the beginning of the next chapter. Then, fractionation distribution in each sludge type is studied in order to determine the main discriminant parameters as far as biodegradability concerned. Biochemical characterization is also detailed to clearly understand the types of molecules that are extracted. Finally, chemical accessibility, associated with chemical extraction, and biological accessibility correlations are investigated through 3 experimental assays.

III. BIOACCESSIBILITY AND CHEMICAL ACCESSIBILITY CORRELATION INVESTIGATION

III.1. Preliminary results : Biochemical methane potential (BMP) test and sequential extractions 100
III.1.1. Biochemical Methane Potential: S/X ratio investigation 100
III.1.2. Sequential extraction and sludge profile 102
III.1.2.1. Validation extractions number 102
III.1.2.2. Fractions extraction repartition and sludge type 104
III.1.2.3. Effect of size particle distribution on chemical extractions protocol 108
III.1.3. Biochemical nature of sludge and extracted organic matter 110
III.1.3.1. Non-fractionated sludge characterization 110
III.1.3.2. Fractionated sludge characterization 111
III.1.4. Sludge fractionation conclusion 114
III.2. Correlation between chemical and biochemical accessibility investigation 115
III.2.1. Material flow investigation : anaerobic stabilization test 115
III.2.2. Biodegradability and bioaccessibility investigation of sequential extraction fractions 121
III.2.3. Methane production curve and correlation of fractions extracted 126
III.3. Conclusions 129

Note for the reader:

This first chapter of results begins with the preliminary results in order to validate assumptions about the BMP test used for X_{RC} calculation and the number of sequential extractions. Repartition and global composition of each sludge fraction are also studied in order to evaluate what molecules are extracted and if they are the main component of the studied sludge. The results obtained in the laboratory reactors tests (batch and continuous) are presented to validate the hypothesis that chemical accessibility simulates biological accessibility. This hypothesis is the basis for the overall methodology. Therefore, this section is important and introduces the next chapter based on fluorescence spectroscopy and the correlation with biodegradability.

III.1. Preliminary results : Biochemical methane potential (BMP) test and sequential extractions

Before investigating the hypothesis of the correlation between bioaccessibility and chemical accessibility, the conditions of the experimental test BMP described in the previous chapter is studied. In order to choose the most relevant S/X ratio for the X_{RC}/X_{SC} interpretation, several tests were performed at different ratios. Later, the results of the sequential extractions are analyzed in order to optimize the extractions number and also to check the fractionation repartition in each kind of sludge as well as their organic composition.

III.1.1. Biochemical Methane Potential: S/X ratio investigation

As described in the Material and Methods Chapter, the BMP test is usually performed with an optimal S/X ratio of 0.5 gCOD.gVS^{-1} for the degradation.

However, the optimal ratio is highly dependent on the objective. In the current study, this ratio has to be chosen for an optimal assessment of both BD and X_{RC}. Using a typical ratio of 0.5 gCOD.gVS^{-1}, the observed methane production rate might not allow the interpretation of the X_{RC}/X_{SC} decomposition. Indeed, Figure 22 (a) and figure 22 (b) represent the degradation of a sludge sampled at different time, and analyzed with different S/X ratios, 0.5 and 1 gCOD.gVS^{-1} respectively. At S/X= 0.5 gCOD.gVS^{-1}, the interpretation was very difficult because the kinetic observed through the curve is too fast (figure 22 a). From this observation, and in order to investigate the ratio value that gives the most accurate result, three ratios have been studied: 0.5, 1 and 2 gCOD.gVS^{-1}.

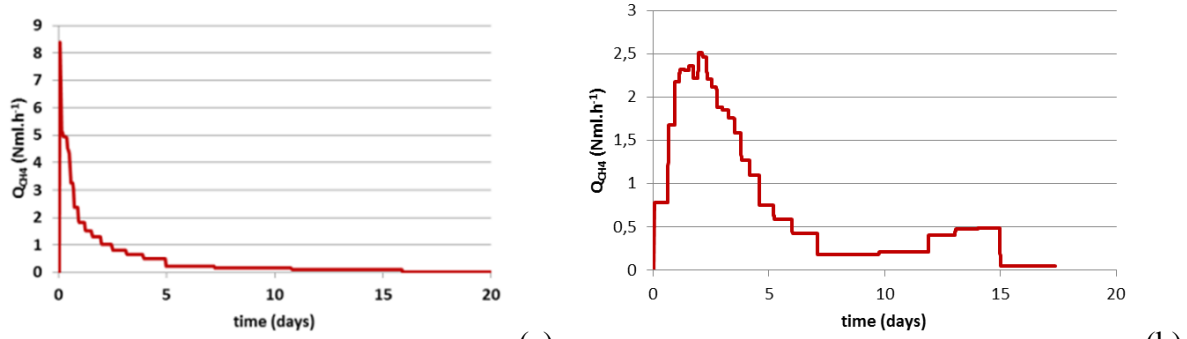

Figure 22 : Methane production rate curves from a secondary sludge BMP test with (a) S/X=0.5 gCOD.gVS^{-1} and (b) S/X=1 gCOD.gVS^{-1}

Results of X_{RC} calculation are presented in table 18. As shown by the percent values of X_{RC} obtained, the ratio 2 gCOD.VS^{-1} led to an overestimation of the variable.

Indeed, this ratio was too high as shown by the very slow reactions of methane production rate curve (figure 23). The plateau was reached after 40 days and BD obtained was lower 30±5% than with the traditionally ratio 0.5 or 1 gCOD.VS^{-1}, respectively 46±7% and 40±9%.

Table 18 : Results obtained in the comparison test of S/X ratios: impact of DOM in X_{RC} assessment

	Duration test	**X_{RC} (*%COD*)**		**BD (%COD)**	
gCOD.VS^{-1}	days	Average	Standard Deviation	Average	Standard Deviation
Ratio 0.5	21	32.3	5.4	46	7
Ratio 1	35	35.8	0.5	40	9
Ratio 2	40	30.8	1.1	30	5

Additionally, the methane production curve (figure 23) did not highlight the X_{RC}/X_{SC} location and the X_{RC} value obtained was close to the final BD. One assumption could be that the kinetic was too low to observe a complete X_{SC} degradation. Therefore, this ratio has been eliminated since the test was too long and the results underestimated BD and X_{RC} compared to the others ratios.

From a kinetic point of view, the methane production rate curves were not so significantly different between both ratios 0.5 and 1 gCOD.VS^{-1} in this test. However, determination of X_{RC} was difficult to assess with the ratio 0.5 gCOD.VS^{-1} test because methane production curve did not present a visible decomposition of X_{RC}/X_{SC} in both cumulated and methane production rate curves.

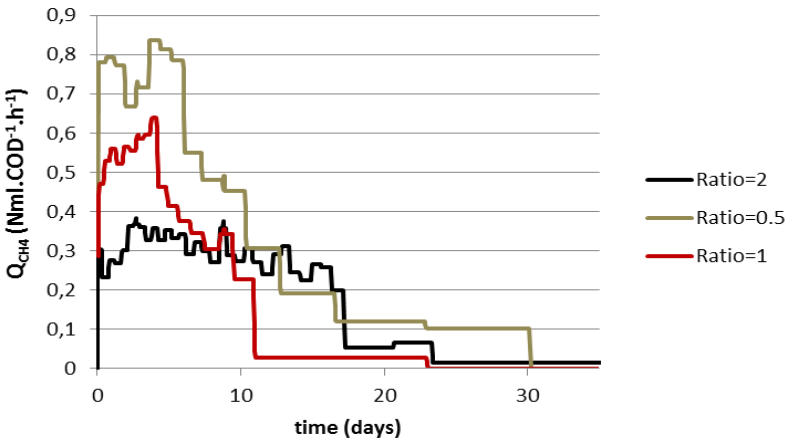

Figure 23 : methane production rates for several S/X ratios

Finally, the ratio 1 $gCOD.VS^{-1}$ seemed to be the most relevant for X_{RC} calculation. The value obtained was underestimated by both ratios 0.5 $gCOD.VS^{-1}$ and 2 $gCOD.VS^{-1}$. The ratio 2 $gCOD.VS^{-1}$ did not present a clearly decomposition of X_{RC}/X_{SC}.

III.1.2. Sequential extraction and sludge profile

In the material and methods section, the extraction protocol defined was based on. However, some modification on the extraction number was done. Indeed, Muller *et al.* (*in press*) used more than 20 sequential extractions for each fraction. In order to simplify the protocol, this number has been significantly reduced.

From Muller *et al.* (*in press*) results, it appears that RE-EPS and HSL were respectively extracted with a yield of on average 70% and 90% with only 4 extractions for the 3 tested sludge. Concerning S-EPS, one sludge was extracted with more than 90% after 4 extractions whereas the 2 others were extracted at 50%. Thus, general trend seems indicate that 4 extractions could be sufficient to reach an extraction yield between 50 and 90% for a given fraction.

Protocol based on 4 extractions would be suitable because it would be less long and more practical. For that reason, next section aims at studying this extraction number and its ability to be representative of a compartment.

III.1.2.1. Validation extractions number

The main objective of the organic matter extraction is to extract sufficient organic matter from each sludge compartment to be representative of a fraction.

In the current work, the patterns of the COD concentration from 6 different sludge show that there was a depletion of each fraction after 4 extractions (figures 24).

Whatever the sludge nature, profiles were indeed similar and most of the time the lower detection limit of COD analyzer during the fourth extraction was reached.

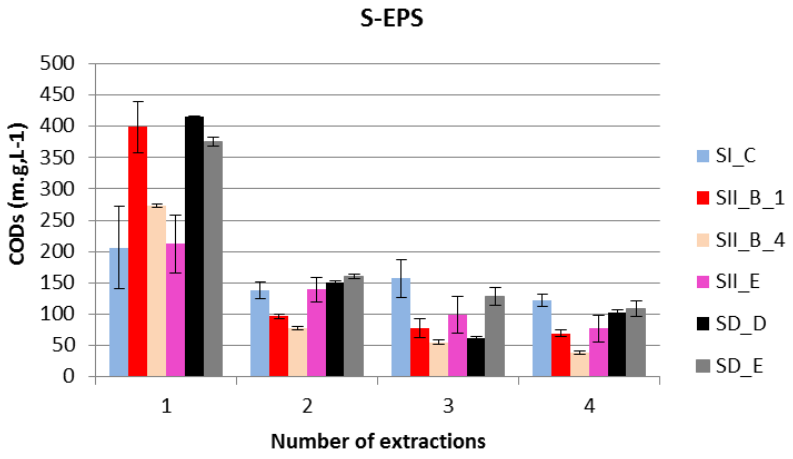

(a)

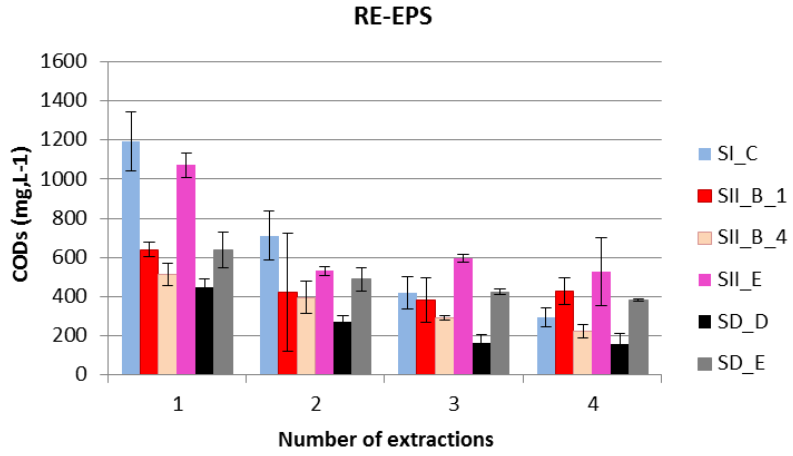

(b)

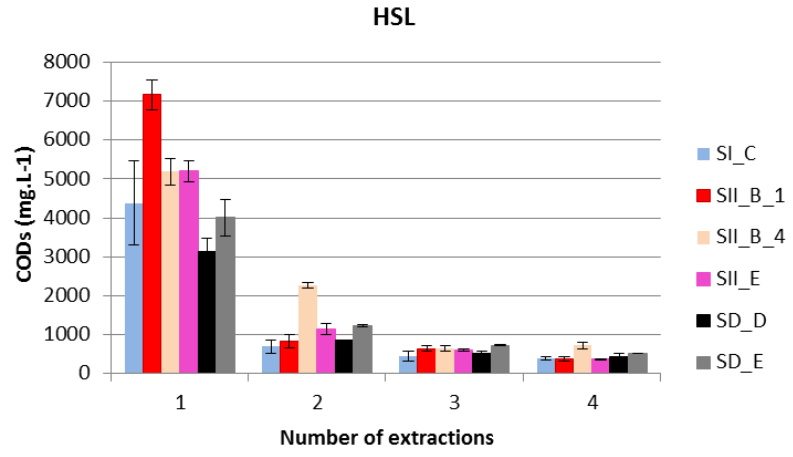

(c)

Figure 24 : Extracted sludge COD concentration depletion for (a) S-EPS, (b) RE-EPS and (c) HSL for six different sludge

Cumulated mass COD extracted profiles of the 6 sludge (figure 25) showed that a plateau was reached for each compartment before increasing again in the following extraction. This means that there are three compartments of different nature as regard the amount of organic matter extracted. An extraction number of 4 is a good compromise between efficiency and easiness of practical implementation to extract the main organic matter of all the sludge types, minimizing contamination by other remained fraction to the following one.

The representativeness of the extracted organic matter will be studied at the same time than chemical and biological accessibility correlations.

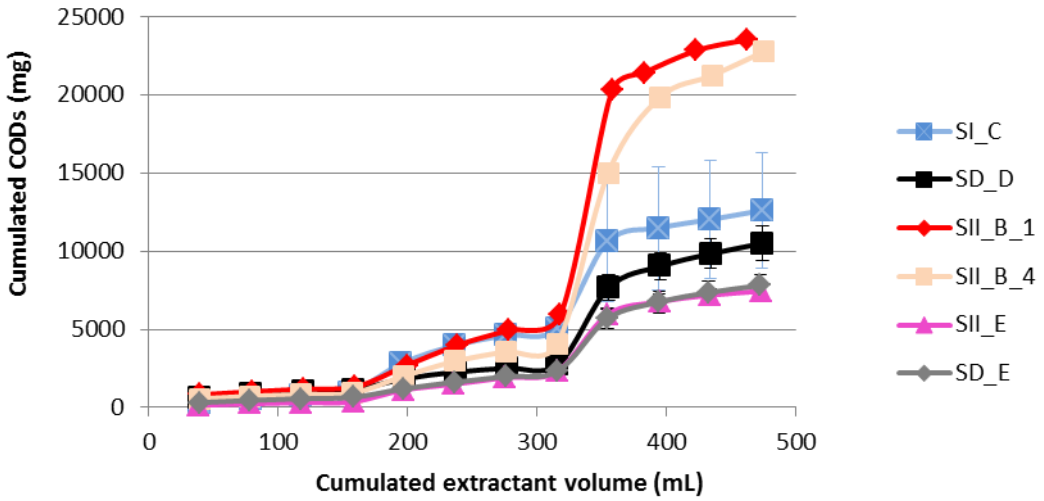

Figure 25 : Extracted sludge CODs profiles for several sludge studied

III.1.2.2. Fractions extraction repartition and sludge type

Fractionation obtained by chemical extractions has been performed for 52 sludge samples defined in the previous chapter. As primary, secondary, digested and thermally treated sludge have been used, analysis of the repartition of the fractions was performed in order to check the variability and profile differences of each sludge. The fractionation for all the studied sludge samples is presented in a boxplot in figure 26. 6 primary sludge samples, 23 secondary sludge samples, 15 anaerobic digested sludge samples and 8 thermally treated sludge samples were tested. As can be seen, total extraction percentage is asymmetrically distributed. The median is about 41% of total COD and half of the sludge samples are extracted with percentages between 38% and 52% of total COD (limits of the box).

This means indeed that about 50% of matter is not extracted. Thus, representativeness of the accessible organic matter in extractible fractions has to be validated.

Concerning each fraction, only the fractions S-EPS and RE-EPS present low variations of percentage of extraction with 1 to 5% and 5 to 8% of COD respectively. Identified outliers for S-EPS come from the thermally treated sludge where solubilization of particular matter has occurred. DOM and HSL are the fractions with higher variations. Whereas HSL is better distributed with a median of 25% and few outliers, DOM repartition is not symmetric. This aspect is mainly due to thermally treated sludge, for which DOM goes from 17% to 34% (outliers). Moreover, HSL is the largest fraction which represents half of the total fraction followed by DOM, RE-EPS and S-EPS. As variability is represented by the large box and whiskers, an analysis of the same distribution is performed for each kind of sludge in order to identify sludge specificities.

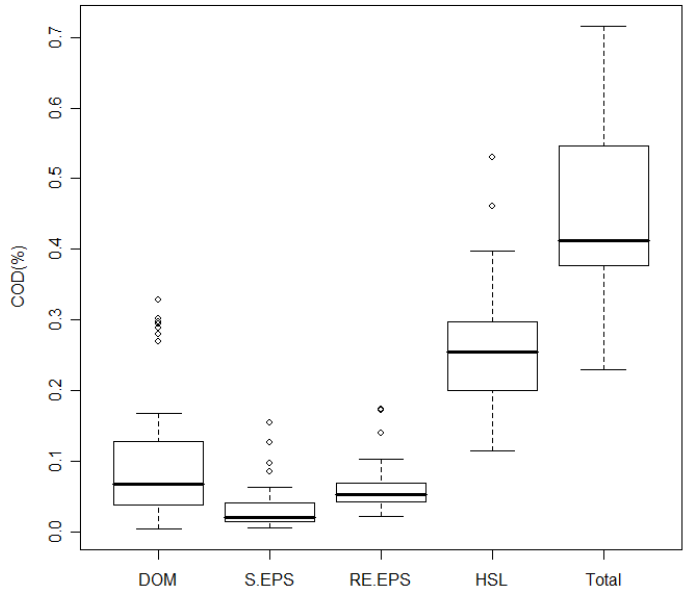

Figure 26 : Boxplot representation of the COD fractions from sequential extractions of all the sludge

One of the most heterogeneous categories of sludge is the primary sludge. The boxplot presented in figure 27a, shows that there is an asymmetric repartition in each fraction. Median of total extraction is about 35% but the range goes from 22 to 40% of total COD, below the median obtained for all the sludge samples. S-EPS, RE-EPS and DOM are concentrated around their median whereas HSL is more expanded.

This can be explained by the fact that primary sludge mainly depends on wastewater quality and settler efficiency. Large particles from wastewater can indeed affect primary sludge characteristic and make them very heterogeneous for analysis.

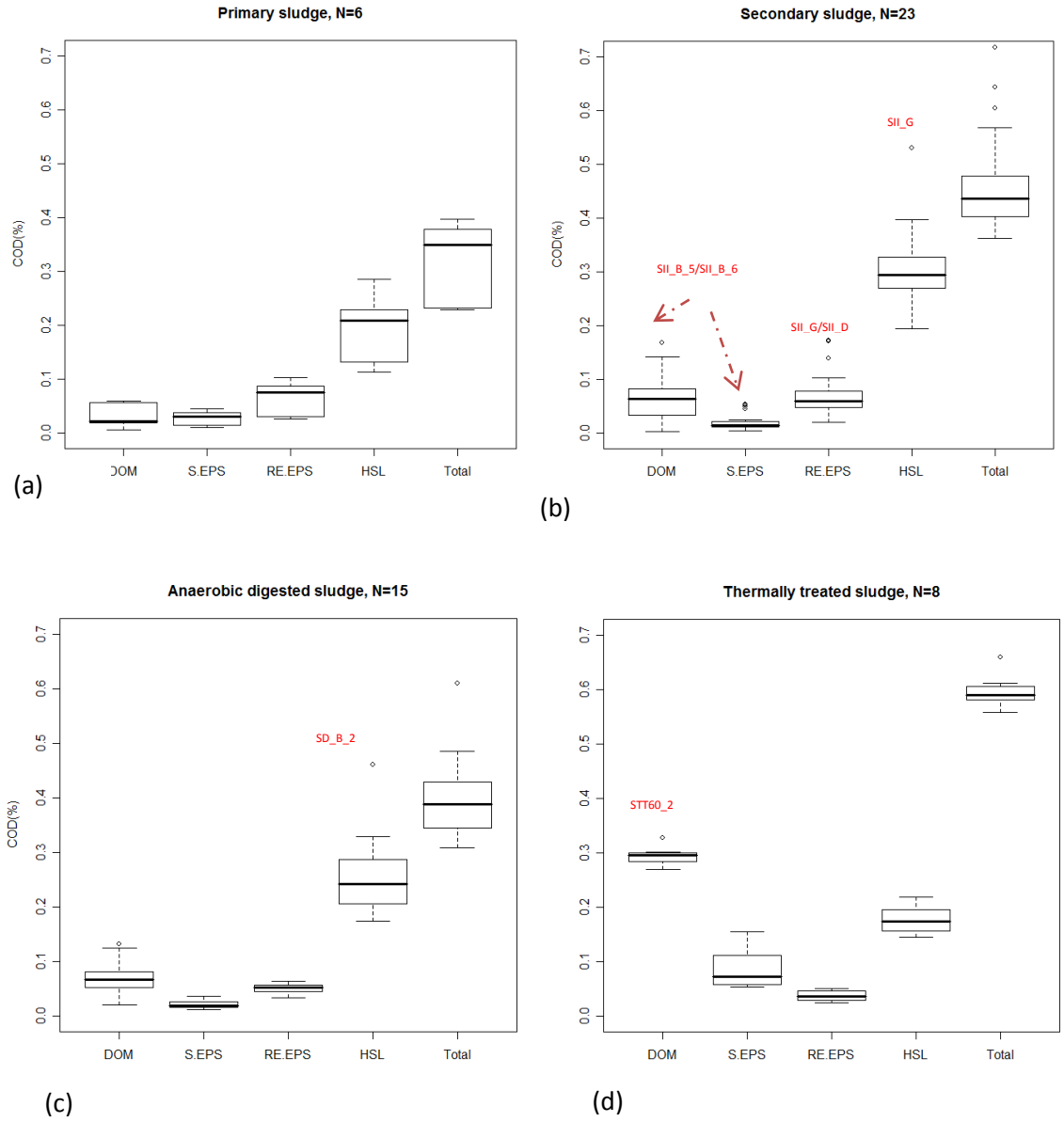

Figure 27 : Boxplot representation of COD fractions from sequential extractions for (a) primary sludge, (b) secondary sludge, (c) anaerobic digested sludge and (d) thermally treated sludge

Concerning the secondary (figure 27b) and anaerobic (figure 27c) sludge, similar profiles are observed. The total extraction median is about 45 and 38% of COD respectively. HSL is the main extracted fraction (30 and 25% respectively), followed by DOM, RE-EPS and S-EPS. Only one outlier sample is identified for anaerobic sludge whereas three are identified in secondary sludge.

These three outliers are two sludge samples coming from the same wastewater treatment plant sampled at different times (SII_B_5 and SII_B_6). In fact, unexplained problem occurred during this period in which DOM was very high, close to thermally treated sludge (17%). The third outlier SII_G comes from a membrane bioreactor (MBR) where the HSL fraction was very high (55%) as the total extraction (71%).

MBR process has indeed the particularity to work at high SRT in order to concentrate biomass. With this system, EPS do not cross the membrane and they are concentrated in the sludge.

A better repartition is found for thermally treated sludge (figure 27d). Distributions are symmetric and concentrated around the median for all fractions. In fact, this homogeneous feature is probably due to the fact that the 8 sludge thermally treated at different temperatures (60°C and 165°C) came from the same plant (B) but sampled at different times. At the contrary of the general trend obtained for all sludge, DOM is the main fraction extracted (30%), followed by HSL (18%), S-EPS (8%) and RE-EPS (5%). This is due to the solubilization of particular compounds into soluble during the thermal treatment. Thus, HSL and RE-EPS were impoverished whereas DOM and S-EPS content increased.
Whereas thermally treated sludge has a specific profile in agreement with the thermal solubilization occurring in the pre-treatment, fractionation does not lead to discriminant profile from primary, secondary and anaerobic sludge. They are mainly composed of HSL and RE-EPS representative of the less chemically accessible fractions. However, primary sludge has the lowest percentage of HSL and of total extraction.
In parallel, some granulometry tests have been performed on several sludge samples. Globally primary sludge has the highest median size particles (100µm) with the poorest total extraction yield whereas the lowest median size particles (28µm) was obtained for SII_MBR which had one of the highest extraction yield (72%). Based on this observation, the limitation of the extraction protocol by the sludge granulometry gives rise to questions.

Does granulometry limit the sequential extraction protocol and accessibility sludge simulation? Does accessibility correlate with granulometry of sludge?

The next section investigated these points.

III.1.2.3. Effect of size particle distribution on chemical extractions protocol

In order to evaluate the correlation between extraction and granulometry, a test has been set up. It consisted in comparing the extraction of three kind of sludge in duplicate (primary, secondary, anaerobic) before and after grinding with an Ultrathurax system which reduced the granulometry (78%, 81% and 72% respectively of initial median size particles d50). Results are shown in the Table 19. COD extraction percentages were similar before and after Ultraturax with relative deviations of 4.82, 2.29 and 0.73% of total COD respectively for primary, secondary and anaerobic sludge.

These values were closed to the mean standard deviation calculated between two replicate for the extractions of all the sludge samples (2.93 ±2.70% COD). Thus, deviations were not significant. And over all, the same distribution of the fractionation was shown on the range of d50 from 19.6 to 153.5µm.

Table 19 : COD extraction comparison before and after grinding for primary, secondary and anaerobic sludge

	Primary sludge			*Secondary sludge*			*Anaerobic digestion sludge*		
%COD	Raw	Grinded	Standard deviation (%)	Raw	Grinded	Standard deviation (%)	Raw	Grinded	Standard deviation (%)
DOM	2.06	3.01	0.67	0.32	1.64	0.94	6.70	8.10	0.99
S-EPS	1.45	1.94	0.34	0.80	0.99	0.14	2.63	2.83	0.14
RE-EPS	10.28	8.41	1.32	10.32	8.85	1.04	3.38	3.35	0.02
HSL	22.94	16.55	4.52	30.32	33.51	2.26	18.13	17.60	0.38
Total	36.73	29.91	4.82	41.76	45.00	2.29	30.84	31.88	0.73
d50 size particle (µm)	98.16	21.49	78*	153.5	29.46	81*	69.89	19.57	72*

**percentage t of variation calculation*

Moreover, figure 28 presents the total extraction of COD obtained for several kind of sludge versus the median size particle. No correlation appeared between total extraction and sludge granulometry between 20 to 153µm.

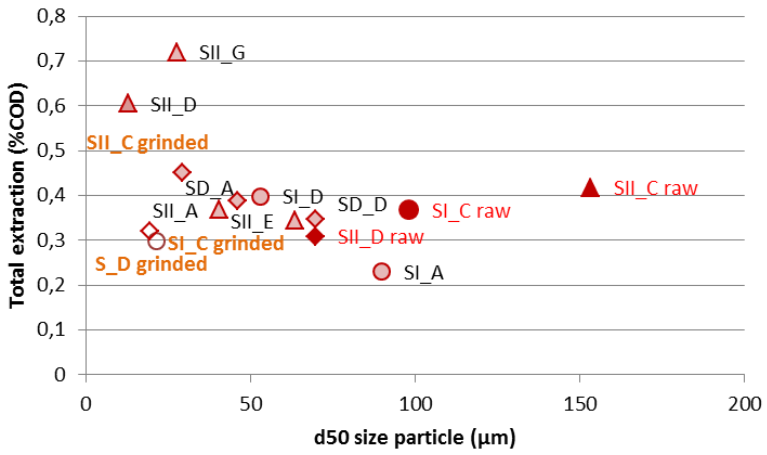

Figure 28 : COD total extraction versus median size particle for several kinds of sludge

This means that chemical extraction protocol is thus not limited by sludge granulometry. Consequently, chemical accessibility is not perturbed by particle size in a granulometry range of (20-153µm).

One hypothesis is that the increase of the specific area of particles between 20 and 153µm does not impact the accessibility of sludge. Indeed, results obtained are in adequacy with the literature. The accessibility and the enzymatic kinetic are not influenced by the range of the granulometry studied. Silva et al. (2012) showed that enzymatic kinetic of straw by decreasing its particle size (800µm) by sieve-based grindings was enhanced until a limit of granulometry. The limits were found at 270 µm for glucose release and 100 µm for reducing sugars release. According to authors, cellulose crystallinity was not enough altered by these techniques and accessibility was not improved below these granulometry values. Moreover, Bougrier *et al.*, (2006) found that thermally treated sludge subjected to deflocculating in thermal treatment had twice higher median size particles (77 µm) than secondary sludge (36 µm) due to chemical bonds creation. They showed that thermal treatment enhances biodegradability kinetics (50%) by solid solubilization effect but not by decreasing granulometry. Authors compared pretreatments such as ultrasonication and thermal treatment before anaerobic digestion and showed that ultrasonication made particles smaller (10 µm, 70% of median diameter reduction) but did not solubilize solids. Enhancement of kinetics and bioaccessibility is less important than after thermal treatment. That means that bioaccessibility is not directly linked to granulometry (<200 µm) but is linked with macromolecules solubilization potential.

III.1.3. Biochemical nature of sludge and extracted organic matter

Biochemical characterization of non-fractionated and fractionated sludge were further performed in order to investigate what types of molecules were extracted and if they were representative of sludge organic compounds.

III.1.3.1. Non-fractionated sludge characterization

As previously mentioned in chapter I, the main biochemical fractions composing sludge are proteins, lipids and carbohydrates. In order to investigate what kind of macromolecules are extracted, the global nature of sludge was analyzed. Boxplots of each kind of sludge are presented in figure 29. Primary sludge (figure 29a) is mainly composed of carbohydrates (median of 32% of total COD) coming from settled wastewater fibers compounds. Then, proteins and lipids follow with respectively a median of 20% and 13% of total COD. The outlier identified in the lipids fraction is the grease treatment refusal which is obviously mainly composed of lipids. These results are coherent with the literature (Table 1 in chapter I). In the same way, secondary (figure 29b) and anaerobic digested sludge (figure 29c) are also in agreement with values presented in Table 1.

Both type of sludge are mainly composed of proteins (41% in both cases) from microbial aggregates and microbial products. Then, carbohydrates and lipids are less important for both (respectively 16 and 8% for secondary sludge and 15 and 10% for anaerobic digested sludge). However, high variations in the biochemical composition of primary, thermally treated and anaerobic digested sludge are observed. Boxplots from secondary sludge are less expanded around the median.

Analytical methods succeeded in characterizing most of the matter: median values of 82% of COD for primary sludge, 71% of COD for secondary sludge and 61% for anaerobic digested sludge. The remaining organic matter molecules not characterized could be humic acids, lignocellulose-like and nucleic acids compounds that could not be measured in these experiments.

Concerning thermally treated sludge, proteins are the main component with a median of 26%, followed by carbohydrates (8%) and VFA with 7% of COD (figure 29 d). VFA fraction is more important because unsaturated lipids and long-chain fatty acids are broke-down by thermal treatment as suggested by (Wilson and Novak, 2009). As a consequence, lipids content is very low, with a median at 2.7% of COD. From our results, 70% of thermally treated lipids from secondary sludge are solubilized.

Around 30% of lipids solubilized are found through VFA content but the remaining 40% is not measured. This fraction is probably under LCFA form not measured in this study.

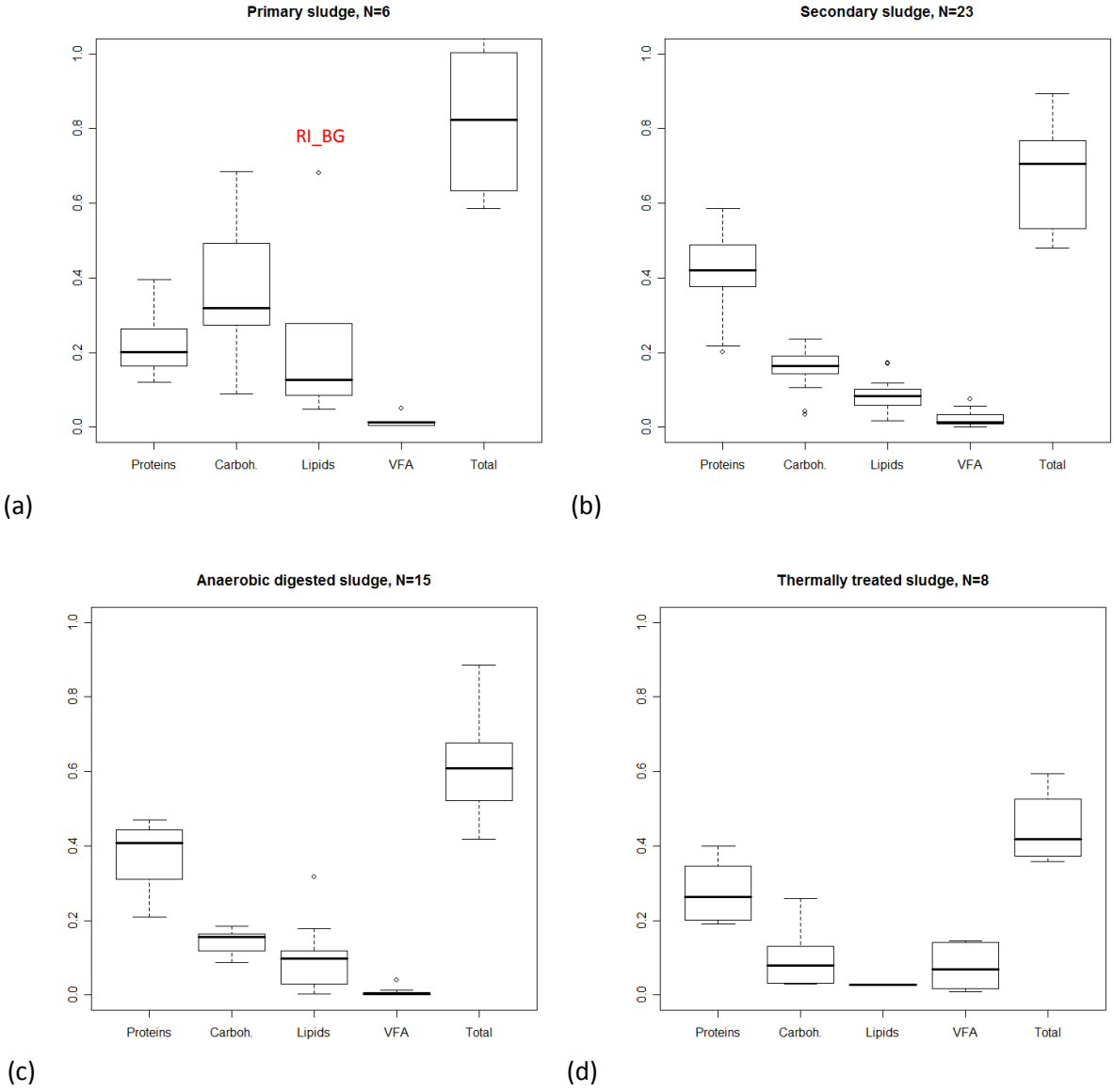

Figure 29 : Biochemical fractionation of primary (a), secondary (b), anaerobic digested (c) and thermally treated (d) sludge

III.1.3.2. Fractionated sludge characterization

In order to investigate what type of molecules is obtained from the chemical extraction protocol, proteins, VFA and carbohydrates were measured in the fractions samples (represented by the merge of the 4 extractions by compartment). VFA concentration, contained in the DOM fraction, is null for SE-EPS, RE-EPS and HSL. As lipids measurement is only applicable on total sludge, soluble extracts were not analyzed. Figures 30 a, b and c present the repartition of protein and carbohydrates measured into respectively S-EPS, RE-EPS and HSL fractions.

As no significant discrimination from sludge type could be noticed on extracted organic matter measured on S-EPS, RE-EPS and HSL, boxplots represent the entire sludge category. Concerning DOM, its interesting biochemical repartition is studied in Table 20 by category of sludge.

S-EPS, RE-EPS and HSL are mainly composed of proteins (respective medians of 55%, 74% and 56% of COD). However, these proteins could have different structural properties since they are not extracted with the same strength. Carbohydrates compounds were extracted with a median yield between 9% and 12% of COD for the three fractions. Remaining material could be composed of lipids (long chain fatty acids), humic acids, uronic and nucleic acids, and other minor compound (Comte *et al.,* 2006).

Indeed, extraction with soda could cause a saponification reaction with a solubilization of lipids. So, RE-EPS and above all HSL (higher soda concentration) should contain between 10% and 20% of COD from total sludge lipids.

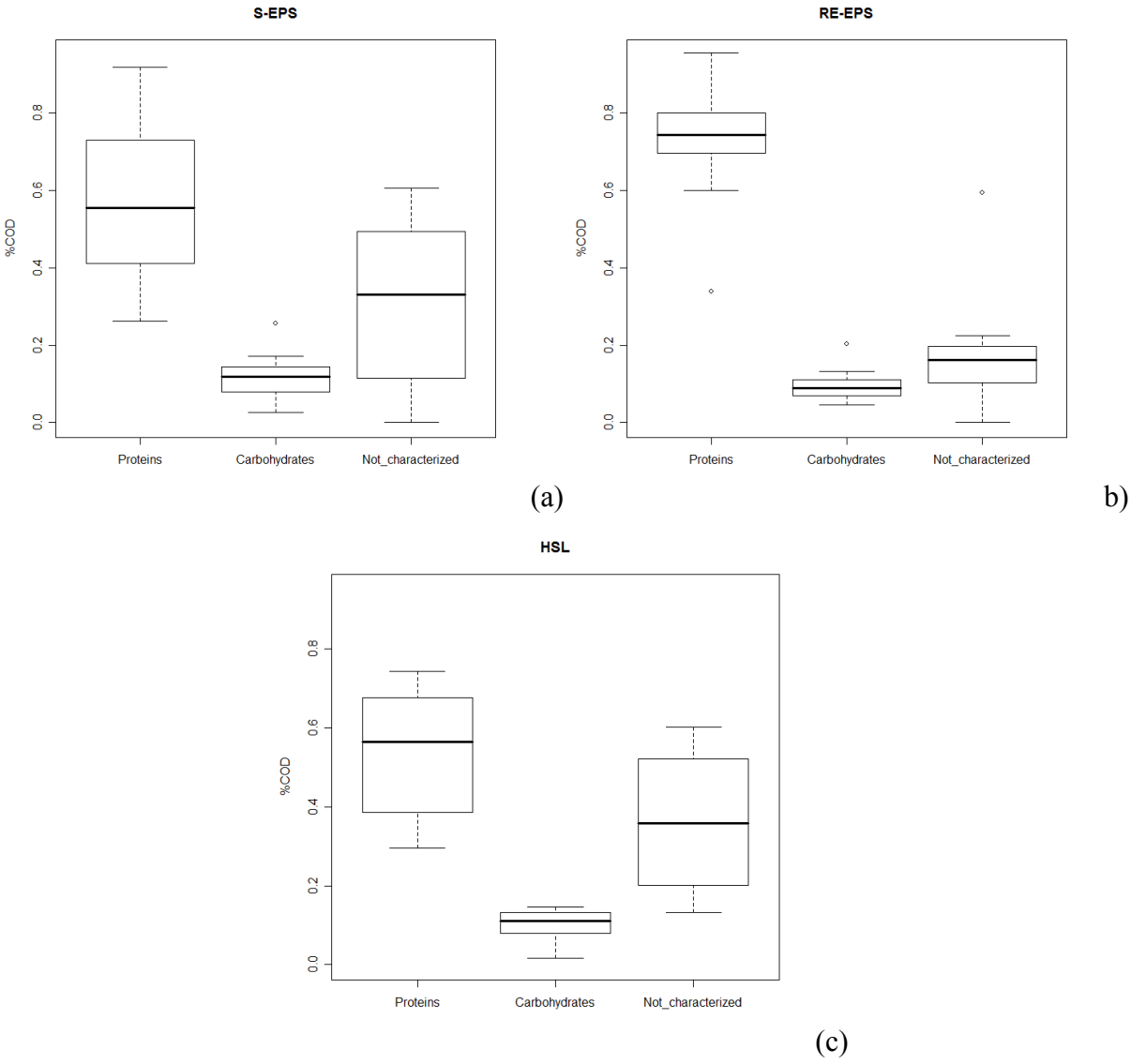

Figure 30 : Organic matter repartition in S-EPS (a), RE-EPS (b) and HSL(c) fractions

Concerning the DOM organic matter repartition (Table 20), carbohydrate is also the lowest component measured, between 6.42% and 17.45% for anaerobic digested sludge. Anaerobic digested sludge still contained hydrolysis products not degraded during the anaerobic digestion from protein (53.23%) and carbohydrates macromolecules. VFA, rapidly degradable, is the lowest fraction in anaerobic digested sludge. DOM from primary and secondary sludge are mainly composed of VFA (with high standard deviation for secondary sludge) and then of proteins.

In these cases, VFA could result from a pre-hydrolysis step performed in buffer tanks (usually installed before anaerobic digesters), samples transport or in settler for primary sludge.

DOM from thermally treated sludge contains mainly proteins (52.98%), VFA (23%) while carbohydrates content is low (8.35%). Thus, solubilization of macromolecules has mainly targeted proteins and long chain fatty acids. This observation is in agreement with Mottet (2009) on waste activated sludge thermal treatment.

Table 20 : Organic matter repartition in DOM fraction for each kind of sludge

	g eq COD.g COD DOM^{-1}					
Sludge	Proteins	*SD*	VFA	*SD*	Carbohydrates	*SD*
Primary	12.19	7.62	67.55	15.64	6.42	6.15
Secondary	36.13	10.63	36.58	21.29	10.19	7.95
Anaerobic digested	53.23	21.35	9.43	12.25	17.45	15.33
Thermally treated	52.98	20.57	23.00	20.46	8.35	7.65

Considering all the extracted fractions, the proteins are the molecules the most solubilized by the chemical extraction protocol whereas the carbohydrates are the least ones. As the 3D-SE-LPF characterization protocol uses the combination of sequential extraction and fluorescence spectroscopy, this result is important. Monosaccharides and VFA are not naturally fluorescent whereas proteins molecules are fluorescent. This means that fluorescence spectroscopy could measure the main compounds of all the extracted fractions and could reveal more specific information about structural complexity in each fraction than the global measurement.

III.1.4. Sludge fractionation conclusion

The main component of fractionated sludge is the proteins as well as in the non-fractionated sludge. However, 45% of total COD is extracted. The question to investigate not yet answered is the following: is the organic matter extracted representative of the bioaccessible and biodegradable part of the sludge?

We already saw that sludge granulometry between 20 µm and 153 µm does not affect the sequential extraction protocol, neither the accessibility. Size distribution analysis has not been performed on thermally treated sludge which have high COD extraction yields (median of 60% COD). However extraction profiles of thermally treated sludge have the particularity to be in adequacy with solubilization of particulate organic matter occurring during thermal pretreatment.

Indeed, whereas particulate organic matter extracted HSL and RE-EPS become impoverished, soluble organic matter DOM and S-EPS rise in thermally treated sludge in comparison of the others sludge.
Shifts in matter organization occur in thermal treatment and affect the fraction distribution. Additionally, thermally treated sludge has a readily hydrolysable fraction higher than without thermal treatment (Mottet, 2009) and this aspect is reflected through the fractionation analysis.

In order to go further and to correlate chemical accessibility provided by sequential extraction protocol with bioaccessibility, several tests have been set up to investigate this hypothesis.

III.2. Correlation between chemical and biochemical accessibility investigation

To investigate that the chemical accessibility simulated by extraction protocol is linked with the biological accessibility, several tests have been set up. The first one consists in an anaerobic digestion of secondary sludge through a batch test. The extracted fractions analyses were performed at several times of the biodegradation.

Then, in order to go further on kinetics visualization of fractions, two tests were performed on thermally treated sludge and secondary sludge in respectively batch and continuous mode. Thermally treated sludge was deprived of all the successive fractions and batch tests were performed on each remaining samples. Secondary sludge was deprived of DOM and of DOM+S-EPS+RE-EPS and fed the continuous lab scale reactors.

III.2.1. Material flow investigation : anaerobic stabilization test

Two batch reactors (4 L) of anaerobic stabilization have been set up (see chapter II). Secondary sludge (named SII_F_1 and SII_F_2) sampled from the same wastewater treatment plant F have been used. The reactors were operated under mesophilic conditions (37°C) without addition of inoculum. In fact, since the aim of the test is to follow the evolution of chemical extraction fractions, the inoculum presence could perturb extraction analysis. The mean COD concentration was about 9000 mg $COD.L^{-1}$ composed of 22% of proteins, 23% of carbohydrates and 4% of lipids for both sludge. A two-phase profile was observed in methane production (figure 31).

Similar results were obtained with SII_F_1 but are not shown for clarity of the figure.

Sequential extraction protocol was applied at 4 different instants: at initial time (A), at the end of the first plateau (B), during transitory degradation (C) and at the end of the final plateau (D). Figure 31 shows the several samples depending on the cumulate methane production profile of SII_F_1 reactor.

The first plateau is linked with the readily biodegradable fraction (X_{RC}) and the second one with the slower fraction (X_{SC}) composed of more complex macromolecules as found in literature (cf. chapter I).

BD and X_{RC} were calculated as described in chapter II and are equal to respectively 35+/- 5% and 19+/-8% of total COD. Then, X_{SC} represents 16+/-4% of total COD.

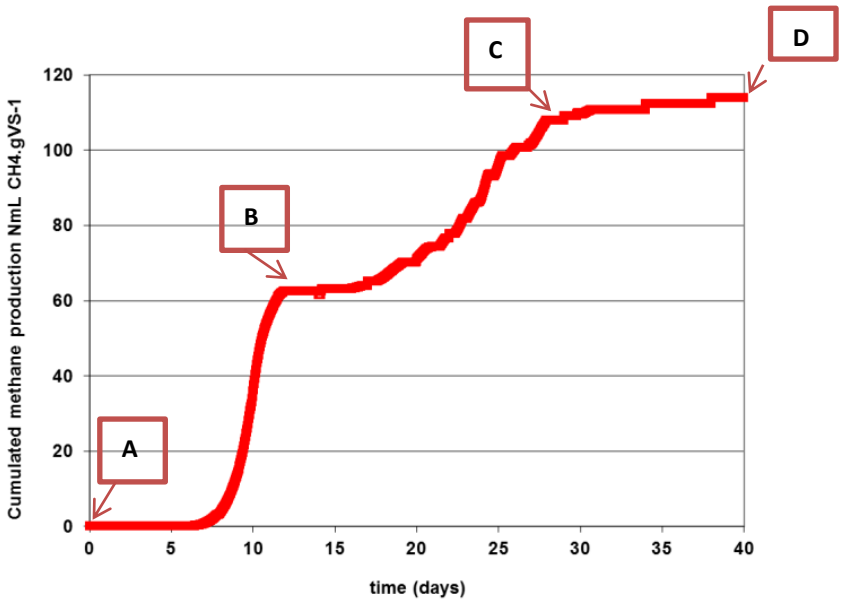

Figure 31 : Cumulated methane production obtained during the anaerobic digestion of SII_F_1 and sampled recovered for sequential extraction analysis

VFA concentration measurements have been performed daily with time (Figure 32). The concentration profiles are in adequacy with the two-phase profile of cumulated methane production, as noticed by Mottet (2009) and Ramirez *et al.* (2009). Acetate and propionate evolution are quite similar in both reactors. During the first phase corresponding to the period between A and B, acetate is produced until day 8 and then consumed. This lag time (8 days) corresponds to the methanogens growth (generation time).

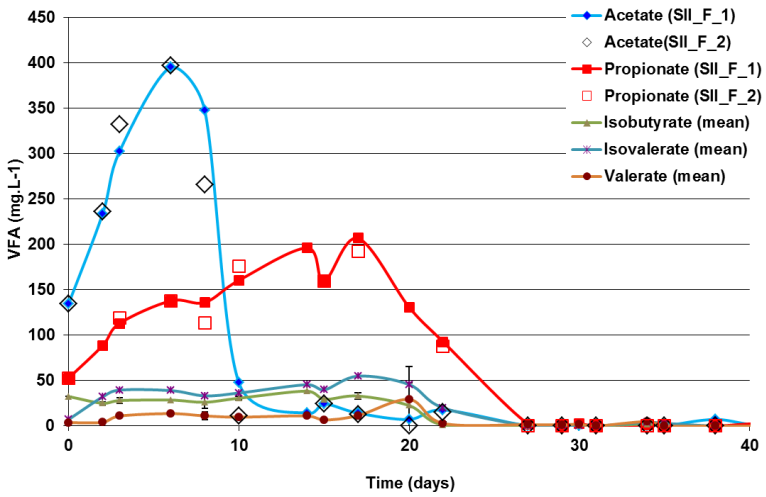

Figure 32 : Evolution of VFA in both anaerobic digestion of SII_F1 and SII_F2

At the beginning, acetate production (acetogenesis) was faster than acetate uptake (methanogenesis) because inoculum was absent and because methogens needed to grow up. After this period, acetate production was slower than methanogenesis as regard the low acetate residual content. The second phase corresponding to the period between B and D, propionate was produced and accumulated until day 18. Then, it was transformed into acetate (acetogenesis) and was degraded until reach a concentration closed to 0. According to Mottet (2009), propionate and acetate accumulation was due to a limiting effect of hydrolysis step. VFAs of higher molecular weights were degradation products of sugars and amino acids, themselves products of hydrolysis. Evolution of the sequential extraction fractions was analyzed (figure 33) through the extracted COD mass. Bar errors are standard deviations obtained on both reactors.

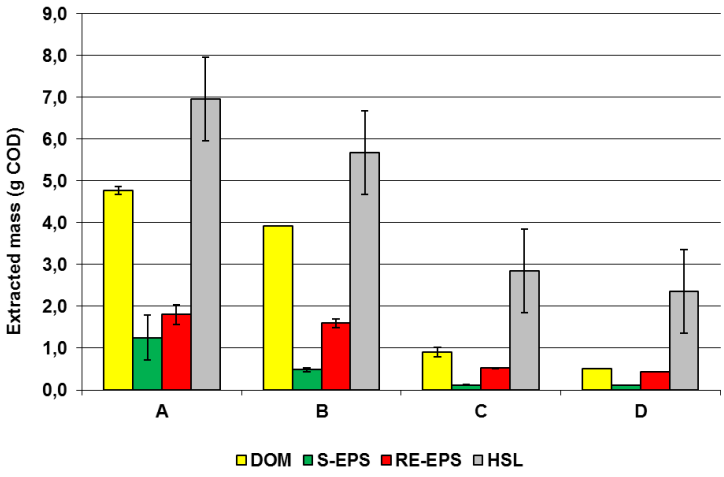

Figure 33 : Evolution of extracted fractions during anaerobic digestion of SII_C_2 and SII_C_3

During anaerobic digestion, total extracted COD mass decreased with time. COD mass balance was performed (Table 21) between initial sample (A), X_{RC} uptake sample (B), and final sample (D). The total extracted COD was mainly biodegraded (77%) and the non-extracted fraction represented 23% of the total COD biodegraded. Therefore, the sequential extraction protocol was targeting the main part of the biodegradable fractions. Thus, the 4 sequential extractions representing 50% of total COD are enough to be representative of the biodegradable fraction.

Table 21 : Mass balance calculated between samples A-B and B-D

Samples	DOM	S-EPS	RE-EPS	HSL
COD mass degraded (mg COD)				
A-B	849	767	205	1288
B-D	3408	375	1158	3307
A (initial mass)	14782			
Total (A-D)	11358			
%COD degraded				
(A-B)/A	*18%*	**61%**	11%	19%
(B-D)/A	*71%*	30%	**64%**	**48%**
Total	*89%*	91%	76%	66%
Total (A-D)/A	**77%**			

In both studied secondary sludge, DOM was higher (14% of sludge total COD) than previously analyzed secondary sludge (median of 7% of COD). However, DOM biodegradation mass balance during the first phase could not be performed. Indeed, the sample B was taken when solubilization of slowly hydrolysable macromolecules occurred. Thus, initial DOM was affected by the hydrolysis products not yet degraded (VFA, protein, LCFA and monosaccharides). This observation explained the production of organic matter at the phase B (figure 34).

Biochemical analyses were also performed during this test (figure 34a and b). Soluble proteins contained in DOM were biodegraded at 56% during A-B period from 1200 to 550 mg $COD.L^{-1}$ and at 27% during the B-D period from 550 to 400 mg $COD.L^{-1}$ whereas soluble carbohydrates were produced during the first phase and then biodegraded at 98% at the end of the second phase. Moreover, 50% of particulate carbohydrates uptake (4 g COD) matched with soluble carbohydrates production (2 g COD), representing hydrolysis products. The remaining 50% could have been degraded before sample B.

Concerning the particulate organic matter fractions, the accessible EPS (external floc layer) S-EPS was uptaken at 61% during the first phase (A-B). Less accessible fractions RE-EPS and HSL were mainly hydrolyzed during the second phase (B-D) at respectively 64 and 48% associated with X_{SC}. This means that RE-EPS and HSL were slowly biodegraded whereas S-EPS was rapidly uptaken. Thus, chemical accessibility goes to the same way that biological accessibility. Moreover, the percentage of total degradation of each fraction showed a decreasing profile: from table 21, S-EPS was the most biodegraded fraction (91% of COD) at the contrary of RE-EPS and HSL (76 and 66% of COD respectively).

Concerning macromolecules content, particulate proteins were degraded at 37% during the first phase and at 30% during the second one (figure 34a), whereas particulate carbohydrates were only degraded during the first phase (figure 34b). Thus, proteins were the main component degraded in RE-EPS and HSL.

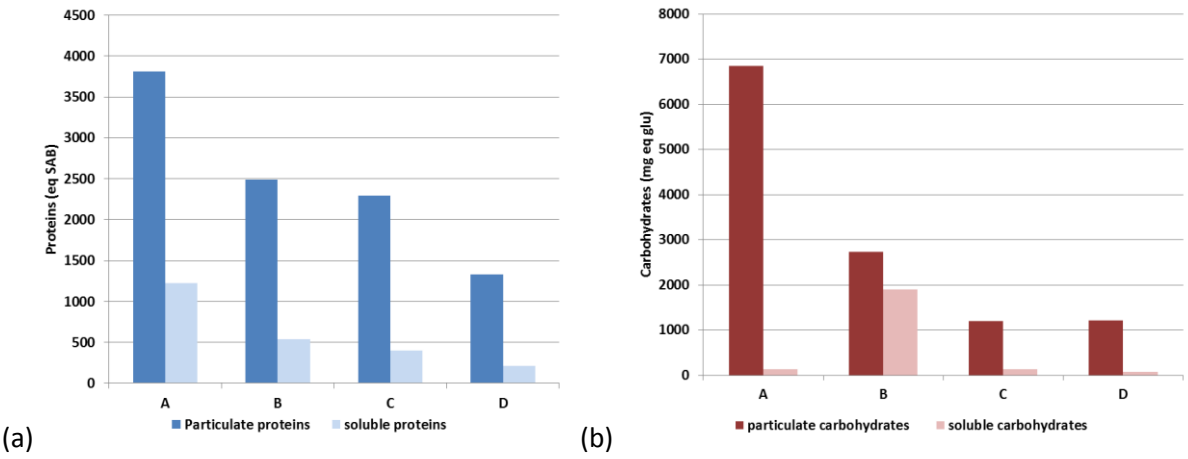

Figure 34 : Biochemical fractionation evolution during stabilization test: (a) proteins and (b) carbohydrates

In order to calculate the fraction contribution in each biodegradation phase, mass balance was performed during the periods A-B for the first phase and B-D for the second phase. Table 22 represents mass balance performed between two phases A-B and B-C where respectively X_{RC} and X_{SC} were biodegraded. The aim of this mass balance was to calculate the participation of each in the X_{RC} and X_{SC} biodegradation. As DOM mass balance cannot be made directly, biodegraded DOM was calculated by subtracting the sum of the biodegraded mass of the others fractions from total COD mass biodegraded in this first phase as following:

$$DOM_{biodegraded} = COD_{biodegraded} - (SEPS+RE\text{-}EPS+HSL)_{biodegraded}$$

Table 22 : COD mass balance and recovery of X_{RC} and X_{SC}

Period A-B	DOM	S-EPS	RE-EPS	HSL	SEPS+RE-EPS+HSL	Biodegradable COD
Initial COD (mg COD)	4651	1611	1938	6834	10383	6669
Degraded COD (mg COD)	*4175	983	213	1298	2494	6669
COD degraded (%)	90%	61%	11%	19%	24%	
Readily biodegradable composition (%COD)	**63%**	**15%**	**3%**	**19%**		**100%**

Period B-D	DOM	S-EPS	RE-EPS	HSL	SEPS+REEPS+HSL	Biodegradable COD
Degraded COD (mg COD)		483	1240	3280	5004	5616
COD degraded (%)		30%	64%	48%	48%	
Slowly biodegradable composition (%COD)		**9%**	**22%**	**58%**		**89%**

*: $DOM_{biodegraded} = COD_{biodegraded} - (SEPS+RE\text{-}EPS+HSL)_{biodegraded} = 6669-2494 = 4175$ *mg COD*

It appeared that DOM contributes to 63% of A-B COD degradation. Moreover, from this calculation, degradation of DOM in the A-B phase was about 90%, it represented the fraction the most available. S-EPS and HSL followed with respectively 15% and 19%. Only 3% was represented by RE-EPS.

From B-D period mass balance, DOM calculation could not be made because initial DOM biodegradation could not be determined in this second part. One assumption is that all the biodegradable DOM has been biodegraded in the first phase. Considering particular organic matter, mass balance was closed in the B-D period between the total biodegradable COD and the biodegradable S-EPS, RE-EPS and HSL. Biodegradable particular organic matter explains the X_{SC} fraction at 89% (table 22). X_{SC} contains mainly HSL (58%), then RE-EPS (22%) and S-EPS (9%). The remaining 11% of total slowly biodegradable fraction could be provided by non-extracted biodegradation.

On the contrary, in the A-B period, mass balance showed that (SEPS+RE-EPS+HSL) were not sufficient to explain this fraction because DOM is missing. This means that the most chemically available part of these fractions represented by DOM was degraded in the first phase and the less chemically accessible (RE-EPS+HSL) and slowly biodegradable in the second one.

These results are in accordance with the floc model description (figure 7, chapter II) used in sequential extractions.

General trends show that the S-EPS fraction was mainly degraded in the first phase of anaerobic digestion whereas RE-EPS and HSL were degraded in the second one. Another point observed is that biodegradability percentage of each fraction decreased with the accessibility. However, the main drawback of this stabilization test is the absence of visualization of exchange between each fraction and their degradation rates. A typical illustration is the DOM fraction. This fraction is the central place where organic matter flow in and out through hydrolysis, and product hydrolysis uptake. In order to solve this problem, another test has been set up and is presented in the next section.

III.2.2. Biodegradability and bioaccessibility investigation of sequential extraction fractions

Previous results have shown that the most accessible fractions, DOM and S-EPS, contributed to the fastest degradable fraction whereas the least accessible fractions RE-EPS and HSL contributed to the slowest degradable COD.

However, kinetics of each fraction could not be observed. The following test aimed at investigating the kinetic behavior of the degradation of each fraction. The sludge used for the test was a thermally treated sludge STT165_B.

Thermally treated sludge has been chosen because DOM and S-EPS were there more important, and DOM or S-EPS removal would be more impacting on the methane production than in secondary or primary sludge. The COD fractionation for DOM, S-EPS, RE-EPS and HSL is respectively 29.2%, 7.6%, 3.2% and 12.0%.
The test consisted in performing successive BMP tests on sludge after removing each fraction until the non-extractible fraction. By applying the sequential extraction protocol, remaining samples of each stage were used after adjusting the pH to 7 with NaOH (1N). Five BMP curves were recorded (figure 34): Total sludge (T), Total sludge without DOM (T-DOM), T-DOM without S-EPS (T-DOM-SEPS), T-DOM-S-EPS without RE-EPS (T-DOM-SEPS-RE-EPS) and T-DOM-SEPS-RE-EPS without HSL (NE).

The BMP tests have been performed with the same COD concentration (9000 mg COD.L^{-1}) and the same inoculum acclimated to this sludge in order to be able to compare the results. Then, by subtracting the methane production biogas from the total sludge one, the methane production rate of DOM, S-EPS, RE-EPS and HSL could be obtained (figure 36) as following:

BMP(DOM)=BMP(T)-BMP(T-DOM)

BMP(S-EPS)=BMP(T-DOM)-BMP(T-DOM-SEPS)

BMP(RE-EPS)=BMP(T-DOM-S-EPS)-BMP(T-DOM-S-EPS-RE-EPS)

BMP(HSL)=BMP(T-DOM-S-EPS-RE-EPS)-BMP(NE)

The cumulated methane production curve of total sludge shows a profile with four periods (figure 34). The first one occurred from 0 to 5 days (I), and then a plateau was reached after 17 days (II). The final plateau was obtained at day 26 (III). The last period was the stabilization of the methane production (IV).

As shown by figure 35, it appears that DOM removal highly impacted the biodegradability, contrary to the results obtained for not thermally treated sludge (cf. chapter II). Using the graphical analysis described in Material and Methods for X_{RC} and X_{SC} assessment, results show that total sludge X_{RC} is about 35% of COD whereas T-DOM is about 24% of COD (deviation of 11%). Indeed, DOM represents here 29.2% of the COD whereas DOM from secondary sludge was about 7% of COD.

Moreover, the DOM impact concerns phase I and mainly phases II and III, whereas previously results showed that DOM contributed mainly to the first phase degradation. This result is due to the product from thermal hydrolysis.

At temperature as high as 165°C, protein and reduced sugars react together through the Maillard reaction (glucose and glycine) in order to form molecules called melanoidins (Miyata *et al.,* 1996). These molecules are recalcitrant (Chandra *et al.,* 2008) and slowly bioaccessible. They can contribute to the third phase degradation.

Then, with particular organic matter fraction removal, both kinetic and biodegradability were affected. Cumulated methane production curves show that total biodegradability decreased when the chemical accessibility decreased. NE fraction was biodegradable at 16%. These results validate the hypothesis that extracted COD is mainly contained in the biodegraded fraction as for the previous test.

Concerning kinetics, there was also a hierarchical classification depending on the chemical accessibility considered.

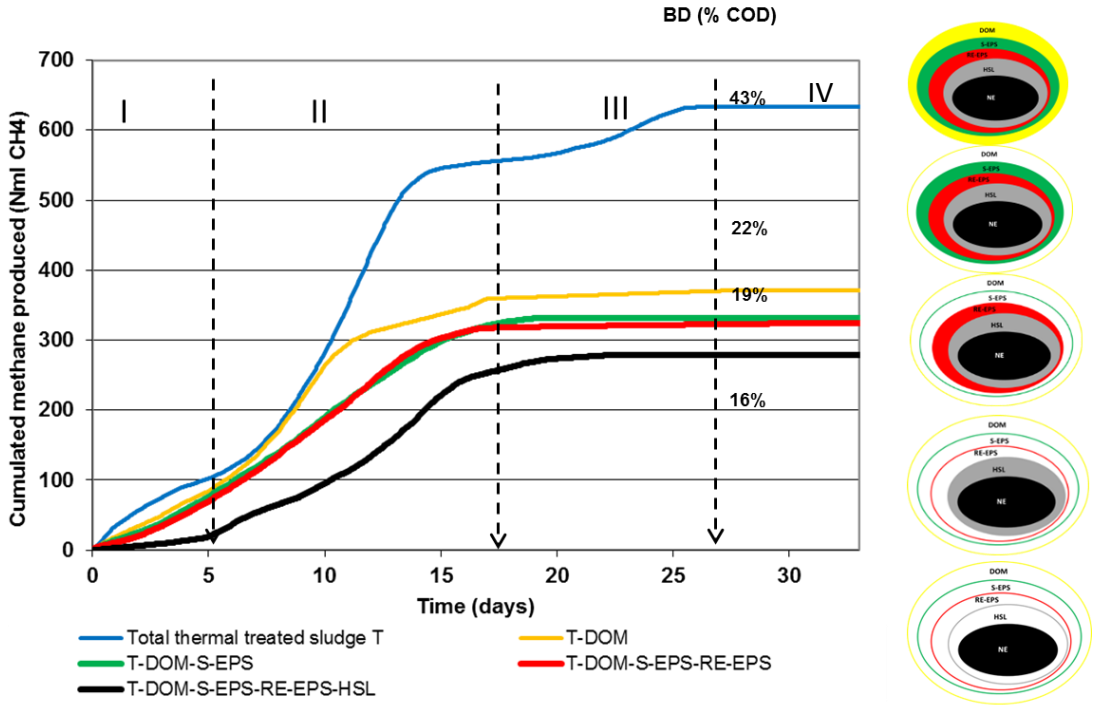

Figure 35 : Cumulated methane produced obtained for total sludge deprived of successive fractions (the highest to the least accessible) by BMP tests

A zoom between 0 and 2 days is presented in figure 36. The most the accessible fractions were removed, the slowest were the initial curve slopes. Indeed, total sludge was characterized by the highest slope value of 33 NmL $CH_4.d^{-1}$.

After DOM removal, slope was lower with a value of 20 NmL $CH_4.d^{-1}$. S-EPS removal from T-SEPS led to a slope value twice lower than total sludge with 15 NmL $CH_4.d^{-1}$.

Then, RE-EPS removal had a small impact on the slope with a value of 12 NmL $CH_4.d^{-1}$. Removing of S-EPS and RE-EPS led to similar curves because RE-EPS content was low in thermally treated sludge (3.2%) due to the solubilization.

Finally, the BMP curve of the NE degradation was the slowest fraction with an initial slope of 3 Nml $CH_4.d^{-1}$.

Removing extracted fractions impacted both kinetic and degradation methane production. That means there is a link between chemical accessibility and biological accessibility.

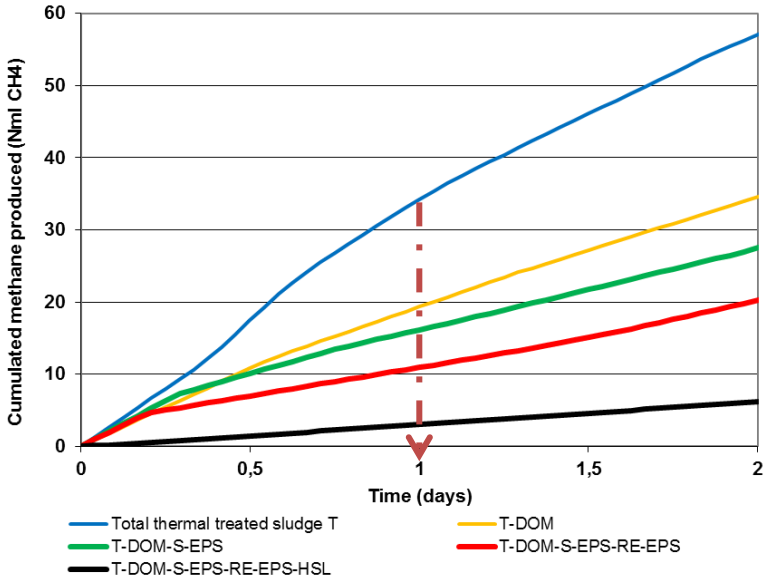

Figure 36 : Zoom [0-2] days of cumulated methane produced obtained for total sludge deprived of successive fractions (the highest accessible to the least one)

Kinetic of methane production is presented in figure 37a for DOM and S-EPS and in figure 37b for R-EPS, HSL and NE. Thanks to the superposition of each fraction with the total sludge, an interpretation of the biodegradable sludge composition can be made.

In phase I, the most bioavailable fraction was already uptaken, due certainly to VFA and available biochemical molecules consumption (figure 37a). In this phase, DOM contributed with a fast production peak but its main contribution was in the two first phases with 70% of the total (I+II) area and 30% in the last area (III). Superposition of T and DOM curves (figure 37a) shows that phase II and phase III were constituted of slowly biodegradable DOM, certainly due to the melanoidins-like compounds produced during thermal treatment at 165°C. Concerning the particulate organic matter fractions, S-EPS was also biodegraded in the two first phases as the DOM fraction (figure 37a). Between 0 and 2 days, a production peak was also visible for S-EPS degradation. For this fraction, phase II was divided into II and II_1 at 13 days. After 13 days, a very few part of S-EPS was biodegraded until phase III.

Methane production for RE-EPS and HSL in this period was slower and lower (figure 37b). Besides, kinetics of RE-EPS and HSL was very slow during the phase II traducing slowly hydrolysis profiles. We already saw that thermal treatment had solubilized particulate fractions into soluble fractions. Thus, particulate organic matter solubilized could have been impacted on its bioaccessible and biodegradable fraction.

Finally, the NE fraction was mainly composed of two-degradation peaks in phase II (figure 37b). Phase II was thus divided in 2 phases II and II_2 at 10 days for HSL.

The biodegradation after 10 days represented the slowest degradable of all the particulate fractions.

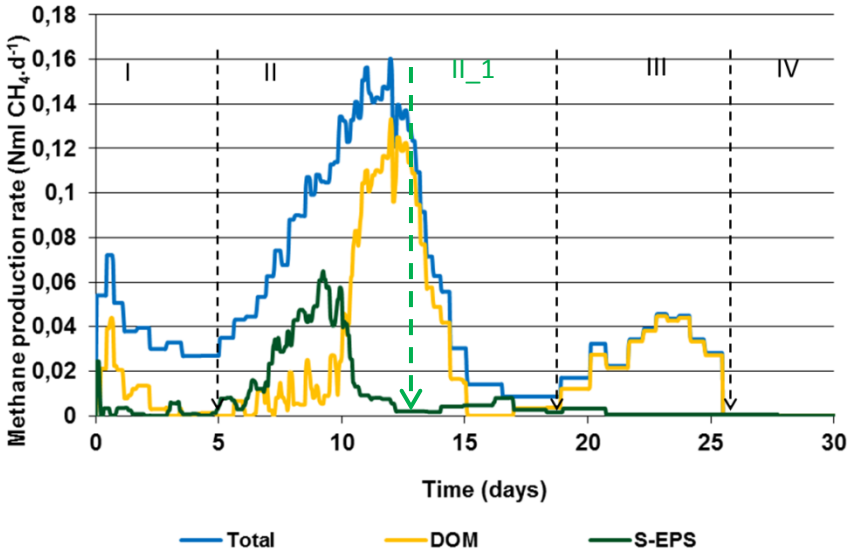

(a)

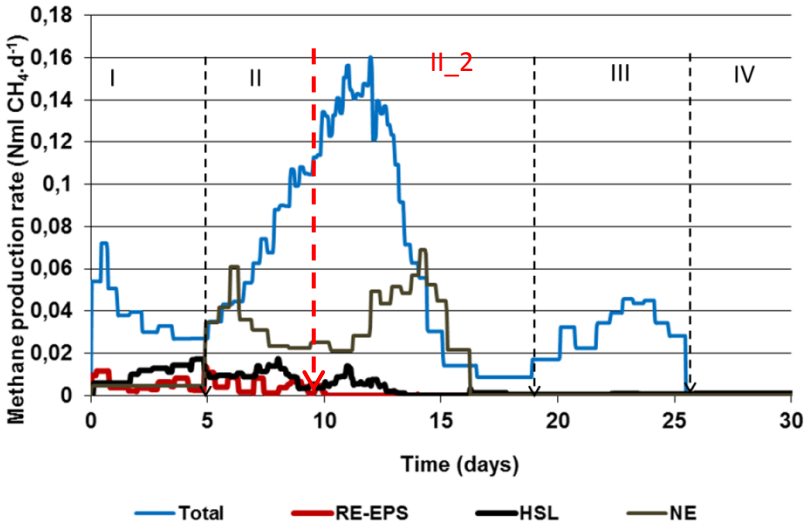

(b)

Figure 37 : Methane production curves of fraction extracted from thermally treated sludge for Total, DOM and S-EPS fractions (a) and for Total, RE-EPS, HSL and NE fractions

NE kinetic was the slowest one in comparison with the others particulate fractions. No methane production was indeed observed between 0 and 5 days. This means that no bioavailable COD was contained in this fraction but only slowly bioaccessible COD.

These results validated that both kinetics and biodegradability were impacted when accessible fractions were removed. DOM was the most accessible fraction but not necessarily the most readily biodegradable as observed in the thermally sludge case.

Because of thermal treatment, some part of DOM was indeed composed of melanoidin compounds slowly biodegradable fraction that is not naturally present in other sludge types. RE-EPS as HSL were impoverished by solubilization whereas they are larger in primary, secondary and digested sludge.

In order to go further, secondary sludge tests in continuous mode have been performed for modeling purpose (described in chapter II). The next section presents the kinetic results when total secondary sludge was deprived of DOM, and of (DOM+SEPS+RE-EPS).

III.2.3. Methane production curve and correlation of fractions extracted

In this experiment, two lab scale reactors named here after pilot 1 (P1) and pilot 2 (P2) were used together fed by total secondary sludge (SII_B) in successive batches with a low organic matter loading 0.13 $gCOD.gVS^{-1}$and at HRT of 18 days.

P1 was named as the "reference test" fed by the total sludge SII_B. On the opposite, P2 was dedicated to "disturbing tests" fed by the same total sludge deprived of some fractions: DOM and (DOM+SEPS+RE-EPS). For each disturbing phases, both reactors ran in parallel. Before the disturbing phase, a reference period has been performed where both pilots were fed by the same sludge in the same operating conditions. The results showed that biogas production and kinetics were similar (cf. chapter V). This allowed the DOM and DOM+SEPS+RE-EPS+HSL degradation kinetics determination by subtracting kinetic of P2 from P1.
In order to validate that chemical and biological accessibility were closely linked, biogas production rates from both reactors are observed.
The first disturbing consisted in removing DOM (7.4% of COD) from the total sludge (figure 38). The biogas production rate was impacted at the beginning of the curve, corresponding to the most bioavailable COD (yellow area in figure 38). Relative standard deviations between 6 and 20% were found between the Total secondary curve area and the Total-DOM curve area. By subtracting area of both curves, biodegradable COD represented biodegradable DOM.
The biodegradable DOM represented 88% of the total DOM. The remaining DOM (12%, corresponding to 1530 mg $COD.L^{-1}$) was found in the output P1.

In conclusion, DOM was a part of the readily biodegradable fraction and was well correlated to the bioaccessible COD fractions.

The second disturbing test consisted in removing DOM but also S-EPS and RE-EPS. S-EPS representing only 1.3% of total COD, its impact on the methane production rate would not be significant.

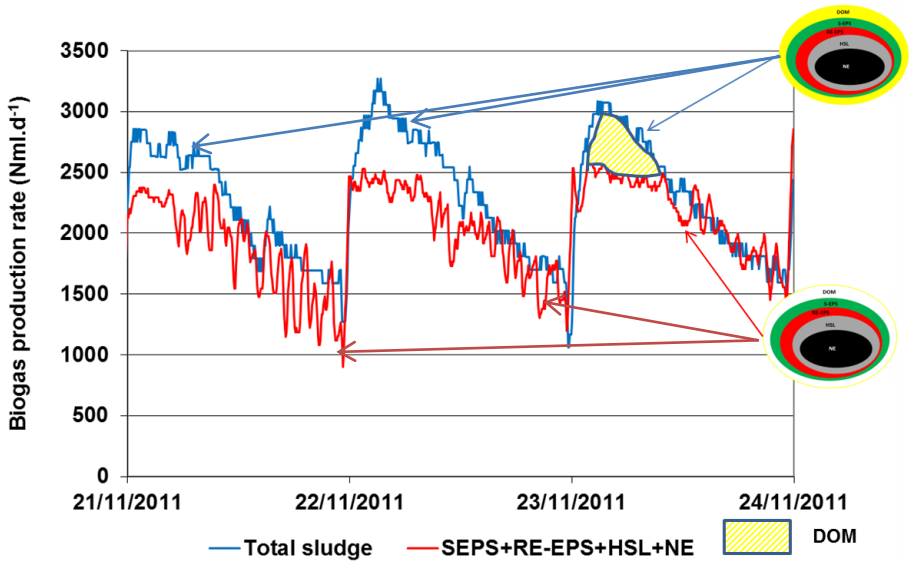

Figure 38 : Biogas production rate comparison between total sludge and total sludge without DOM (S/X=0.13 gCOD.gVS^{-1})

Biogas production rate (figure 39) from P2 was here much lower than P1. Kinetics showed that the removal of the most accessible fractions impacted the readily biodegradable fraction. The biogas production profiles obtained in the reactor P2 fed by only (HSL+NE) were representative of a slowly biodegradable fraction. Relative deviations of the areas between the P1 and P2 curves went from 30% to 52%.

By subtracting the biogas production of HSL+NE from the one obtained with the total sludge, the remaining area colored in blue in figure 39 (a) represented (DOM+SEPS+RE-EPS). Results clearly revealed that these three fractions constituted the readily biodegradable fractions whereas HSL and NE constituted the slowest ones.

A parallel with a literature results from Yasui et al. (2006) has been made. The authors performed “respirometry anaerobic tests” on secondary wastewater treatment sludge in order to find some mapping between ASM1 and ADM1 variables. As shown by the figure 39 (b), results obtained in our study was close to the Yasui et al. (2006) ones. Two degradations phases were observed and two fractions, readily and slowly biodegradable, are described. In our case, biodegraded DOM+S-EPS+RE-EPS was close to the readily biodegradable fraction whereas biodegraded HSL and NE were linked with the slowly biodegradable fraction.

In conclusion, biodegraded chemically extracted fractions simulated bioaccessibility and biodegradation kinetics.

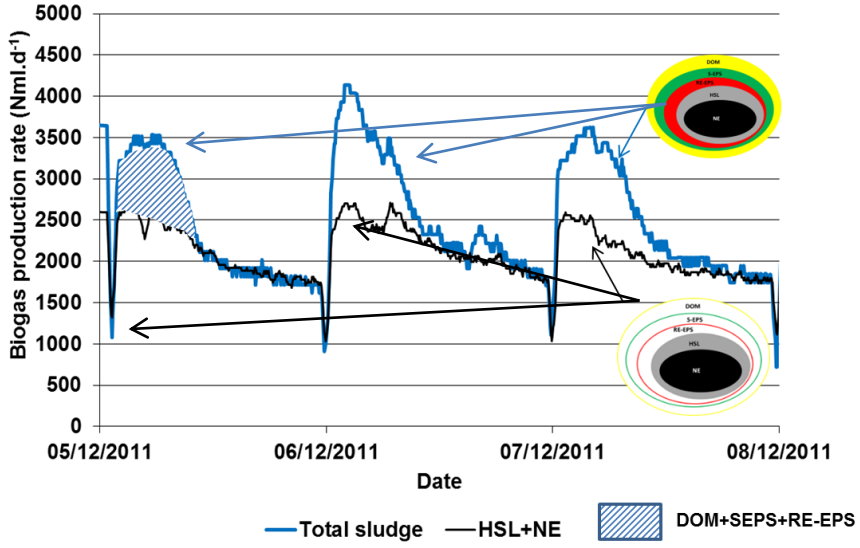

(a)

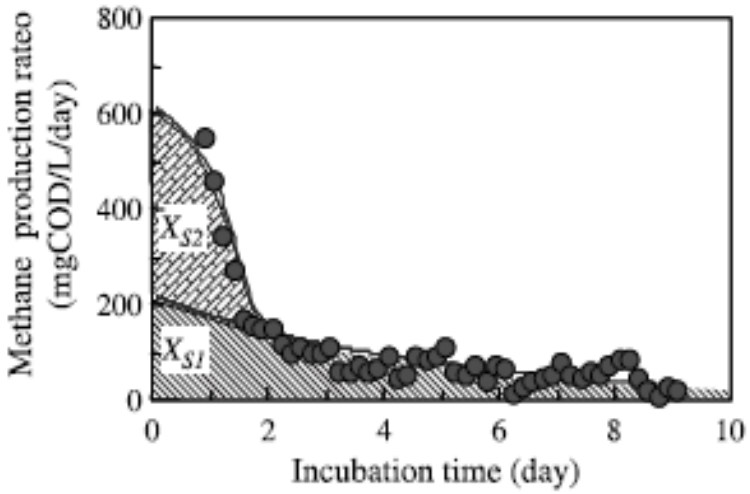

(b)

Figure 39 : (a) Superposition of biogas production rate comparison between total sludge and total sludge without (DOM+SEPS+RE-EPS) at S/X=0.08 gCOD.gCOD^{-1}); (b) Methane production rate at S/X=0.24 gCOD.gCOD^{-1} (Yasui et al., 2006)

Moreover, even if the uptake of these chemically accessible fractions behaves like bioaccessible fractions degradation, PLS regression tests have been performed to correlate X_{RC} and BD (Y-variables) with DOM, S-EPS, RE-EPS and HSL (X-variables). Figures 40a and b present the correlation circles graphs from a PLS regression following the two first components (t_1 as abscissa and t_2 as ordinate). In order to be correlated, two variables have to be in the same correlation circle close to the circle of radius 1.

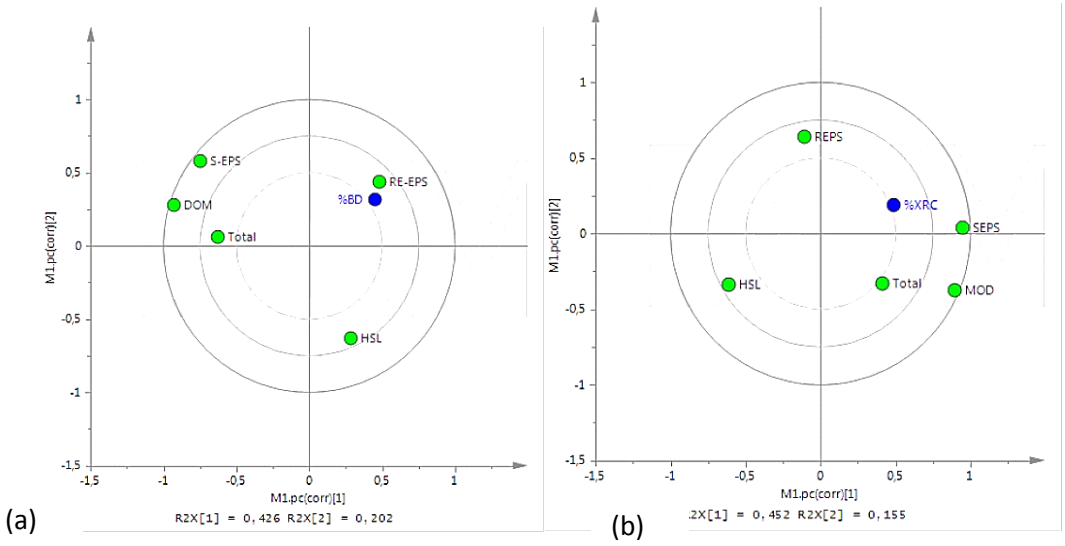

Figure 40 : PLS regression correlation circles obtained for BD (a) and X_{RC} (b) prediction

As observed in the correlation circles, no direct correlation is found for both X_{RC} and BD and the fractions as far as BD and X_{RC} are not in the circle of radius close to 1. BD model is fitted with 2 components with lower values of the PLS quality parameters (Q^2=0.158, R^2X=0.628 and R^2Y=0.299). X_{RC} model is fitted with 1 component with very low values of PLS quality parameters too (Q^2=0.133, R^2X=0.452 and R^2Y=0.241). We can conclude that the biochemical characterization of the extracted fractions is not enough to predict both BD and X_{RC}.

III.3. Conclusions

The main objective of chapter III was to investigate the links between chemical accessibility provided by sequential extraction protocol and biological accessibility provided by methane production curves. Three tests have been used, the first two ones being in batch conditions and the third was in continuous mode.

The first assay aimed at investigating the organic material flows through fractionation performed at several biodegradation times. COD mass balance has shown that DOM and S-EPS, which are the most chemically accessible fractions, and mainly biodegraded in the first degradation phase. The two others fractions, less chemically accessible, participated mainly in the second phase of organic matter degradation. Final results also showed that the readily biodegradable fraction was composed of DOM (63%), S-EPS (15%), RE-EPS (3%) and HSL (19%), while slowly biodegradable fraction was composed of S-EPS (9%), RE-EPS (22%) and HSL (58%), and NE (11%). Remaining fractions (2% of DOM, 0% of S-EPS, 1% of RE-

EPS, 7% of HSL and 47% of NE) were not biodegraded. Same conclusions have been found in the organic matter disturbing test. Disturbing organic matter have been applied on one continuous reactor by removing the most accessible fractions, DOM, SEPS and RE-EPS while another reactor was fed by the same total secondary sludge. Kinetics showed clearly that DOM mainly participated to the readily biodegradable fraction together with S-EPS and RE-EPS whereas HSL and NE contributed to the slowly bioaccessible fraction.

In order to validate these conclusions with visualization of the kinetics for each fraction, another test was set up with thermally treated sludge. Main results showed that chemical accessibility had an impact on both biodegradability and bioaccessibility. From the most accessible fraction removal to the least one, there was a progressive decrease of the initial slope obtained from BMP curves and of the biodegradability values. However, the most chemical accessible fraction DOM was also the most bioaccessible fraction but slowly biodegradable in this case. So, biodegradability could not be predicted with the only bioaccessibility information. The recalcitrant nature of the accessible molecules has to be taken into account. All the fractions extracted are not entirely biodegraded (77% of COD extracted is degraded in the first test).

Indeed, no correlations have been found between COD fractions and BD or X_{RC} variables. **The sequential extractions fractions are thus correlated with bioaccessibility as proven by reactor tests but not with the biodegradable and bioaccessible fraction represented by X_{RC}.**

Moreover, as shown in section II.1, no discriminant fractionation has been found between primary sludge, secondary sludge and anaerobically sludge. This means that the complexity of molecules extracted cannot be explained, even with a PLS regression from only the chemically extracted fractions and their biochemical composition. Figure 41 shows a schematic overview of this issue.

How to characterize the biodegradable part of each fraction? A possible answer has been given by the literature review. Spectroscopy fluorescence indeed seems to be a promising tool for complexity characterization. But this aspect has to be investigated, in particular since the results obtained in this chapter have shown that the extracted organic matter is mainly composed of fluorescent compounds (proteins). The next question is then: Is it possible to find a biodegradability and bioaccessibility indicator from both sequential extraction and fluorescence analysis?

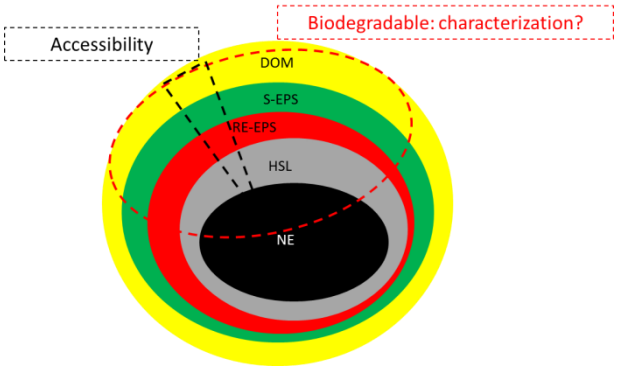

Figure 41 : Schematic overview of the next chapter issue

IV. BIODEGRADABILITY AND BIOACCESSIBILITY INDICATORS INVESTIGATION FROM SEQUENTIAL EXTRACTIONS COUPLED WITH 3D-EEM FLUORESCENCE SPECTROSCOPY

IV.1.1. Fluorescence spectroscopy and organic matter complexity 134
IV.1.1.1. Sequential extractions fractions fluorescence 134
IV.1.1.2. Evolution of fractions during anaerobic treatment 139
IV.1.1.3. Thermally treated sludge 142
IV.2. Definition of indicators from sequential extractions coupled with 3D-EEM liquid phase fluorescence spectroscopy (3D-SE-LPF) results 145
IV.2.1. General complexity indicator 145
IV.2.2. Zone-specific biodegradability indicator 148
IV.3. Correlations between 3D-SE-LPF indicators and biodegradability 150
IV.3.1. Exploratory PLS regressions 150
IV.3.2. PLS regression model set up for biodegradability prediction 154
IV.3.2.1. Calibration and validation datasets 154
IV.3.2.2. Validation results of PLS regression 155
IV.4. Correlations between 3D-SE-LPF indicators and bioaccessibility 157
IV.4.1. Exploratory PLS regressions 157
IV.4.2. Validation PLS regression for X_{RC} prediction 162
IV.5. Identification of recalcitrant molecules to biodegradation: sensitivity analysis 163
IV.5.1. Sensitivity analysis of PLS models 163
IV.5.1.1. Sensitivity analysis of PLS models: fractionation variables 164
IV.5.1.2. Sensitivity analysis of PLS models: fluorescence zones variables 164
IV.5.1.3. Sensitivity analysis of PLS models: scenario analysis 165
III.1. Conclusions 169

Note for the reader:

The chapter IV presents the "heart" of this study. Indeed, this section reveals the fluorescence spectroscopy potential for biodegradability prediction. Combining chemical fractionation with fluorescence information leads to new biodegradability indicators able to predict both biodegradability and bioaccessibility. This chapter is crucial for quantifying the inputs of the modified ADM1 presented in the chapter V.

Previously, chemical accessibility fractions were shown to be linked with biological accessibility fractions. However, the only information provided by the chemical fractions was not sufficient to predict both BD and X_{RC}. Indeed, the biodegradable part of each fraction was not taken into account. Consequently, the COD fractionation is not enough discriminant to predict both biodegradability and bioaccessible fraction X_{RC} for all kind of sludge. In order to solve this problem, the fluorescence spectroscopy highlighted by the literature review could be a promising tool. This aspect is strengthened especially since, as previously shown in chapter III, the sludge organic matter is mainly composed of proteins naturally fluorescent. The main objective of this chapter is thus to find correlations between biodegradability, bioaccessibility and the analytical information provided by fluorescence spectra from the sequential extractions of sludge.

To this end, fluorescence from chemical fractions is first studied in order to highlight its ability to be discriminant with respect to the biodegradability. Then, investigation about indicators provided by coupling the sequential extraction protocol and fluorescence is performed.

IV.1. Biodegradability and bioaccessibility indicators investigation

Fluorescence spectroscopy of sequential extractions from sludge fractions is studied in this section. Preliminary tests were performed in order to investigate the ability of the 3D spectra from sludge fractions to be discriminant according to the anaerobic biodegradability.

IV.1.1. Fluorescence spectroscopy and organic matter complexity

First, the 3D liquid phase fluorescence (3D-LPF) spectroscopy is studied for each sludge found in a wastewater treatment line from plant A.

IV.1.1.1. Sequential extractions fractions fluorescence

Additionally to biochemical analysis, the 3D-LPF spectra were obtained for each fraction extracted (DOM, S-EPS, RE-EPS and HSL) for all the sludge. Chapter II described the fluorescence spectroscopy methodology in order to obtain the 3D spectra.

The spectra obtained after the fractionation of a secondary sludge sample (figure 42) show that the molecules complexity increased when the fractions accessibility decreased as yet highlighted by Muller *et al. (in press*). Indeed, from the DOM spectra to the HSL spectra,

there was a shift of the fluorescence peaks to the right. This evolution means that the organic matter became more complex.

In the DOM fraction, the main fluorescence peaks are the protein-like compounds (zone I, II and III). This distribution is also met in the S-EPS spectra with a fluorescence zone III more intense, related to the soluble EPS (mainly proteins) composed of microbial products. In the third fraction RE-EPS, the protein-like compounds are still extracted but a new peak appears in the fluorescence zone VI, defined as lignocellulose-like compound, humic-like or melanoidin-like compound, known to be recalcitrant or very slowly biodegradable (Muller *et al., in press*, Chandra *et al.*, 2008). Finally, the least extracted accessible fraction HSL is mainly composed of intense peaks in the fluorescence zones VI and IV defined by fulvic acid-like compounds. Therefore, the complexity has grown with the decrease of the accessibility. This result goes in the same direction than results from chapter III where it was shown that the fraction biodegradability decreased with the fraction accessibility.

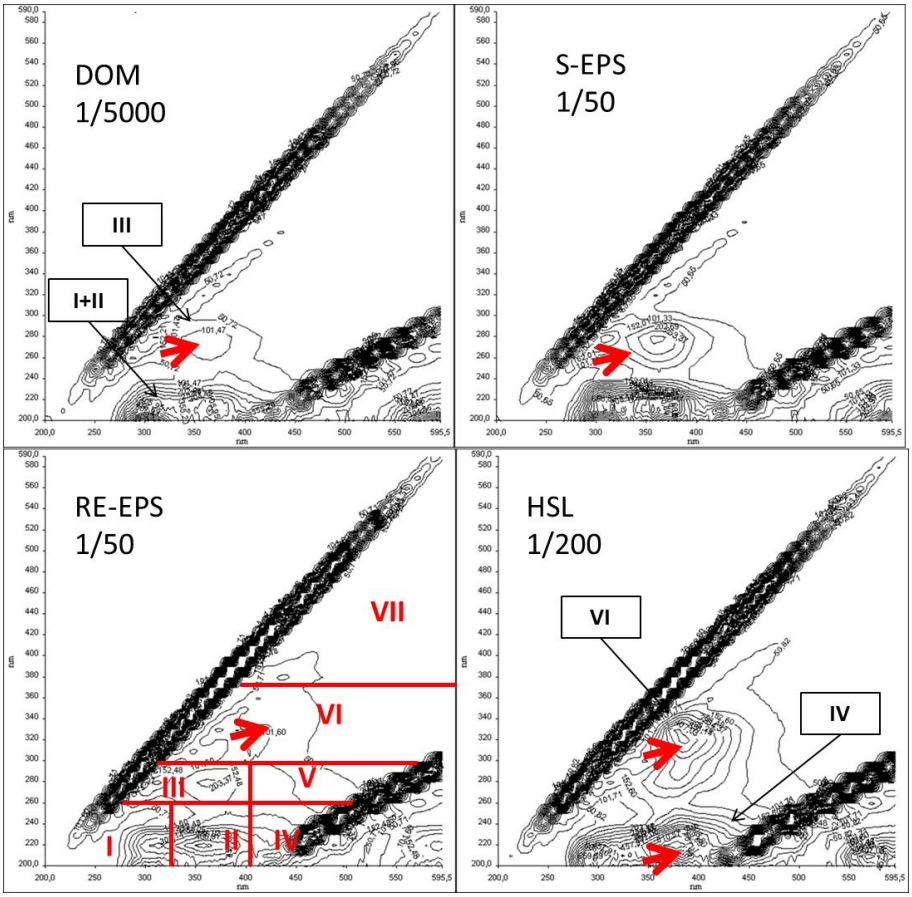

I: protein-like (Tyrosine); II: protein-like (Tryptophan); III: protein-like (Tryptophane, microbial products); IV: fulvic acid-like; V: inner filter, glycolated protein-like; VI: melanoidin-like, lignocellulose-like, humic acid –like; VII: humic acid-like, consensed protein-like

Figure 42 : 3D-LPF spectra obtained for SII_F_2 sludge chemical fractionation

In order to go further, spectra from fractions extracted from different kind of sludge are studied. These sludge, sampled in the same WWTP, have different biodegradability values corresponding to their nature: primary (SI_A), secondary (SII_A) and anaerobically digested sludge (SD_A), respectively 51.1%, 43.5% and 16.5%. Evolution of the fluorescence spectra for each fraction is presented by the figures 43 to 46. The general trend shows that the least biodegradable is the total sludge, the most complex peaks appear in each fraction.

Concerning the DOM fraction, the fluorescence zone I, II and III (protein-like compounds) contain the main peaks whereas the DOM from the digested sludge has a poorest zone III and a main peak in the zone VI (complex compounds). Moreover, a shoulder appears in the fluorescence zone VI of the secondary sludge's DOM, showing that the DOM from primary sludge is less complex. Similar observations are made for the S-EPS fraction where a peak apparition in the zone VI for secondary sludge and digested sludge is observed and a decrease of the fluorescence of the zone III in the digested sludge. In the chapter III, the proteins from DOM, S-EPS, RE-EPS and HSL were biodegraded in the anaerobic stabilization test of a secondary sludge. The fluorescence observations on zone I to III are in adequacy with this result.

In the RE-EPS fraction, primary sludge has a fluorescence zone III higher than in secondary sludge. The protein-like compounds from the zone III has been used as a BOD_5 indicator in the 2D-EEM by Reynolds *et al.* (1997). This zone is still present in the RE-EPS fraction of the digested sludge but the peak in the zone VI shows that this fraction is complex too. Additionally, the dilution applied (1/20) shows that the RE-EPS fluorescence is less important for digested sludge than the other sludge (1/100).

Finally, the fluorescence of the HSL fractions evolves too. The three spectra are mainly composed of the fluorescence zones IV and VI peaks showing that this slowly accessible fraction is the most complex too. According to the dilution applied, the HSL fluorescence is not so important for primary sludge (1/50) than for secondary and digested sludge (1/200). Besides, a fluorescence peak in the zone III is still present for the primary sludge whereas it tends to disappear for the secondary sludge and is absent for the digested sludge. The fluorescence of the zone VI is also higher in the digested sludge than in the primary and in the secondary sludge.

Therefore, from this qualitative observation, we can see that the total sludge biodegradability changes accordingly to the complexity.

The complexity described by the fluorescence zones IV and VI of all the fractions of a sludge sample increases when the sludge biodegradability decreases. Whereas the fluorescence of the zone III (protein-like) increases in the fractions of the most biodegradable sludge. Wan *et al.* (2012) found similar results concerning the evolution of the DOM fluorescence after co-digestion. Fulvic and humic acid structures remained stable during the digestion whereas tyrosine-like compounds disappeared due certainly to molecules hydrolysis into non fluorescence structures.

Depending on the fraction, complexity is more or less important. The HSL fraction contains more complex compounds than the other fractions whereas it is less fluorescent for primary sludge. On the contrary, RE-EPS is less important for digested sludge whereas it contains more fluorescence in zone III of primary sludge as S-EPS. Thus, it seems that the whole spectra information is promising for sludge biodegradability characterization.

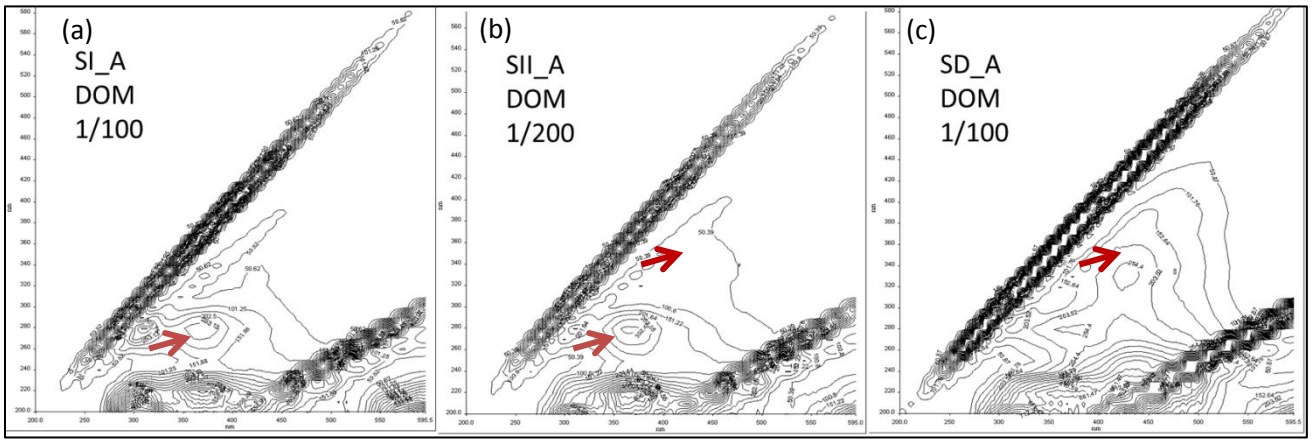

Figure 43 : DOM 3D-LPF spectra obtained for SI_H (a), SII_H (b) and SD_H (c)

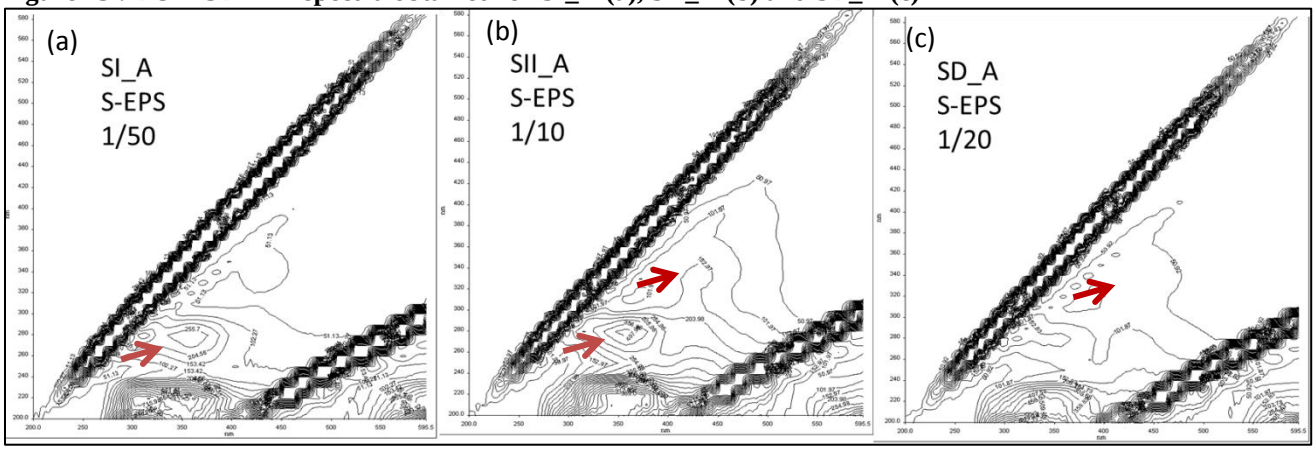

Figure 44 : S-EPS 3D-LPF spectra obtained for SI_A (a), SII_A (b) and SD_A (c)

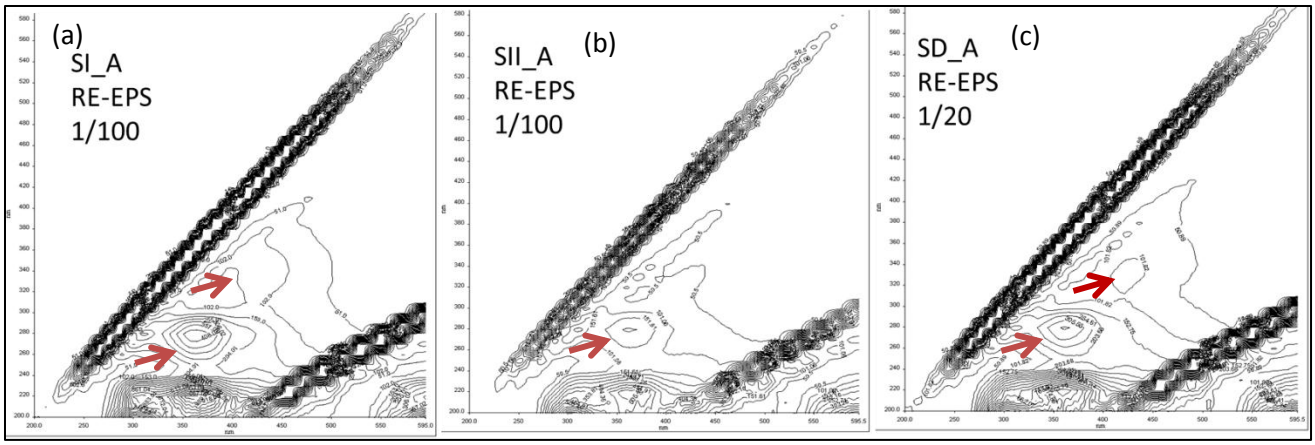

Figure 45 : RE-EPS 3D-LPF spectra obtained for SI_A (a), SII_A (b) and SD_A (c)

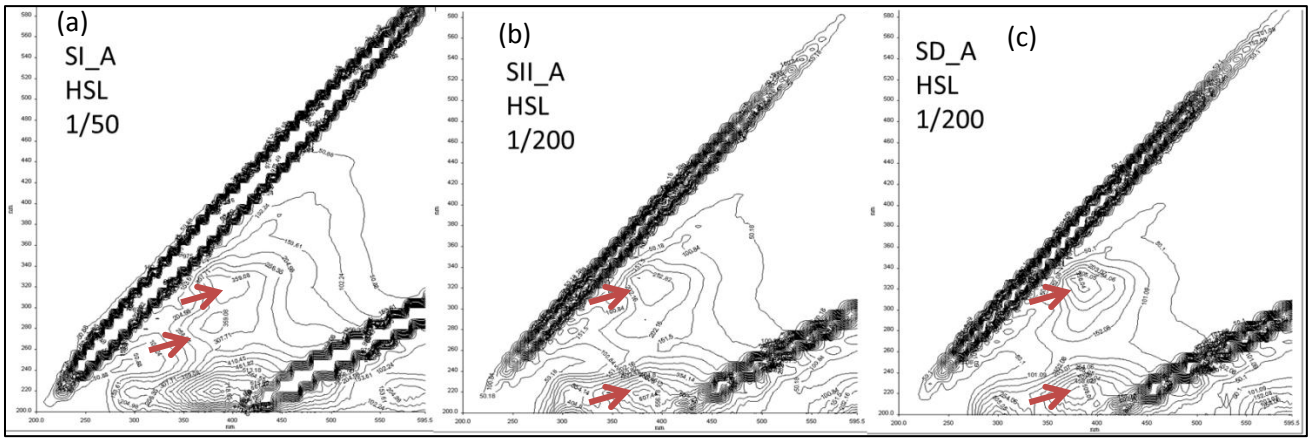

Figure 46 : HSL 3D-LPF spectra obtained for SI_A (a), SII_A (b) and SD_A (c)

The last fraction not characterized is the non-extracted one (NE). As described in chapter II, the NE fraction is freeze-dried and grinded in order to use the solid phase fluorescence (SPF) spectroscopy. As highlighted by Muller *et al.* (2011), the photons excitation of the 3D-SPF is not enough powerful for the dark-colored substrates such as secondary sludge or compost. In this study, only the NE fraction of primary sludge, less dark-colored, had fluorescence signature (figures 47a and b). The fluorescence observed appears in the zone VI describing complex lignocellulose-like compounds. Another peak, less important, appears in the fluorescence zone V corresponding to inner filter for melanoidins-like proteins. Both florescent zones represent complex compounds, slowly biodegradable or recalcitrant. This result goes to the same direction than the low biodegradable fraction found for NE in chapter III.

Spectra from secondary and digested sludge NE have no fluorescence signal because of their higher dark color (figure 47 c and d). Dilutions have been tested with sodium carbonate without success. Nevertheless, some signal has been recorded in the primary sludge case.

As the fluorescence of NE depends on the sludge origin, this fraction has not been considered for the biodegradability indicator study.

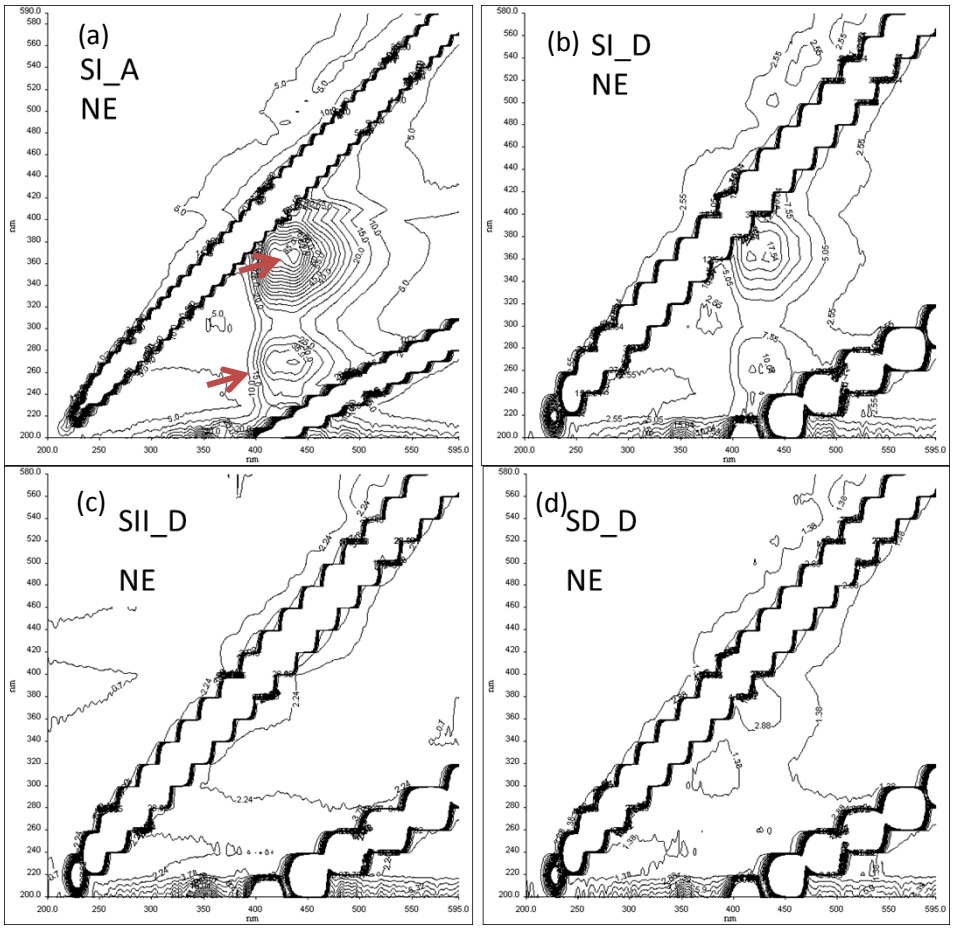

Figure 47 : NE 3D-SPF spectra obtained for SI_A (a), SI_D (b), SII_D (c) and SD_D (d)

IV.1.1.2. Evolution of fractions during anaerobic treatment

Previous observations have shown the potential of fluorescence spectroscopy to characterize biodegradability. Next results show the evolution of 3D-LPF spectra of extracted fractions from SII_F_2 before (figure 48) and after (figure 49) the anaerobic stabilization test (chapter III).

Qualitatively, spectra observations lead to the same conclusions than the previous paragraph. After anaerobic digestion, the fluorescence zones describing complex compounds appear whereas the zones describing the protein-like compounds have lower signal. The protein-like compounds have been probably hydrolyzed into no fluorescence structure.

The fluorescence from the zones I to III of the secondary sludge decreased in all the fractions of the digested sludge, letting the complex compounds (zones IV and VI) more visible in the DOM, S-EPS and RE-EPS fractions. Concerning the HSL fraction, the fulvic acid (zone IV) and lignocellulose-like compounds (zone VI) seem to remain stable through the anaerobic digestion and the dilution (1/200) applied to samples remain identical.

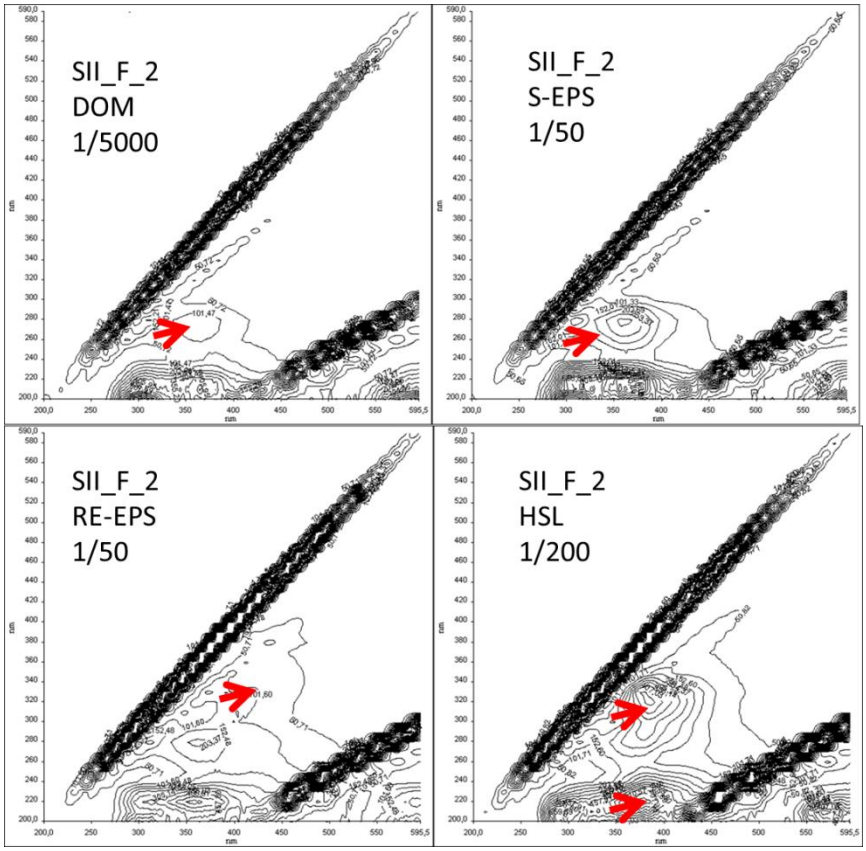

Figure 48 : 3D-LPF spectra obtained for sequential extractions of SII_F_2 before anaerobic stabilization

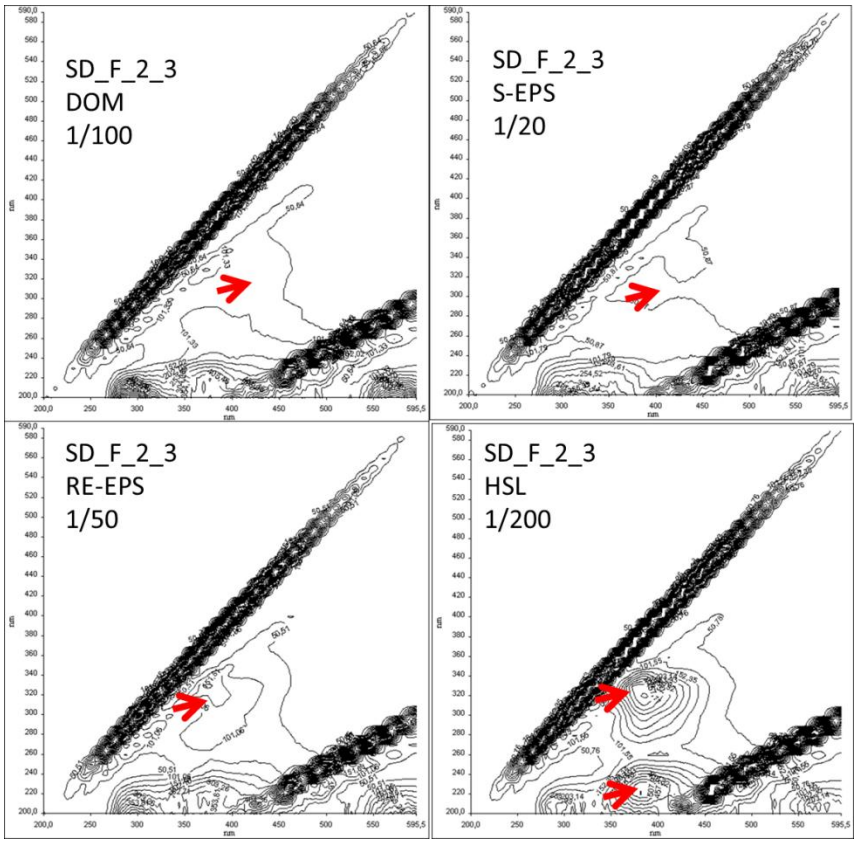

Figure 49 : 3D-LPF spectra obtained for sequential extractions after anaerobic stabilization test of SII_F_2 named SII_F_2_3

Quantitatively, based on Wang *et al.* (2010) and He *et al.* (2011) studies, a ratio is calculated between the complex structures fluorescence and the protein-like compounds fluorescence. Using the fluorescence intensity volumes of each zone for each fraction, the ratio between the fluorescence percentage of zones (IV to VI) on the fluorescence percentage of zones (I to III) $P_f(IV+V+VI+VII)/P_f(I+II+III)$ is calculated (figure 50).

Results show that for all the fractions, this ratio increases significantly after anaerobic digestion. This confirms that the fluorescence of the protein-like compounds decreases due to their biodegradation or hydrolysis into non fluorescent molecules such as VFA. Consequently, the fluorescence intensity percentage of zones IV to VI increases because the complex zones remain stable as explained by Wan *et al.* (2012). These molecules seem to be recalcitrant to the anaerobic digestion. Thus, this "complexity" ratio is related to the biodegradability. This observation is more important when the biodegradability is low. Moreover, the "complexity" ratio increases from the most accessible organic particulate fraction (S-EPS) to the least one (HSL), reinforcing the previous results.

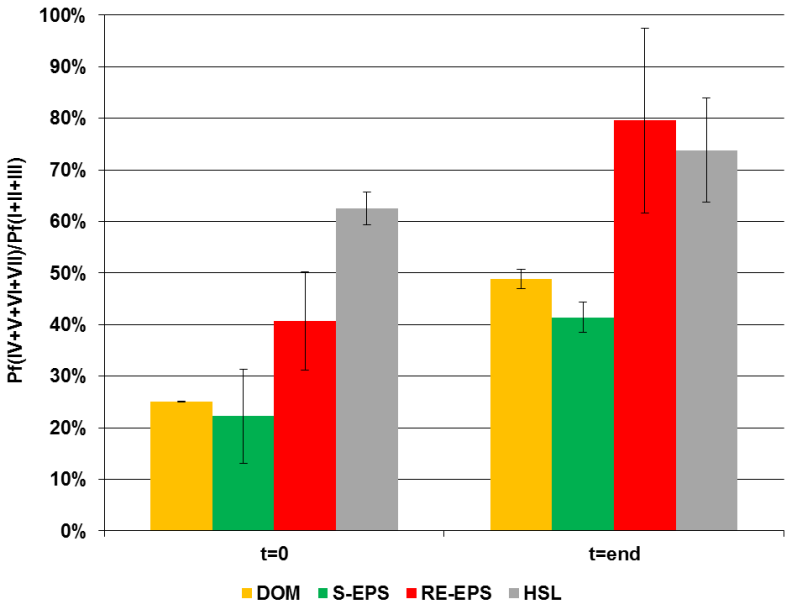

Figure 50 : Evolution of the ratio of fluorescence percentage between complex zones (IV-VII) and protein-like zones (I-III)

IV.1.1.3. Thermally treated sludge

Spectra of the thermally treated sludge sample have been analyzed together with spectra obtained on the whole line of the sludge treatment from the plant B. The secondary sludge, pretreated by thermal treatment at 165°C, feed an anaerobic digestion reactor. COD mass balance and the characterization of the three samples have been performed (figure 51). .

It appears that the RE-EPS and the HSL fractions from the secondary sludge are respectively hydrolyzed (-45% and -56% of COD) into DOM and S-EPS. The COD mass produced in the two first fractions is 20% higher than those from thermally treated sludge. This is probably due to a part of solubilization of COD from the NE fraction (biodegradability of 16%).

After the thermal treatment, the fluorescence of the DOM and the S-EPS fractions goes to the same direction than the COD mass balance. The fluorescence intensity in all the zones, proportional to the sample concentration, is more important considering their higher sample dilution. New fluorescent molecules seem to be produced during the pretreatment, mainly in zone V and VI, corresponding to glycated proteins as melanoidins compounds. As previously mentioned, at high temperatures like 165°C, the Maillard reaction produces glycated proteins. Additionally, the fluorescence zones I to III from RE-EPS and HSL and a part of fluorescence zone VI from HSL decreased strongly after the thermal treatment.

These molecules have probably been hydrolyzed and the protein-like compounds could have participated to the Maillard reaction or be hydrolyzed into non fluorescent molecules.

After that, the anaerobic digestion of thermally treated sludge removes 84% of COD of each fraction. The remaining fluorescence at the end of anaerobic digestion is mainly composed of complex molecules located in zones IV and VI for all the fractions, confirming that these molecules are recalcitrant to biodegradation.

Combining chemical extraction with 3D-LPF has thus a high potential to analyze the organic matter degradation during sludge treatment. In order to go further in this direction, the next section aims at investigating some indicators provided by the 3D-SE-LPF methodology. Statistic tools are used to validate or invalidate correlations between those indictors and both biodegradability and bioaccessibility of sludge.

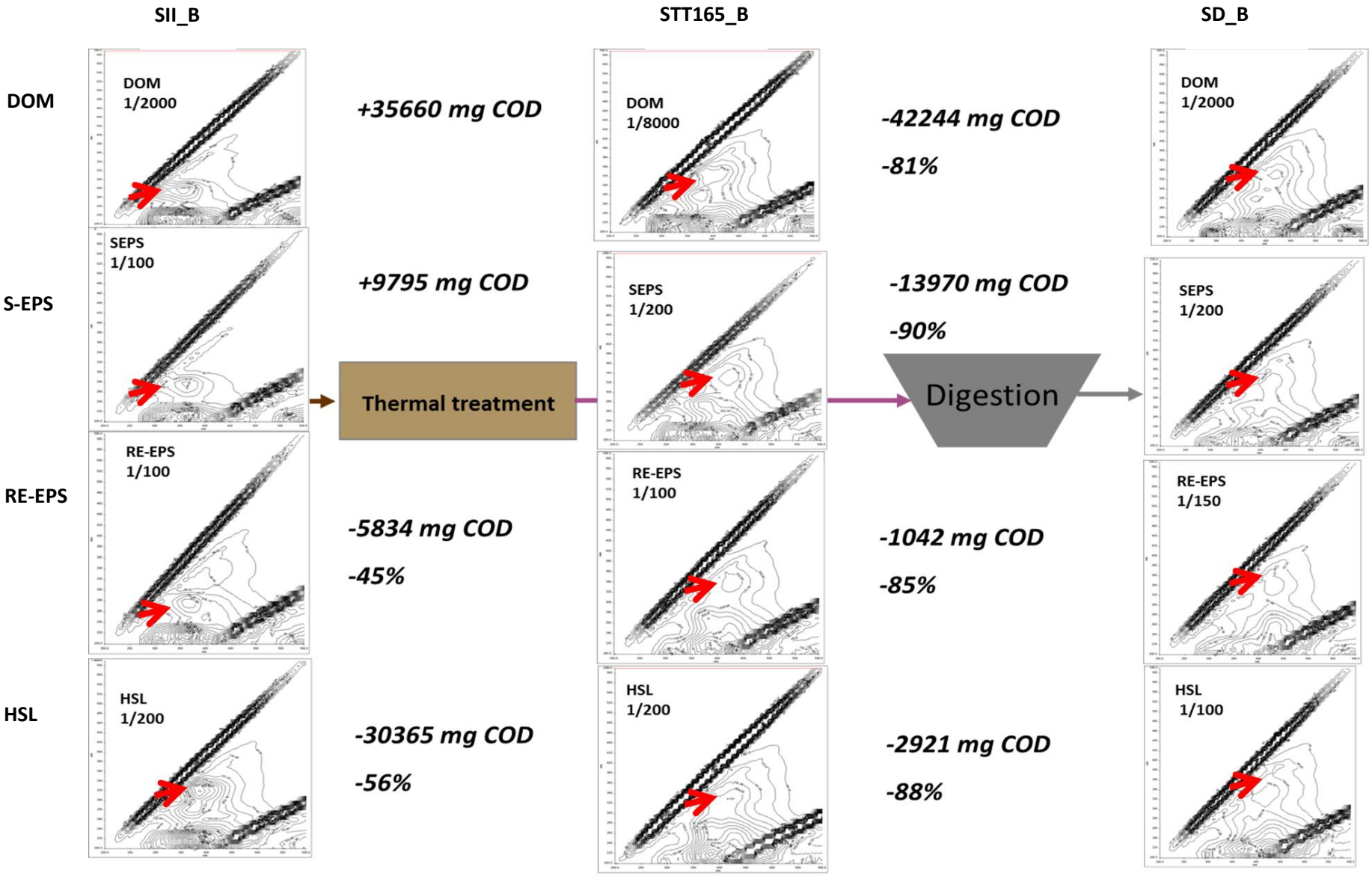

Figure 51 : 3D-LPF spectra obtained at 3 sampling points from a sludge treatment unit: raw sludge, thermally treated sludge and anaerobically digested sludge

IV.2. Definition of indicators from sequential extractions coupled with 3D-EEM liquid phase fluorescence spectroscopy (3D-SE-LPF) results

We saw that the biodegradability prediction seems to be linked with the complexity of each fraction extracted from the sludge. As the previous chapter conclusion mentioned, the only fractionation information is not sufficient to predict the biodegradability of the sludge. Thus, each fraction has to be weighted by an indicator translating their biodegradable part, or, inversely their not biodegradable part, thanks to the complexity (figure 52). In the first section of this chapter, the potential of the 3D-LPF methodology to describe complexity has been proven. Therefore, in this section, investigations on the definition of indicators from both spectra interpretation and chemical extractions are set up. First, the objective of these indicators is to predict the biodegradability of the sludge. Then, thanks to the chemical fractionation simulating accessibility, correlation between biodegradable accessible fraction X_{RC} and these new indicators are tested. Indeed, as no really parameter is defined for the bioaccessibility characterization, we decided to quantify this notion with the fraction readily accessible X_{RC}. Nevertheless, a bioaccessible fraction can be biodegradable or not (as the melanoidins compounds in the DOM accessible fraction of thermally treated sludge). In this case, X_{RC} characterizes the readily bioaccessible and biodegradable fraction.

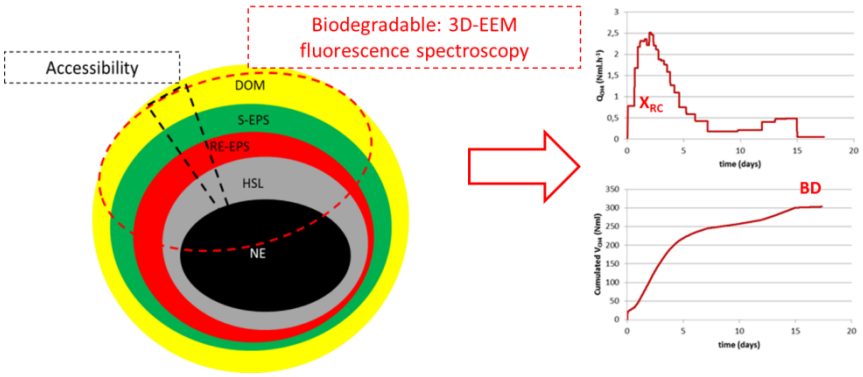

Figure 52 : Approach used for biodegradability and bioaccessibility prediction of sludge

IV.2.1. General complexity indicator

Based on the literature (Wang *et al.* (2010), He *et al.* (2011)), the ratio of fluorescence percentage from complex compounds in the zones IV to VII on the fluorescence percentage from protein-like compounds in the zones I to III has been set up in the previous section. This complexity ratio increased in all the fractions extracted after anaerobic digestion (i.e. when sludge biodegradability decreased).

From this observation, a complexity indicator can be proposed: each fraction (percentage of total COD) is weighted by this complexity ratio. We could translate the complexity in each fraction in percentage of COD.

In order to go beyond this first assumption, boxplots of the complexity indictors are performed for the 52 sludge samples studied (figure 53).

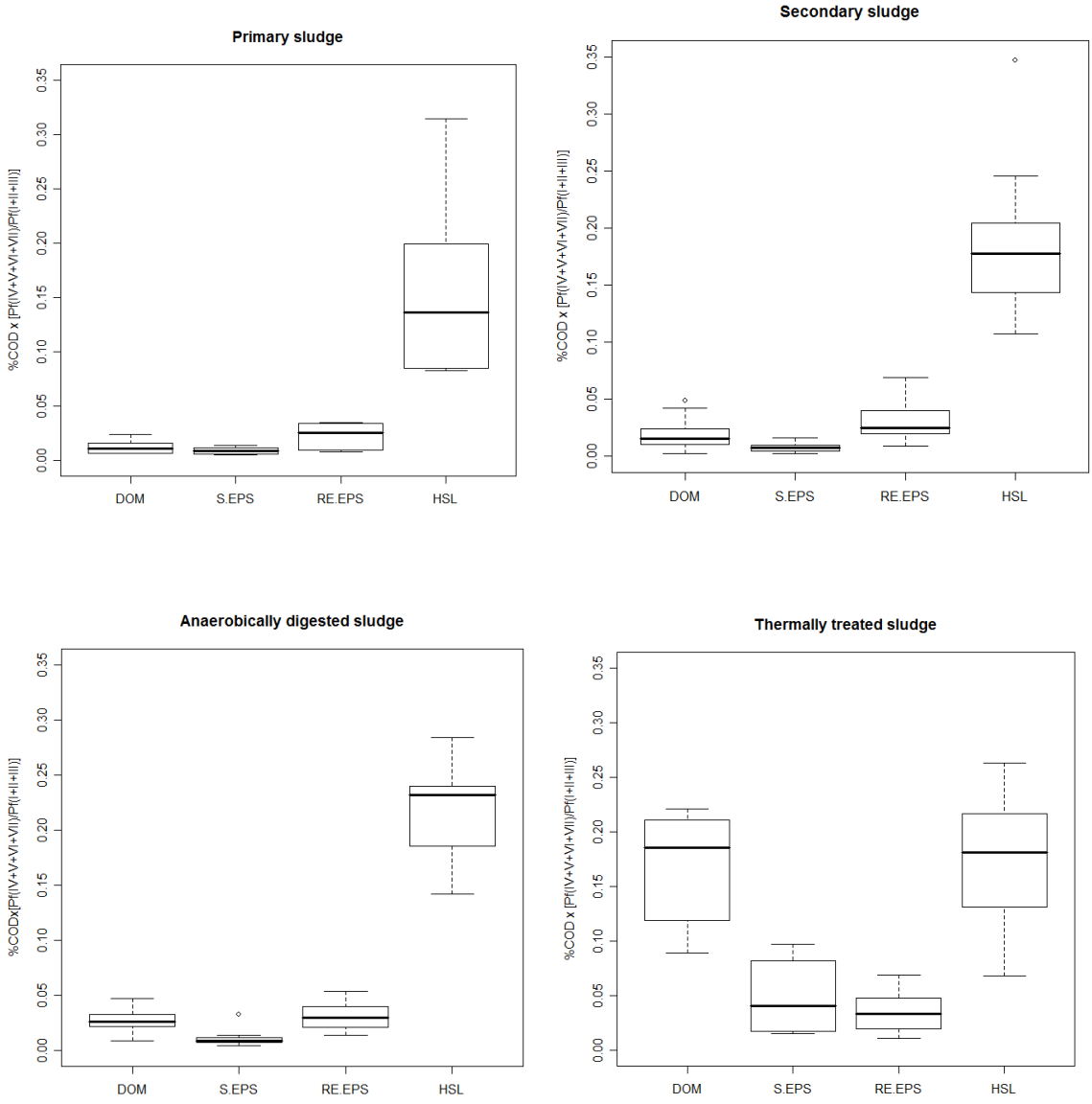

Figure 53 : Boxplots of the "complexity indicator" relative to each fraction for primary, secondary, anaerobically digested and thermally treated sludge

Concerning the primary, secondary and anaerobically digested sludge, no discriminant parameter for the biodegradability prediction is highlighted. Indeed, the medians of the indicators are similar and low for DOM, S-EPS and RE-EPS (<0.05) for the three sludge.

However, the HSL indicator median (0.12) is weaker in the primary sludge than in the secondary sludge (0.17) or in the anaerobically digested sludge (0.22). Additionally, HSL indicator is higher for anaerobically digested sludge than secondary sludge. The HSL complexity indicator of the primary, secondary and anaerobically digested sludge increases when the sludge biodegradability decreased.

The distribution repartition of the complexity indicator is different for thermally treated sludge. The HSL indicator is about 0.17 as for the secondary sludge but the DOM indicator is also high (0.18). This is due to the high value of COD percentage of DOM and to the fluorescence melanoidins in zone VI. However, the mean biodegradability of thermally treated sludge is about 49%, higher than the mean biodegradability of the secondary sludge.
Thus, in order to evaluate the correlation between the complexity indicator and the biodegradability, a PLS regression is performed. The X-variables are the fourth complexity indicators for DOM, S-EPS, RE-EPS and HSL fractions and the Y-variable is defined by BD.

Results show that there is no correlation between the X-variables and BD (figure 54a and b). Nevertheless, the correlation circles are proposed for the two first components when all sludge are considered (figure 54 a) and when thermally treated sludge is not considered (figure 54 b). No correlation exists between BD and complexity indicators even if thermally treated sludge samples (atypical repartition sludge) are removed.

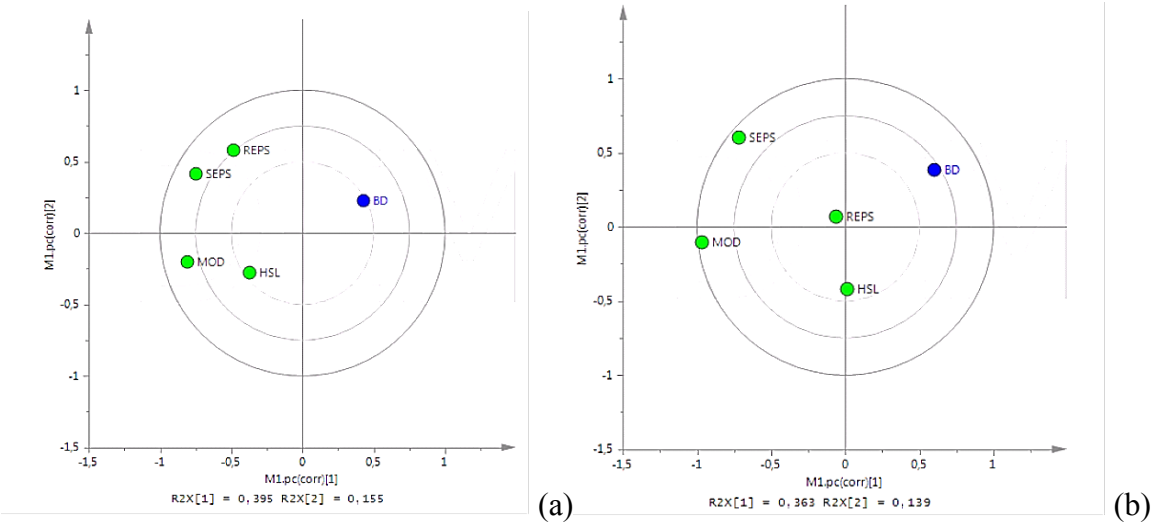

Figure 54 : Correlation circle obtained in PLS regression of BD with the complexity indicators calculated for each fraction, considering all the sludge (a) and not considering the thermally treated sludge (b)

By analyzing in more details the complexity indicators for identical nature of sludge samples (see figures 55a for primary sludge and 55b for secondary sludge), it appears that there is no sufficient internal discrimination to explain BD.

This ratio is thus discriminant from a group of sludge to another but not between two identical types of sludge. Thus, another type of complexity indicator has to be investigated.

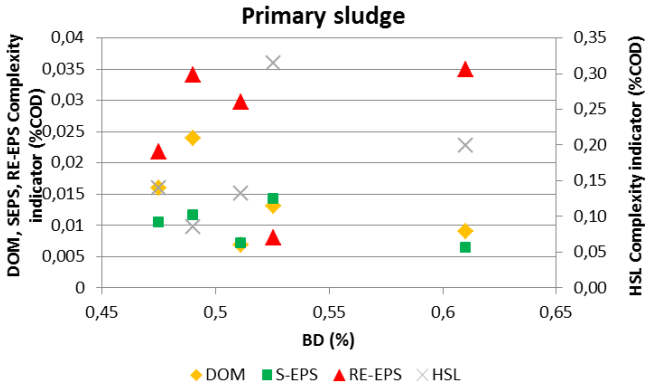

(a)

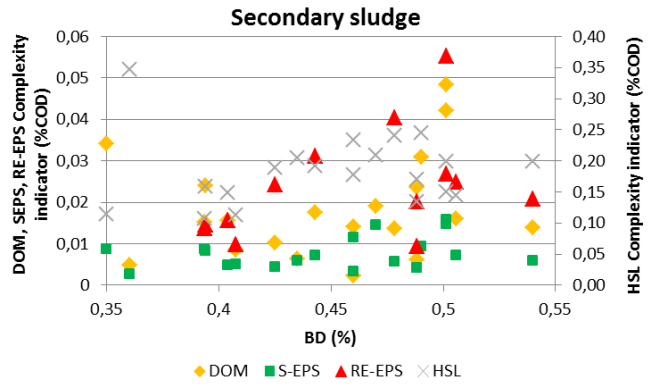

(b)

Figure 55 : BD versus complexity indicators for primary sludge (a) and secondary sludge (b)

IV.2.2. Zone-specific biodegradability indicator

The main purpose of the biodegradability indicator is to represent both complex and biodegradable compounds contained in the sludge fractions. One solution is to use the information provided by the whole spectra, using the volume of the fluorescence intensity of each zone associated to each fraction. This new indicator is described by the equation 4.1. The fraction COD percent ***Fract*** is weighted by the percent of fluorescence of volume intensity of a zone i $\boldsymbol{P_f(i)}$. 28 indicators are determined for a given sludge as far as 4 fractions are considered (DOM, S-EPS, RE-EPS and HSL) and 7 fluorescence zones (I to VII) are taken into account.

$$\boldsymbol{Fract_{zone\ i} = \sum_{i=I}^{VII} P_f(i) \times Fract(\%COD)}$$ **Equation 4.1**

In the chapter III, we saw that the DOM fraction from the primary, secondary and thermally treated sludge contain a significant part of VFA. However, the VFA molecules are not naturally fluorescent. Thus, concerning the DOM fraction, the COD associated to the VFA is removed. The DOM fraction used in the calculation (equation 4.1) is a new fraction called ***DOM_fluo***. Moreover, since VFA is the easiest biodegradable compound, this variable is added to the 28 others X-variables.

The same methodology could be applied to soluble carbohydrates contained in all fractions, but they are in minority in all the sludge and their impact on COD is not significant. Additionally, the soluble carbohydrates are higher in the anaerobic digested sludge. Thus, this variable cannot be linked with easily biodegradable compounds as VFA.

A Hierarchical Cluster Analysis (HCA) has been performed before the PLS regression in order to classify the sludge depending on their X-variables. Applied on all the sludge studied, a dendogram has been drawn (figure 56). Four groups appear in coherence with their nature: thermally treated in green color, digested sludge in blue, secondary and primary sludge in yellow and 3 atypical secondary sludge in red. Then, a first exploratory PLS regression is tested on all the samples.

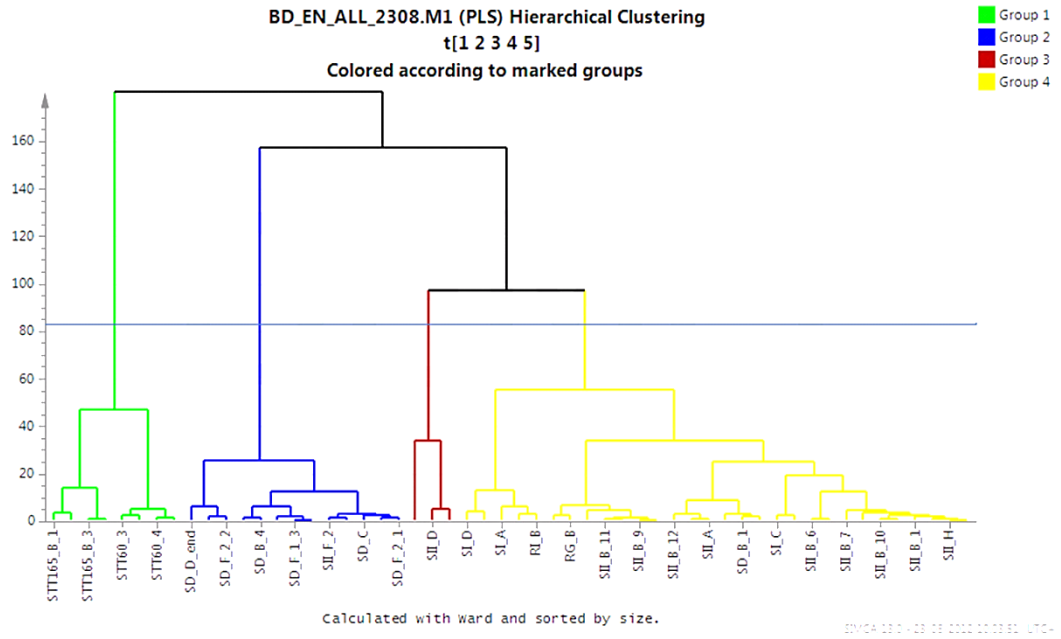

Figure 56 : Hierarchical Cluster Analysis performed on all indicators data from the 52 sludge studied

IV.3. Correlations between 3D-SE-LPF indicators and biodegradability

In order to investigate the correlation between the new indicators and the biodegradability of sludge, two PLS regressions were performed using the 52 sludge samples.

In a first PLS regression, the X-variables are defined by the 28 indicators and the VFA percentage of the total COD. Y-variable is defined by the biodegradability BD. In the second PLS regression, the X-variables are defined only by the 28 indicators previously defined.

IV.3.1. Exploratory PLS regressions

The PLS regressions show that there is a good correlation between X and Y variables. The number of components used in the PLS for reducing the number of X-variables is 5 for both regressions. This number is obtained by the algorithm of the software (i.e. the algorithm considers a compromise between R^2 and Q^2 parameters). The quality parameters of the PLS models obtained with 5 components for R^2X, R^2Y, Q^2 and RMSE are presented in the Table 23.

Table 23 : PLS regression performances parameters

PLS regressions	R^2X	R^2Y	Q^2	RMSE
28 variables+VFA	0.877	0.802	0.687	7.6%
28 variables	0.877	0.827	0.694	7.1%

The components give a good description of both X and Y variables with R^2X and R^2Y close to 1. Q^2 is higher than 0.5 indicating a good predictivity in both cases. The RMSE gives low errors percent for BD prediction. However, it seems that the model performance is better when the PLS considers only the 28 variables. When the correlation circles are plotted (figures 57a and b), the two first components are linked with all the zones from the HSL, DOM and S-EPS fractions in the 28 variables case whereas in the second one, VFA appears correlated to BD only in the third component (more results of PLS with VFA are presented in Annex 3). As expected, the VFA variable has a positive influence on BD and is linked with the thermally treated sludge (cf. figure A4.3 in Annex 4). However, this variable is not strongly correlated with BD as presented by the correlation circles graph (figure 57b shows). Moreover, as the addition of this variable does not improve the prediction of biodegradability, the 28 variables model is selected.

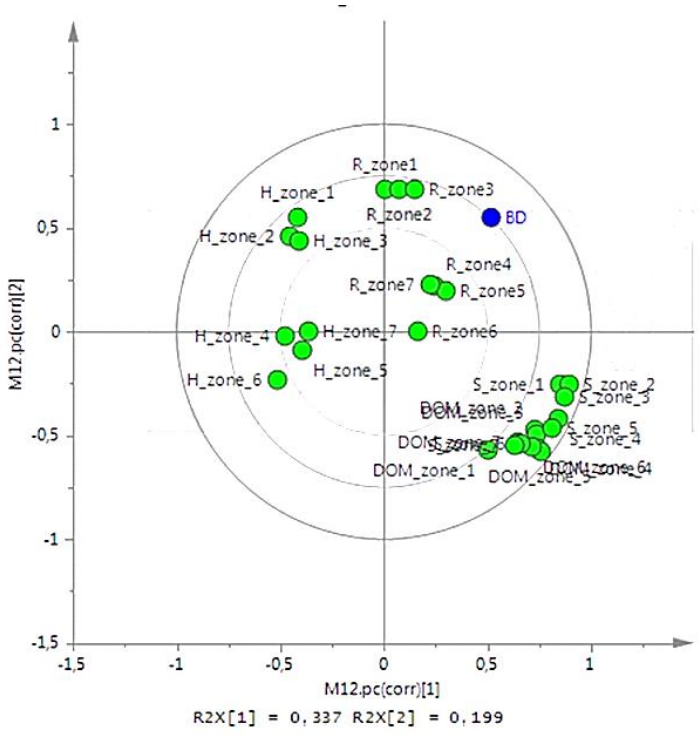

(a)

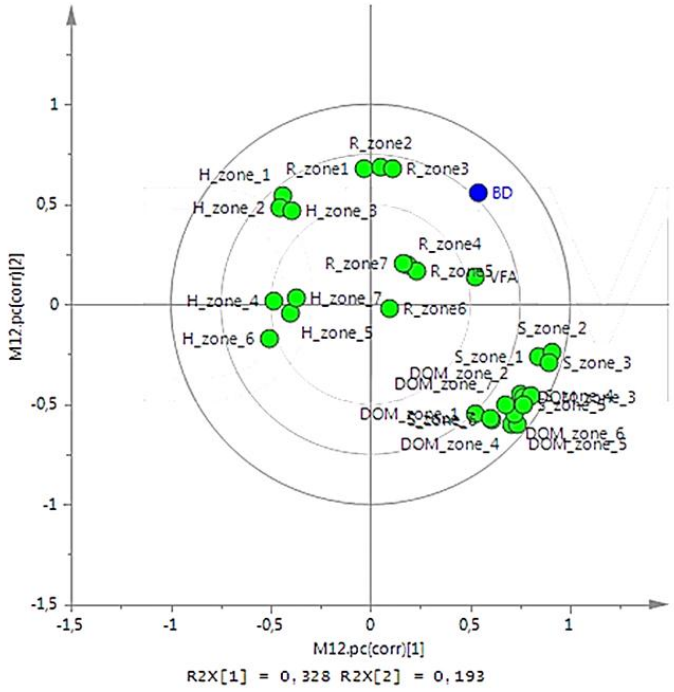

(b)

Figure 57 : Correlation circle obtained for the two first components in PLS regression of 28 variables (a) and 28 variables and VFA (b)

The correlation circles graph of the 28 variables PLS (figure 57a) show that BD is correlated positively with RE-EPS variables and soluble variables (S-EPS and DOM) in the first component whereas it is correlated negatively with all zones from HSL.

Then, in the second component, BD is correlated negatively with zone IV to VI from HSL and with all SEPS and DOM zones.

Observation from the correlation circles of the sludge samples repartition (figure 58) highlights that each sludge is grouped in accordance with its biodegradability as observed in the HCA analysis previously performed.

To a better interpretation of the PLS regression results, the correlation circles from the figure 58 representing the sludge samples have to be analyzed at the same time than the figure 57a representing the X-variables. Indeed, this analyze could provide useful interpretation on how the X-variables impact the BD prediction and what kind of sludge are responsible of this impact.

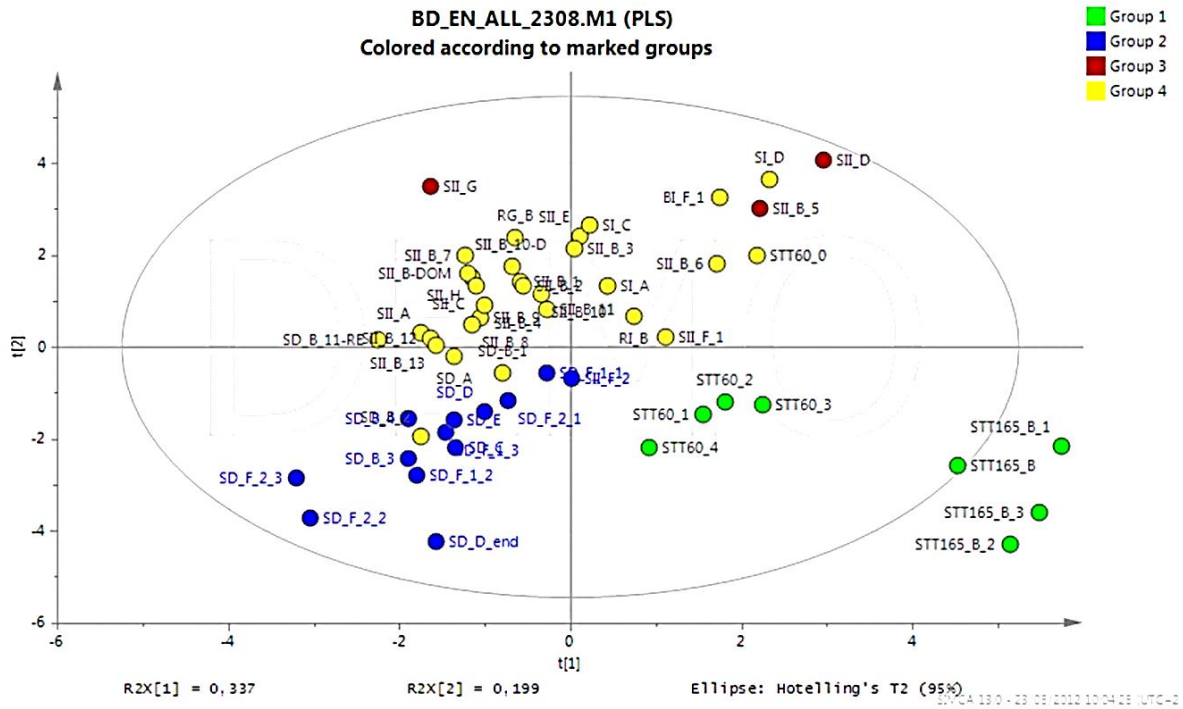

Figure 58 : Correlation circle of sludge samples repartition obtained in PLS regression

The thermally treated sludge (red color) has an influence on the biodegradability through the DOM and SEPS variables for all the fluorescence zones, as these samples and the DOM and S-EPS variables are located in the same part of the correlation circle. They are all located indeed in the right bottom corner of the circle. The negative influence of these sludge samples in the second component is certainly due to the complex compounds present at high temperatures whereas their positive influence is due to the high accessibility level of DOM and S-EPS.

Indeed, DOM and S-EPS of the fluorescence zones IV to VII are located in the right lowest part of the circle as the four 165°C treated sludge. The 60°C treated sludge points are above and more correlated with the zones I to III since no complex molecules are formed at this temperature.

The anaerobically digested sludge samples are in the same location in the circles than the HSL for the zones IV to VI. As expected, these variables, lower accessible and complex, have a negative influence on BD. In the contrary, the primary sludge samples are all correlated positively with BD and have an influence through all the zones of the RE-EPS fraction. Finally, the secondary sludge samples are located on the top half circle, depending on their biodegradability. The most biodegradable secondary sludge samples are close to the primary sludge samples with a positive influence in the two first components. The least biodegradable samples are located in the top left circle quarter as HSL zones I to III.

The biodegradability is predicted by combining information from spectra zones and accessibility provided by fractionation. Moreover, the correlation circles analyses are coherent with the sludge nature and with the interpretation of the fluorescence zones.

Observed versus predicted values of BD graph is plotted in the figure 59. The RMSE is about 7.15% and the correlation coefficient of the straight line is 1, as the line of perfect fit. Regression coefficient of 0.827 shows that regression is good but the predicted data are a little bit dispersed. In order to validate these results, another PLS regression has been performed using calibration samples values and validation samples values.

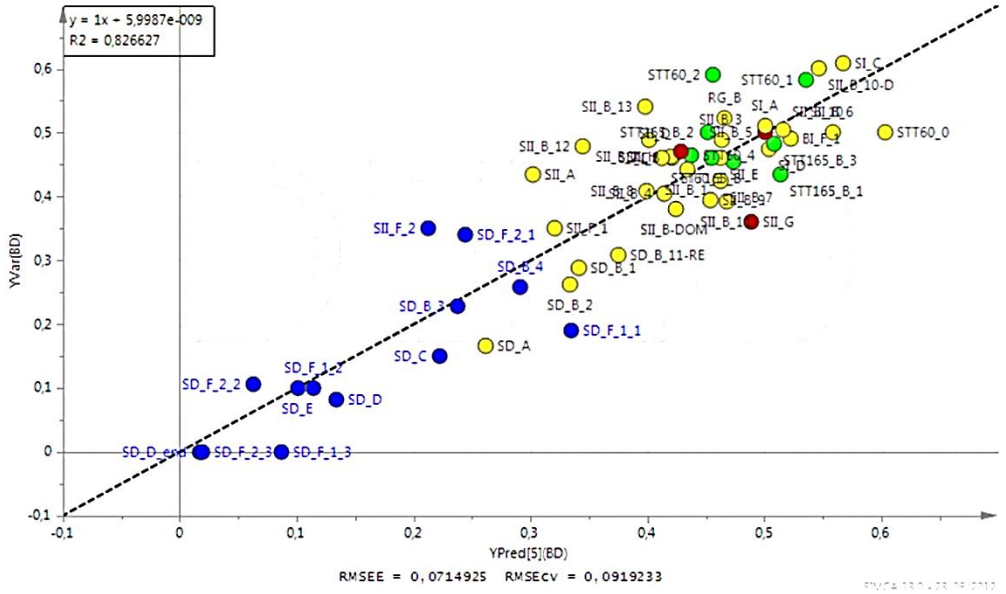

Figure 59 : Observed versus predicted values of biodegradability in PLS regression

IV.3.2. PLS regression model set up for biodegradability prediction

IV.3.2.1. Calibration and validation datasets

In order to validate the previous promising prediction model, some samples have been removed from the calibration dataset and used as validation samples. These samples were chosen over a homogeneous biodegradability repartition going from 0% (anaerobic digested sludge) to 60% (primary sludge). To this end, the dataset was sorted according to increasing biodegradability and one sample in four was removed from calibration dataset to be used as validation samples.

Finally 12 samples were used for model validation. Table 23 presents these validation samples according to their nature and biodegradability range.

Table 24 : Validation samples used for PLS regression

Sludge nature	Anaerobic digested	Secondary	Primary	Thermally treated
Names	SD_D, SD_C, SD_B_4, SD_F_2_1	SII_B-DOM, SII_B_8, SII_B_1, SII_C, SII_D, SII_B_2, SII_B_5, SII_B_11-RE-EPS	SI_A	STT60_2
Biodegradability range	0-34%	38-50%	51%	59%

Boxplot representation of both calibration and validation biodegradability samples (figure 60) validates that there is a similar repartition.

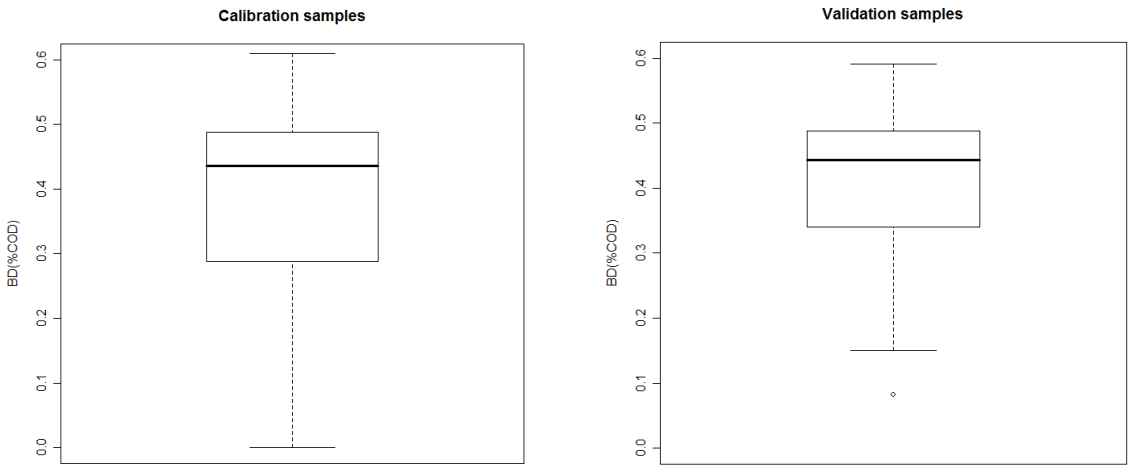

(a) (b)

Figure 60 : Boxplot of biodegradability repartition in calibration (a) and validation (b) samples

IV.3.2.2. Validation results of PLS regression

The PLS model has been recalculated with the newly built calibration dataset. Five components were needed to obtain the maximum Q^2 value (0.615) which is higher than 0.5. R^2X and R^2Y are higher than the previous PLS model with respectively 0.881 and 0.855 values. The observed versus predicted biodegradability is plotted in the figure 60. The line of perfect fit is still reached but with less dispersion. The RMSE is about 6.9% of biodegradability.

Concerning validation data, samples are predicted with RMSEP of 8.6% and a mean error of 5.5%. Thus, statistical parameters are sufficient to validate the obtained PLS model.

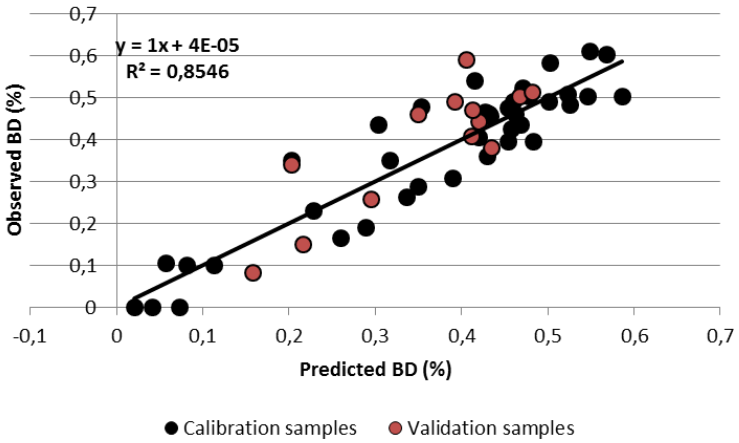

Figure 61 : Observed versus predicted biodegradability

Scaled and centered coefficients are plotted together with their respective error bars, for sludge data with a confidence interval of 95% (figure 61). If the errors bars are two high and cover the 0 value, coefficients are not significant to explain the biodegradability. In this study, 6 coefficients are significant. Two additional coefficients (RE-EPS_VI and HSL_IV) are added because of their low bar error (close to 0), and their important value. This leads to the following coefficients, by order of importance:

- Positive influence: HSL_III, RE-EPS_III, S-EPS_III and S-EPS_II
- Negative influence: DOM_I, HSL_VI, RE-EPS_VI and HSL_IV.

The positive's impact variables, corresponding to the zones II and III of all the fractions, are protein-like compounds fluorescence zones.

Indeed, as mentioned in Henderson et al. (2009) study, several authors made correlations between the protein fluorescence intensity from the tryptophane peak and the BOD concentration.

The negative's impact variables correspond to the zones IV and VI of the HSL fraction (less accessible complex zones), the complex zone VI of the RE-EPS fraction and the zone I of the DOM fraction. The negative effect of the zone I was not expected because the zone I defined the protein-like compounds. Moreover, in all the fractions, the fluorescence zone I has a negative impact on BD whereas the two others zones (II and III) describing the protein-like compounds have a positive impact. The zone I contains in fact fluorescence from tyrosine-like compound and this amino acid is known to contain a phenol group, more or less hydrophobic. One assumption is that the zone I describe proteins imprisoned in a hydrophobic structure. More generally, the fluorescent proteins compounds are suspected to not be directly accessible. The zone VI of all the fractions has also a negative impact. It represents the complex slowly biodegradable compounds such as humic acid compounds (Chen et al., 2003), melanoidins or lignocellulose-like compounds (Muller et al., 2011, in press). That means the PLS interpretation is coherent with the meaning of the fluorescence zones and the extracted fractions.

Concerning the zones IV and V extracted from the S-EPS and the RE-EPS fractions, they have a positive influence whereas in the HSL and DOM fractions, they have a negative influence. No conclusion can be proposed for these zones.

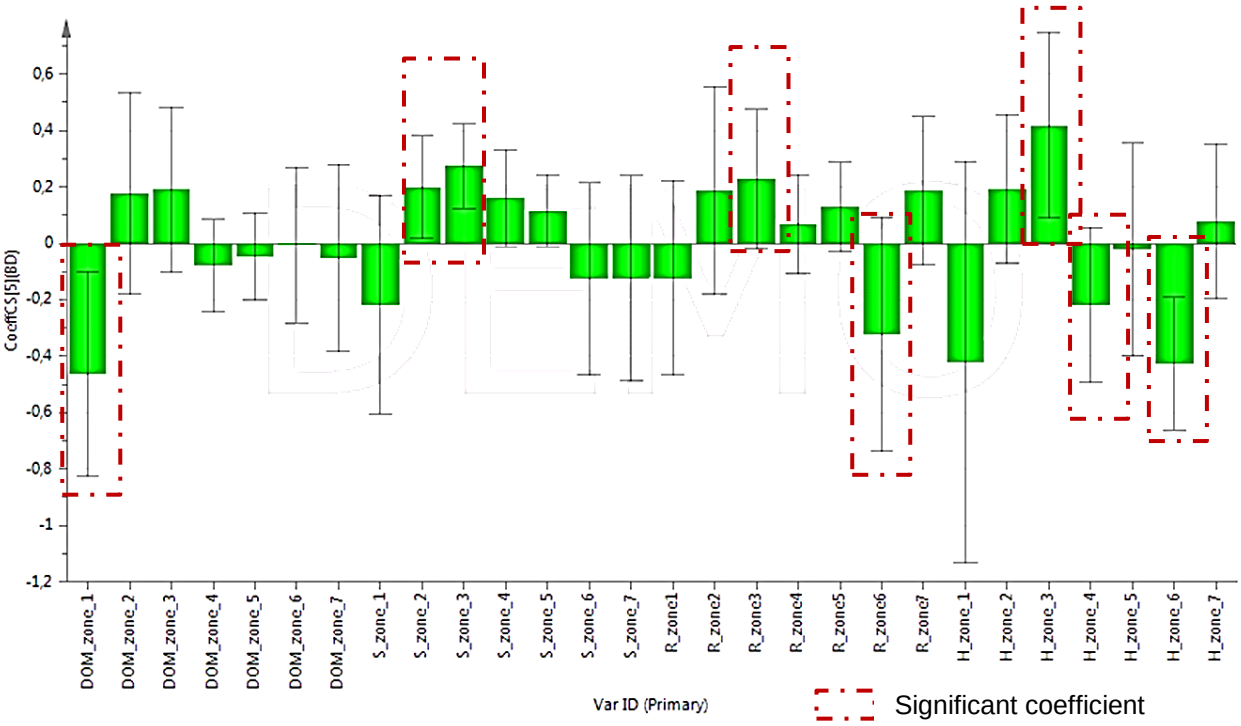

Figure 62 : BD PLS regression coefficients scaled and centered and error bars obtained with a confidence interval of 95%

New biodegradability indicators from 3D-SE-LPF methodology are able to predict all kind of sludge biodegradability in a range of 0 to 60%. The next step aims at validating that these new indicators are able to predict the biodegradable and bioaccessible variable X_{RC}.

IV.4. Correlations between 3D-SE-LPF indicators and bioaccessibility

First, exploratory PLS regressions were performed for all sludge samples with X_{RC} as Y-variable. Then, validation samples were sorted for validation of the PLS model.

IV.4.1. Exploratory PLS regressions

Indicators similar to BD are used for the X_{RC} prediction.

As previously, two PLS regressions were tested considering the 28 indicators as X-variables in a first one and the VFA variable added to the 28 indicators in a second one. Y-variable is defined by X_{RC} variable defined in chapter II. For both PLS regression, the number of components is 6. The quality parameters of the PLS regressions are summarized in table 25.

Table 25 : PLS regressions performances parameters for X_{RC} prediction

PLS regressions	R^2X	R^2Y	Q^2	RMSE
28 variables+VFA	0.909	0.882	0.723	5.5%
28 variables	0.912	0.863	0.631	5.9%

Unlike the BD prediction, the VFA variable addition to the X-variables improves the X_{RC} prediction without increasing the component number. All the regression quality parameters are better with VFA, above all the Q^2 value that increases from 0.631 to 0.723. Moreover, the correlation circle graph in the VFA addition case (figure 63 b) shows that this variable is strongly correlated with X_{RC} in the first component. Thus, this variable is more important in the X_{RC} prediction than in the BD prediction, in sludge case. This means that the easy accessibility feature of the VFA compounds is more important than their readily biodegradablity, in sludge case.

In the 28 variables case (figure 63 a), the correlation circle is similar to the BD results previously obtained.

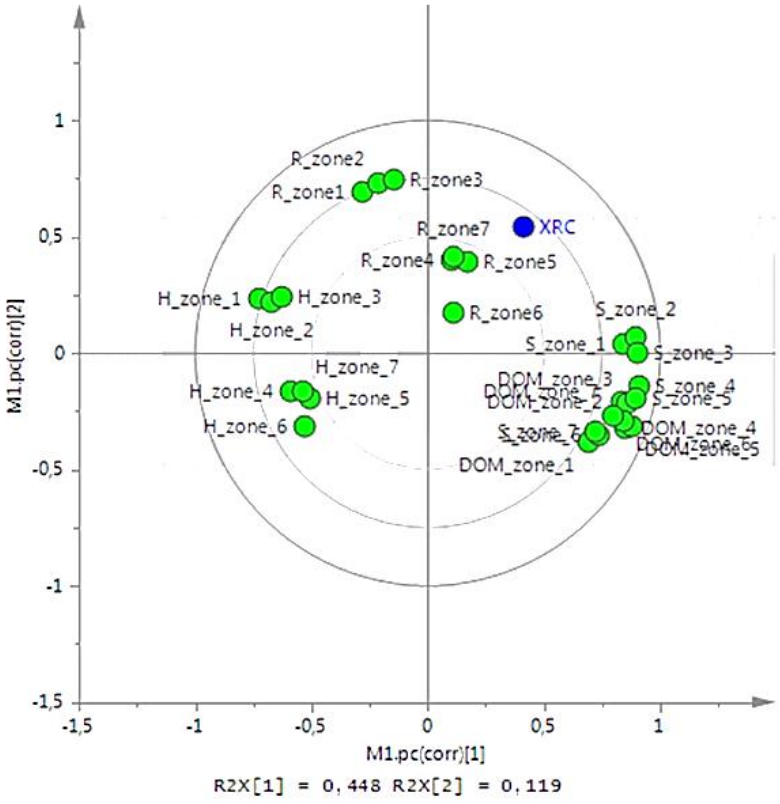

(a)

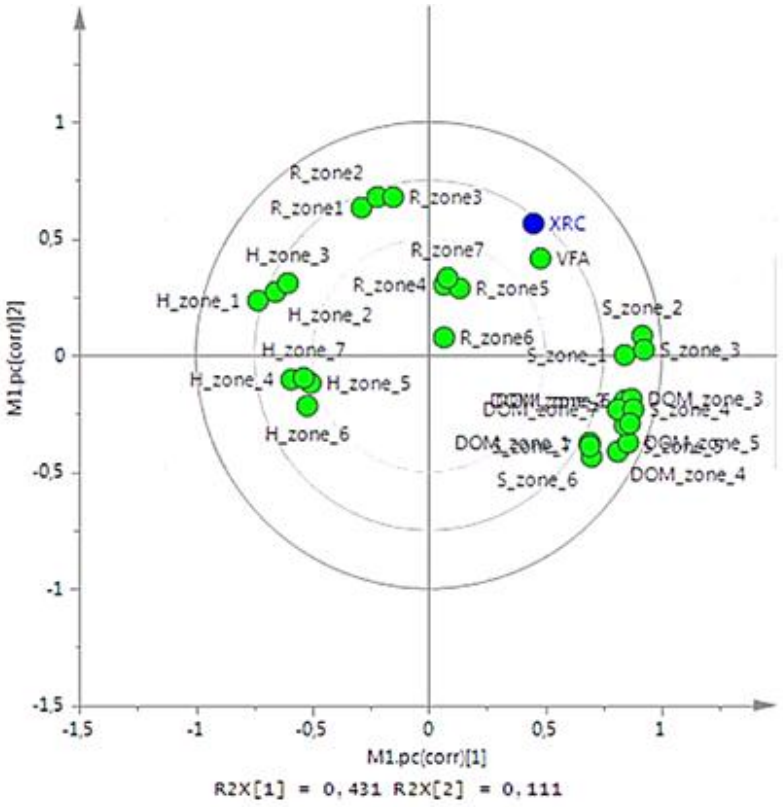

(b)

Figure 63 : Correlation circle obtained for the two first components in PLS regression of 28 variables (a) and 28 variables and VFA (b) for X_{RC} prediction

Study of the scaled and centered coefficients and their error bars (figures 64a and b) shows that the 28 variables PLS regression has less significant variables than with the VFA addition. Indeed, for the 28 variables regression, the most significant variable is only S-EPS_I. RE-EPS_VI, HSL_I can be added because of the very low error bar containing 0 (figure 64 a). In the VFA addition case, 7 variables are significant: HSL_I, VFA, SEPS_IV, SEPS_V REPS_VI, HSL_VI and REPS_VII. VFA is the third most significant variable after HSL_I and HSL_VI and the first that have a positive effect.

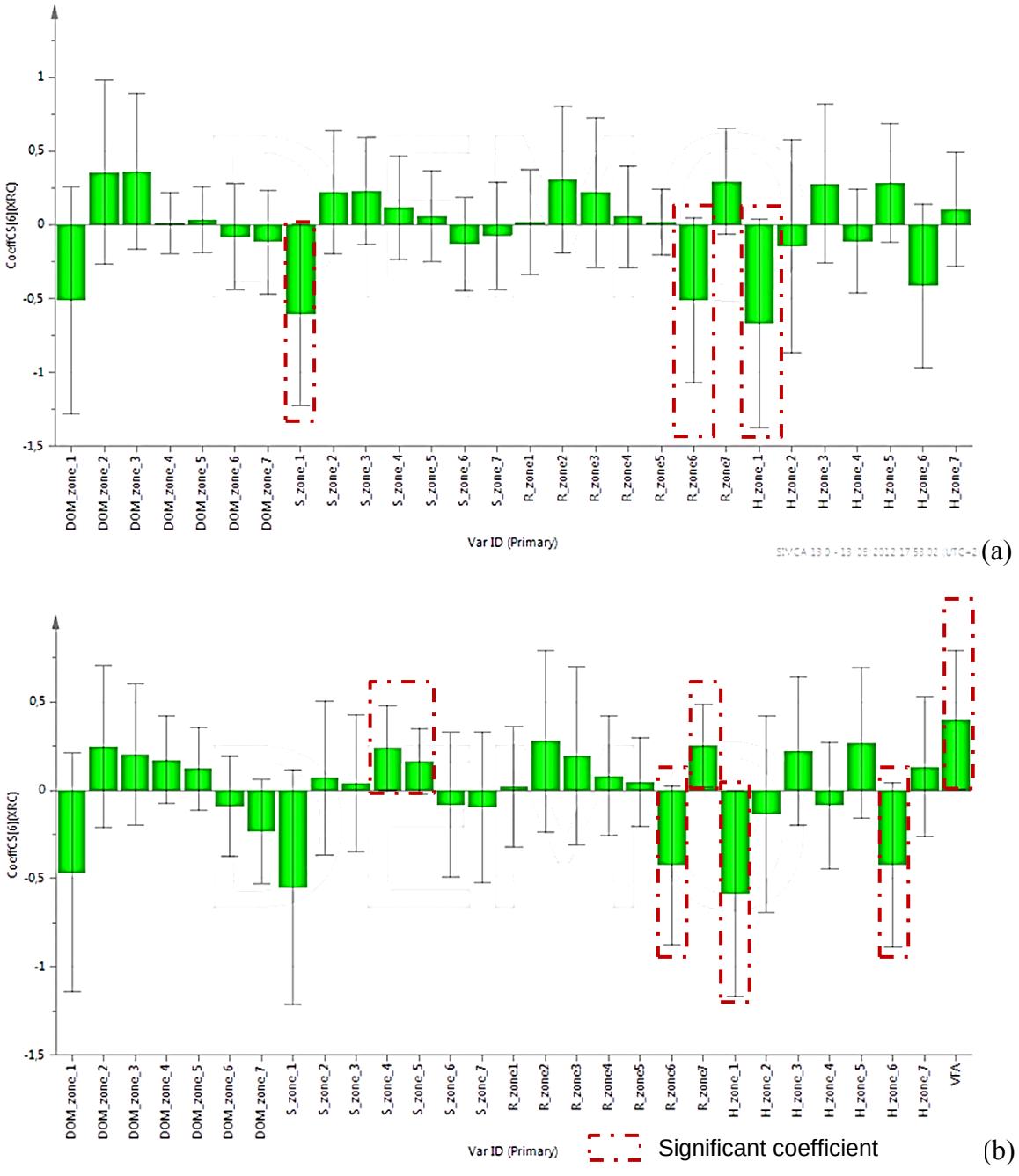

Figure 64 : Scaled and centered coefficient values from X_{RC} PLS regression of 28 variables (a) and 28 variables with VFA (b) obtained with a confidence interval of 95%

A classification analysis through the HCA has been performed as for BD. The sludge groups, close to the BD's groups, were formed on PLS regression with VFA consideration. The green group defined by the thermally treated sludge in BD case is split in two groups: the thermally treated sludge at 165°C (green) and the thermally treated sludge at 60°C (red). Observations from both correlation plots for sludge samples (figure 65) and for X and Y variables (figure 63 b) highlights that VFA positive influence comes from sludge containing high DOM percentage as the 60°C thermally treated sludge. VFA are easily bioaccessible and biodegradable. These sludge samples are grouped with zones I to III from S-EPS that are also responsible of their positive impact (biodegradable and easily accessible).

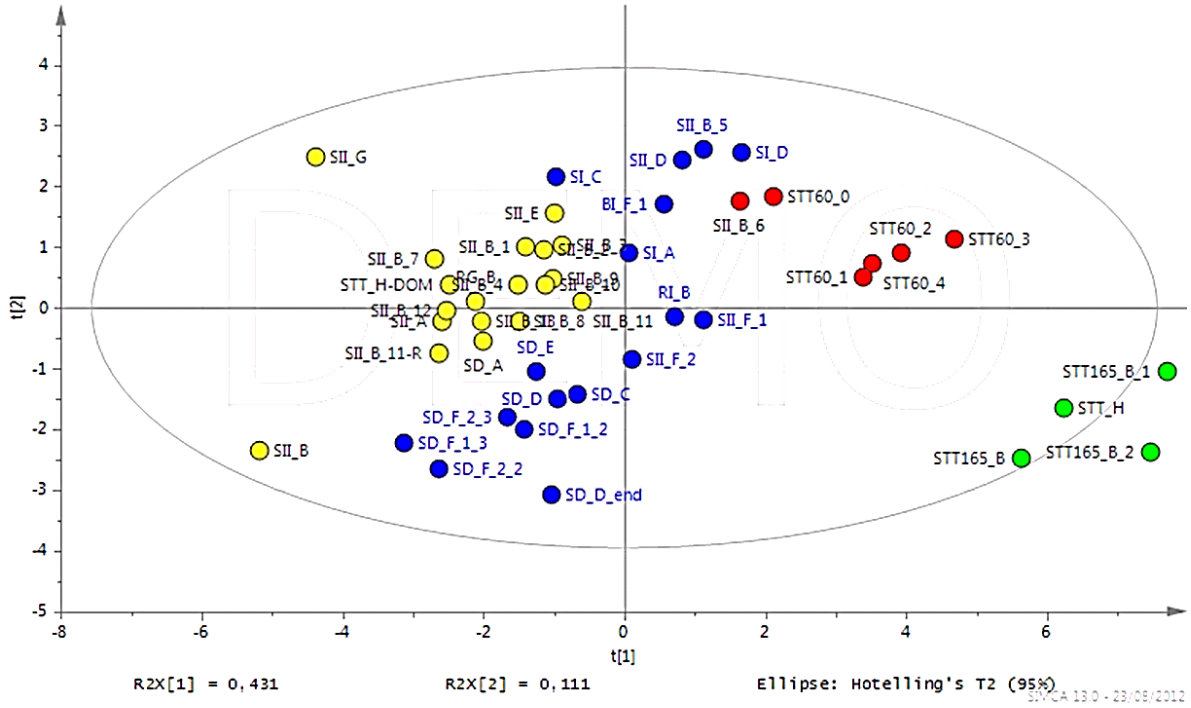

Figure 65 : Correlation circle obtained for sample sludge in PLS regression for 28 variables and VFA

The green colored thermally treated sludge samples (165°C) have a positive influence on X_{RC} in the first component whereas they have a negative impact in the second one. This is due to the complex indicators from S-EPS and DOM (corresponding to the zone IV to VI defined by the melanoidins and lignocellulose-like compounds). These compounds are easily bioaccessible but slowly biodegradable.

The yellow group is composed of the secondary sludge samples. They have a positive influence in the first component but negative in the second one.

Observation from the X and Y variables correlation circle graph shows that the positive influence comes from the zones I to III of the RE-EPS and HSL fractions. The negative influence comes from the low bioaccessibility brought by the RE-EPS and HSL fractions. Moreover there is a hierarchy on this negative impact. The RE-EPS fraction location is less negative than the HSL fraction. This point is coherent with the accessibility concept brought by the fractionation. Finally, the correlation circles interpretation is coherent with the X_{RC} meaning. VFA, the easiest biodegradable and accessible fraction has the most positive impact on X_{RC}.

The blue colored group is composed of digested sludge samples (negatively correlated with X_{RC}) and primary sludge samples (positively correlated with X_{RC}). Complex zones (IV to VII) from HSL are responsible for anaerobically digested sludge location in the correlation circle, as for the BD prediction. Concerning primary sludge, VFA and zones I to III of RE-EPS are responsible of their location in the circle. However, anaerobically digested and primary sludge are not grouped in accordance with their X_{RC} values but both kind of sludge have slowly biodegradable characteristics.

In conclusion, for the X_{RC} prediction, the VFA addition in the X-variables improves the PLS model. Thus, the validation test has been performed with these X-variables. The PLS regression give a good model quality (figure 66). The observed versus predicted X_{RC} curve is closed to the line of perfect fit with a regression coefficient of 1. The dispersion of the straight line is satisfying through a correlation coefficient of 0.88.

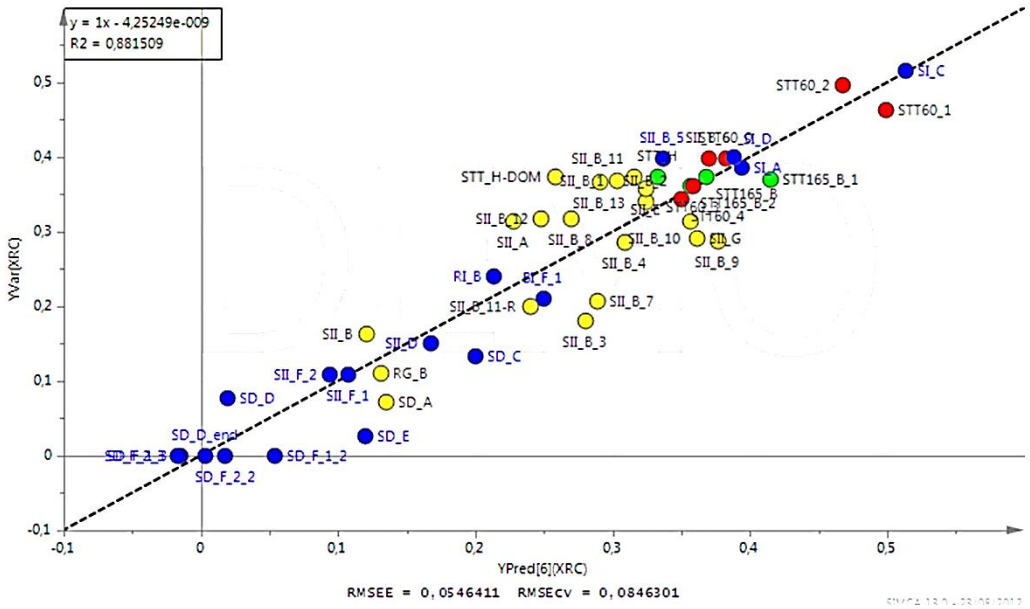

Figure 66 : Observed versus predicted X_{RC} obtained in PLS regression of all sludge in 28 variables and VFA case

IV.4.2. Validation PLS regression for X_{RC} prediction

The validation samples are chosen as the same way than for the BD prediction. Table 26 summarizes the validation samples used for several ranges of X_{RC} values.

Table 26 : Validation samples used for X_{RC} regression

Sludge nature	Anaerobic digested	Secondary	Thermally treated
Names	SD_F_2_2, SD_D, SD_C,	SII_B_11-REPS, SII_B_4, SII_B_10, SII_B_13, SII_B_5	STT60_4, STT165_B, STT60_1
Biodegradability range	0-13%	20-39%	34-46%

The observed versus the predicted X_{RC} plot (figure 67) shows that regression quality is very satisfying. Line of perfect fit is reached with a regression coefficient of 1 and the dispersion is improved with R^2 of 0.896. The X-variables variance is well described by the 6 components with R^2X=0.912. The predictivity is also good with a Q^2 value of 0.64. The RMSE and RMSEP values are low, respectively 5.34% and 6.37% of COD. The mean prediction deviation error of X_{RC} is evaluated at 3.88% of COD.

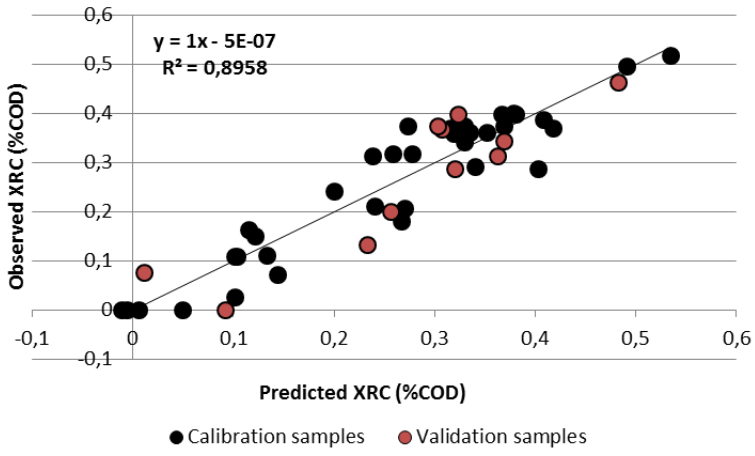

Figure 67 : Observed X_{RC} versus predicted X_{RC} from PLS regression

The indicators set up in this section have successfully predicted both BD and X_{RC}. The VFA information used for the DOM_fluo calculation has been necessary for a better X_{RC} prediction. As previously said, the VFA variable is more necessary for bioaccessibility prediction than for biodegradability in the sludge case. Their rapidly accessibility feature has priority.

In order to study further the PLS models, sensitivity analysis and "simulations" are performed in the next section in order to identify the recalcitrant compounds limiting the anaerobic biodegradation of sludge.

IV.5. Identification of recalcitrant molecules to biodegradation: sensitivity analysis

In this section, the main idea is to identify what molecules have to be targeted to improve both accessibility and biodegradability and to improve anaerobic digestion biodegradability. To this purpose, a sensitivity analysis test has been performed on the PLS regression models previously set up.

IV.5.1. Sensitivity analysis of PLS models: definition

Petersen *et al*. (2002) proposed a model calibration procedure for the ASM1 model. In this methodology, one step is dedicated to the sensitivity analysis of the model parameters. For this purpose, sensitivity is evaluated with the Relative Sensitivity Function (RSF) (equation 4.2). This function calculates the impact of a parameter change on the state variables. Based on this study, RSF is calculated for some parameters used on the PLS in order to identify the X-variables impact.

$$\boldsymbol{RSF} = \frac{\boldsymbol{\Delta y}}{\boldsymbol{y}} \times \frac{\boldsymbol{p}}{\boldsymbol{\Delta p}} \qquad \textbf{Equation 4.2}$$

Where

y is the initial value variable

Δy is the deviation between initial and end final values after a parameter change

p is the initial parameter value

Δp is the deviation between initial and final parameter value

From Petersen et al. (2002), depending of the RSF value, a parameter is considered more or less influential as following:

- RSF<0.25: parameter is considered no influential, "0"
- 0.25<RSF<1: parameter is influential, "+/-"
- if 1<RSF<2: parameter is very influential and finally "++/--"
- if 2<RSF: parameter is extremely influential "+++/---"

The sign "+" means that both parameter and variable evolve in the same way whereas sign "-" means that they do not evolve in the same way.

The PLS X-variable sensitivity is analyzed in this section on the BD and X_{RC} prediction. As already shown for each variable, some X-variables are more or less significant. In order to go further in interpretation, the percentage of COD is tested as well as the fluorescence zones.

IV.5.1.1. Sensitivity analysis of PLS models: fractionation variables

For the sensitivity analysis, the initial sludge chosen is the secondary sludge named SII_E. The final value used for the RSF study is 0 in order to study their removal impact.

The results of the COD fractions sensitivity analysis (table 27) reveal that the DOM and the S-EPS fractions have a low influence on both BD and X_{RC} prediction whereas the RE-EPS fraction has a positive impact and the HSL fraction a negative impact. In fact, the RE-EPS fraction takes part of the more accessible fractions, as shown by the continuous test presented in the chapter III, whereas the HSL fraction is considered as one of the least accessible fraction. Thus, this observation is coherent.

Table 27 : Relative sensitive function calculated for COD fractions on BD and X_{RC} variables obtained in PLS

Variables	Parameters values		BD		X_{RC}	
	Initial value	Final value	RSF value	Code	RSF value	Code
DOM	3.40%	0	-0.009	0	-0.140	0
S-EPS	1.80%	0	0.070	0	-0.260	-
RE-EPS	8.90%	0	0.260	+	0.430	+
HSL	24.50%	0	-0.250	-	-0.990	--

The PLS significance analysis has shown that some variables such as DOM_I were very influential on the BD prediction. Thus, depending on the fluorescence zone and their complexity level, the variables will be more or less influential.

IV.5.1.2. Sensitivity analysis of PLS models: fluorescence zones variables

The fluorescence zones are the second important information considered in the BD and X_{RC} prediction. In the same way than the fractions, sensitivity analysis of each fluorescence zone is studied. To this purpose, the sum of one zone i in all fractions (DOM_i+S-EPS_i+RE-EPS_i+HSL_i) is used. Fluorescence zone impact on the BD prediction is presented in the table 28. As for the fractions, the final values used are 0 in order to simulate their removal by a pre-treatment for example. Three zones influence strongly the BD prediction: the zones I, III and VI. These zones have been already highlighted. The fluorescence zone I and VI have a negative impact on the BD prediction whereas the zone III representing protein-like has a positive impact. These observations are confirmed with the RSF study. When the zone I is

removed from all the fractions, the predicted BD increases from 0.463 to 0.797 (72%). When the zone VI is removed, the predicted BD increases from 0.463 to 0.649 (40%). The fluorescent molecules of the zones I and VI are the main responsible of the low biodegradability.

Table 28 : Relative sensitive function calculated for fluorescence zones on BD variable obtained in PLS

Zones	Initial sum of X-variables on zone i	Final sum of X-variables on zone i	BD_0	BD_{final}	RSF value	code
I	0.059	0	0.463	0.797	-0.722	-
II	0.128	0	0.463	0.356	0.231	0
III	0.058	0	0.463	0.271	0.415	+
IV	0.083	0	0.463	0.369	0.203	0
V	0.033	0	0.463	0.407	0.121	0
VI	0.018	0	0.463	0.649	-0.401	-
VII	0.004	0	0.463	0.371	0.199	0

The same analysis is made in the case of X_{RC} prediction (table 29). In this case, only the zones I and VI have an influence on the X_{RC} prediction. When the zone I is removed, the predicted X_{RC} increased from 0.259 to 0.751 (190%) and when the zone VI is removed, the predicted X_{RC} increased from 0.259 to 0.446 (72%). Thus, both zones have to be targeted to increase both bioaccessibility and biodegradability.

Table 29 : Relative sensitive function calculated for fluorescence zones on X_{RC} variable obtained in PLS

Zones	Initial sum of X-variables on zone i	Final sum of X-variables on zone i	X_{RC0}	$X_{RCfinal}$	RSF value	code
I	0.059	0	0.259	0.751	-1.898	--
II	0.128	0	0.259	0.202	0.219	0
III	0.058	0	0.259	0.223	0.138	0
IV	0.083	0	0.259	0.199	0.230	0
V	0.033	0	0.259	0.258	0.005	0
VI	0.018	0	0.259	0.446	-0.721	-
VII	0.004	0	0.259	0.207	0.202	0

IV.5.1.3. Sensitivity analysis of PLS models: scenario analysis

As the RE-EPS and HSL are the main influential fractions as well as the fluorescence zone I and VI have the most negative impact on the BD prediction, some scenarii analyses are performed using the PLS models. The aim of these tests is to simulate some pretreatment able to uptake the recalcitrant molecules.

A final value of 0 is used successively for the fluorescence zones I and VI from RE-EPS and HSL in order to simulate their removal.
Concerning the RE-EPS fraction, the predicted BD increases from 0.463 to 0.766 (65%) and the predicted X_{RC} increases from 0.259 to 0.447 (74%) when zone I and VI are equal to 0. In the case of the HSL fraction, the predicted BD increases from 0.463 to 0.789 (70%) and the predicted X_{RC} increases from 0.259 to 0.711 (174%). The zones I and VI of the HSL fraction removal have a more positive impact than the zone I and VI of the RE-EPS fraction removal, as far as HSL is the least accessible fraction. However, if another scenario is performed with the zones I and VI removal on the RE-EPS and HSL fractions, the predicted BD and X_{RC} increase respectively to 109% and 86%. This means that molecules from the zones I and VI located in the HSL fraction and in the RE-EPS fraction have to be targeted to improve biodegradability and bioaccessibility. In the S-EPS and the DOM fractions cases, removal of zones I and VI leads to an increase of only 8.5% (0.463 to 0.506), not so significant.

N.B: However, we can notice that the prediction results go out of the validity range of the PLS models (0-60%). These results represent only a diagnostic of the interest to remove such recalcitrant molecules.

Another scenarii tests have been performed on digested sludge SD_E which is the anaerobic digested sludge of SII_E. As previously, the zones I and VI are successively tested into the RE-EPS and HSL fractions. This analysis leads to the results presented in the table 30.
Concerning the HSL fraction, the removal of the zones I and VI increases more the predicted BD and X_{RC} than in the RE-EPS fraction. As already mentioned, the HSL is the fraction the most influential on the BD and X_{RC} prediction.

However, the results obtained with the removal of both zones I and VI in the fractions RE-EPS and HSL show that the biodegradability and the bioaccessibility from the digested sludge could be improved by targeting these molecules located in both floc layers. Indeed, the pre-treatment of the anaerobic digestion feed sludge or post-treatment of anaerobic digested sludge could improve significantly the biodegradability and thus the energetic balance from methane production.

Table 30 : Predicted BD and X_{RC} by PLS models for several scenarios where zone I and VI are removed from RE-EPS and HSL in digested sludge SD_E

R-EPS		HSL		BD	X_{RC}
Zone I*	Zone VI	Zone I	Zone VI		
X	X	X	X	0.100	0.025
0	X	X	X	0.215	0.112
X	0	X	X	0.287	0.239
X	X	0	X	0.286	0.291
X	X	X	0	0.333	0.245
0	0	X	X	0.389	0.384
X	X	0	0	0.506	0.573
0	0	0	0	0.781	0.722

*: 0 means that fluorescence zone is removed from X-variables; X means that fluorescence zone is not removed

The identification of these compounds is relevant in order to target the molecules to remove to improve the sludge biodegradation and to propose some pre-treatment. The table 31 is a literature survey of the fluorescent molecules and their location in the 3D spectra.

As reported by the literature, the fluorescence zone I is due to the tyrosine-like fluorescence. However, this amino acid is composed of a phenol group which provides a feature more or less polar to the compound. In addition, the phenol fluorescence has been found into the zone I too (Prahl, 2012). One assumption is that the zone I is formed by non-polar structure where the proteins biodegradable are imprisoned but non bioaccessible because of their hydrophobicity structure. Hexane or methanol extraction of some fraction containing the zone I could be performed and analyzed through the 3D-LPF spectroscopy in order to identify the hydrophobic protein fluorescence location. Moreover, these compounds seem to be extractible because of their absence in non-extracted samples.

According to the literature, the fluorescence zone VI can correspond to several compounds: humic acids, fulvic acids, melanoidins, polysaccharides, Nicotinamide Adenine Dinucleotide dehydrogenase (NADH) and lignocellulose-like markers. The annex 4 presents some 3D spectra obtained for several samples studied. Concerning the melanoidins, as already mentioned, thermally treated sludge at high temperature contains these glycated proteins. By studying thermally treated sludge spectra of DOM from STT165_B_2, the fluorescence peak of zone VI is about $\lambda_{excitation}/\lambda_{emission}$ of 340nm/420nm and corresponds with melanoidin compounds as explained by Muller *et al.* (2011).

However, the fluorescence peak found in the zone VI of the HSL fraction from primary, secondary and digested sludge have coordinates at 320/390 nm, close to the humic acids substances (Dominguez *et al.,* 2010).

In the RE-EPS fraction of primary, secondary and digested sludge, the zone VI peak is around 340nm/420nm like the melanoidin but they could also be humic acid substances as defined by Sheng *et al*. (2006) or lignocellulose-like compounds as observed by 3D-SPF Muller *et al*., (2011) at 370/430 as lignin and paper fluorescence compounds.

Thus, depending on the peak location and the sample nature, the recalcitrant compounds will be glycated proteins, humic acids substances or lignocellulose compounds. The peak location corresponding to NADH at 370-390/450-470 is not observed on the samples studied.

Concerning fulvic acid compound, some authors found two peak locations, one in the zone IV and another in the zone VI. However, as Hao *et al.* (2012) showed, standard solution of fulvic acid has two peaks of fluorescence but the peak located in zone VI has a very low intensity of fluorescence.

When humic acid is present in the sample, its fluorescence intensity can recover the fulvic acid one.

Therefore, more investigation has to be done in order to complete the recalcitrant molecules identification and to found the appropriate treatment to remove them.

Table 31 : Literature survey of fluorescent molecules location in 3D spectra

$\lambda_{excitation},\lambda_{emission}$	Compound-like	Zone (this study)	Sample type	References
<250,300-320	Tyrosine	I	DOM from wastewater, rivers, Recycled water systems, bound EPS extracted from MBR sludges, DOM from MBR, waste activated sludge, DOM from anaerobic co-digestion sludge, disinfection by-products	Chen et al. 2003, Henderson et al., 2009, Dominguez et al. 2010 Wang et al. 2009, 2010, Muller et al. 2011, Wan et al 2012
<250,320-400	Tryptophane	II		
250<λ_{ex}<300, 300-400	Tryptophane, microbial products	III		
<250,400-500	Fulvic acid	IV		Chen et al. 2003, Wang et al. 2010, Muller et al. 2011, Wan et al 2012, He et al. 2011, Hao et al. 2012
245-290,306	Phenol	I	Phenol , bisphenol A	Del Olmo et al., 1999
250<λ_{ex}<300, 400-550	Polyaromatic acid humic	V	DOM from MBR sludge	Wang et al. 2010
>280, >380	Humic acid	V-VI	DOM from wastewater, rivers	Chen et al. 2003
>300, 350-400	Polysaccharides	VI	DOM from MBR sludge	Wang et al 2010
>300, 400-550	Polycarboxylate humic acid	VI	DOM from MBR sludge	Wang et al. 2010
330-340,420-430	Humic acid	VI	EPS from anaerobic sludge, DOM from winery compost and distillery residues	Sheng et al. 2006, Egea et al. 2007
305-315,405-415	Humic acid	VI	DOM from MBR sludge and anaerobic digestion sludge	Wang et al. 2009, 2011
390,450	Humic acid	VI	Extracellular and intracellular products from activated sludge	Li et al. 2006
340,420	Melanoidin	VI	Waste activated sludge, lignine (standard solution)	Muller et al. 2011
320,390	Humic acid derived	VI	bound EPS extracted from MBR sludges	Dominguez et al. 2010
320-340,400-420	Fulvic acid	VI	Biomedia, EPS from aerobic and anaerobic sludge, disinfection by-product	Pons et al. 2004, Li et al. 2008, Ni et al. 2009, Hao et al. 2012, Lee et al. In press.
237,420 and 326,415	Fuvic acid	IV and VI	Standard solution	Hao et al., 2012
290,460	Humic acid	VI	Standard solution	Hao et al., 2012
380,470	Humic acid	VI	Biomedia	Pons et al. 2004
380,440	Lignine, cellulose, paper, humic acid	VI-VII	Activated sludge, lignine (standard solution)	Muller et al. 2011, In press
370-390,450-470	NADH/NADPH : metabolic activity of bacteria	VI-VII	Activated sludge	Kobbero et al. 2008
430,510	Humic substances	VII	Activated sludge	Kobbero et al. 2008
420,480	Lipofuscin, protein condensed	VII	Activated sludge, lignine (standard solution)	Muller et al. 2011

IV.6. Conclusions

From the results obtained, the fractionation and the fluorescence spectra information have predicted both bioaccessibility and biodegradability.

The contribution of the extracted fractions and the fluorescence zones to these predictions can be represented in a matrix format as shown in figure 68.

This matrix is defined by two axes:

- The bioaccessibility level depending on the extracted fraction considered,
- The biodegradability level depending on the fluorescence zone found in the extracted fractions.

Each indicator translates a compound characterized by its bioaccessibility and biodegradability level. The following compounds are sorted from the most biodegradable and bioaccessible until the least biodegradable and bioaccessible:

- VFA: very biodegradable and very accessible
- S-EPS III-II-I: easily biodegradable and accessible
- DOM II-III: easily biodegradable and easily accessible
- DOM I-IV-V-VI-VII: slowly biodegradable and easily accessible
- S-EPS IV-V-VI-VII: slowly biodegradable and accessible
- RE-EPS I-II-III: biodegradable and slowly accessible
- HSL I-II-III: biodegradable and very slowly accessible
- RE-EPS IV-V-VI-VII: slowly biodegradable and very slowly accessible
- HSL IV-V-VI-VII: very slowly biodegradable and very slowly accessible
- NE: very slowly biodegradable and no accessible

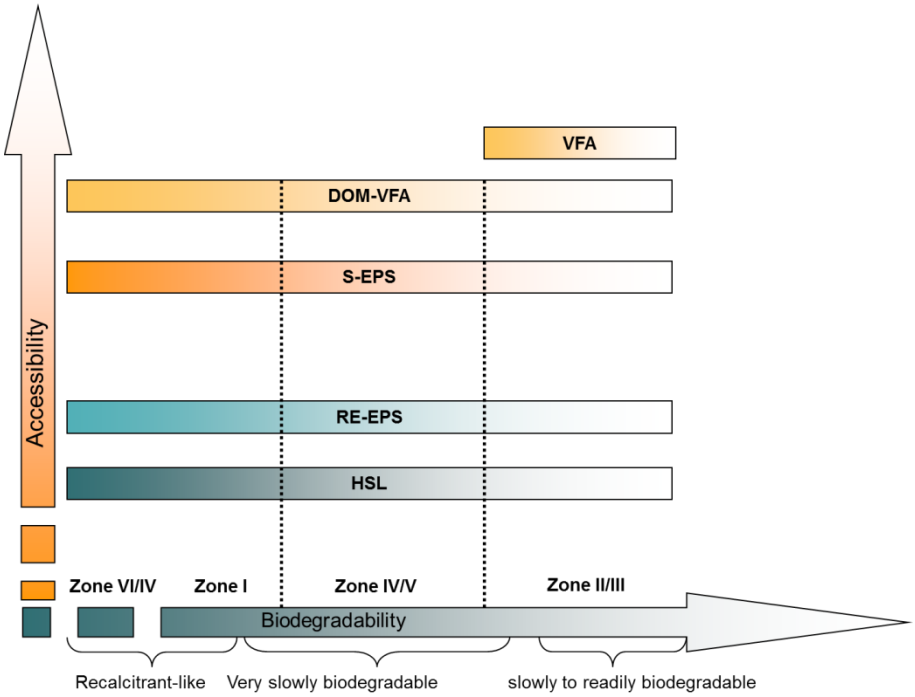

Figure 68 : Matrix representation of the indicators contribution to BD and X_{RC} prediction

The scheme simulating the sludge composition can thus be updated (cf. figure 69) to include this hierarchy.

This result is very promising because it opens several applications and research studies. First, cartography of the sludge can be made. From the identification of the recalcitrant compounds, it will be possible to better target and optimize the pretreatments aiming at increasing the biodegradability and bioaccessibility. This cartography could also be used as a performance diagnostic of a specific treatment. Besides, the sludge composition is better described and richer than global analysis such as the BMP test.

From the PLS sensitivity analysis, the conclusions revealed that the HSL and RE-EPS fractions are the most influential concerning both biodegradability and bioaccessibility predictions. Concerning the fluorescence zones, it appeared that the zone I and the zone VI have a negative impact on the BD and X_{RC} prediction. When a sludge sample is tested considering that the zone I and VI have been removed by a given pre-treatment from HSL and RE-EPS in models, the gain of BD and X_{RC} is very significant (closed to 100% of biodegradation). As found by the sensitivity analysis of the models, the fluorescent compounds from zone I and VI in the HSL fraction are the most recalcitrant molecules limiting the sludge biodegradability.

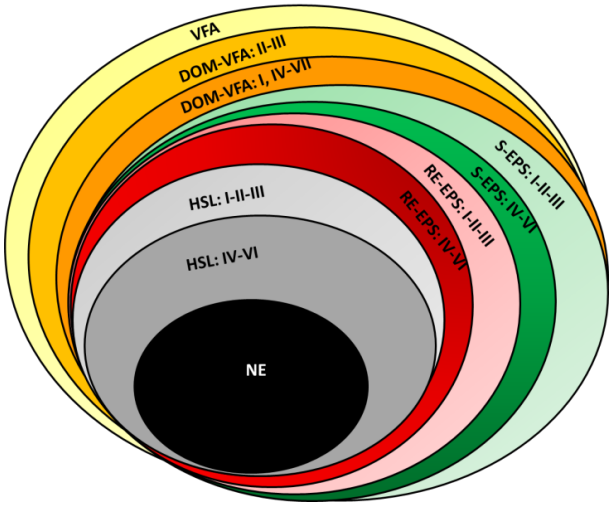

Figure 69 : Detailed scheme representation of sludge bioaccessibility and biodegradability according to fractionation and fluorescence results

Another application is the prediction of the anaerobic digestion performance. Thanks to the process modeling, methane production, performance, design, system dysfunctions or experiment guidelines could be proposed. The bioaccessibility and biodegradability information that are now available will be useful to better calibrate dynamic models. Next chapter purpose is to validate this last application: are the variables provided by the cartography able to obtain a better fit of the experimental data?

V. METHODOLOGY GLOBAL VALIDATION : MODIFIED ADM1 MODELLING AND DIGESTERS DESIGN IMPACT

V.1. Continuous lab pilots performances 175
V.1.1. Reference period 176
V.1.2. Disturbing period 177
V.2. Modified ADM1 modeling 180
V.2.1. Modeling procedure 180
V.2.2. Input implementation and parameters 181
V.2.3. Model calibration 182
V.2.3.1. Steady state calibration 182
V.2.3.2. Dynamic state calibration 186
V.3. Model validation 192
V.3.1. Dynamic validation with disturbing data 192
V.3.1.1. Input data during both references and disturbing period 192
V.3.1.2. Dynamic validation 193
V.3.1.3. Sensitivity analysis 199
V.4. Bioaccessibility variables and impact on hydraulic retention time 199
V.4.1. Scenarii analysis 200
V.4.2. Correlations found between bioaccessibility variables and HRT 201
V.5. Conclusions and discussion 205

Note for the reader:

Chapter V is the last results chapter. It presents the validation of the sludge characterization methodology using the previously determined variables predicted by PLS as inputs of a dynamic model of anaerobic digestion processes. The chosen model is a modified version of ADM1 that has been demonstrated to be appropriate for sludge digestion. Reference data are used for calibration whereas disturbing data are used for validation. A discussion based on the sensitivity analysis of ADM1 input variables is also presented. Investigation about the impact of the fractionation on the process design is developed. Finally, several perspectives of the study are highlighted.

One of the aims of the characterization methodology proposed in this study is to quantify the ADM1 input variables for a better description of the sludge treatment. Statistical tests have shown that the fluorescence spectroscopy information describing complexity coupled with chemical extraction describing accessibility leads to both biodegradability and bioaccessibility prediction applied on different municipal sludge. In the ADM1, the biodegradability is one of the main information needed in order to calculate the non-biodegradable fractions X_I and S_I. Additionally, previous tests have highlighted that all the sludge are mainly composed of slowly accessible fractions (HSL is the main fraction). In this context, hydrolysis is the rate-limiting step and is crucial for evaluate an optimal solids retention time. To this purpose, a modified version of the IWA ADM1 model has been selected (Mottet, 2009). Compared to the standard ADM1, this model explains the bioaccessibility concept through the definition of two new variables representing the slowly and the readily hydrolysable organic matter. A Contois kinetics term is also used to simulate the slow hydrolysis kinetics of sludge. Contois considers specific hydrolysis microorganisms producers of dedicated enzymes. Thus, the purpose of this chapter is to use the variables obtained by the PLS regressions (BD and X_{RC}) to validate the methodology with the simulations of two lab scale reactors continuously fed by a secondary sludge.

In order to obtain an accurate validation, one lab scale reactor has been dedicated to disturbing tests consisting of organic matter intrinsic modification (i.e. removing some fractions of the sludge). The other reactor is used as a reference in order to compare the performances and the disturbing impacts. Summary of this strategy is described in the figure 70.

First, the reactors performances and the mass balances are checked to be used for modeling purpose. Second, the model input implementation and the model calibration are described followed by the validation step. Third, a sensitivity analysis and discussions about the impact of the variables predicted on process design conclude this chapter.

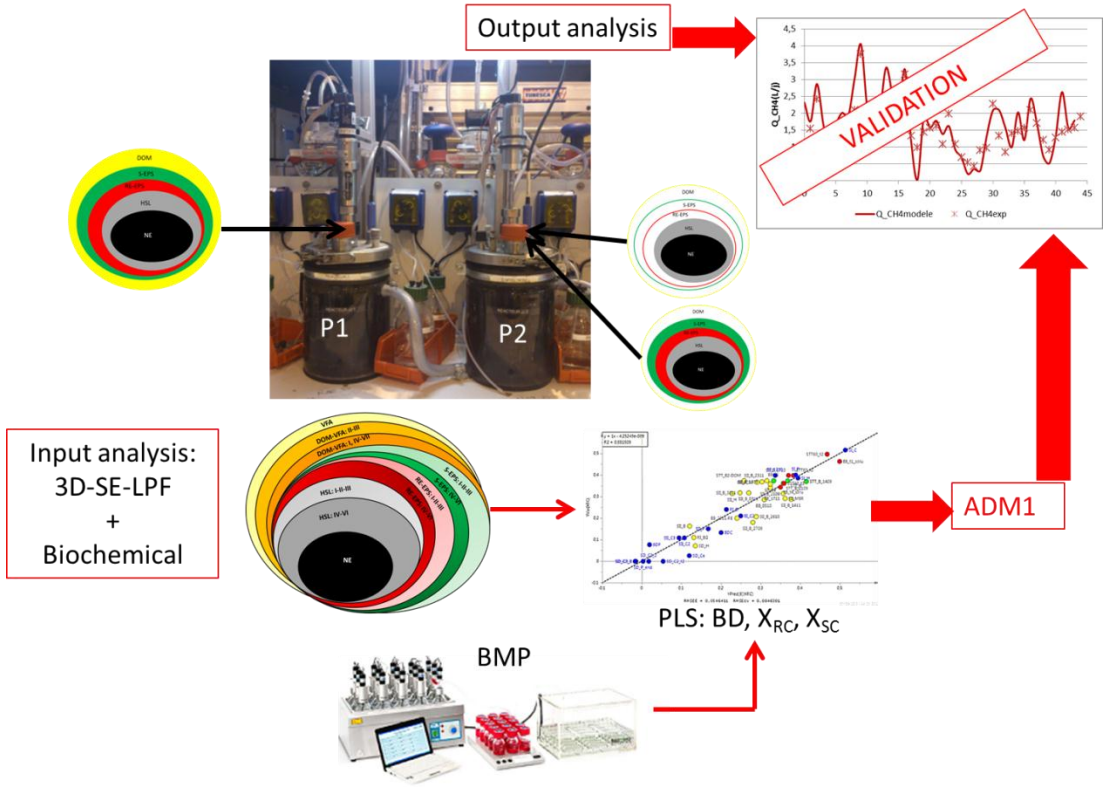

Figure 70 : Strategy used for characterization methodology validation

V.1. Continuous lab pilots performances

The reactors P1 and P2 operating conditions were described in Chapter II. The secondary sludge used as feed is the SII_B. SII_B. It was collected every week from the wastewater treatment plant B and stored at 4°C until a new sample was received. At the beginning of the experiments, in order to reach rapidly the steady state, the anaerobic digested sludge from plant B was used as inoculum for both reactors. Solids concentration stabilization (figure 71) defines the beginning of the steady state period (corresponding to 3 HRTs). The HRT applied is about 18 days which is the value commonly found in European anaerobic digesters.

When both reactors reached the steady state, two periods were defined:

- 06/10/11-17/11/11: the “reference” period is defined by the same feed and operating conditions for both reactors. Data provided in this period constitutes the calibration dataset for the ADM1 model.
- 18/11/11-10/12/11: The “disturbing” period. P1 is fed with the same sludge but the sludge feeding P2 is modified. Indeed, the DOM fraction (7.4% COD) is first removed. Later, the DOM+S-EPS+RE-EPS (10.3-13.9% COD) fractions are removed. The same organic load is performed on both reactors by thickening the sludge modified. This second period is used as validation for ADM1 model.

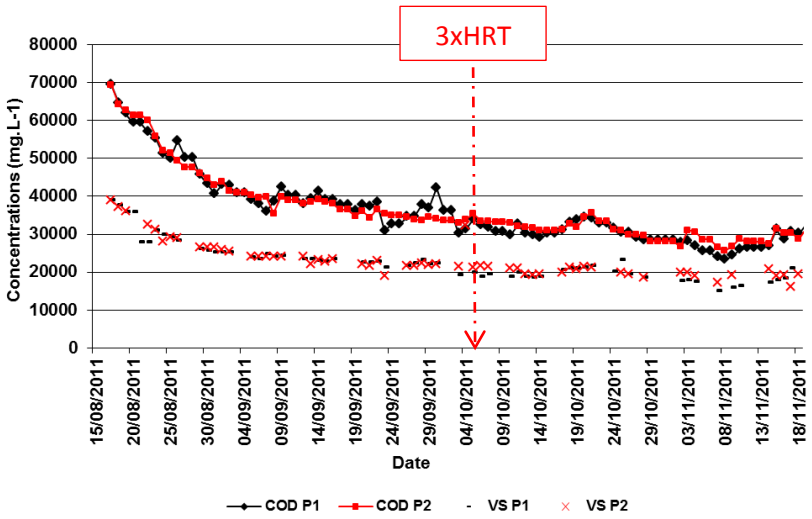

Figure 71 : Evolution of total solids and volatile concentration of output reactors

Performances of P1 and P2 are first studied during the reference period and then during the disturbing period.

V.1.1. Reference period

After reaching the steady state, both reactors are operated similarly during 42 days. The sludge, the HRT and the organic load applied are the same for both pilots (figure 72a). For practical reasons, the reactors were fed constantly during the working days of each week while, in order to manage the week-end, the feed was increased on the Fridays. The load was three times higher in order to keep constant the HRT over the whole week. This explains the loading profile in the figure 72a where every 5 days, the organic loading reaches a peak and then decreases down to 0 for 2 days. Consequently, the biogas production profiles are impacted as shown by the figure 72b. This evolution constitutes a hydraulic disturbing which brings more validation to the model.

Concerning the output profiles of biogas (figure 72 b) and solids (figure 72 c), they evolved similarly for both reactors. However, a deviation was observed between the methane production of P1 and of P2 during the working days although the COD concentration is similar. The methane production from P1 is higher than P2 one. This phenomenon was due to a technical problem on the P1 counter gas which overestimated the biogas production. The COD and TC mass balance errors of P1 in this period were respectively 12% and 18% whereas those of P2 were respectively 0.3% and 5.46%. One can conclude that data from P1 and P2 were repeatable during the reference period.

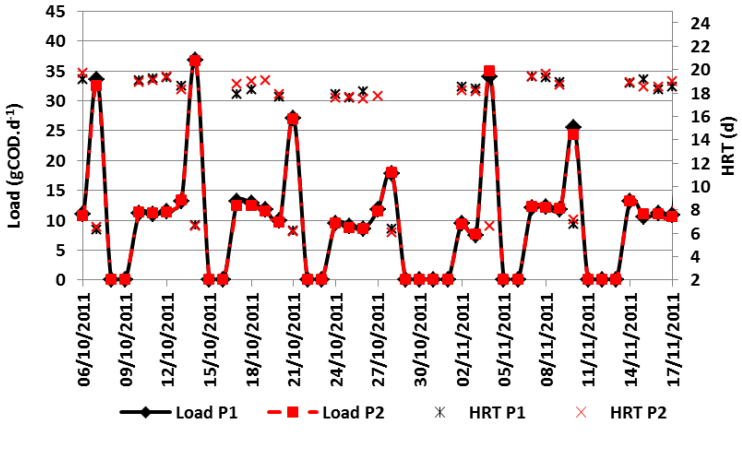

(a)

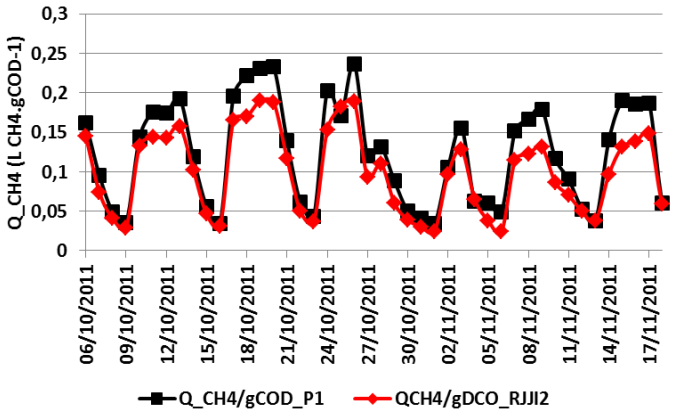

(b)

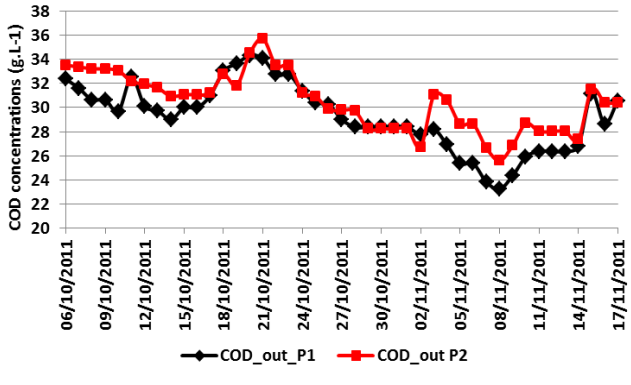

(c)

Figure 72 : Reference period performances comparison in P1 and P2 reactors in terms of (a) organic loads and HRT, methane production rate (b) and output COD concentration (c)

V.1.2. Disturbing period

The disturbing period was initiated after 42 days of the reference period. The Figure 73a presents the organic load and the HRT applied on both reactors. The operating conditions were the same for both reactors. The only difference was the intrinsic organic fractionation of the sludge feeding P2.

During 6 days (from 18/11/11 to 24/11/11), the DOM fraction was removed from the sludge by centrifugation. Comparison between the P1 and P2 output performances shows that there was an impact on the methane production. The methane produced by P2 was lower than P1 one. Relative errors go from 6 to 20% (figure 73c). Another impact was on the kinetics of the daily profiles. The figure 38 in the chapter III presented 3 days of the biogas production in P1 and P2 during the perturbation period. As mentioned, the DOM fraction impacted the first part of the kinetics curve, meaning that DOM participated to the most bioaccessible and biodegradable fraction of the sludge.

After 4 days being back to the "reference" feeding, another disturbing period is applied. The DOM, S-EPS and RE-EPS fractions were removed from the sludge by centrifugation, after chemical extraction and sludge neutralization during 9 days (28/11/11-07/12/11). The methane produced by P2 was strongly impacted by this removal compared to the methane produced by P1, as shown by the figure 73b. Indeed, the methane production yield decreased in P2. Relative errors between the P1 and P2[1] total biogas production go from 16 to 52%. The kinetics impact was also higher than for the DOM fraction removal as highlighted by the Figure 39 in chapter III. This means that the HSL and the NE fractions constituting the P2 sludge feed were slowly bioaccessible and slowly biodegradable. Thus, these disturbing tests were very useful to validate the bioaccessibility correlation with the chemical fractionation in addition to provide useful data for modeling purpose.

On the other hand, the output total COD impact was limited in the first disturbing period (figure 73 c). Indeed, the DOM fraction was removed. Thus, process output led to less soluble COD. However, during the second disturbing period, accessible fractions were removed and particular COD was accumulated certainly due to a lower biodegradation of the disturbing sludge in comparison of the reference sludge (02/12/11-09/12/11). Between the 4 days of reference period (24/11/11-28/11/11) the total COD from P2 was still higher than P1 one but finally led to come back at the same value.

[1] Relative error = [Q_BG(P1)-Q_BG(P2)]/Q_BG(P1)

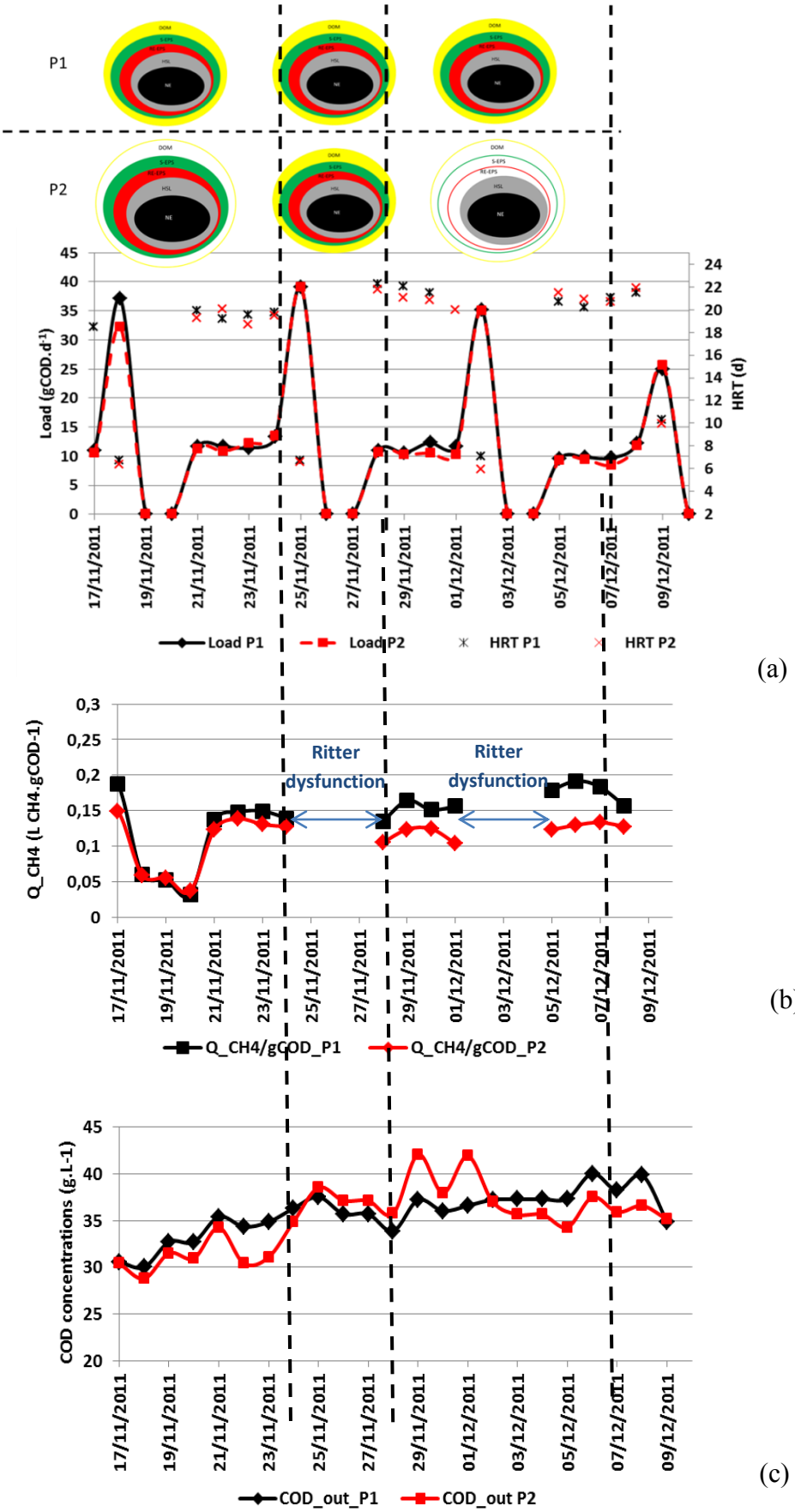

Figure 73 : Disturbing period performances comparison in P1 and P2 reactors in terms of (a) organic loads and HRT, methane production rate (b) and output COD concentration (c)

V.2. Modified ADM1 modeling

V.2.1. Modeling procedure

The biological process modeling follows a procedure as summarized by the figure 74. After the objective of modeling definition, a relevant model has to be selected. In this study, as yet mentioned, the objective is to validate the 3D-SE-LPF methodology ability to characterize the ADM1 input variables. This methodology can predict biodegradability and bioaccessibility. Thus, the model has to take into account substrate bioaccessibility as the modified ADM1 model by Mottet (2009) which is chosen in the following.

Then, the data collection step is crucial for the model calibration and validation. In this study, experimental analysis consists in 3D-SE-LPF analysis, biochemical characterization and global parameters measured as COD in particulate and soluble phases.

COD mass balances on reactors P1 and P2 were performed (table 32) considering the sludge accumulation in both reactors. Indeed, the ADM1 is based on COD units. In both periods, the P2 mass balance is closed at 96%. In P1, the reference period overestimates the COD output mass and the mass balance is closed at 88% because of the technical problem with the gas counter. Before the disturbing period, the counter gas was changed and the mass balance was better, closed at 93%.

Table 32 : COD mass balance on P1 and P2

		COD mass balance error (%)	
Period	Total	Reference	Disturbing
P1	-12%	-12%	-7%
P2	-3.7%	0.3%	-6.9%

Since the data from P2 are more accurate than P1 during the reference period, they were used for the calibration step. Concerning the manual simulation feed, the real flow rate was used in order to simulate the disturbing phase created by the week-end strategy.

The calibration steps consist in several stages. As the reactors are run in continuous mode, a steady-state has to be reached. For this purpose, a static feed is applied in the simulation during 200 days. When the steady-state is reached, the final values of the state variables obtained are used as initial values for dynamic simulation. During the steady state period, a first calibration can be proposed to get model outputs closed to the mean experimental values. Then, the dynamic inputs are applied, and the first calibration is validated or modified by returning to the data collection step.

Finally, the validation step uses a dataset different from the one used for calibration. In this study, the dataset used for validation is obtained from the disturbing period applied to P2.

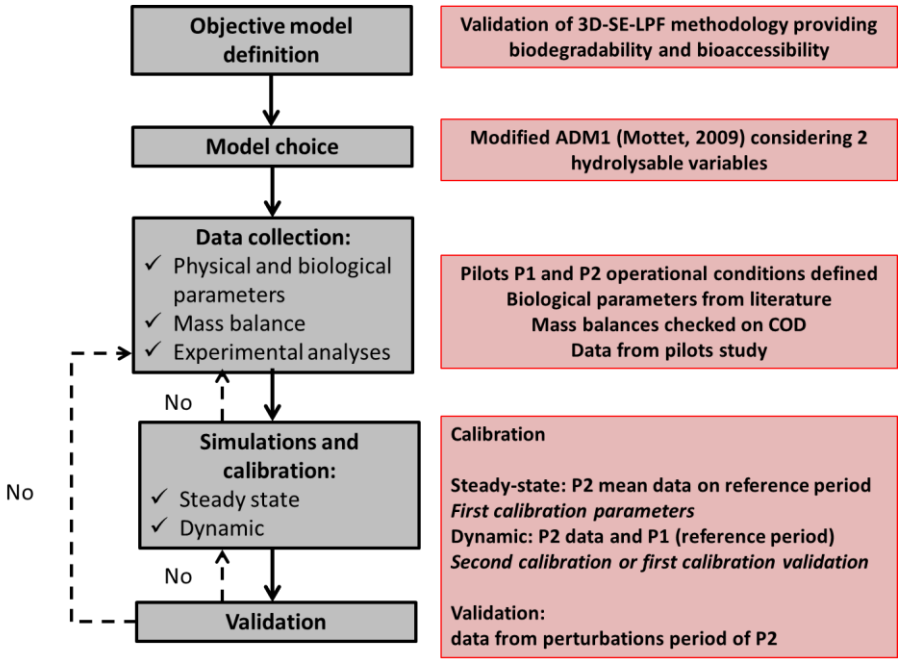

Figure 74 : Modeling procedure

V.2.2. Input implementation and parameters

The particulate and soluble input variables are characterized as explained in chapter II.

The particulate COD is decomposed on X_{RC} and X_{SC} variables. According to the values predicted by the PLS results, X_{RC} is defined (percentage of biodegradable COD). By subtracting X_{RC} from BD, X_{SC} is calculated. Then, the biochemical parameters $f\_X_{RC,SC}\_X_I$, $f\_X_{RC,SC}\_X_{PR}$, $f\_X_{RC,SC}\_X_{CH}$, $f\_X_{RC,SC}\_X_{LI}$ become dynamics and are obtained from respectively BD (PLS), protein, carbohydrate and lipids analysis (cf. Chapter II). These parameters vary according to the variations of the sludge composition. The stoichiometric parameter f_X_I (non-biodegradable fraction) is calculated from the Predicted BD by the previous PLS model.

The classical ADM1 kinetics and stoichiometric parameters values are taken from the standard ones proposed by the ADM1 report at 35°C (Batstone *et al.*, 2002). Concerning the new parameters brought by the modified ADM1, a first approach is to use the parameters found by Mottet (2009) at 55°C (table 33).

Table 33 : New parameters from modified ADM1 values used in this study before calibration step

Parameters	Unit	Value	Reference
kdec _(Xbio_X_{PR}, Xbio_X_{CH}, Xbio_X_{LI})	d^{-1}	0,04	Mottet(2009)
kdec_Xbio_X_{RC}		0,2	
kdec_Xbio_X_{SC}		0,4	
km_Xbio_X_{RC}		9	
km_Xbio_X_{SC}		5,7	
Km_(Xbio_X_{PR}, Xbio_X_{CH}, Xbio_X_{LI})		10	
K_S_(Xbio_X_{PR}, Xbio_X_{CH}, Xbio_X_{LI})	$kgCOD.m^{-3}$	0,5	
K_S_ Xbio_X_{RC}		0,4	
K_S_ Xbio_X_{SC}		0,3	
Y_ Xbio_X_{RC}	$kgCOD.kgCOD^{-1}$	0,1	
Y_ Xbio_X_{SC}		0,09	
Y_ (Xbio_X_{PR}, Xbio_X_{CH}, Xbio_X_{LI})		0,1	

V.2.3. Model calibration

Before the model calibration, a simulation with the default variables of ADM1 is performed in order to reach the steady state. A static feed is applied to the model, corresponding to the average values of the reference period during 200 days. When the state variables of ADM1 are stabilized, the final values are saved as the new initial state values.

V.2.3.1. Steady state calibration

The results of the steady-state reached with default values of ADM1 parameters are presented in the table 34 together with the average experimental values of P2 during the reference period. From the VFA compounds, only the acetate and the propionate concentrations are presented. Indeed, the others VFAs content are very low values as regard experimental data and model results found.

Table 34 : Steady-state values of state variables from ADM1 with default values parameters

Variable	Units	Model	P2	Relative error (%)
pH	-	7.76	7.51	3
COD particulate	$kg.m^{-3}$	36.05	30.44	18
COD total	$kg.m^{-3}$	38.09	32.53	17
COD soluble	$kg.m^{-3}$	2.04	2.08	-2
S_ac	$kg.m^{-3}$	0.006	0.016-0.316	62
S_pro	$g.L^{-1}$	0.019	0.020	7
Q_BG	$kg.m^{-3}$	2.93	2.50	17
%CH4	%	0.68	0.64	6
S_INN	$kmol.m^{-3}$	2310.00	1331.00	74

One can see that the model overestimates the particulate COD value (18%). A pie graph of the repartition of the state variables into particulate COD is plotted (figure 75). As expected with the HRT of 18 days, the main variable is the non-biodegradable fraction X_I which represents 70% of output particular COD. However, a high percentage (17% of particulate COD) is obtained from the sum of hydrolytic biomass of protein, carbohydrates and lipids. This means the growth/decay kinetics of these hydrolytic biomasses are too fast. As a matter of fact, they were directly taken from Mottet (2009) who worked with a reactor operating at 55°C while our reactors are operated at 35°C. Growth rates from Mottet (2009) were thus reduced to account for the mesophilic temperature of our experiment, with the assumption that mesophilic hydrolytic biomass is slower than thermophile biomass. Moreover, the total biogas is also overestimated (17%). After the calibration with new values of hydrolytic biomass kinetic parameters, the particular COD decreases due to a lower hydrolytic biomass as the total biogas. Nevertheless, the acetate concentration and ammonium concentration do not fit.

The ammonium concentration is mainly produced by the hydrolysis of proteins and depends on pH equilibrium. Two phenomena could bring an overestimation of this value (74%). First, the pH predicted is higher than the experimental one (7.76 versus 7.51). Secondly, the proteins hydrolysis is overestimated. However, after the hydrolysis biomass parameters calibration, the pH and the S_INN values decrease but they are still overestimated (respectively 7.6 and 1960 $kmol.m^{-3}$). The pH model in ADM1 is not enough robust to predict

directly the real pH value. Several authors have tried to complete the ADM1 model by considering all ionic species (Grau *et al.*, 2007). In this study, in order to overcome this problem, the predicted pH is directly controlled by the experimental pH by calibrating the cations concentrations.

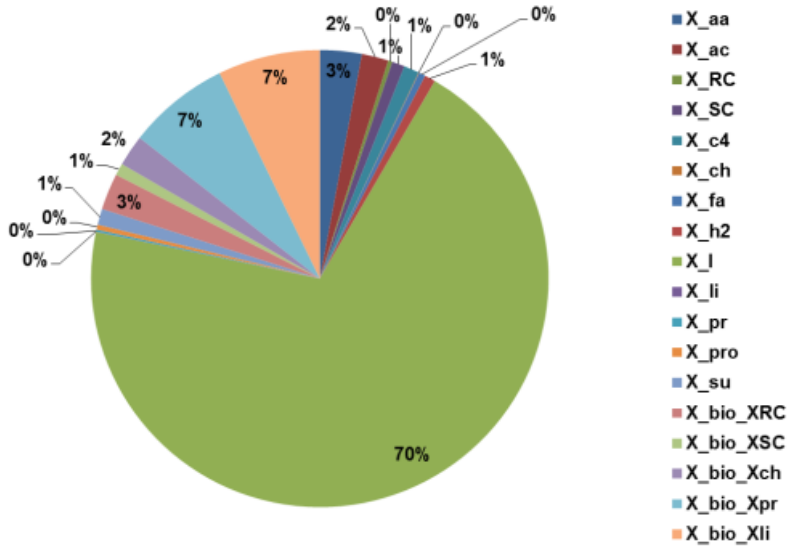

Figure 75 : Particulate COD repartition on ADM1 state variables obtained by steady-state simulation without calibration

After the pH calibration, the acetate concentration is still underestimated. This means that the acetate uptake kinetics is too high. Indeed the S_ac concentration varies widely from 0.016 to 0.316 kg.m^{-3}. The default half saturation parameter for acetate degraders ($K_S\_X_{AC}$) used is 0.15 kg.m^{-3}. However, when acetate concentration is above this value, there is a lower limitation of the X_ac kinetics and the S_ac concentration is low. Thus, in order to obtain higher S_ac values, $K_S\_X_{AC}$ is increased at 0.40 kg.m^{-3}.

The calibration parameters values are summarized in the Table 35 with their respective effect on the state variables. Growth rate of hydrolytic bacteria is decreased from 10 d^{-1} to 5 d^{-1} (close to X_{RC} and X_{SC} hydrolytic biomass values). Then, as calibration is not sufficient, decay rate is raised from 0.04 d^{-1} to 0.2 d^{-1} (value of X_{RC} hydrolytic biomass).

The growth and the decay rates of hydrolytic biomass are assumed to be the same for carbohydrates, proteins and lipids as far as we cannot have this data for each biochemical fraction.

Concerning the acetate concentration calibration, the half-saturation constant calibrated increases up to 0.40 kg.m^{-3} to reach the expected acetate concentration. Finally, the cations concentration is decreased in order to fit with experimental values of pH.

Table 35 : Steady-state values of state variables from ADM1 with calibrated values parameters

Calibration parameter	Unit	Default value (Temperature °C)	Calibration value	Impact
Km ($Xbio\_X_{PR}$, $Xbio\_X_{CH}$, $Xbio\_X_{LI}$)	*d-1*	10 (55°C)	5 (35°C)	Decrease the COD particulate concentration of hydrolytic biomass
kdec ($Xbio\_X_{PR}$, $Xbio\_X_{CH}$, $Xbio\_X_{LI}$)	*d-1*	0,04 (55°C)	0,2 (35°C)	
K_S_X_ac	$kg.m^{-3}$	0.15 (35°C)	0.40 (35°C)	S_ac calibration (increase)
Constant k S_cat=S_IC+k	-	0.035 (Roesen *et al*., 2002)	0.025	pH calibration S_INN

After the new calibration performed, another steady-state is achieved by simulating a static feed during 200 days.

Comparison between the new values of state variables predicted and the experimental ones is presented in table 36.

As expected, relative errors have decreased for all the problematic state variables previously identified. The COD particulate fit with experimental value at 1%.

Biogas flow rate predicted fits well the experimental values with relative errors for Q_BG of 3%. Finally, the pH value is better predicted with the new cations concentrations and ammonium too with relative error of 14%.

The repartition of particulate COD is plotted (figure 76). X_I represents now 83% and sum of the protein, carbohydrates and lipids hydrolytic biomass concentrations have decreased from 17% to 3% of particulate COD which is more realistic.

Table 36 : Steady-state values of state variables from ADM1 with calibrated values parameters

Variable	Units	Model	P2	Relative error (%)
pH	-	7.49	7.51	-0,3
COD particulate	$kg.m^{-3}$	30.39	30.44	-1
COD total	$kg.m^{-3}$	32.61	32.53	0
COD soluble	$kg.m^{-3}$	2.23	2.08	8
S_ac	$kg.m^{-3}$	0.12	0.016-0.316	27
S_pro	$g.L^{-1}$	0.02	0.02	7
Q_BG	$kg.m^{-3}$	2.58	2.50	3
%CH4	%	0.64	0.64	0
S_INN	$kmol.m^{-3}$	1512.09	1331.00	14

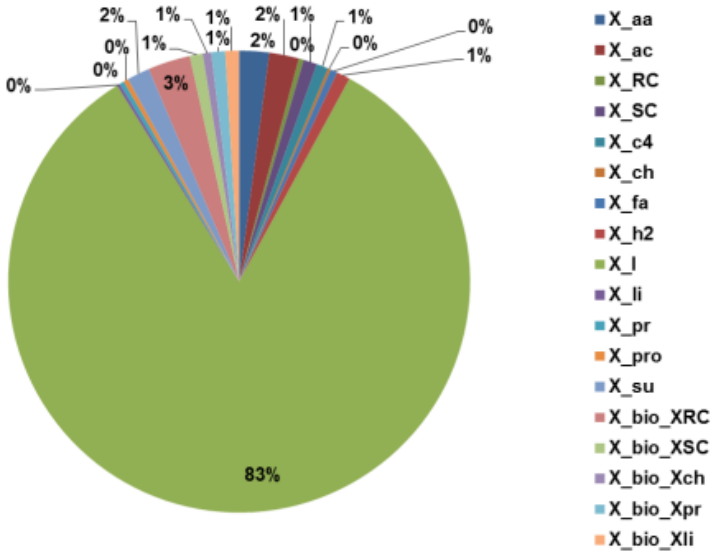

Figure 76 : Particulate COD repartition on ADM1 state variables obtained by steady-state simulation after calibration

V.2.3.2. Dynamic state calibration

The dynamic data feed is applied to the model using the values of calibrated parameters previously found. The figures 77 to 82 present the evolution of the state variables before (a) and after calibration (b).

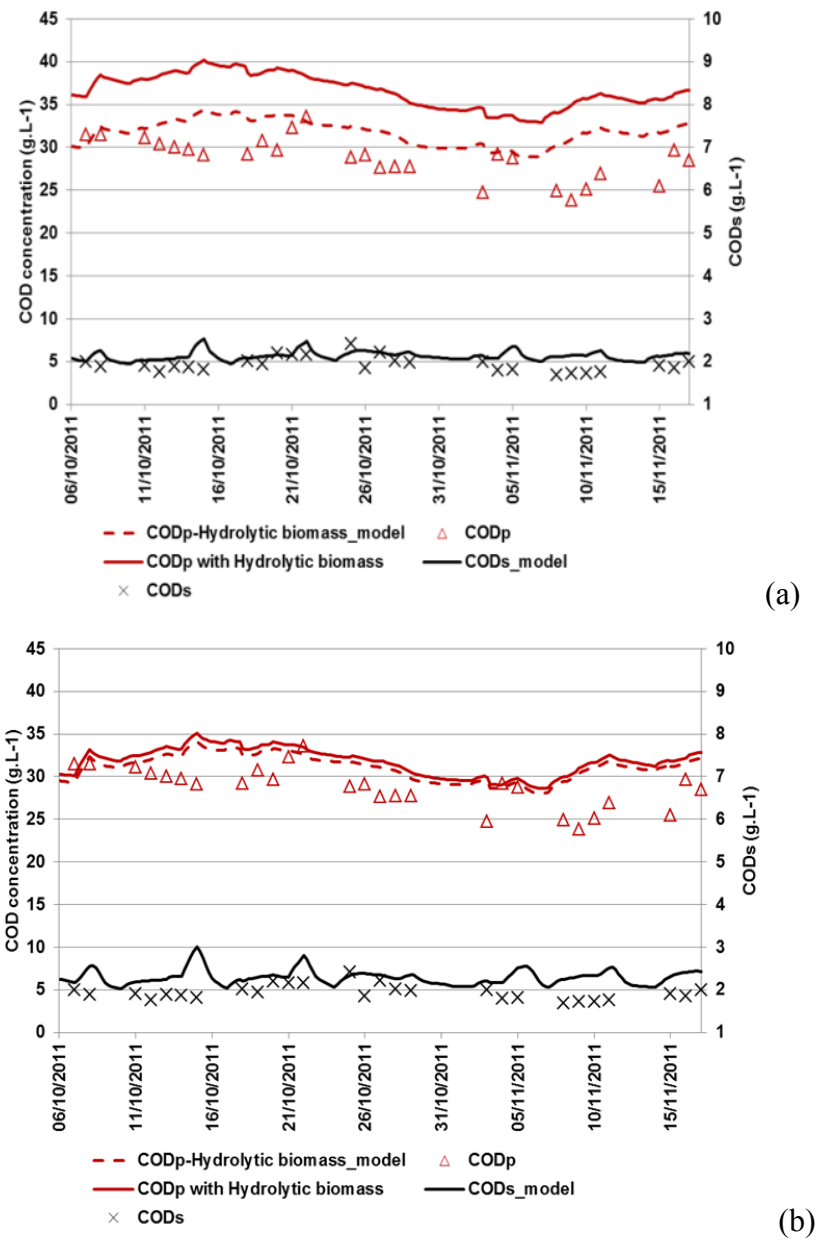

Figure 77 : COD output prediction before (a) and after (b) calibration P2

The particulate COD is better predicted by the new parameters values. As previously mentioned, the hydrolytic biomass COD was too high before calibration and particulate COD was overestimated. This overestimation is clearly decreased after the calibration. The soluble COD fits well the experimental values. This is due to the S_I implementation corresponding directly to the soluble COD not degraded in the reactor.

The calibration of the cations concentrations allows the pH to fit with experimental data (figure 78).

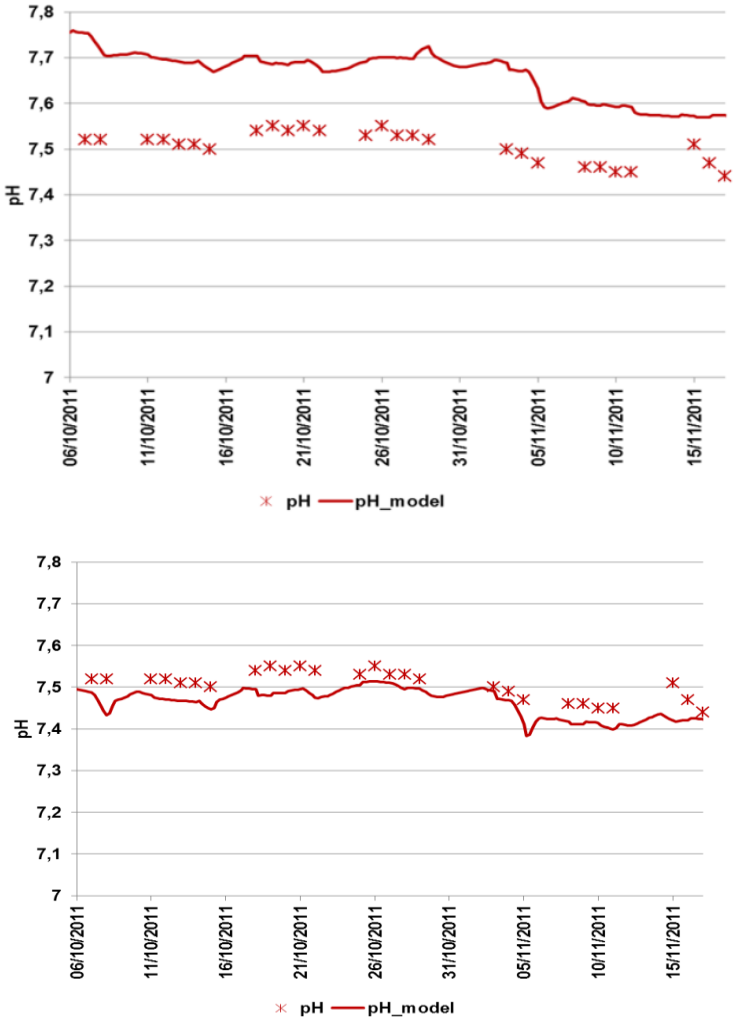

Figure 78 : pH output prediction before (a) and after (b) calibration

When the pH decreases with the cations calibration, the carbon dioxide increases and the biogas composition change and fits better with the experimental data (figures 79 and 80).

This calibration impacts also the ammonium concentration (figure 82) which is overestimated before this step.

Indeed, the hydrolytic biomass calibration has impacted the biogas flow and the methane content by decreasing their values. This leads to a better prediction of both experimental data.

The dynamic evolution of the biogas is mainly driven by the input organic load flow. Indeed, the week-end strategy implies high production peaks. This leads to hydraulic disturbing well supported by the ADM1 model.

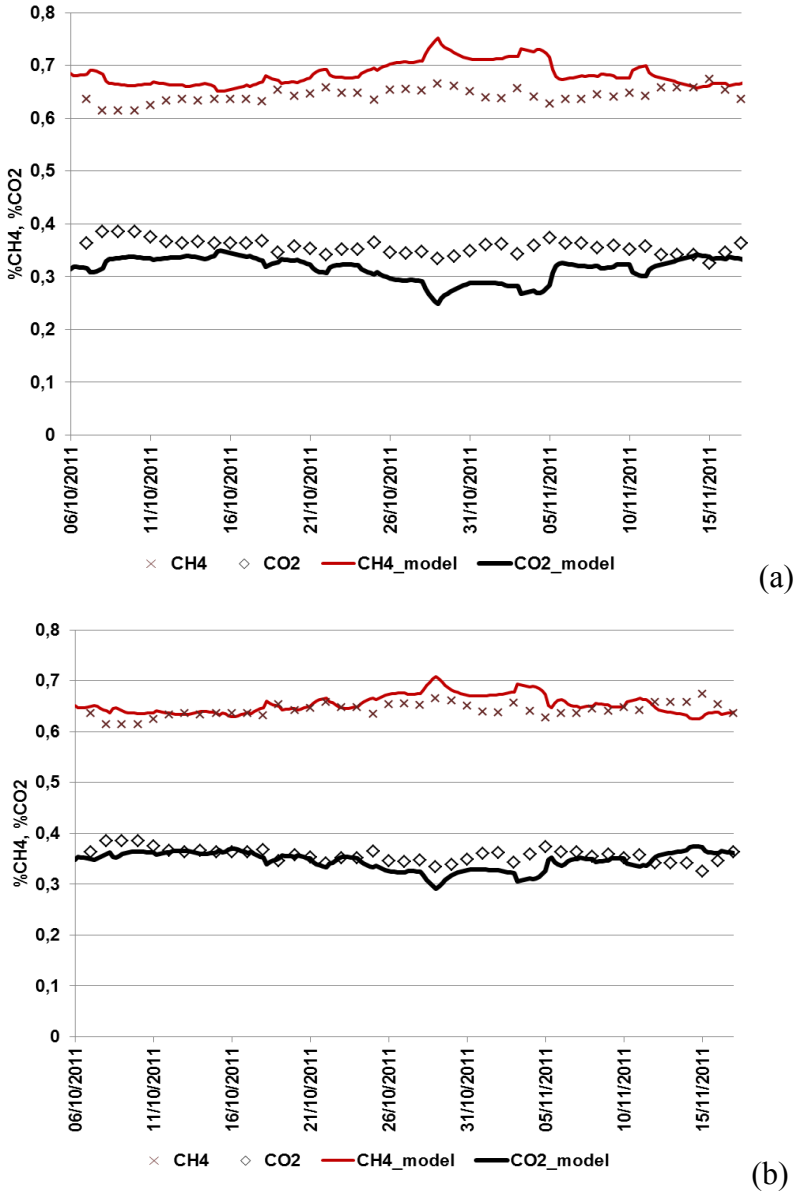

Figure 79 : Methane and carbon dioxide proportion in biogas prediction before (a) and after (b) calibration

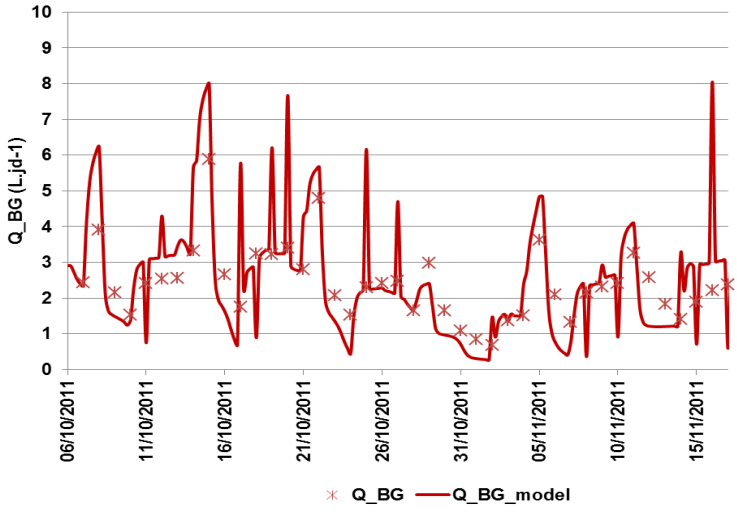

(a)

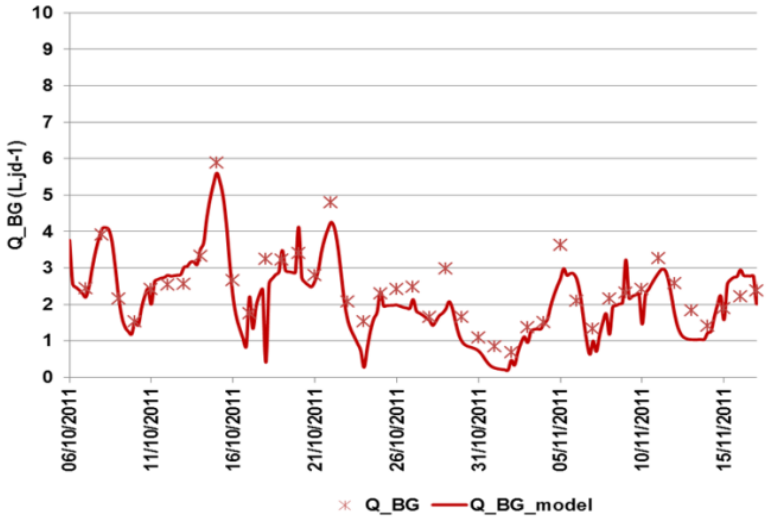

(b)

Figure 80 : Total biogas flowrate output prediction before (a) and after (b) calibration for P2

Finally, the calibration parameters (hydrolytic biomass growth kinetic, pH and K_S_X_ac) have improved model prediction in steady-state as well as in dynamic state.

The model calibrated and simulated in dynamic conditions is satisfying to predict methane production and anaerobic digestion reactions. Moreover, the hydraulic disturbing brought by the flowrate variations validates that the model can handle high load disturbing.

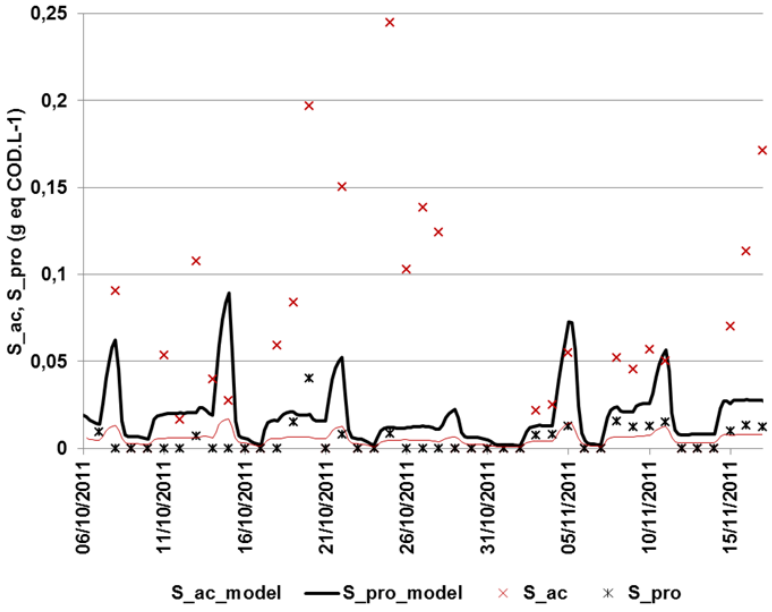

(a)

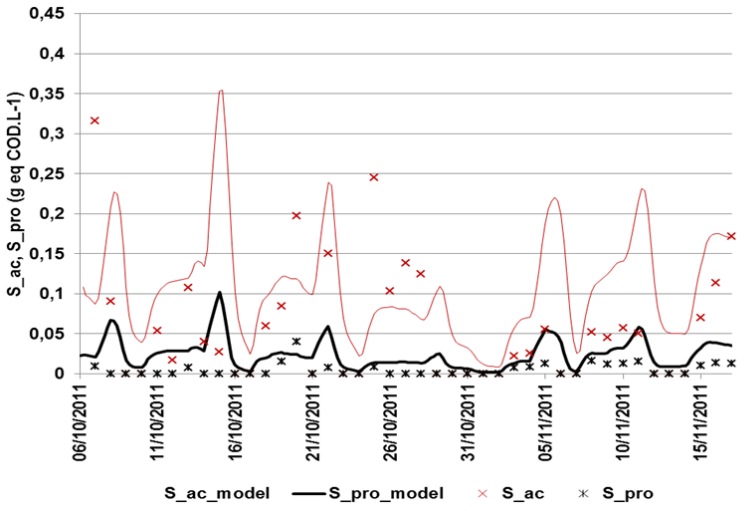

(b)

Figure 81 : Acetate and propionate concentrations output prediction before (a) and after (b) calibration

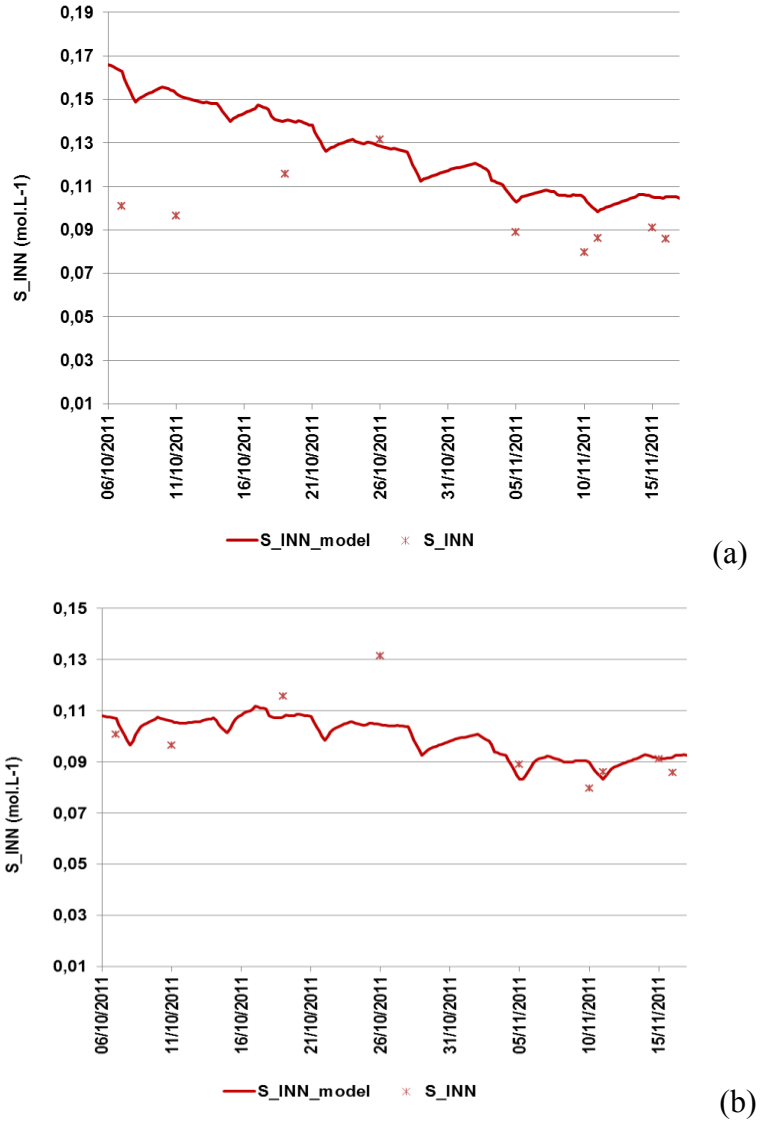

Figure 82 : Ammonium concentration output prediction before (a) and after (b) calibration

V.3. Model validation

V.3.1. Dynamic validation with disturbing data

V.3.1.1. Input data during both references and disturbing period

In order to validate that the input model with the BD and X_{RC} predicted by the PLS leads to better, a plot of X_I and X_{SC} resulting of the calculation from the two variables is performed (figure 83). As expected, the evolution and the values of X_I and X_{SC} match with experimental analysis.

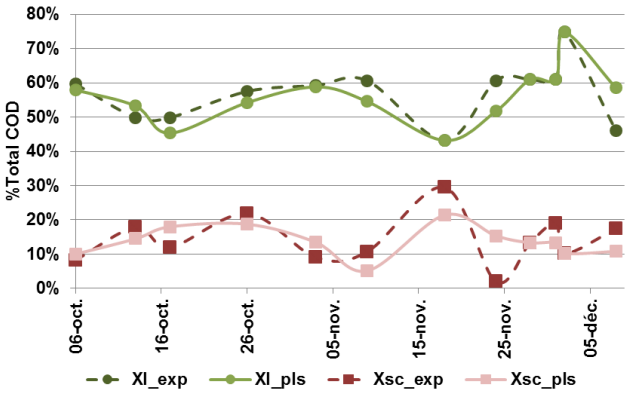

Figure 83 : Validation of input state variables X_I and X_{SC} obtained from PLS (respectively 1-BD and BD-X_{RC})

During the disturbing period, one or several fractions were removed from the feed sludge. First, the DOM fraction was removed from the sludge SII_B_10. The PLS result shown in table 37 highlights that the X_{RC} variable decreases to about 25% from its initial value.

Then, the DOM, S-EPS and RE-EPS fractions were removed from the sludge SII_B_9 and SII_B_12. Table 37 shows that the PLS predicted X_{RC} decreases respectively by 19% and 30%, such as BD with relative deviation of 25% and 27%.

Table 37 : PLS results for disturbed sludge

	BD (%COD)	X_{RC} (%COD)
SII_B_10	52	36
SII_B_10-DOM	56	27
SII_B_9	48	33
SII_B_9-DOM-S-EPS-REEPS	39	26
SII_B_12	35	26
SII_B_12- DOM-S-EPS-REEPS	25	15

Thus the removal of the most accessible fraction leads X_{RC} to decrease which is coherent with the previous results.

V.3.1.2. Dynamic validation

The reference and disturbing periods are simulated for reactors P1 and P2 with the values of the calibrated parameters found in last section.

All the simulation results of P1 and P2 are plotted in Annex 5. The main results (methane production flow rate and particulate COD in reactors) are plotted in the figures 84-89.

As for the reference period (06/10/2011-17/11/2011), the total biogas flow rate (figure A5.2a) and the biogas composition (figure A5.2b) followed the evolution of experimental data during the disturbing period (18/11/2011-10/12/2011).

A zoom of the disturbing period is highlighted in the figure 84 for methane production from P1 and P2. Both reactors are properly simulated by the model calibrated during the disturbing period.

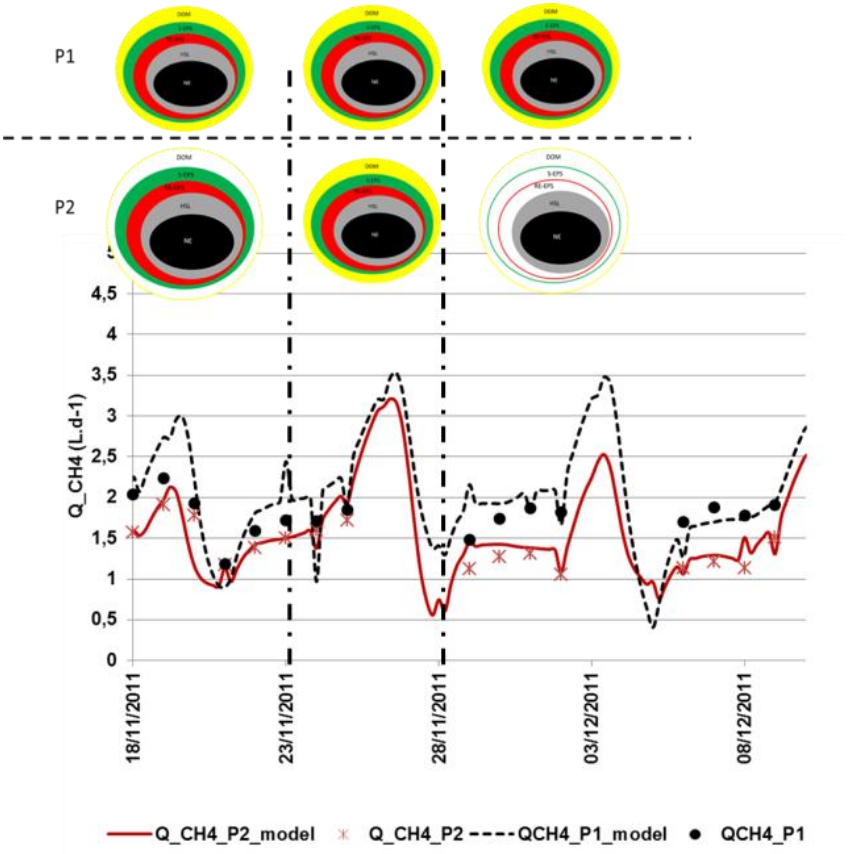

Figure 84 : Methane flow rate simulated during disturbing period

In P2, the disturbing step applied does not degrade the methane flow rate prediction. For P1, without disturbing periods, model still fits the experimental data. P1 methane production flow rate is clearly higher than in P2 in which fractions were removed from total sludge. Thus, model translates well the removal through the methane production.

In order to have an idea of the quality of the model, a plot of measured versus simulated values from P2 is presented in figure 85.

There is a good correlation between predicted methane production and observed methane production with a curve close to the line of perfect fit (y=x). The correlation coefficient is close to 0.8. Regarding the disturbing period, the mean standard deviation of the methane flow rate in P2 is about 11%.

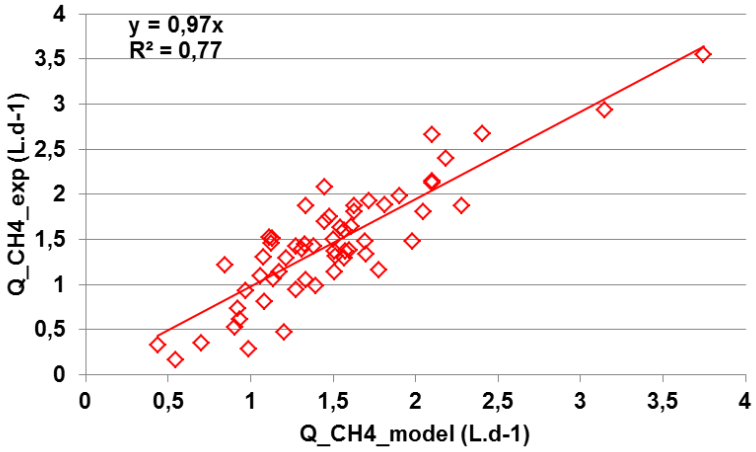

Figure 85 : Observed methane versus predicted methane in P2

However, the Ritter dysfunction led to miss some biogas flowrate measurement during two weekends: 26-27/11 and 03-05/12 (figure 84). Consequently, the peak load brought by the weekend strategy was missed too. Nevertheless, this hydraulic disturbing has been handled by the model on the reference period. So, in the organic matter disturbing period, the focus is made on the kinetics of methane production.

Concerning the particulate COD, this variable is also well predicted in all the periods (figure 86).

The simulation considers that the disturbed reactor contains more particulate COD than the reference reactor. The bar errors represent the measurement incertitude (7%). This deviation, which is low at the beginning, increases with the fraction removal. This is due to the X_I fraction which is higher in sludge feeding P2 than in the sludge feeding P1. As previous PLS model shows, the BD is lower when the DOM, S-EPS and RE-EPS fractions are removed.

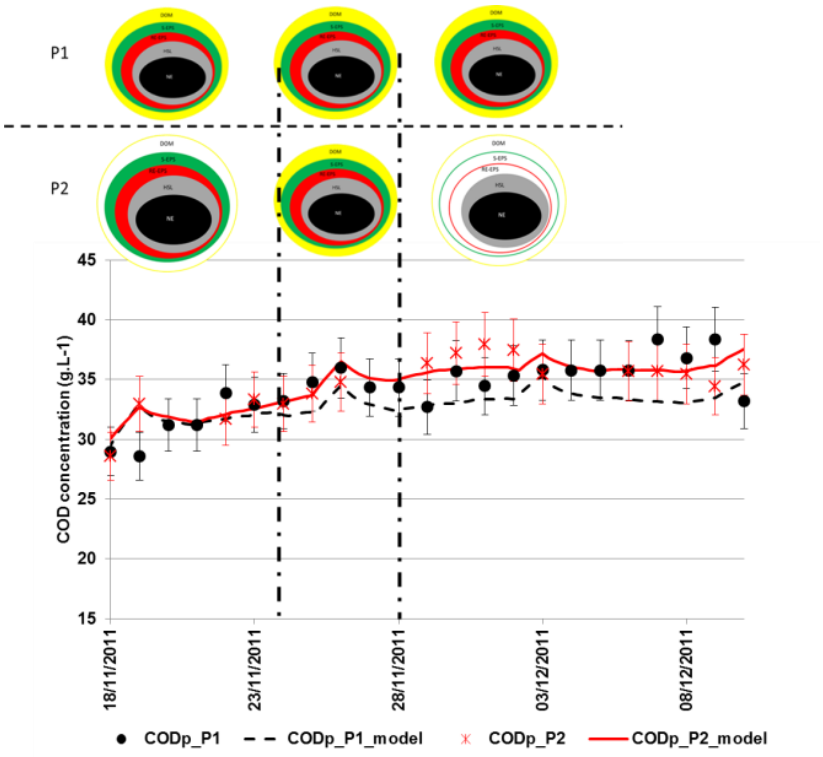

(b)

Figure 86 : Particulate COD simulated in reactors P1 and P2 during the disturbing period

Concerning pH, its value is still imposed by experimental values with cations concentrations as in calibration section (figure 87). Contrary to P2, the modeled pH from P1 did not fit with experimental one until the disturbing period. A pHmeter drift was suspected. At the beginning of the disturbing period, it was changed.

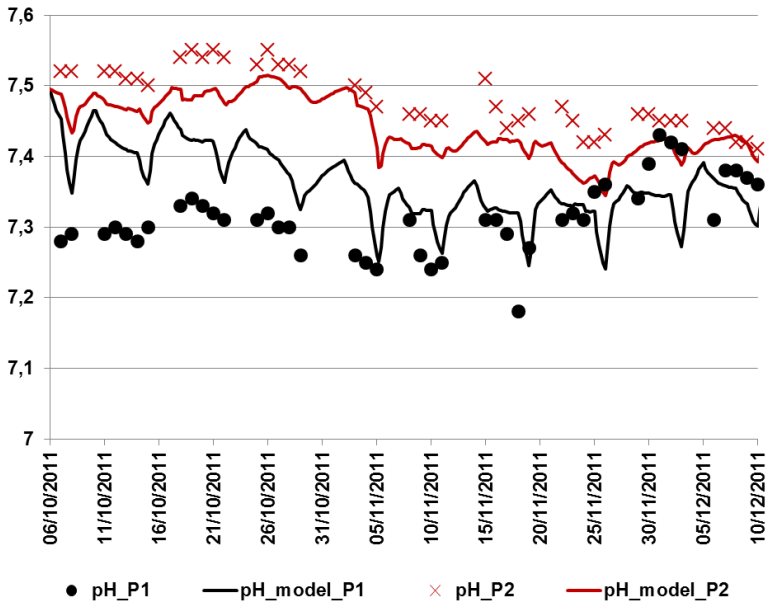

Figure 87 : pH evolution in P1 and P2 during the reference and the disturbing periods

The predicted ammonium concentrations for both pilots evolve as experimental values. The acetate concentration trend is similar to the experimental values (figure 89). However, after the first disturbing period and till the end, the acetate concentration is overestimated by the model in both reactors. The experimental concentration was under the limit of quantification (5 $mg.L^{-1}$) as the propionate and the others VFAs. Nevertheless, no calibration is made for the VFAs concentrations.

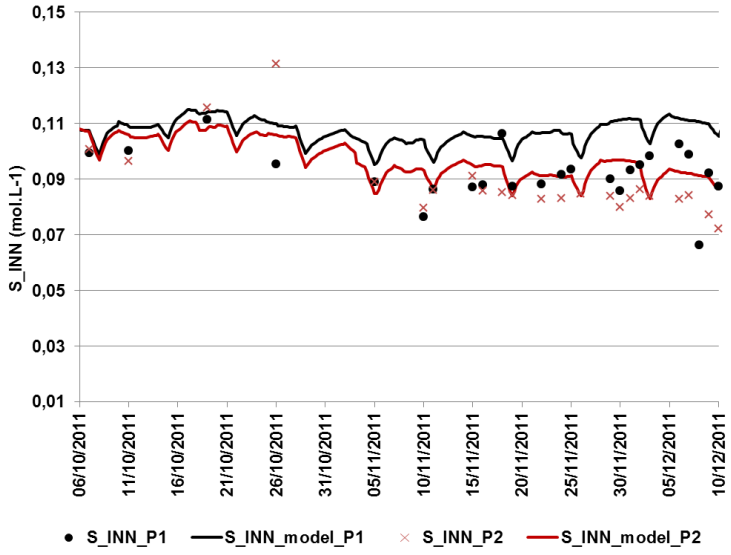

Figure 88 : Output ammonium concentration in P1 and P2 during the reference and the disturbing periods

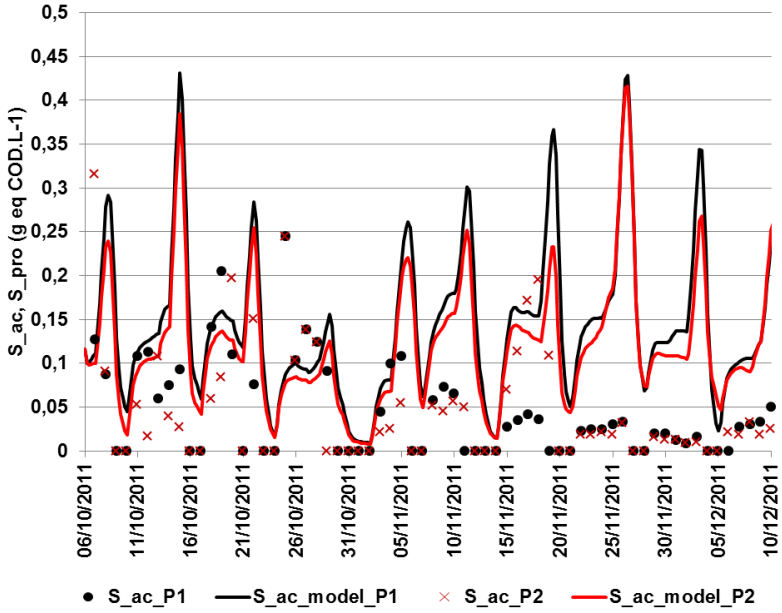

Figure 89 : Output acetate concentration in P1 and P2 during the disturbing period

In order to go further with the model validation, kinetics of 2 days of disturbing step in P2 are simulated with the calibrated model.

Focus has been done on the DOM, S-EPS and RE-EPS removal because their high impact on kinetics as shown on chapter III. The methane flow rate of the days 06/12/2011 and 07/12/2011, corresponding to the last disturbing period, are plotted in the figure 90. As highlighted by the simulated methane flow rate, the model fits well the experimental data for P2.

The curve plotted is closed to slowly particulate hydrolysis kinetics, corresponding to the X_{SC} degradation kinetics. Indeed, X_{RC} is rapidly uptaken whereas X_{SC} is the limiting variable not totally consumed at the end of the day.

On the contrary, the P1 methane kinetics shows a more important first peak profile due to a higher part of X_{RC} uptake at the beginning. This is due to the presence of the most accessible fractions in the feeding sludge i.e. DOM, S-EPS and RE-EPS.

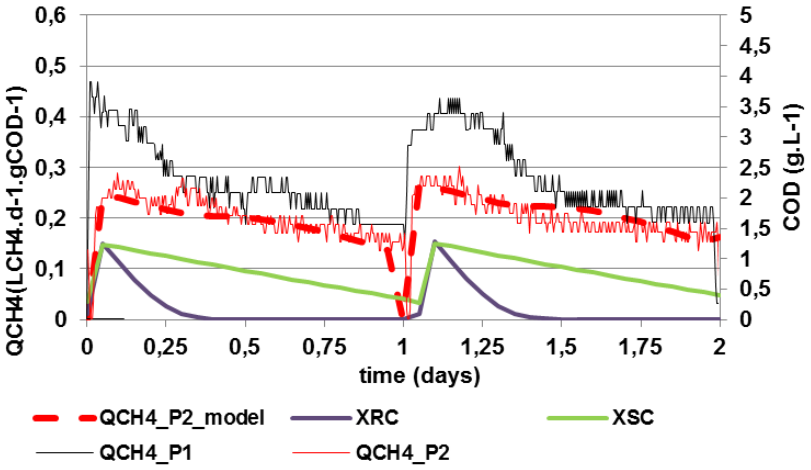

Figure 90 : Methane flow rate kinetic simulation on DOM, S-EPS and RE-EPS removal in P2 (06-07/12/2011)

With this modeling exercise, we have shown that the variables predicted by the PLS model are relevant to predict anaerobic digestion of sludge performances in a continuous lab scale reactor as well as its kinetics. Thus, the methodology based on the fluorescence spectroscopy and the chemical fractionation that we proposed has been validated as analytic tool to characterize the ADM1 input variables.

The substrate description and the analysis time have been highly optimized.

Next section analyses the sensitivity of the variables generated by the PLS on the ADM1 predictions.

V.3.1.3. Sensitivity analysis

An evaluation of the influence of the PLS variables BD and X_{RC} on ADM1 predictions as well as the biochemical fractionation calculated from biochemical measurement are investigated.

The RSF (cf. Chapter IV, Petersen *et al.,* 2002) is evaluated for the particulate COD fractionation parameters in ADM1 (table 38). The model previously calibrated is used at steady-state in order to simplify the RSF calculation. Care has to be taken with this sensitivity analysis which is specific of the calibrated model, in the defined operating conditions (35°C, HRT=18 days).

The results summarized in the table 38 show that protein and carbohydrates biochemical fractionation influenced the quality of biogas (composition of methane) whereas the biodegradable fraction impacted the quantity of biogas as well as the output COD.

Nevertheless, the X_{SC}/X_{RC} ratio, translating the part of the COD bioaccessibility, has no influence on the ADM1 performances in these conditions. Indeed, the HRT of the reactors is 18 days. It is too long to observe some impacts.

In order to study the impact of the HRT on the degradation of both X_{RC} and X_{SC}, scenarii analyses based on the variable HRT are performed using the WEST software.

Table 38 : RSF analysis on input characterization of ADM1 obtained by biochemical measurement and PLS

Parameters\Variables	VFA	$\%CH_4$	$\%CO_2$	Q_{BG}	COD	Influence
$f\_X_{RC,\,SC}\_X_{PR}$	-	0	-	0	0	Biogas quality
$f\_X_{RC,\,SC}\_X_{CH}$	+	-	+	0	0	
$f\_X_{RC,\,SC}\_X_{LI}$	+	0	0	0	0	
$f\_X_{RC,\,SC}\_X_I$ (1-BD)	0	0	0	--	+	Biogas quantity and COD
X_{SC}/X_{RC} ratio	0	0	0	0	0	HRT=18 days, no influential

V.4. Bioaccessibility variables and impact on hydraulic retention time

The main drawback of the steady-state local sensitivity analysis is that the interpretation of the results is limited to the defined operating conditions and calibrated parameters values.

Concerning this study, the high value of HRT was chosen in order to maximize the visualization of X_{RC} and X_{SC} kinetics degradation during the experiments. Another reason was that the average value of the HRT in European anaerobic digesters is about 18 days. Designers lead to overestimate the anaerobic digesters HRT in order to prevent non expected loads and to secure the process. However, this value is too high to evaluate the accessibility

impact and thus the process design impact. This section aims at studying deeper the correlation between the HRT and the ratio X_{SC}/X_{RC} in order to highlight the bioaccessibility impact on digester design.

V.4.1. Scenarii analysis

Scenarii analyses were performed with the calibrated model for sludge with different X_{SC}/X_{RC} fractionation.

Some sludge come from this study, others have been modified in order to emphasize the X_{SC}/X_{RC} ratio.

For each sludge, the "scenario analysis" function of the WEST software is used in order to consider several HRT values (variation from 1 day to 30 days).

The scenarii analysis answer is plotted in the figure 91. The biogas production is plotted versus the HRT. The profile of this graph is asymptotical. Depending on the biodegradability and the biodegradable sludge organic matter, the biogas quantity is more or less important. That is why, for several sludge with different X_{SC}/X_{RC} ratios, the final value (HRT=30) changes.

However, let focus on the curve slope between 0 and 10 days. When the X_{SC}/X_{RC} ratio increases, the slope decreases. This result show that when the X_{SC}/X_{RC} ratio is high, optimal design of digester is impacted and the HRT have to be increased.

For example, the primary sludge S_ID_R=0.2 reaches its asymptote at HRT 6.5 days whereas the secondary sludge SII_B_12-RE-EPS_R=1.33 reaches its asymptote at HRT 11 days.

This result was expected. Indeed, when slowly biodegradable fraction increases in particulate COD, time needed to uptake this fraction increases too.

For all the cases studied, at HRT=18 days which is the HRT chosen in the reactors P1 and P2, the biogas production was stabilized and no impact of the bioaccessibility fractionation was observed. Moreover, during our European wastewater treatment plant campaign, we noticed that anaerobic digesters mainly worked at HRT between 15 and 25 days.

With a similar study applied to the industrial cases, optimized HRT or minimal HRT depending on the characterization of the sludge could be evaluated and optimized design.

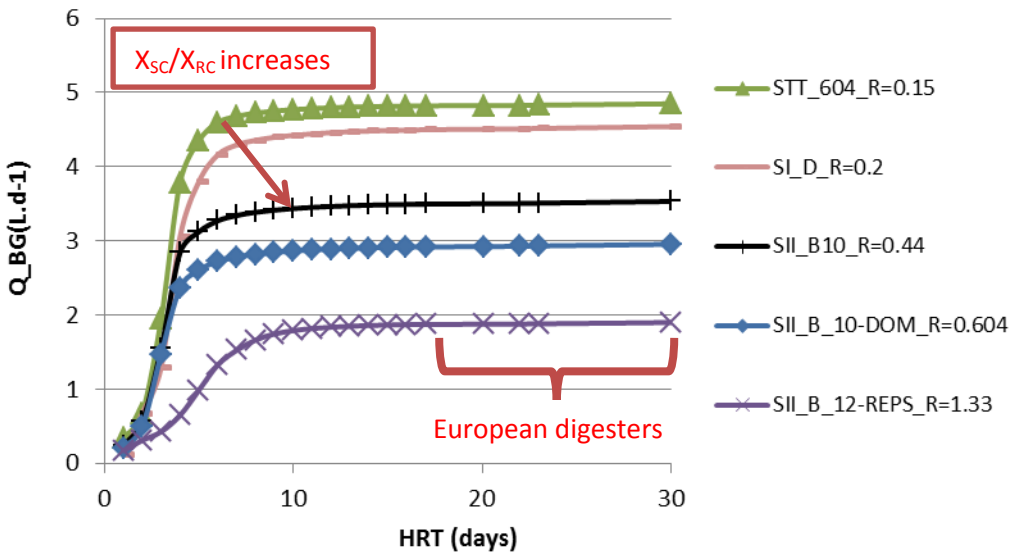

Figure 91 : Total biogas versus HRT for several R=X_{SC}/X_{RC} ratios obtained by simulations

V.4.2. Correlations found between bioaccessibility variables and HRT

A minimal HRT definition could provide optimized design of digesters. Then, by changing the X_{SC}/X_{RC} ratio, simulations with calibrated ADM1 could give some security factor and avoid to over or underestimate anaerobic digester volumes.

In order to simplify the simulation work at mesophilic conditions, a correlation between the ratio X_{SC}/X_{RC} and the HRT is investigated.

First, the meaning of the minimal HRT is crucial. The figure 92 shows the methodology to obtain the minimal HRT. It represents the HRT corresponding to the beginning asymptote, between 95 and 98% of the maximal biogas production.

In the biogas flow rate graph from the figure 92, the maximal degradation of the secondary sludge where the DOM fraction was removed is reached at a HRT of 8 days.

In the same way, the degradation of the sludge where the DOM, S-EPS and RE-EPS fractions were removed is reached 11 days. Thus, it is obvious that the fractionation ratio is influential when HRT is under 15 days.

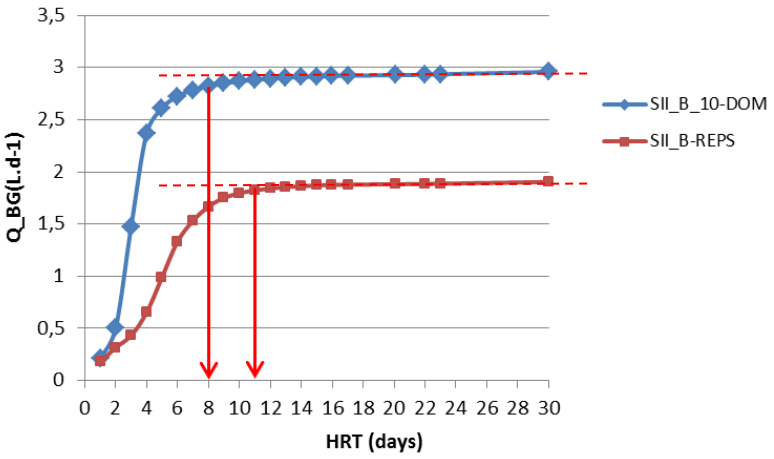

Figure 92 : Methodology definition for minimal HRT assessment

Based on the minimal HRT definition, a scenario analysis can be performed to generate biogas curves and to identify corresponding minimal HRTs. The X_{SC}/X_{SC} ratio used for each simulation is confronted to the minimal HRT found. The plot of the HRT versus the X_{SC}/X_{RC} ratio is presented in the figure 93a.

A first calibration curve is obtained with 6 different sludges with ratios from 0.03 to 1.33. A good linear regression is found between the HRT and the fractionation ratio. Indeed, the correlation coefficient is about 0.995.

This model quality is highlighted by the figure 93b with the observed HRT versus the predicted HRT plot.

Both regression and correlation coefficient are close to 1 (i.e. close to the line of perfect fit). As previously mentioned, the relation has a positive trend. Then, 10 sludges (provided by other sludge values from this study) are used as validation data (figure 93a). Primary, thermally treated and secondary sludge are used.

Their fractionation fit with minimal HRT obtained by linear regression. When stronger P2 disturbing is tested, the minimal HRT found is lower than 14 days (figure 93a). Thus, HRT of 18 days was too higher in the local sensitivity analysis performed in the last section.

Moreover, this means that HRT was overestimated, as well as the reactor volume. As plotted in figure 93c, minimal reactor volume is calculated from HRT. The reactor volume used in the study (3.8 L) could be decreased down to 2.5 L without affecting total X_{RC} and X_{SC} degradation. From the fractionation of the particulate COD, the HRT and the design of the digester can thus be assessed.

However, two important remarks have to be taken into account:

- The correlation found is obtained in the operating conditions studied (35°C). To apply this result at other temperatures, calibration parameters could change and other studies should be performed with changing temperatures.
- The correlation found could be used to optimize the digester design but care has to be taken with the sludge and substrate variations inducing fractionation ratio variations.

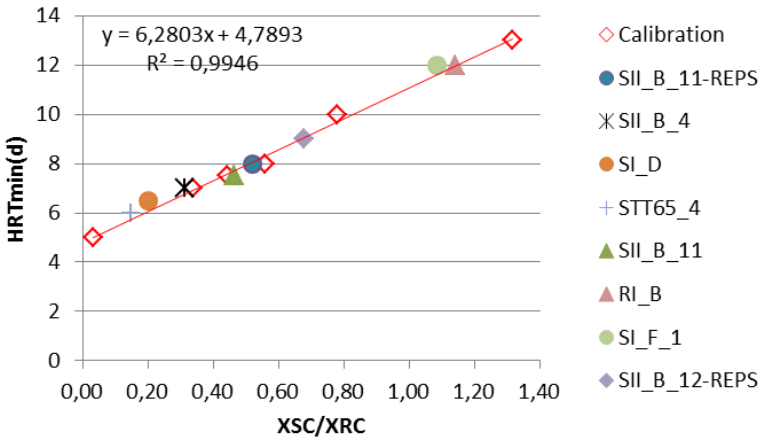

(a)

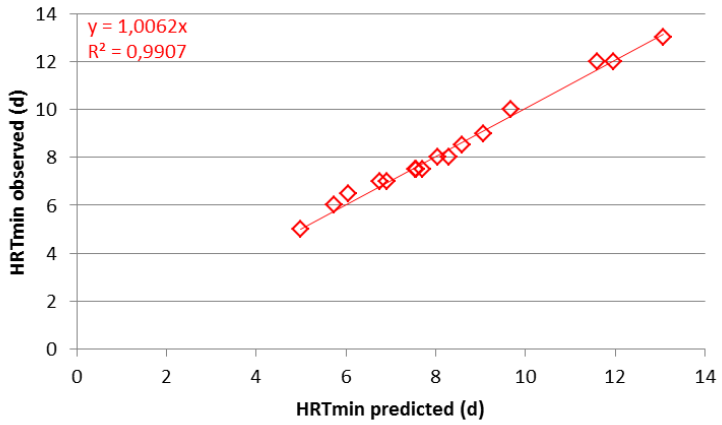

(b)

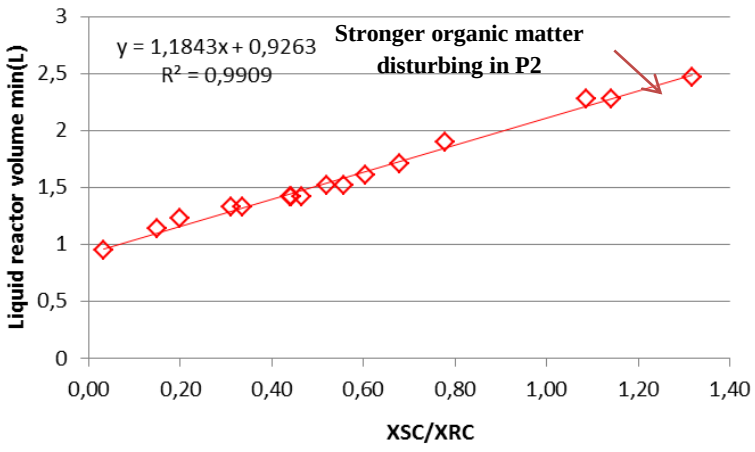

(c)

Figure 93 : Correlation obtained between minimal HRT and X_{SC}/X_{RC} ratio (a) Observed HRT versus predicted HRT (b) minimal liquid volume of reactor versus X_{SC}/X_{RC} (c)

The repartition of the X_{SC}/X_{RC} ratios and the minimal HRT predicted by models are presented in boxplots (figure 94). For each type of sludge, some relevant distribution is found. The minimal HRT repartition from anaerobic digested sludge (figure 90c) shows that this type of sludge has the lowest accessibility. However, this repartition is wide and asymmetric with a median value of 10 days and a mean value of 27 days. The fractionation ratio goes from 0.12 to 13 and the HRT from 5 to 89 days. For the SD_D sludge, the HRT reaches 89 days with a ratio of 13. This sludge is an extreme sample with a very low predicted X_{RC} fraction (1.1% of total COD). Since at the end of digestion, the main part of the accessible fraction has been uptaken, only the slowly biodegradable fraction composed these sludges.

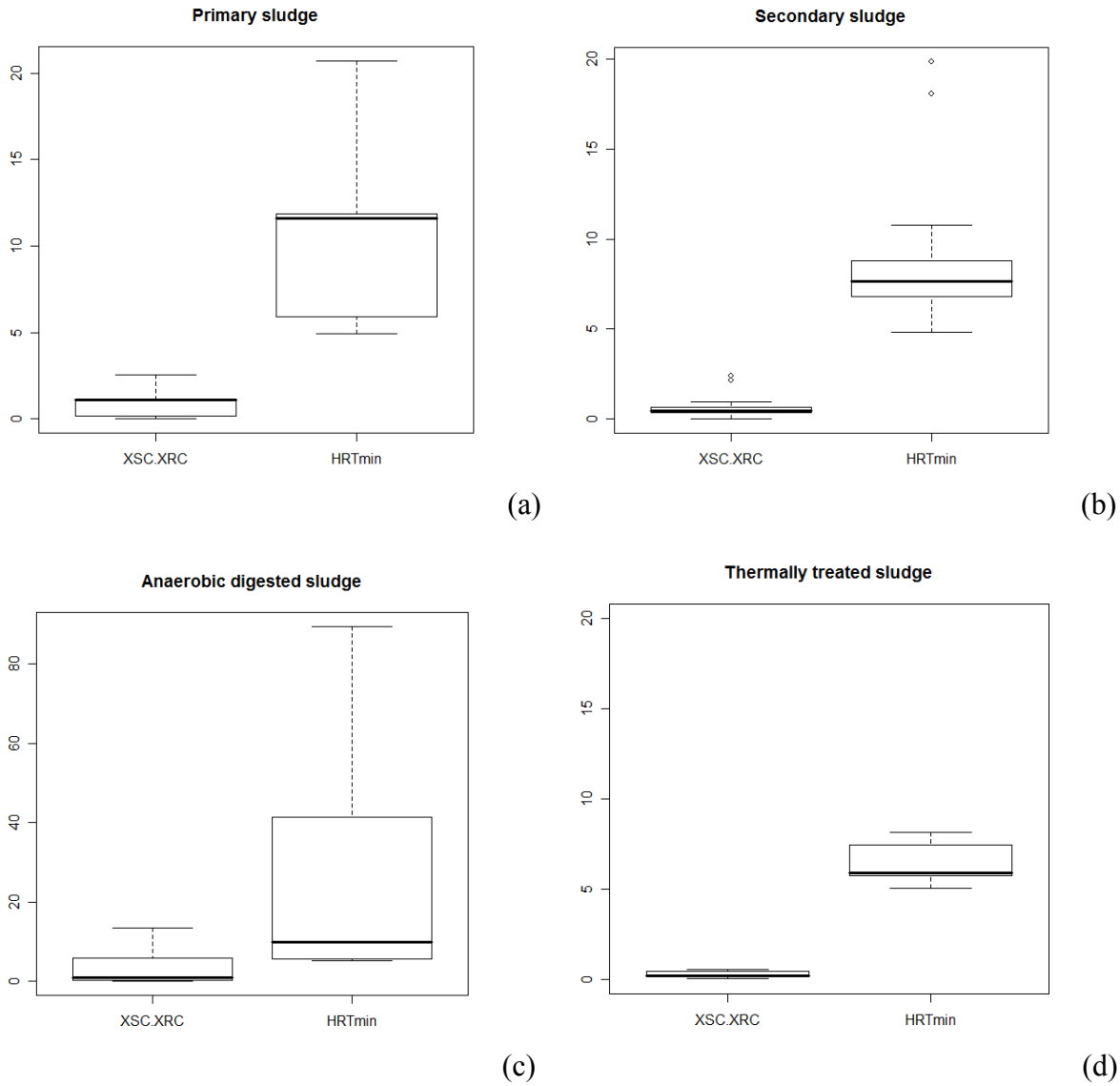

Figure 94 : Repartition of X_{SC}/X_{RC} ratio and minimal HRTobtained by model prediction for primary sludge (a), secondary sludge (b), anaerobic digested sludge (c) and thermally treated sludge (d)

The primary sludge (figure 94a) also presents a slowly accessible feature with a mean value of 11 days closed to the median value of 11.6 days. The fraction ratio goes from 0.03 to 1.09 and HRT from 5 to 12 days. The grease treatment refusal RG_B is an extreme sample with a minimal HRT of 20.7 days and a ratio of 2.53. Without the RG_B sample, the mean and the median values of the minimal HRT become respectively 8.6 days and 8.7 days. This means that, even if this type of refusal is one of the most biodegradable substrate (52.3%), it is also one of the least bioaccessible.
The mean value of the minimal HRT for secondary sludge (figure 94b) is found at 8.5 days with a median of 7.7 days. The fraction ratio goes from 0.12 to 2.4 and the HRT from 6 to 20 days. The repartition is more concentrated around the median and more symmetric. Two sludges are considered as outliers: SII_F_1 and SII_D with ratios of respectively 2.1 and 2.4 and HRT of respectively 18 and 19 days.
A sludge sample with the fluorescence zones I and VI removed from HSL studied in sensitive analysis of PLS models (cf. chapter IV) leads to the minimal HRT of 5.4 days instead of 7.6 days without any removal corresponding to a 30% savings in the digester.

Finally, the most accessible sludge is the thermally treated sludge type (figure 94d). The mean minimal HRT is 6.4 days close to the median (6.37 days). Despite an asymmetric repartition, the values are not dispersed. The fraction ratio goes from 0.04 to 0.54 and HRT from 5 to 8 days. This result is coherent with the results previously obtained. The thermally treated sludge is more bioaccessible than the secondary sludge, thus predicted minimal HRT is lower.
Finally, the most bioaccessible sludge are mainly contained in the thermally treated and primary sludge, followed by the secondary and the anaerobic sludge.
Therefore, the X_{SC}/X_{RC} ratio knowledge allows the estimation of the mesophilic digester design.

V.5. Conclusions and discussion

Over this chapter, the 3D-SE-LPF methodology of characterization has been validated with an experimental modeling exercise. The ADM1 modified model fits very well with the experimental data even with intrinsic organic matter is disturbed.

A local sensitivity analysis has shown that biochemical fractions have an influence on biogas quality whereas non-biodegradable fraction has an influence on the quantity. However, as the analysis is performed locally, bioaccessible fractions have no influence at 18 days HRT.

In order to show this fractionation impact on the ADM1 model, scenarii analysis has been performed for several sludge having different X_{SC}/X_{RC} ratios, with HRT going from 1 to 30 days. Results showed that the ratio had an impact when HRT is less than 14 days. Finally, the X_{SC}/X_{RC} ratio and the minimal HRT are positively correlated with a linear regression.

Therefore, the 3D-SE-LPF tool has allowed us to find three main following results:

- Biodegradability prediction
- Biodegradable readily and slowly bioaccessible fractions X_{RC} and X_{SC}
- Minimal HRT advised to obtain 95 to 98% of maximal biogas flow rate.

From the chapter IV, the sludge SII_E used for the RSF study has been tested in the correlation for minimal HRT assessment. This HRT is significantly decreased leading to important cut costs for reactor design. The use of this methodology tool through the correlations set up in this study would allow design optimization.

Conclusions

The main objective of this study was to develop a methodology to characterize the organic matter from wastewater treatment sludge. More specifically, this method aimed at characterizing input variables of ADM1. These variables are above all composed of the biochemical and non-biodegradable fractions. Moreover, the limiting step of anaerobic digestion of sludge is the hydrolysis. In order to better simulate this step, a modified version of ADM1 from Mottet (2009) has been chosen. Indeed, this model considers a Contois kinetic term that is more appropriate to the enzymatic colonization of particulate organic matter occurring during the hydrolysis. It also considers two distinct biodegradable fractions, similarly to the ASM1 model. One challenge was thus to define a methodology able to characterize the biodegradable fraction (for non-biodegradable fraction assessment) and the readily and slowly biodegradable fractions.

A literature review focused on this topic has shown that several methods exist for biodegradability characterization. Originally, they were based on BMP tests which are tedious and time consuming. Thus, several authors have developed correlations between measurements easy to obtain and biodegradability. However, few correlations were developed for sludge. Concerning fractionation of X_{RC} and X_{SC}, the methods reviewed are mainly based on batch tests.

The lack of tools for characterizing these variables has been highlighted in this review chapter. However, spectral techniques (e.g. infra-red spectroscopy or fluorescence spectroscopy) seemed promising. In fact, the infra-red spectroscopy has been already used as a biodegradability indicator but is not sensitive enough and the structural interpretation is difficult. The 3D fluorescence spectroscopy has not yet been correlated with biodegradability but recent scientific papers have shown its potential for this and for representing a characterization map of the organic matter. This technique is also very sensitive allowing the identification of complexity. Muller et al. (2011) applied this technique to sludge. Unfortunately, because of the dark color of this matrix, the 3D-SPF technique could not be used. In their last work, Muller et al. (*in press*) avoided this problem by defining sequential extraction methods and measuring these sludge extracts by 3D-LPF. The results obtained were promising and the extraction protocol was an efficient approach to simulate the sludge bioaccessibility.

However, extraction yield was only 50% of the total COD. Thus, the assumption that the extractible fractions were linked with bioaccessibility had to be proven.

In our study, the sequential protocol was first slightly optimized and applied on 52 sludge samples. The number of 4 extractions (instead of 20 as proposed by Muller et al.) has been demonstrated to extract the main part of organic matter represented by the proteins. Thermally treated sludge samples extracts indicated that the chemical accessibility was linked with the bioaccessibility since the most accessible fractions were increased by thermal pretreatment. However, correlation between chemical and biological accessibility had to be validated together with the ability of the low extraction yield to represent the biodegradable and bioaccessible fractions.

To investigate these issues, three laboratory tests had been performed. Results showed that during the anaerobic biodegradation, there was a coherent organic matter shift between the extracted fractions. The mass balances revealed that 80% of the extractible matter was biodegradable. There was also coherent kinetics. Indeed, the most accessible fractions were biodegraded in a first phase of degradation and the less accessible fractions were biodegraded at the end. This result was validated by the BMP tests performed on sludge in which each fraction is removed. The third test made on continuous reactors showed that the slowest biodegradable fractions were mainly composed of HSL and NE fractions. Thus, the chemical and the biological accessibility were linked. However, no statistical correlation could be between the extracts and the X_{RC} variable. Indeed, X_{RC} is the biodegradable bioaccessible fraction and all the extracts are not totally biodegradable. Therefore, the correlation has to take into account the non-biodegradable part of the fractions.
From this assumption, fluorescence spectroscopy was studied on liquid extracts in order to measure their complexity. Preliminary results showed that the least accessible is the organic matter, the most complex are the 3D fluorescent spectra. Moreover, the spectra observations before and after anaerobic digestion highlighted the complexity revealed in the non-biodegraded sludge.

Our objective was then to build an indicator based on the fluorescence complexity and on the accessibility simulated by the extractions. These indicators have been defined as the multiplication of each COD percentage of the fractions with the seven fluorescence zones percentage. 28 variables were thus obtained and tested in a PLS regression model for BD and

X_{RC}. The VFA percentage was also added in the PLS model because this not fluorescent compound was easily biodegradable and represented the second main component of several sludge.
The BD prediction with the 28 indicators was a success but was not enhanced by the VFA addition. X_{RC} was also well predicted but here, the accounting for VFA improved the PLS model.

In order to apply this technique, two lab scale reactors were run and simulated with a modified ADM1 model. The influent organic matter was modified to check the robustness of the model and both reference and disturbed periods were correctly simulated, demonstrating the interest of the approach.

A local sensitivity analysis was also performed for the input variables of the ADM1 model. Biochemical fractions influenced to the methane quality and the non-biodegradable fractions influenced the methane quantity. However, no influence was noticed for X_{SC}/X_{RC} ratio at this HRT (18 days). In order to further investigate this point, a scenario analysis was performed simulating several HRT values for sludge samples with different X_{RC}/X_{SC} ratios. Results showed that below 15 days, the X_{SC}/X_{RC} ratio impacted the biogas production. From the curves obtained, an optimal HRT for each X_{SC}/X_{RC} ratio could be defined and a linear correlation between this ratio and HRT was found. This result leads to a digester design optimization.

Another powerful observation was provided by the sensitivity analysis of the PLS models prediction of BD and X_{RC}. The HSL fraction was the main influential fraction for both models. Concerning the fluorescence zones, the zone I (protein-like compounds) and VI (humic acid-like, melanoidin-like, and lignocellulose-like compounds) are responsible of the biodegradation limitation of the organic matter contained in the sludge. Identifying these compounds can lead to optimize pre- or post-treatment of sludge leading to a significant enhancement of both accessibility and biodegradability and thus to a decrease of the minimal HRT or an increase of the energy produced.

Finally, the 3D-SE-LPF methodology has shown its ability to predict organic matter biodegradability and bioaccessibility in 5 days (extractions protocol and fluorescence spectroscopy) instead of 30 to 40 days as with the classical BMP tests.

This methodology has also shown its ability to characterize the ADM1 input variables with accuracy. Beyond these applications, this approach can provide a useful map of the organic matter in order to evaluate the performances of a process, or to investigate substrate limitations and to identify recalcitrant compounds.

Perspectives

The methodology developed and tested in this study has shown to be useful for several applications. Nevertheless, to go further, optimization and complementary studies can be performed to bring practicality and powerfulness to this characterization tool.

A first development could be the optimization and automation of the sequential extraction protocol. This would lead to large time savings in comparison to the manual protocol as well as a better optimization of the number of chemical extractions. On-line instrumentation tool would be an application of this automation. However, the methodology is based on the florescence spectroscopy and extractions coupling. 3D-LPF probe does not exist. There are only 2D wavelength probes which can be multiplexed with others at different excitation wavelength. This means that relevant excitation wavelengths should be chosen. For example, 7 probes can be tested at excitation wavelengths corresponding to the main peak of the 7 zones highlighted in this study.
With such a portative instrumentation, the organic matter would be rapidly characterized to diagnose process offsets. This method would also help the human operator to evaluate and optimize the performance of a sludge pre-treatment.

A complementary study would be to perform the same work but at different temperatures of anaerobic digestion such as thermophilic (55°) or low temperature conditions (20°). The BMP tests for biodegradability assessment at the temperature targeted would be performed and validation with ADM1 would be also made with lab scale reactors at the same temperature. This perspective would lead to the diversification of temperature process design.

In the same way, application of the protocol could be tested on matrices other than sludge. Indeed, in an environmental biorefinery context, others potential substrates (agro-food, organic fractions from municipal solid wastes, etc…) could be studied for others applications/process (fertilizing, reuse, compost, interest molecules production, etc…).
In this study, two refusals have been used: grid refusal solids and grease treatment refusals, both from the same wastewater treatment.

As shown, 3D-SE-LPF worked for both samples. Thus, application of the methodology to others matrix such as solids wastes or composts can be imagined and this opens exciting routes to the optimization of anaerobic digestion in general.

Another complementary study would be the improvement of anaerobic digestion process by recalcitrant compounds identification.
Therefore, identification of the compounds from fluorescence in zones I and VI constitutes a very promising perspective. However, from the literature review, the fluorescence zone VI is associated to several types of molecules depending on the sample studied. In the same way, the fluorescence zone I is associated to protein-like which might be hydrophobic. Thus, additional laboratory tests should be performed to identify these compounds by extracting them (extraction with hexane or methanol) and by measuring their fluorescence. Concerning the fluorescence zone VI, advanced measurement of humic acids-like and others compounds should be performed on HSL samples. Once these recalcitrant compounds are identified, an interesting perspective would be to find relevant and dedicated treatment before or after anaerobic digestion of sludge.

But the methodology applications and complementary studies listed above are not exhaustive! Fluorescence spectroscopy has not yet been fully investigated. And from the results obtained during this work, it is strongly believed that this will lead to main achievements in the near future for better knowledge of organic matter and for optimization of anaerobic digestion processes.

References

Abbassi-Guendouz, A., Brockmann, D., Trably, E., Delgenes, J-P., Steyer, J-P., Escudié, R. (2012) Total solids content drives high solid anaerobic digestion via mass transfer limitation. *Bioresource Technology* **111**, 55-61.

Allen, M. S., Welch, K. T., Prebyl, B. S., Baker, D. C., Meyers, A. J. and Sayler, G. S. (2004) Analysis and glycosyl composition of the exopolysaccharide isolated from the floc-forming wastewater bacterium Thauera sp. MZ1T. *Environmental Microbiology* **6** (8), 780-790.

Andrews, J. F. and Graef S. P. (1971) Dynamic Modelling and Simulation of the AD Process. *Advances in Chemistry Series No.105, Anaerobic Biological Treatment Processes.* American Chemical Society, Washington, D.C.126.

Andrews, J. F. (1971) Kinetic models of biological waste treatment. *Biotechnology and Bioengineering* **2**, 5-33.

Angelidaki, I., Ellegaard, L. and Ahring, B. K. (1993) A mathematical model for dynamic simulation of AD of complex substrates: Focusing on ammonia inhibition. *Biotechnology and Bioengineering* **42** (2), 159-166.

Angelidaki, I., Ellegaard, L. and Ahring, B. K. (1997) Modelling anaerobic codigestion of manure with olive oil mill effluent. *Water Science and Technology* **36** (6-7), 263-270.

Angelidaki, I. and Sanders, W. (2004) Assessment of the anaerobic biodegradability of macropllutants. *Reviews in Environmental Science and Bio/Technology* **3**, 117-129.

Angelidaki, I., Alves, M., Bolzonella, D., Borzacconi, L., Campos, J.L., Guwy, A.J., Kalyuzhnyi, S., Jenicek, P. and van Lier, J. B. (2009) Defining the biomethane potential (BMP) of solid organic wastes and energy crops: a proposed protocol for batch assays. *Water Science and Technology* **59** (5), 927-934.

Appels, L., Baeyens, J., Degreve, J. and Dewil, R. (2008) Principles and potential of the AD of waste-activated sludge. *Progress in Energy and Combustion Science* **34** (6), 755-781.

Appels, L., Lauwers, J., Gins, G., Degreve, J., Van Impe, J. and Dewil,R. (2011) Parameter identification and modeling of the biochemical methane potential of waste activated sludge. *Environmental Science & Technology* **45** (9), 4173-4178.

Aquino, S. F., Chernicharo, C. A. L., Soares, H., Takemoto, S. Y. and Vazoller, R. F. (2008) Methodologies for determining the bioavailability and biodegradability of sludges. *Environmental Technology* **29** (8), 855-862.

Barret, M., Barcia, G. C., Guillon, A., Carrére, H. and Patureau, D. (2010) Influence of feed characteristics on the removal of micropollutants during the AD of contaminated sludge. *Journal of Hazardous Materials* **181** (1-3), 241-247.

Batstone, D. J., Keller, J., Newell, R. B. and Newland, M. (2000) Modelling anaerobic degradation of complex wastewater. I: model development. *Bioresource Technology* **75** (1), 67-74.

Batstone, D. J., Keller, J. and Steyer, J. P. (2006) A review of ADM1 extensions, applications, and analysis: 2002-2005. *Water Science and Technology* **54** (4), 1-10.

Batstone, D. J., Keller, J., Angelidaki, I., Kalyuzhnyi, S. V., Pavlostathis, S. G., Rozzi, A., Sanders, W. T. M., Siegrist, H. and Vavilin, V. A. (2002) AD Model No.1. (ADM1). *IWA Scientific and Technical Report No. 13*. IWA, ISBN:1-900222-78-7.

Battersby, N. S. and Wilson, V. (1989) Survey of the anaerobic biodegradation potential of organic chemicals in digesting sludge. *Applied and Environmental Microbiology* **55** (2), 433-439.

Beech, I. B., Cheung, C. W. S., Johnson D. B. and Smith, J. R. (1996) Comparative studies of bacterial biofilms on steel surface using atomic force microscopy and environmental scanning electron microscopy. *Biofouling* **10**, 65-67.

Blumenkrantz, N. and Asboe Hansen, G. (1973) New method for quantitative determination of uronic acids. *Analytical Biochemistry* **54** (2), 484-489.

Bougrier, C., Albasi, C., Delgenès, J.P. and Carrère, H. (2006) Effect of ultrasonic, thermal and ozone pre-treatments on waste activated sludge solubilisation and anaerobic biodegradability. *Chemical Engineering and Processing: Process Intensification* **45** (8), 711-718.

Bradford, M. M. (1976) A rapid and sensitive method for the quantitation of microgram quantities of protein utilizing the principle of protein-dye binding. *Analytical Biochemistry* **72** (1-2), 248-254.

Brinkmann, K., Blaschke, L. and Polle, A. (2002) Comparison of different methods for lignin determination as a basis for calibration of near-infrared reflectance spectroscopy and implications of lignoproteins. *Journal of Chemical Ecology* **28** (12), 2483-2501.

Bryers, J. D. (1985) Structured modelling of the AD of biomass particles. *Biotechnology and Bioengineering* **27**, 638-649.

Buendía, I.M., Fernández, F.J., Villaseñor, J. and Rodríguez, L., 2008. Biodegradability of meat industry wastes under anaerobic and aerobic conditions. *Water Research* **42** (14), 3767-3774.

Buffiere, P., Loisel, D., Bernet, N. and Delgenes, J. P. (2006) Towards new indicators for the prediction of solid waste AD properties.*Water Science and Technology* **53** (8), 233-241.

Burton, K. (1956) A study of the conditions and mechanism of the diphenylamine reaction for the colorimetric estimation of deoxyribonucleic acid. *The Biochemical Journal* **62** (2), 315-323.

Cao, Y. and Pawlowski, A. (2012) Sewage sludge-to-energy approaches based on AD and pyrolysis: Brief overview and energy efficiency assessment. *Renewable and Sustainable Energy Reviews* **16** (3), 1657-1665.

Cecchi, F., Mata-Alvarez, J., Marcomini, A. and Pavan, P. (1991) First order and step-diffusional kinetic models in simulating the mesophilic AD of complex substrates. *Bioresource Technology* **36** (3), 261-269.

Chandler, J. A., Jewell, W. J. and Gossett, J. M. (1980) Predicting methane fermentation biodegradability. *Biotechnology Bioengineering Symposium* **NO.10** (10), 93-107.

Chandra, R., Bharagava, R.N., and Rai, V. (2008) Melanoidins as major colorant in sugarcane molasses based distillery effluent and its degradation. *Bioresource Technology* **99** (11), 4648-4660.

Chen, W., Westerhoff, P., Leenheer, J. A. and Booksh, K. (2003) Fluorescence excitation-emission matrix regional integration to quantify spectra for dissolved organic matter. *Environmental Science & Technology* **37** (24), 5701-5710.

Costello, D. J., Greenfield, P. F. and Lee, P. L. (1991) Dynamic modelling of a single stage high rate anaerobic reactor-I. Model derivation and II. Model verification. *Water Research* 25, 847-871.

Chynoweth, D. P., Turick, C. E., Owens, J. M., Jerger, D. E. and Peck, M. W. (1993) Biochemical methane potential of biomass and waste feedstocks. *Biomass and Bioenergy* **5** (1), 95-111.

Chynoweth, David P. and Ron Isaacson, Anaerobic digestion of biomass. Published by Springer, edited by Hardcover , -296. 23-7-1987.

Comte, S., Guibaud, G. and Baudu, M. (2006) Relations between extraction protocols for activated sludge extracellular polymeric substances (EPS) and EPS complexation properties Part I. Comparison of the efficiency of eight EPS extraction methods. *Enzyme and Microbial Technology* **38** (1-2), 237-245.

Comte, S., Guibaud, G. and Baudu, M. (2007) Effect of extraction method on EPS from activated sludge: An HPSEC investigation. *Journal of Hazardous Materials* **140** (1-2), 129-137.

Copp, J. B., Jeppsson, U. and Osen, C. (2003) Towards an ASM1 – ADM1 state variable interface for plant-wide wastewater treatment modeling. *Proceedings of the 76th Annual WEF Conference and Exposition (WEFTEC)*. Oct.11-15, Los Angeles, USA.

Cossu, R. and Raga, R. (2008) Test methods for assessing the biological stability of biodegradable waste. *Waste Management* **28** (2), 381-388.

D'Abzac, P., Bordas, F., Van Hullebusch, E., Lens, P. N. L. and Guibaud, G. (2010) Extraction of extracellular polymeric substances (EPS) from anaerobic granular sludges: comparison of chemical and physical extraction protocols. *Applied Microbiology Biotechnology* **85** (5), 1589-1599.

Davidsson, A., Gruvberger, C., Christensen, T. H., Hansen, T. L. and Jansen, J. (2007) Methane yield in source-sorted organic fraction of municipal solid waste. *Waste Management* **27** (3), 406-414.

De Baere, L. (2000) AD of solid waste: state-of-the-art. *Water Science and Technology* **41** (3), 283-290.

del Olmo, M., Zafra, A., Navas, A., and Vilchez, L. (1999) Trace determination of phenol, bisphenol A and bisphenol A diglycidyl ether in mixtures by excitation fluorescence following micro liquid-liquid extraction using partial least squares regression. *Analyst* **124** (3), 385-390.

Derbal, K., Bencheikh-lehocine, M., Cecchi, F., Meniai, A. H. and Pavan, P. (2009) Application of the IWA ADM1 model to simulate anaerobic co-digestion of organic waste with waste activated sludge in mesophilic condition. *Bioresource Technology* **100** (4), 1539-1543.

Dignac, M. F., Urbain, V., Rybacki, D., Bruchet, A., Snidaro, D. and Scribe, P. (1998) Chemical description of extracellular polymers: Implication on activated sludge floc structure. *Water Science and Technology* **38** (8-9), 45-53.

Dominguez, L., Rodriguez, M., and Prats, D. (2010) Effect of different extraction methods on bound EPS from MBR sludges. Part I: Influence of extraction methods over three-dimensional EEM fluorescence spectroscopy fingerprint. *Desalination* **261** 19-26.

Donoso-Bravo, A., Garcia, G., Pérez-Elvira, S. and Fernandez-Polanco, F. (2011) Initial rates technique as a procedure to predict the anaerobic digester operation. *Biochemical Engineering Journal* **53** (3), 275-280.

Doublet, J., Ponthieux, A., Laroche, C., Bougrier, C., Poitrenaud, M. and Cacho Rivero, J. (2011) Predicting the Biochemical Methane Potential of a wide range of organic waste and biomass by Near Infrared spectroscopy. *Proceedings of the IWA International Symposium on AD of Solid Waste and Energy Crops*. Vienna , 8 pp.

Dreywood, R. (1946) Qualitative Test for Carbohydrate Material. *Industrial & Engineering Chemistry Analytical Edition* **18** (8), 499.

Dubois, M., Gilles, K. A., Hamilton, J. K., Rebers, P. A. and Smith, F. (1956) Colorimetric method for determination of sugars and related substances. *Analytical Chemistry* **28** (3), 350-356.

Dufrêne, Y. F. and Rouxhet, P. G. (1996) X-ray photoelectron spectroscopy analysis of the surface composition of Azospirillum brasilense in relation to growth conditions. *Colloids and Surfaces B: Biointerfaces* **7** (5-6), 271-279.

Ekama, G.A., Dold, P.L. and Marais v., G.R. (1986). Procedures for determining influent COD fractions and the maximum specific growth rate of heterotrophs in activated sludge systems.*Water Science and Technology* **18** (6), 91-114.

Ekama, G. A., Sottemann, S. W. and Wentzel, M. C. (2007) Biodegradability of activated sludge organics under anaerobic conditions. *Water Research* **41** (1), 244-252.

Elefsiniotis, P. (1993) The effect of operational and environmental parameters on the acid-phase AD of primary sludge. PhD thesis National Technical University of Athens, Greece M. A. Sc. University of Toronto, pp206. 1993.

Elefsiniotis, P. and Oldham, W. K. (1994) Influence of pH on the acid-phase AD of primary sludge. *Journal of Chemical Technology & Biotechnology* **60** (1), 89-96.

Elefsiniotis, P. and Oldham, W. K. (1994) Anaerobic acidogenesis of primary sludge: The role of solids retention time. *Biotechnology and Bioengineering* **44** (1), 7-13.

Esparza-Soto, M. and Westerhoff, P. K. (2001) Fluorescence spectroscopy and molecular weight distribution of extracellular polymers from full-scale activated sludge biomass. *Water Science and Technology* **43**(6), 87-95.

Esposito, G., Frunzo, L., Panico, A. and Pirozzi, F. (2011) Modelling the effect of the OLR and OFMSW particle size on the performances of an anaerobic co-digestion reactor. *Process Biochemistry* **46** (2), 557-565.

Fenu, A., Guglielmi, G., Jimenez, J., Spérandio, M., Saroj, D., Lesjean, B., Brepols, C., Thoeye, C. and Nopens, I. (2010) Activated sludge model (ASM) based modelling of membrane bioreactor (MBR) processes: A critical review with special regard to MBR specificities. *Water Research* **44** (15), 4272-4294.

Frings, C. S. and Dunn, R. T. (1970) A colorimetric method for determination of total serum lipids based on the sulfo-phospho-vanillin reaction. *American Journal of Clinical Pathology* **53** (1), 89-91.

Frølund, B., Palmgren, R., Keiding, K. and Nielsen, P. H. (1996) Extraction of extracellular polymers from activated sludge using a cation exchange resin. *Water Research* **30** (8), 1749-1758.

Giovanela, M., Parlanti, E., Soriano-Sierra, E.J., Soldi, M.S. and Sierra, M.M.D. (2004). Elemental compositions, FT-IR spectra and thermal behavior of sedimentary fulvic and humic acids from aquatic and terrestrial environments. Geochemical Journal 38(3): 255-264.

Girault, R., Bridoux, G., Nauleau, F., Poullain, C., Buffet, J., Steyer, J.-P., Sadowski, A.G. and Béline, F. (2012) A waste characterisation procedure for ADM1 implementation based on degradation kinetics, *Water Research* (2012).

Girault, R., Bridoux, G., Nauleau, F., Poullain, C., Buffet, J., Steyer, J.P., Sadowski, A.G., and Béline, F. (2012) A waste characterisation procedure for ADM1 implementation based on degradation kinetics. *Water Research* **46** (13), 4099-4110.

Gledhill, W. E. (1979) standard practice for the determination of the anaerobic biodegradability of organic chemicals. Work document. Draft 2, no.35.24. American Society for Testing Materials, Philadelphia.

Gornall, A. G., Bardawill, C. J. and David, M. M. (1949) Determination of serum proteins by means of the biuret reaction. *Journal of Biochemical Chemistry* **177**, 751-766.

Graef, S. P. and Andrews, J. F. (1974) Stability and control of AD. *Journal of the Water Pollution Control Federation* **46**, 667-682.

Grau, P., de Gracia, M., Vanrolleghem, P. A. and Ayesa, E. (2007) A new plant-wide modelling methodology for WWTPs. *Water Research* **41** (19), 4357-4372.

Gunaseelan, V. N. (2007) Regression models of ultimate methane yields of fruits and vegetables solid wastes, sorghum and napiergrass on chemical composition. *Bioresource Technology* **98**, 1270-1277.

Gunaseelan, V. N. (2009) Predicting ultimate methane yields of Jatropha curcus and Morus indica from their chemical composition. *Bioresource Technology* **100** (13), 3426-3429.

Hansen, T. L., Schmidt, J. E., Angelidaki, I., Marca, E., Jansen, J. l. C., Mosbæk, H. and Christensen, T. H. (2004) Method for determination of methane potentials of solid organic waste. *Waste Management* **24** (4), 393-400.

Hao, R., Ren, H., Li, J., Ma, Z., Wan, H., Zheng, X. and Cheng, S. (2012) Use of three-dimensional excitation and emission matrix fluorescence spectroscopy for predicting the disinfection by-product formation potential of reclaimed water. *Water Research* **46** (17), 5765-5776.

Hill, D. T. (1982) A comprehensive dynamic model for animal waste methanogenesis. *Transactions of ASAF* **25**, 1374-1380.

He, X. S., Xi, B. D., Wei, Z. M., Jiang, Y. H., Yang, Y., An, D., Cao, J.L. and Liu, H.L. Fluorescence excitation-emission matrix spectroscopy with regional integration analysis for characterizing composition and transformation of dissolved organic matter in landfill leachates. *Journal of Hazardous Materials* **In Press, Corrected Proof**.

Henderson, R.K., Baker, A., Murphy, K.R., Hambly, A., Stuetz, R.M., and Khan, S.J. (2009) Fluorescence as a potential monitoring tool for recycled water systems: A review. *Water Research* **43** (4), 863-881.

Henneberg, W. and Stohmann, F. (1860) Beiträge zur Begründer einer rationellen. *Fütterung der Wiederkäer I & II*. Braunschweig.

Hill, D. T. and Barth, C. L. (1977) A dynamic model for simulation of animal waste digestion. *Journal of the Water Pollution Control Federation* **49** (10), 2129-2143.

Holm-Nielsen, J. B., Lomborg, C. J., Oleskowicz-Popiel, P. and Esbensen, K. H. (2008) On-line near infrared monitoring of glycerol-boosted AD processes: Evaluation of process analytical technologies. *Biotechnology and Bioengineering* **99** (2), 302-313.

Huang, M. H., Li, Y. M. and Gu, G. W. (2010) Chemical composition of organic matters in domestic wastewater. *Desalination* **262** (1-3), 36-42.

Huete, E., de Gracia, M., Ayesa, E. and Garcia-Heras, J. L. (2006) ADM1-based methodology for the characterisation of the influent sludge in anaerobic reactors. *Water Science and Technology* 54 (4), 157-166.

ISO 11734, 1995 ISO 11734, Evaluation of the "ultimate" anaerobic biodegradability of organic compounds in digested sludge – method by measurement of the biogas. 1995

Jeong, H. S., Suh, C. W., Lim, J. L., Lee, S. H. and Shin, H. S. (2005) Analysis and application of ADM1 for anaerobic methane production. *Bioprocess and Biosystems Engineering* **27** (2), 81-89.

Ji, Z., Chen, G. and Chen, Y. (2010) Effects of waste activated sludge and surfactant addition on primary sludge hydrolysis and short-chain fatty acids accumulation. *Bioresource Technology* **101** (10), 3457-3462.

Jimenez, J., Grelier, P., Meinhold, J., and Tazi-Pain, A. (2010) Biological modelling of MBR and impact of primary sedimentation. *Desalination* **250** (2), 562-567.

Jones, R., Parker, W., Khan, Z., Murthy, S. and Rupke, M. (2011) Characterization of sludge for predicting anaerobic digester performance. *Water Science and Technology* **57** (5), 721-726.

Jorand, F., Zartarian, F., Thomas, F., Block, J. C., Bottero, J. Y., Villemin, G., Urbain, V. and Manem, J. (1995) Chemical and structural (2D) linkage between bacteria within activated sludge flocs. *Water Research* **29** (7), 1639-1647.

Kameya, T., Murayama, T., Kitano, M. and Urano, K. (1995) Testing and classification methods for the biodegradabilities of organic compounds under anaerobic conditions. *Science of The Total Environment* **170** (1-2), 31-41.

Kleinstreuer, C. and Poweigha, T. (1982) Dynamic simulator for AD process. *Biotechnology and Bioengineering* **24**, 1941-1951.

Kayhanian, M. (1995) Biodegradability of the organic fraction of municipal solid waste in a high-solids anaerobic digester. *Waste Management & Research* **13** (2), 123-136.

Kiely, G., Tayfur, G., Dolan, C. and Tanji, K. (1997) Physical and mathematical modelling of AD of organic wastes. *Water Research* **31** (3), 534-540.

Kjeldahl, J. (1883) A new method for the determination of nitrogen in organic matter. *Zeitschreft fur Analytische Chemie*. 22:366.

Kleerebezem, R. and van Loosdrecht, M. C. M. (2006) Waste characterization for implementation in ADM1.*Water Science and Technology* **54** (4), 167-174.

Kobbero, C., Keiding, K., Larsen, K.L. and Halkjaer Nielsen, P. (2008) Quenching effects in the application of multi-channel fluorescence in activated sludge suspended solids. *Water Research* **42,** 2449-2456.

Labatut, R. A., Angenent, L. T. and Scott, N. R. (2011) Biochemical methane potential and biodegradability of complex organic substrates. *Bioresource Technology* **102** (3), 2255-2264.

Larpent, J.-P. and Champiat, D. (1988) Biologie des eaux-Méthodes et techniques. Masson.

Laurent,J., Casellas,M., Carrère,H. and Dagot,C. (2011) Effects of thermal hydrolysis on activated sludge solubilization, surface properties and heavy metals biosorption. *Chemical Engineering Journal* **166** (3), 841-849.

Lattner, D., Flemming, H. C. and Mayer, C. (2003) 13C-NMR study of the interaction of bacterial alginate with bivalent cations. *International Journal of Biological Macromolecules* **33** (1-3), 81-88.

Lee, M. Y., Suh, C. W., Ahn, Y. T. and Shin, H.S. (2009) Variation of ADM1 by using temperature-phased AD (TPAD) operation. *Bioresource Technology* **100** (11), 2816-2822.

Lee, B.M., Shin, H.S. and Hur, J. (2012) Comparison of the characteristics of extracellular polymeric substances for two different extraction methods and sludge formation conditions. *Chemosphere* **In Press, Corrected Proof**.

Lesteur, M., Bellon-Maurel, V., Gonzalez, C., Latrille, E., Roger, J. M., Junqua, G. and Steyer, J. P. (2010) Alternative methods for determining anaerobic biodegradability: A review. *Process Biochemistry* **45** (4), 431-440.

Lesteur, M., Latrille, E., Maurel, V. B., Roger, J. M., Gonzalez, C., Junqua, G. and Steyer, J. P. (2011) First step towards a fast analytical method for the determination of Biochemical Methane Potential of solid wastes by near infrared spectroscopy. *Bioresource Technology* **102** (3), 2280-2288.

Lettinga, G., van Velsen, A. F. M., Hobma, S. W., de Zeeuw, W. and Klapwijk, A. (1980) Use of the upflow sludge blanket (USB) reactor concept for biological wastewater treatment, especially for anaerobic treatment. *Biotechnology and Bioengineering* **22** (4), 699-734.

Li, B. and Logan, B. E. (2004) Bacterial adhesion to glass and metal-oxide surfaces. *Colloids and Surfaces B: Biointerfaces* **36** (2), 81-90.

Li, W. H., Sheng, G. P., Liu, X. W. and Yu, H. Q. (2008) Characterizing the extracellular and intracellular fluorescent products of activated sludge in a sequencing batch reactor. *Water Research* **42** (12), 3173-3181.

Lowry, O. H., Rosebrough, N. J., Farr, A. L. and Randall, R. J. (1951) Protein measurement with the Folin phenol reagent. *The Journal of Biological Chemistry* **193** (1), 265-275.

Lyberatos, G. and Skiadas, I. V. (1999) Modelling of AD - A review. *Global Network for Environmental Science and Technology: the International Journal* **1** (2), 63-76.

Manca, M. C., Lama, L., Improta, R., Esposito, E., Gambacorta, A. and Nicolaus, B. (1996) Chemical composition of two exopolysaccharides from Bacillus thermoantarcticus. *Applied and Environmental Microbiology* **62** (9), 3265-3269.

Marhuenda-Egea, F.C., Martinez-Sabater, E., Jordi, J., Moral, R., Bustamante, M.A., Paredes, C. and Perez-Murcia, M.D. (2007) Dissolved organic matter fractions formed during composting of winery and distillery residues: Evaluation of the process by fluorescence excitation-emission matrix. *Chemosphere* **68** (2), 301-309.

Mata-Alvarez, J., Macé, S. and Llabrès, P. (2000) AD of organic solid wastes. An overview of research achievements and perspectives. *Bioresource Technology* **74** (1), 3-16.

Mc Carty, P. L. (1964) Anaerobic waste treatment fundamentals, part two. *Public works* **95** (10), 123-126.

Miyata, N., Ike, M., Furukawa, K. and Fujita, M. (1996) Fractionation and characterization of brown colored components in heat treatment liquor of waste sludge. *Water Research* **30** (6), 1361-1368.

Moletta, R., Verrier, D. and Albagnac, G. (1986) Dynamic modelling of AD. *Water Research* **20** (4), 427-434.

Mosey, F. E. (1983) Mathematical modelling of the AD process: regulatory mechanisms for the formation of short-chain volatile acids from glucose. *Water Science and Technology* **15**, 209-232.

Mottet, A. (2009) Research of anaerobic biodegradability indicators and Modelling of thermophilic AD: Application to waste activated sludge with and without a thermal pretreatment. PhD thesis, LBE INRA Narbonne and VEOLIA, France, -221.

Mottet, A., François, E., Latrille, E., Steyer, J. P., Déléris, S., Vedrenne, F. and Carrère, H. (2010) Estimating anaerobic biodegradability indicators for waste activated sludge. *Chemical Engineering Journal* **160** (2), 488-496.

Muller, M., Milori, D., Deleris, S., Steyer, J.P. and Dudal, Y. (2011). Solid-phase fluorescence spectroscopy to characterize organic wastes. *Waste Management* **31**(9-10): 1916-1923.

Muller, M., Antonini, M., Dudal, Y., Latrille, E., Vedrenne, F. and Steyer, J.P. (*In press*). Combination of sequential extractions with liquid phase fluorescence spectroscopy to characterize sludge organic matter.

Ndira, V. Substances humiques du sol et du compost analyse elementaire et goupements atomiques fictifs: vers une approche thermodynamique. PhD thesis INP Toulouse, France, 1-223. 2006 (in French).

Neave, S. L. and Buswell, A. M. (1930) The anaerobic oxidation of fatty acids. *Journal of the American Chemical Society* **52** (8), 3308-3314.

Nielsen, P. H. and Jahn, A. (1999) Extraction of EPS. J. Wingender, T. R. Neu and H. C. Flemming, Editors, Microbial extracellular polymeric substances: characterization, structure and function, Springer-Verlag, Berlin Heidelberg , 49-72.

Nielsen, P. H., Thomsen, T. R. and Nielsen, J. L. (2004) Bacterial composition of activated sludge-importance for floc and sludge properties. *Water Science and Technology* **49** (10), 51-58.

Nopens, I., Batstone, D. J., Copp, J. B., Jeppsson, U., Volcke, E., Alex, J. and Vanrolleghem, P. A. (2009) An ASM/ADM model interface for dynamic plant-wide simulation. *Water Research* **43** (7), 1913-1923.

Ortega-Morales, B. O., Santiago-Garcia, J. L., Chan-Bacab, M. J., Moppert, X., Miranda-Tello, E., Fardeau, M.L., Carrero, J.C., Bartolo-Pérez, P., Valadéz-Gonzalez, A. and Guezennec, J. (2007) Characterization of extracellular polymers synthesized by tropical intertidal biofilm bacteria. *Journal of Applied Microbiology* **102** (1), 254-264.

Owen, W. F., Stuckey, D. C., Healy, J., Young, L. Y., and McCarty, P. L. (1979) Bioassay for monitoring biochemical methane potential and anaerobic toxicity. *Water Research* **13** (6), 485-492.

Park, C. and Novak, J.T. (2007) Characterization of activated sludge exocellular polymers using several cation-associated extraction methods. *Water Research* **41** (8), 1679-1688.

Park, C., Helm R. F. and Novak, J.T. (2008) Investigating the fate of activated sludge extracellular proteins in sludge digestion using sodium dodecyl sulphate polyacrylamide gel electrophoresis. *Water Environnement Research* **80** (12) 2219-2227.

Parker, J. W. (2005) Application of the ADM1 model to advanced AD. *Bioresource Technology* **96** (16), 1832-1842.

Parnaudeau, V. and Dignac, M.F. (2007) The organic matter composition of various wastewater sludges and their neutral detergent fractions as revealed by pyrolysis-GC/MS. *Journal of Analytical and Applied Pyrolysis* **78** (1), 140-152.

Pavlostathis, S. G. and Gossett, J. M. (1986) A kinetic model for AD of biological sludge. *Biotechnology and Bioengineering* **28** (10), 1519-1530.

Petersen, B., Gernaey, K., Henze, M. and Vanrolleghem, P. (2002) Evaluation of an ASM1 procedure on a municipal-industrial wastewater treatmen. Journal of Hydroinformatics 4[1], 15-38.

Pullammanapallil, P., Owens, J. M., Svoronos, S. A., Lyberatos, G. and Chynoweth, D. P. (1991) Dynamic model for conventionally mixed AD reactors. *AIChE Annual meeting*, paper 277c , 43-53.

Ramirez, I., Mottet, A., Carrère, H., Déléris, S., Vedrenne, F. and Steyer,J.P. (2009) Modified ADM1 disintegration/hydrolysis structures for modeling batch thermophilic AD of thermally pretreated waste activated sludge. *Water Research* **43** (14), 3479-3492.

Ras, M., Girbal-Neuhauser, E., Paul, E., Sperandio, M. and Lefebvre, D. (2008) Protein extraction from activated sludge: An analytical approach. *Water Research* **42** (8-9), 1867-1878.

Raunkjaer, K., Hvitved-Jacobsen, T. and Nielsen, P. H. (1994) Measurement of pools of protein, carbohydrate and lipid in domestic wastewater. *Water Research* **28** (2), 251-262.

Raposo, F., De la Rubia, M. A., Fernandez-Cegri, V. and Borja, R. (2012) AD of solid organic substrates in batch mode: An overview relating to methane yields and experimental procedures. *Renewable and Sustainable Energy Reviews* **16** (1), 861-877.

Reynolds, D. M. and Ahmad, S. R. (1997) Rapid and direct determination of wastewater BOD values using a fluorescence technique. *Water Research* **31** (8), 2012-2018.

Réveillé, V., Mansuy, L., Jardé, E. and Garnier-Sillam, E. (2003) Characterisation of sewage sludge-derived organic matter: lipids and humic acids. *Organic Geochemistry* **34** (4), 615-627.

Salemi, A., Lacorte, S., Bagheri, H. and Barcelo, D. (2006) Automated trace determination of earthy-musty odorous compounds in water samples by on-line purge-and-trap-gas chromatography-mass spectrometry. *Journal of Chromatography* **1136** (2), 170-175.

Sanders, W. T. M. (2001) Anaerobic hydrolysis during digestion of complex substrates. Wageningen University. ISBN 90-5808-375-6.

Scaglia, B., Confalonieri, R., D'Imporzano, G. and Adani, F. (2010) Estimating biogas production of biologically treated municipal solid waste. *Bioresource Technology* **101** (3), 945-952.

Shanmugam, P. and Horan, N. J. (2009) Simple and rapid methods to evaluate methane potential and biomass yield for a range of mixed solid wastes. *Bioresource Technology* **100** (1), 471-474.

Shelton, D. R. and Tiedje, J. M. (1984) General method for determining anaerobic biodegradation potential. *Applied and Environmental Microbiology* **47** (4), 850-857.

Sheng, G. P. and Yu, H. Q. (2006) Characterization of extracellular polymeric substances of aerobic and anaerobic sludge using three-dimensional excitation and emission matrix fluorescence spectroscopy. *Water Research* **40** (6), 1233-1239.

Sheng, G. P. Yu, H. Q., and Li, X. Y. (2011) Extracellular polymeric substances (EPS) of microbial aggregates in biological wastewater treatment systems: A review. *Biotechnology Advances* **28** (6), 882-894.

Shimizu, T., Kudo, K. and Nasu, Y. (1993) Anaerobic waste-activated sludge digestion- a bioconversion mechanism and kinetic model. *Biotechnology and Bioengineering* **41** (11), 1082-1091.

Siegrist, H., Renggli, D. and Gujer, W. (1993) Mathematical modelling of anaerobic mesophilic sewage sludge treatment. *Water Science and Technology* **27**, 25-6.

Siegrist, H., Vogt, D., Garcia-Heras, J.L. and Gujer, W. (2002) Mathematical model for meso- and thermophilic anaerobic sewage sludge digestion. *Environmental Science and Technology* **36** (5), 1113-1123.

Silva, F., Nadais, H., Prates, A., Arroja, L. and Capela, I. (2009) Modelling of anaerobic treatment of evaporator condensate (EC) from a sulphite pulp mill using the IWA AD model no. 1 (ADM1). *Chemical Engineering Journal* **148** (2-3), 319-326.

Silva, G.G., Couturier, M., Berrin, J.G., Buléon, A., and Rouau, X. (2012) Effects of grinding processes on enzymatic degradation of wheat straw. *Bioresource Technology* **103** (1), 192-200.

Smidt, E., Lechner, P., Schwanninger, M., Haberhauer, G. and Gerzabek, M. H. (2002) Characterization of waste organic matter by FT-IR spectroscopy: Application in waste science. *Applied Spectroscopy* **56** (9), 1170-1175.

Smidt, E. and Schwanninger, M. (2005) Characterization of waste materials using FTIR spectroscopy: Process monitoring and quality assessment. *Spectroscopy Letters* **38** (3), 247-270.

Smith, P. K., Krohn, R. I., Hermanson, G. T., Mallia, A. K., Gartner, F. H., Provenzano, M. D., Fujimoto, E. K., Goeke, N. M., Olson, B. J. and Klenk, D. C. (1985) Measurement of protein using bicinchoninic acid. *Analytical Biochemistry* **150** (1), 76-85.

Smith, P. H., Bordeaux, F. M., Goto, M., Shiralipour, A., Wilke, A., Andrews, J. F., Ide, S. and Barnett, M. W. Biological production of methane from biomass. Methane from biomass. A treatment approach, 291-334. 1988. Smith, W.H, and Frank, J.R. (Eds), Elsevier, London.

Sophonsiri, C. and Morgenroth, E. (2004) Chemical composition associated with different particle size fractions in municipal, industrial, and agricultural wastewaters. *Chemosphere* **55** (5), 691-703.

Spérandio, M. and Paul, E. (2000) Estimation of wastewater biodegradable COD fractions by combining respirometric experiments in various So/Xo ratios. *Water Research* **34** (4), 1233-1246.

Staudt, C., Horn, H., Hempel, D. C. and Neu, T. R. (2004) Volumetric measurements of bacterial cells and extracellular polymeric substance glycoconjugates in biofilms. *Biotechnology and Bioengineering* **88** (5), 585-592.

Swift, R.S. (1996). Methods of soil analysis. Organic matter characterization. D. L. Sparks. Madison, Soil Science Society of America: 1018-1020.

Tartakovsky, B., Lishman, L. A. and Legge, R.L. (1996) Application of multi-wavelength fluorometry for monitoring wastewater treatment process dynamics. *Water Research* **30** (12), 2941-2948.

Tomei, M. C., Braguglia, C. M., Cento, G. I. O. R. and Minnini, G. I. U. S. (2009) Modeling of AD of Sludge. *Critical Reviews in Environmental Science and Technology* **39** (12), 1003-1051.

Van Haandel, A. C., Catunda, P. F. C. and Araujo, L. (1998) Biological sludge stabilization, part 2-influence of the composition of waste activated sludge on AD. Water S.A. **24** (3), 231-236.

Van Lier, J. B. (2008) High-rate anaerobic wastewater treatment: diversifying from end-of-the-pipe treatment to resource-oriented conversion techniques. *Water Science and Technology* **57** (8), 1137-1148.

Van Soest, P. J. (1963) Use of detergents in the analysis of fibrous feeds. II. A rapid method for the determination of fiber and lignin. *Journal of the Association of Official Analytical Chemists* **46**, 829-835.

Vanrolleghem, P.A., Rosen, C., Zaher, U., Copp, J., Benedetti, L., Ayesa, E. and Jeppsson, U. (2005). Continuity-based interfacing of models for wastewater systems described by Petersen matrices. Water Science and Technology 52 (1-2), 493-500.

Vasiliev, V. B., Vavilin, V. A., Rytov, S. V. and Ponomarev, A. V. (1993) Simulation model of AD of organic matter by a microorganism consortium: basic equations. *Water Research* **20**, 633-643..

Vavilin, V. A., Vasiliev, V. B., Ponomarev, A. V. and Rytow, S. V. (1994) Simulation model 'methane' as a tool for effective biogas production during anaerobic conversion of complex organic matter. *Bioresource Technology* **48** (1), 1-8.

Vavilin, V. A. and Lokshina, L. Y. (1996) Modeling of volatile fatty acids degradation kinetics and evaluation of microorganism activity. *Bioresource Technology* **57** (1), 69-80

Vavilin, V. A., Fernandez, B., Palatsi, J. and Flotats, X. (2008) Hydrolysis kinetics in anaerobic degradation of particulate organic material: An overview. *Waste Management* **28** (6), 939-951.

Vesilind, P. A. Wastewater Treatment Plant Design. Published by Water Environment Federation , -516. 1-8-2003.

Wan, S., Xi, B., Xia, X., Li, M., lv, D., Wang, L. and Song, C. (2012). Using fluorescence excitation emission matrix spectroscopy to monitor the conversion of organic matter during

anaerobic co-digestion of cattle dung and duck manure, *Bioresource Technology*. **In press,** doi: 10.1016/j.biortech.2012.04.001.

Wang, Z. W., Liu, Y. and Tay, J. H. (2005) Distribution of EPS and cell surface hydrophobicity in aerobic granules. *Applied Microbiology and Biotechnology* **69** (4), 469-473.

Wang, Z. W., Liu, Y. and Tay, J. H. (2007) Biodegradability of extracellular polymeric substances produced by aerobic granules. *Applied Microbiology and Biotechnology* **74** (2), 462-466.

Wang, Z., Wu, Z. and Tang, S. (2009) Characterization of dissolved organic matter in a submerged membrane bioreactor by using three-dimensional excitation and emission matrix fluorescence spectroscopy. *Water Research* **43** (6), 1533-1540.

Wang, Z., Tang, S., Zhu, Y., Wu, Z., Zhou, Q. and Yang, D. (2010) Fluorescent dissolved organic matter variations in a submerged membrane bioreactor under different sludge retention times. *Journal of Membrane Science* **355** (1-2), 151-157.

Wilson, C. A. and Novak, J. T. (2009) Hydrolysis of macromolecular components of primary and secondary wastewater sludge by thermal hydrolytic pre-treatment. *Water Research* **43** (18), 4489-4498.

Xiong, H., Chen, J., Wang, H., and Shi, H. (2012) Influences of volatile solid concentration, temperature and solid retention time for the hydrolysis of waste activated sludge to recover volatile fatty acids. *Bioresource Technology* **119** (0), 285-292.

Yasui, H., Sugimoto, M., Komatsu, K., Goel, R., Li, Y. Y. and Noike, T. (2006) An approach for substrate mapping between ASM and ADM1 for sludge digestion. *Water Science and Technology* **54** (4), 83-92.

Yasui, H., Goel, R., Li, Y. Y. and Noike, T. (2008) Modified ADM1 structure for modelling municipal primary sludge hydrolysis. *Water Research* **42** (1-2), 249-259.

Zaher, U., Li, R., Jeppsson, U., Steyer, J.P. and Chen, S. (2009) GISCOD: General Integrated Solid Waste Co-Digestion model. *Water Research* **43** (10), 2717-2727.

Zhang, M. L., Sheng, G. P., Mu, Y., Li, W. H., Yu, H. Q., Harada, H. and Li, Y. Y. (2009) Rapid and accurate determination of VFAs and ethanol in the effluent of an anaerobic H2-producing bioreactor using near-infrared spectroscopy. *Water Research* **43** (7), 1823-1830.

Annex

Annex 1 : A statistical comparison of protein and carbohydrate characterisation methodology applied on sewage sludge samples 231
Annex 2: ADM1 and modified ADM1 (Mottet, 2009) Petersen matrix 255
Annex 3: PLS regression results for BD prediction with X-variables containing VFA percent of total COD 259
Annex 4: Identification of fluorescence compounds in zones VI 263
Annex 5: Simulation results obtained for reactors P1 and P2 for all data 265

Annex 1 : A statistical comparison of protein and carbohydrate characterisation methodology applied on sewage sludge samples

Julie Jimenez [2], Fabien Vedrenne[1], Cécile Denis[1], Alexis Mottet[3], Stephane Déléris[2], Jean-Philippe Steyer[3], Jesús Andrés Cacho Rivero[1]

Affiliations

[1]VERI, VEOLIA Recherche et Innovation, Chemin de la Digue, BP 76, 78603 Maisons Laffitte Cedex, France

[2]VEOLIA Eau direction technique, Immeuble B. 1, rue Giovanni Battista Pirelli. 94417 **Saint- Maurice**

[3]INRA, UR50, Laboratoire de Biotechnologie de l'Environnement, Avenue des Etangs, Narbonne, F-11100, France.

Abstract

Biochemical characterization of organic matter is becoming of key importance in wastewater treatment. The main objectives are to predict organic matter properties, such as granulation or flocculation, and hence treatment performance. Although standardized methods do exist for some organic molecules, such as volatile fatty acids or lipids, there are no standard methods to measure proteins and carbohydrates content. Both biochemical families being the main components of sewage sludge. Consequently, the aim of the present work is to investigate the efficiency of several colorimetric methods to determine proteins and carbohydrates content as well as their compatibility with the sludge matrices. The different methods have been evaluated based on statistical criteria such as sensitivity, linearity, accuracy, rightness, and specificity using standard molecules such as Bovine Serum Albumin (BSA), glucose, cellulose and a certified reference product. The Lowry and the Dubois methods have shown to be the best compromise for the considered criteria after been tested on sewage sludge samples obtained from different locations in a wastewater treatment plant. In average, the measured volatile fatty acids, lipids, proteins and carbohydrates contents represented 80 ± 7% (% volatile solids) of the organic matter. Proteins and carbohydrates represented in average 69 ± 3%.

This study underlins that the choice of a relevant methodology is of great importance for organic matter measurement.

Key words: proteins, carbohydrates, organic matter characterization, wastewater sludge

Abbreviations

[2] Corresponding author: julie.jimenez@veolia.com phone: +33 1 34 93 81 87

a	director coefficient or slope obtained by linear regression
ADM1	Anaerobic Digestion Model N°1
b	origin ordinate obtained by linear regression
BCA	Bicinchoninic Acid
BOD	Biological Oxygen Demand
BSA	Bovine Serum Albumin
COD	Chemical Demand Oxygen
DS	Digested Sludge
EPS	Extra polymer Substances
F_{table}	Fisher test value obtained in Fisher table
F_{test}	Fisher test value calculated
GC-MS	Gas Chromatography Mass Spectroscopy
LCS	Supernatant (Liquid) after centrifugation Sludge
MS	Mixed Sludge
N	Nitrogen
R^2	Regression coefficient obtained by linear regression
SI	Primary Sludge
SII	Secondary Sludge
SCS	Solid after centrifugation Sludge => SCS
STP	Standard conditions of Temperature and Pressure
TKN	Total Kjehdahl Nitrogen
t_{table}	Student test value obtained in Student table
t_{test}	Student test value calculated
VFA	Volatile Fatty Acids

VS	Volatile Solids
WW	WasteWater
x	Concentration value in linear regression model
Y	Absorbance value in linear regression model
Ycalc	Absorbance value calculated
α	Risk factor defined for significant difference

1. Introduction

In the past two decades, organic matter characterisation, through identification of biochemical families, has become crucial in several topics of environmental treatment processes. At first, quantification of organic matter was limited to lumped variables such as chemical oxygen demand (COD), biological oxygen demand (BOD) or volatile solids (VS). Later, with the growing necessity to optimise and model treatment process performance, a more accurate characterisation of the organic matter was required. In this context, detailed organic matter quantification methods have been developed and used. For example, in the field of anaerobic digestion, it has been shown that each biochemical family presents a specific methane yield. According to Angelidaki *et al.* (2004), the theoretical methane yield of carbohydrates, proteins and lipids are 0.415, 0.496 and 1.014 $L_{CH4}.g_{VS}^{-1}$ (in STP conditions) respectively. Similarly, the use of static (Mottet *et al.*, 2010) or dynamic models (ADM1, Batstone *et al.*, 2002) to predict anaerobic biodegradability and process performance is also based on a detailed substrate characterization. Other authors used detailed characterization of organic matter to enhance the knowledge of the mechanisms involved in the hydrolysis and solubilisation pre-treatment of solid substrates (Elefsioniotis *et al.*, 1994; Wilson and Novak, 2009 and Ji *et al.*, 2010). Another interesting topic found in the literature is the characterization of extrapolymer substances (EPS) by successive extraction methods from sludge samples in order to link the biochemical composition to fouling in membrane bioreactors (Wang *et al.,* 2009; Malamis *et al.*, 2009; Pan *et al.*, 2010 and Wang *et al.*, 2010). EPS extraction and characterization is also used to study floc properties (settling, flocculation, granulation) (Frølund *et al.*, 1996; Liu *et al.*, 2002; Novak *et al.*, 2003; Nielsen *et al.*, 2004; Comte *et al.*, 2006 and D'Abzac *et al.*, 2010).

According to Elefsionotis *et al.* (1994), Frølund *et al.* (1996), Wilson and Novak (2009), Ji *et al.* (2010), Mottet *et al.* (2010) and Huang *et al.* (2010) the main components of sewage sludge (primary, activated and anaerobic) are proteins, carbohydrates and lipids. A standard method based on soxhlet extraction and gravimetric determination exists for lipid quantification (APHA, 1995). However no standard method exists for proteins or carbohydrates content measurement.

The most commonly used methods to measure carbohydrates concentrations are the Anthrone method (Dreywood, 1946) and the Phenol–sulfuric acid or Dubois method (Dubois *et al.*, 1956). In the case of proteins, the colorimetric methods used to measure their concentration are the Bicinchonic Acid method (BCA) (Smith *et al.*, 1985), the Lowry method (Lowry et al., 1951), the modified Lowry method (Frølund *et al.* , 1996), the Bradford method (Bradford *et al.*, 1976) and the Biuret method (Gornall *et al.*, 1949). Additionally, proteins content can be calculated by measuring the N-organic content as defined by Frølund *et al.* (1996) and Raunjkaer *et al.* (1994) and assuming that protein contains 16.5% (w/w) of nitrogen.

Critical comparisons of the different methods have been made by several authors with diverse conclusions. In the case of the methods to measure carbohydrates concentrations, Brown and Lester (1980) found that the Dubois method recovered more carbohydrates than the Anthrone method (about 24 % higher recovery). Piccolo *et al.* (1991) withdrawn the same conclusion when both methods were applied on soils: the Anthrone determined a significantly lower amount of carbohydrates that the Phenol-sulfuric method (factor from 7 to 81). Feller *et al.* (1991), quoted by Lesteur *et al.* (2010), added that the Anthrone method underestimated sugars as galactose, mannose, xylose, arabinose which are monomers of the hemicellulose. However, Frølund *et al.* (1996) reported that both methods showed similar yield and accuracy (standard deviation of 5% for the Anthrone and 6% for the Dubois method) when applied on sludge. Raunjkaer *et al.* (1994) compared both methods showing that the Dubois method had the lowest precision with a relative standard deviation of 50%, whereas the Anthrone method, after addition of glucose was significantly more accurate (variation coefficients of 4.8% and 2% for total and filtered wastewater samples respectively) and had no interferences (both regression curves are equal at 5%). Therefore, contradictory conclusions are withdrawn, especially in the case of municipal sludge samples.

Similar results can be observed in the comparisons of the different methods for proteins content measurement. Concerning the Bradford method, authors agreed: it underestimates proteins content, from 2 to 4 times lower than the values obtained with Lowry applied on extracted EPS (Frølund *et al.*, 1996) and on wastewater samples (Raunjkaer *et al.,* 1994). The authors explained that the possible reason for the underestimation of the Bradford method is that the method is more appropriate for pure protein and peptides (8-9 peptides bonds) determination, while the Lowry method can measure dipeptides. Moreover, authors show that particulate proteins are not sufficiently solubilised by the Bradford method. For this reason, the Bradford method is not used in this work, applied on sludge samples. The BCA, the Lowry and the modified Lowry methods are accurate and more often used to determinate the protein concentration (Ras *et al.*, 2008), as well as the N-content method. However, depending on the matrix studied, conclusions do not go to the same direction.

Frølund *et al.*, (1996) made a comparison between the Bradford, the Lowry, and the N-content methods on sludge and EPS extracted from sludge. The Lowry method was modified by the author in order to take into account the humic acids interference. Results showed that the values obtained with the modified Lowry

method was close to the values obtained with the N-content method whereas the non-modified Lowry method is around 1.5 times greater on sludge. In the case of EPS measurement, the factor increased to about 3 to 4. Raunjkaer *et al.* (1994) found different results: they compared the BCA, the Bradford and the classical Lowry methods on filtered wastewater samples with addition of BSA in order to test the specificity of each method. The Lowry method did not present any interference (the slopes of both regression curves are equal at 5%) whereas BCA is not used because glucose interference was found.

In Ras *et al.* (2008), the addition of 2, 4 and 8 $g_{BSA}.L^{-1}$ of BSA was made in three activated sludge samples. The results obtained with the modified Lowry method matched better for the majority of the tested sludge (the error ranged from 0.3 to 0.4 $g_{BSA}.L^{-1}$ and an overestimation of 4% was observed in two cases and underestimation of 40% in the other one). The BCA method overestimated in all the cases (20 to 25%) the BSA addition. The BCA method is based on the Lowry principle using an alternative detection reagent, more stable and sensitive (Raunjkaer *et al.*, 1994). Moreover, the BCA method is not affected by humic acids content for concentrations below 0.2 $g_{BSA}.L^{-1}$. After dilution applied on sludges in the method, that will be the typical range for a sewage sludge sample. However, this method becomes unusable when the sample contains reduced sugars (Massé, 2004). Sugars are potential reducing agents which can respond like proteins in the BCA method (Raunjker *et al.,* 1994; Smith *et al.,* 1985). But interfering simple sugars are rapidly assimilated by bacteria and therefore are less likely to persist in bacterial aggregates. (Ras *et al.*, 2008).

Ras *et al.*(2008) concluded that the BCA method was the best for their application since it showed less interferences with the extractant used for EPS dosage. Frølund *et al.*, (1996) have based their comparison on the N-content method value which is not the most appropriate. Raunjkaer *et al.* (1994) showed that the 16.5% (w/w) of nitrogen in proteins (6.25 g protein.gN^{-1}) varies widely from one protein to another: 5.55 to 6.40 for animal products, 5.30 to 6.31 for plant products (Greenfield and Southgate, 2003). Huang *et al.* (2010) used the aminogram of a wastewater, obtained by GC-MS, to prove that the average nitrogen content in that wastewater was 13% (w/w) and that also for that wastewater the observed ratio of 7.5 g protein.gN^{-1} was higher than the theoretical one.

The accuracy of the method depends on the nature of the sample, for that reason interference, specificity and reliability tests have to be carried out to validate the analysis (Raunjkaer *et al.*, 1994). Moreover, conclusions obtained from the several comparisons described are directly linked to the target defined and could be different from one matrix to another.

Therefore the objective of this work is to determine the best colorimetric methods to measure the protein and carbohydrates content in sewage sludge. Evaluation of the different methods will be based on statistical criteria (linearity, sensitivity, accuracy, rightness and specificity). The N-content method will be tested in order to conclude about its pertinence.

1. Material and methods

1.1. Selected methods for proteins and carbohydrates content determination

Protein content: the chosen colorimetric methods were the Lowry method (Lowry *et al.*, 1951), the modified Lowry method (Frølund *et al.*, 1996) and the BCA method (Smith *et al.*, 1985). Additionally the N-content method will be also used for comparison, considering different methodologies to calculate the N content.

The Lowry and the modified Lowry methods are described with a linearity ranged from 0 to $mg_{BSA}.L^{-1}$. The BCA method was performed with the kit Thermo Scientific Pierce BCA Protein Assay, where the linearity goes from 0 to 2000 $mg_{BSA}.L^{-1}$. The sample volumes were 0.5 and 0.1 mL for the Lowry and the BCA methods respectively. The standard calibration used was the BSA set from Thermo Scientific Sigma P0914, made from 0 to 2000 $mg_{BSA}.L^{-1}$. The absorbance was measured at 750 and 562 nm for the Lowry and the BCA method respectively.

The total kjehdahl nitrogen (TKN) and ammonia nitrogen contents were measured by Buchi® AutoKjehdahl Unit K-370 after mineralization on Buchi® Digestion Unit k-435 (for TKN only). The organic nitrogen content was calculated by difference between TKN and ammonia nitrogen. Another type of practical measurement of total nitrogen (TN) content is by chimioluminesence with the TOC-VCCN from Shimadzu®. The total nitrogen is the sum of nitrates, nitrites, ammonium and organic nitrogen. Organic nitrogen is calculated by subtracting nitrogen oxides and ammonia from TN. Nitrogen oxides were measured with HACH LANGE® kits, (nitrites and nitrates). Protein content is estimated with the assumption that 16.5% (w/w) of proteins contains nitrogen (or 6.25 g proteins.g N^{-1}).

Carbohydrates content: the two colorimetric methods tested were the Dubois method (Dubois *et al.*, 1956) and the Anthrone method (Dreywood *et al.*, 1946). The standard calibration was made with glucose (Merck 1.08337.1000). Sample volume was 1mL for both methods and the absorbance was measured at 490nm for the Dubois and 625nm for the Anthrone method.

1.2. Lipids and Volatile fatty acids content measurement

Lipids were measured by a gravimetric method (APHA, 1995) using the Soxtec™, 2050, FOSS with hexane extraction (1h boiling + 2h rinsing) at 180°C.

Volatile Fatty Acid (VFA) concentrations were measured by gas chromatography (7890A Agilent), from acetate to heptanoate.

1.3. Statistical criteria

Five statistical criteria are defined to carry out the methods comparison:

Linearity: In all the methodologies for biochemical component content determination, a calibration curve, based on known amounts of model substrate, is performed. In our case, the model substrates were BSA and glucose. The curve linear regression is used to calculate the substrate content. The first statistical test is the linearity of the calibration curve and the linearity range.

Sensitivity: The slope of the linear regression defined the sensitivity of the calibration curve. Sensitivity increases with the slope.

Accuracy and rightness are obtained by the same statistical test on certified materials.

Accuracy: It is a dispersion measure calculated with the standard deviation between the real values of a model substrate and the content values measured with the evaluated method. A high accuracy is characterized by a low standard deviation.

Rightness: It is expressed in terms of the difference or error between the values measured with the evaluated method and the real value. In the current study this measurement was performed with six repetitions and by external calibration with the model substrates used for the linearity and sensitivity tests.

Specificity: It translates the applicability of the method to the measured component and revealed possible interferences of the measurement. The test is performed using the dosed addition methodology. It allows the evaluation of the matrix influence by adding known amounts of the targeted component in a defined matrix. In others words, a calibration curve is built in an equivalent environment. The obtained linear model can be compared to the linear model obtained for the model substrate in demineralised water. The parallelism of the linear curves indicates the interferences due to the matrix. Fisher and Student tests are performed to evaluate the similarity of both curves. The slopes of the both populations are compared by the Student test. Before conducting the Student test, the Fisher test has to verify that the residual variances of both populations are not homogenous in order to be comparable. The determination coefficient, R^2, of the obtained linear regression Y=a.X+b (Y the absorbance and X the concentration) is a simple indicator but it does not verify if the model is statistically pertinent. The statistical test used is the Fisher test. The ratio between two residual variances (Equation 1) should be lower than one determined value. The test is positive if Ftest < $Ftable_{\alpha}$ where α is the risk, generally taken at 5%. The hypothesis is therefore verified if two variances are closer at α%.

$$Ftest = \frac{\frac{(Y - Ycalc)^2 \, population_A}{N_A - (N_{max} - N_{min} - 1)}}{\frac{(Y - Ycalc)^2 \, population_B}{N_B - (N_{max} - N_{min} - 1)}} \qquad \text{Equation 1}$$

Where: Y: absorbance read from linear regression

Y_{calc}: absorbance calculated with the regression model (Y_{calc}=*a*.X+*b*)

N_A and N_B: numbers of individus of population A and B,

N_{max} and N_{min}: maximum and minimum of N_A and N_B

And the variance of population A is the higher. In the present case, N_{max} = 6 (calibration curve 0-100 mg.L-1) and N_{min} = 3 (dosed addition).

If the Fisher test is positive, the Student test (Equation 2) can be performed in order to compare the mean value observed with a defined value. In the present case, the objective is to compare the value of the slope of the calibration curve obtained by dosed addition with the slope value obtained by standard calibration curve. If the slopes are equal, curves are parallel and therefore no significant interference by the matrix exists.

$$t_{test} = \frac{|a_1 - a_2|}{\sqrt{s^2c\left[\frac{1}{\sum(x_{1i} - \overline{x_1})^2} + \frac{1}{\sum(x_{2i} - \overline{x_2})^2}\right]}}$$ Equation 2

Where: a_1 and a_2: slope of both populations

x_1 and x_2: biochemical component concentration values from both populations

$\overline{x_1}$ and $\overline{x_2}$:mean values.

For a degree of freedom of 2, the variance s²c is defined by the equation 3:

$$S^2c = \frac{\sum(Y_{1i} - \overline{Y_1})^2 + \sum(Y_{2i} - \overline{Y_2})^2}{(N_1 - 2) + (N_2 - 2)}$$ Equation 3

Where: Y_1 and Y_2: absorbance values for both populations 1 and 2

$\overline{Y_1}$ and $\overline{Y_2}$: mean values of the absorbance values for both populations 1 and 2

N_1 and N_2: individus numbers.

As for the Fisher test, if $t_{test} < t_{table}$ at α/2 % (2.5 % if α = 5 %) of risk, the hypothesis of equal slopes is confirmed.

Finally, the slope, *a*, and the origin ordinate, *b*, of the linear model for the dosed addition curve are calculated. With these two parameters, the corrected concentration Ce of the component is obtained by extrapolation as Ce = b/a.

1.4. Model Substrates and Sewage sludge samples

In order to evaluate the linearity and sensitivity of the compared colorimetric methods, the model substrates used for the calibration curves were Bovine Serum Albumin (BSA) for proteins and Glucose for carbohydrates. The analysis of the accuracy and rightness of the test required a more complex model substrate. In absence of a real certified reference substrate, a food complement "WHEY CREATINE COMPLEX" by EAFIT® (the dried sample presented a brown colour similar to sludge colour) was chosen as a reference sample. Its content in proteins (the aminogram was given), carbohydrates and lipids (Table 1) are certified. This product will be named "reference substrate". The aminogram allow the calculation of N-content in protein measured and a real comparison with N-content method can be made.

Table 39 : Composition of the « Whey Creatine Complex by EAFIT®" used as certified reference

Compound	*Molecules*	*mg compound/g dried product*
Proteins	-	703
Carbohydrates	Glucides (Monosaccharides)	46 (25)
	Inulin	53
	Others fibers	29
Lipids	-	33

Concerning the specificity test, dosed additions of model substrates (BSA and reference for proteins and glucose and cellulose for carbohydrates) have been performed in sewage sludge samples. Three increasing concentration additions have been performed, in triplicate, for the following concentrations: 25, 50 and 75 $mg.L^{-1}$. The protein content has been tested on a secondary sludge (high load) and the carbohydrate content on digested sludge (sludge age of 8 days) from the anaerobic digestion of the previous secondary sludge. The analyses have been performed on the total fraction of sewage sludge samples. The sludge was mixed by an ultrathurax before the dosed addition, in order to have homogeneous samples.

Sewage sludge samples were taken from several locations in a wastewater treatment plant in order to test the robustness and the application of the characterisation methods. Figure 1 presents the wastewater treatment plant and the sampling point.

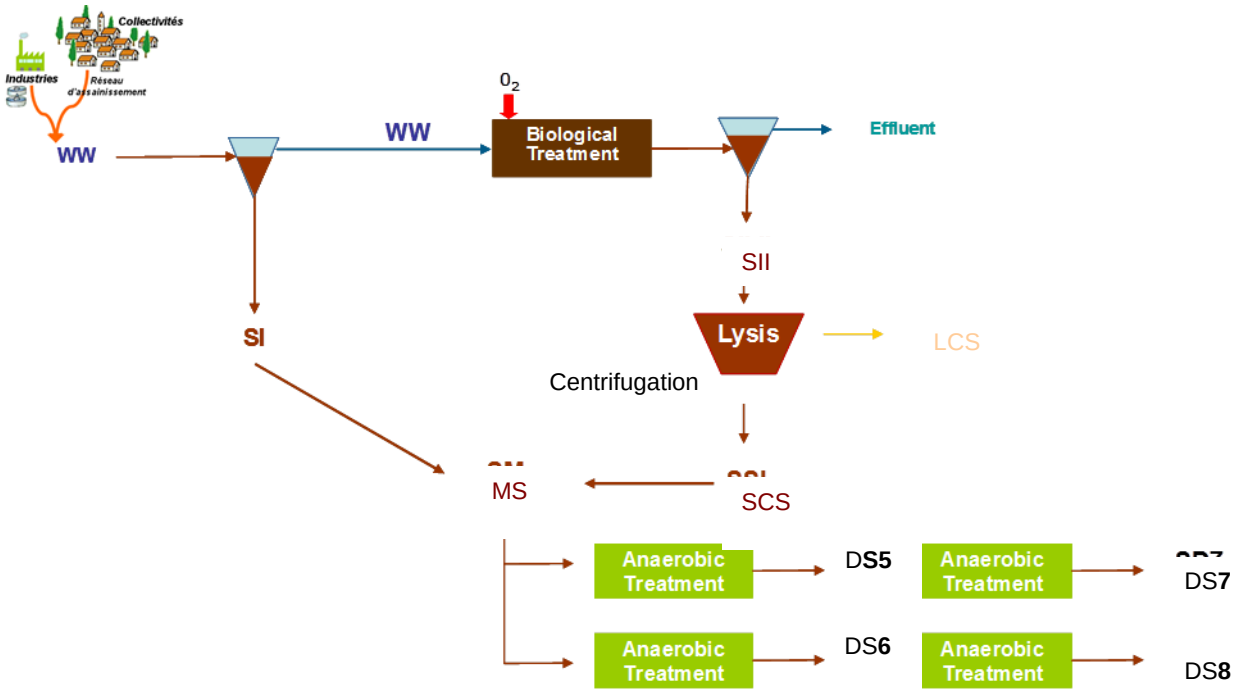

Figure 95 : Wastewater treatment plant providing sludge to analyse
SI: primary sludge (after primary settler)
SII: biological activated sludge
LCS: Supernatant (Liquid) from centrifuged sludge
SCS: solid from centrifuged sludge
MS: mix sludge (SI + SII)
DS 5 to 8: digested sludge

2. Results and discussion

2.1. Linearity and Sensitivity

The linearity and sensitivity criteria were tested on the colorimetric methods selected for comparison. Based on the calibration curve obtained with the substrate model (BSA for proteins and glucose for carbohydrates) a linear regression model was determined.

Figure 2a shows the calibration curve obtained with the Lowry method using BSA as substrate model for protein content determination. The Lowry method is linear between 0 and 100 mg $_{BSA}.L^{-1}$, as indicated in the literature. In order to test the linearity of Lowry method for BSA concentrations higher than 100 mg $_{BSA}.L^{-1}$, another calibration point at 250 mg $_{BSA}.L^{-1}$ has been introduced and impacted negatively the linearity of the Lowry method (lower regression coefficient. Figure 2a also shows the linearity of the BCA method in the range 0 and 100 mg $_{BSA}.L^{-1}$: the regression coefficient is lower than Lowry (0.93 against 0.99 for Lowry method). The linearity of the BCA method is maintained when the range is increased to 2000 mg $_{BSA}.L^{-1}$ (Figure 2b). It is important to notice the fact that the volume samples used in the Lowry method is five times higher than the volume used in the BCA method. The greater volume implies a more representative sample reducing the impact of dilution. The possibility of dilution reduces the negative impact of the smaller range

of linearity of the method. So, a compromise between dilution volume bringing also errors and sample volume has to be made.

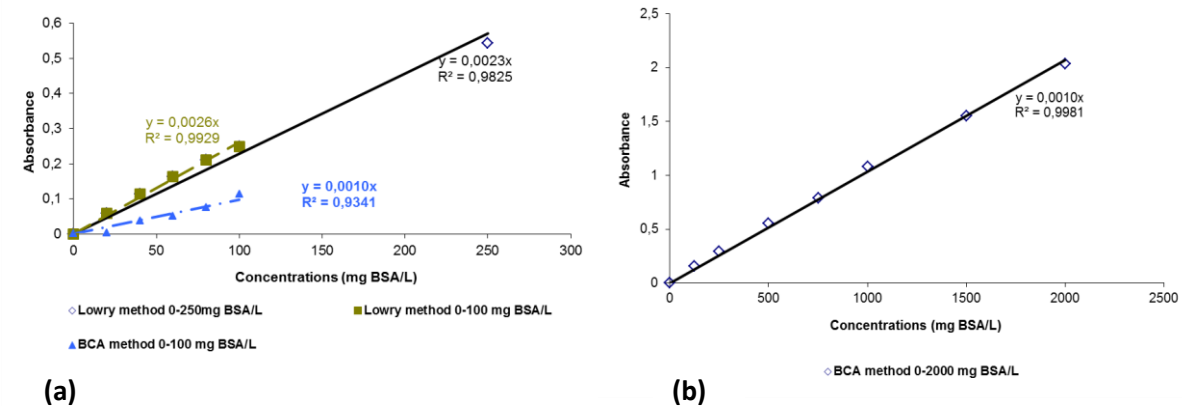

Figure 96 : Standard calibration curves obtained for (a) BCA and Lowry method in range from 0 to 100 mg BSA/L (b) BCA in a range from 0 to 2000 mg BSA/L

Concerning the sensitivity of both methods, a higher slope was observed for the Lowry method (0.0026 versus 0.0010 *Absorbance unit/mg* $_{BSA}$*.L*$^{-1}$ for the BCA method). The Lowry method showed a higher sensitivity.

Figure 3 presents the calibration curves for the Anthrone and the Dubois methods for carbohydrates determination. The same linearity was observed with both methods in the range 0 to 100 mg glucose.L^{-1}. The slope of the linear model obtained for the Anthrone method is higher than the one obtained for the Dubois method (0.0187 versus 0.0100 *Absorbance unit/mg* $_{glucose}$*.L*$^{-1}$). Therefore, the Anthrone method is more sensitive.

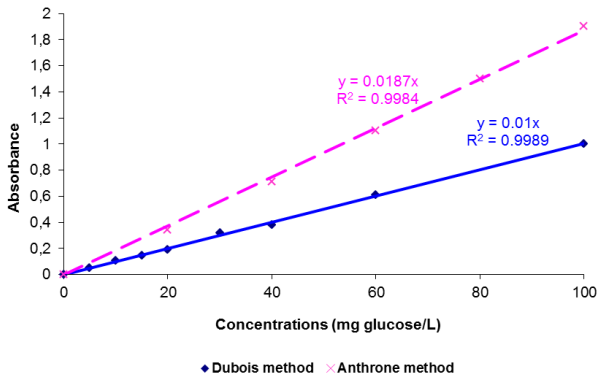

Figure 97 : Standard calibration curves obtained for Dubois and Anthrone methods in a range from 0 to 100 mg glucose/L

2.2. Accuracy and rightness

Accuracy and rightness were determined upon the reference substrate, using an external calibration. The obtained results for the characterisation methods of proteins are summarized in table 2. In all cases, variation coefficients are below 10%, indicating a good accuracy of the methods.

Table 40 : Accuracy and rightness tests: comparison of the characterisation methods with a reference value of protein concentration.

	Reference	Lowry	Modified Lowry	BCA	Organic nitrogen Kjedahl-N	Organic nitrogen Chemioluminescence
Concentration ($mg.g^{-1}$)	703	679	599	728	805	741
Standard Deviation ($mg.g^{-1}$)	-	47	54	22	16	22
Error (%) /reference	-	-3	-15	4	15	5

The modified Lowry method was the less accurate with a maximal standard deviation of 9 %. In terms of rightness, the best results were obtained for the classical Lowry and the BCA methods with less than 4 % error between the reference value and the measured data. The modified Lowry and the Kjehdahl-N methods presented the worst results with errors values around 15 %. The modified Lowry method underestimates the real value due to the correction introduced in the Lowry method (Frolund et al., 1996). The correction is performed by subtracting the supposed humic acid content (consider as an interference molecule) in the sample. In the current case, the methodology gave a concentration for the humic acid substances although the used reference did not contain this kind of molecules. The method is therefore not adapted for the reference.

Both N-content methods (Kjehdahl-N and chimioluminescence) overestimate, with an error of 5%, the concentration of the reference substrate. This was obtained with the hypothesis made on the protein/nitrogen ratio of 6.25 g protein.g N^{-1}. In addition, based on the aminoacids composition of the reference substrate, the actual ratio was calculated to be 8.8 g protein.g N^{-1} (a significant error of 35 %). Considering this new ratio, the values obtained for protein concentration would be 1133 and 1043 $mg.g^{-1}$ for the Kjehdahl-N and the chimioluminescence methods respectively. It means an increase of the overestimation to levels where the relative errors are 61% and 33% respectively.

The first conclusions are that with the calculated protein/nitrogen ratio, based on the aminogram, of 8.8 protein.g N^{-1} the N-content methods are not applicable in this case due to a very poor rightness. For the same reason, the modified Lowry method is also not applicable.Therefore, these three methods will not be tested for the others criteria.

The results of the accuracy and rightness tests for the evaluated methods to quantify the carbohydrates content are summarized in table 3. In terms of accuracy, both methods, Anthrone and Dubois, present low standard deviations (variation coefficients between 2 and 4%).

Table 41 : Accuracy and rightness tests: comparison of the characterisation methods with a reference value of carbohydrate concentration.

	Reference				
	Total carbohydrates	Partial Carbohydrates ***Inulin + glucides***	Partial Carbohydrates ***Others Fibers***	**Dubois**	**Anthrone**
Concentration (mg.g^{-1})	124	95	29	114	92
Standard Deviation (mg.g^{-1})	-	-	-	4,6	1,8
Error (%) /reference	-	-	-	-8	-26

The carbohydrates content of the reference substrate is the sum of simple glucides, inulin (monosaccharide polymer) and other fibers. Concerning the rightness, the concentrations determined by both methods are lower than the reference value. The observed errors were 8 % for the Dubois method and 26 % for the Anthrone method. The Anthrone method seems to dose a less exhaustive panel of sugars. Considering only the fraction of the carbohydrates constituted by the inulin and the glucides, the rightness of the Anthrone method increases significantly (1% error). So, it seems that Anthrone method do not hydrolyse the other fibers constituted of longer oses chains or under crystalline configuration. Similar observation was made by others authors who found an underestimation of the carbohydrates content by the Anthrone method (Frølund *et al.*, 1996; Brown and Lester, 1980).

2.3. Specificity comparison

In order to evaluate the different methods as regard the specificity criteria, dosed addition of simple and complex molecules were carried out.

For the methods aiming at the protein content determination, additions of BSA and reference substrate were performed on secondary sludge. In the case of methods determining carbohydrates content, glucose and cellulose were added on digested sludge.

Figure 4 shows the values obtained for protein content after addition of BSA and reference substrate in demineralised water (standard curve calibration) and secondary sludge (dosed addition calibration curve) using the Lowry (Figure 4a and 4b) and the BCA (Figure 4c and 4d) methods. Table 4 presents the sludge protein concentration calculated using the calibration curve and both linear regression curves obtained with BSA and reference substrate addition for both the BCA and the Lowry methods. Compared to the calibration curve, the BSA dosed addition regression curve is more accurate for the Lowry method than for the BCA method (relative errors are 5% and 11% respectively). In the case of the reference substrate dosage regression, the errors compared to the calibration curve are higher: 33% for the Lowry and 47% for the BCA method. One reason is the difficulty observed to dissolve the reference substrate in the sludge matrix.

Table 42 : Protein concentration of sludge sample obtained by two methods: calibration curve and dosed addition of BSA and reference regression model

Methodologies	**Lowry**		**BCA**	
Substrate Added	BSA	Reference	BSA	Reference
Calibration curve ($g.L^{-1}$)	20	21	18	19
Dosed addition ($g.L^{-1}$)	19	14	16	10
Relative error (%)	5	33	11	47

The specificity of each method was verified by conducting the Fisher and the Student tests (Table 5) on the results reported in Figure 4. The objective was to compare the slopes between the dosed addition curve and the calibration curve. The first step is to verify, through the Fisher test, if the residual variances are not significantly different at 5% (confidence level). A significant difference was observed for the addition of BSA in the BCA method. Therefore the student test cannot be conducted in that case. No significant differences were observed for the Lowry method.

Table 43 : Fisher and Student tests results for the comparison of proteins determination methods: Lowry and BCA

Fisher		F_{test}	$F_{table(\alpha=0.05)}$	Conclusion	Student		t_{test}	$t_{table(\alpha=0.05)}$	Conclusion
BSA	Lowry	1,57	240.50	$F_{test}<F_{table}$	BSA	Lowry	0.07	2.228	$-t_{table}<t_{test}<t_{table}$
	BCA	16,56	5.12	$F_{test}>F_{table}$		BCA	-	-	-
Reference	Lowry	78.22	240.50	$F_{test}<F_{table}$	Reference	Lowry	0.23	2.228	$-t_{table}<t_{test}<t_{table}$
	BCA	1.28	5.12	$F_{test}<F_{table}$		BCA	2.09	2.228	$-t_{table}<t_{test}<t_{table}$

According to the Student test results, for the Lowry method, the positive test shows that both linear regression curves are parallel (equal slopes) for BSA and reference substrate addition. Although the reference substrate addition seems to be accurately measured by the BCA method, the observed high relative error in the sludge protein concentration recovery is too important for this method.

Therefore the results are not reliable. Moreover, the Lowry method is the most specific, sensitive and accurate method. For that reason it is recommended to determine the protein concentration in the evaluate sludge matrix.

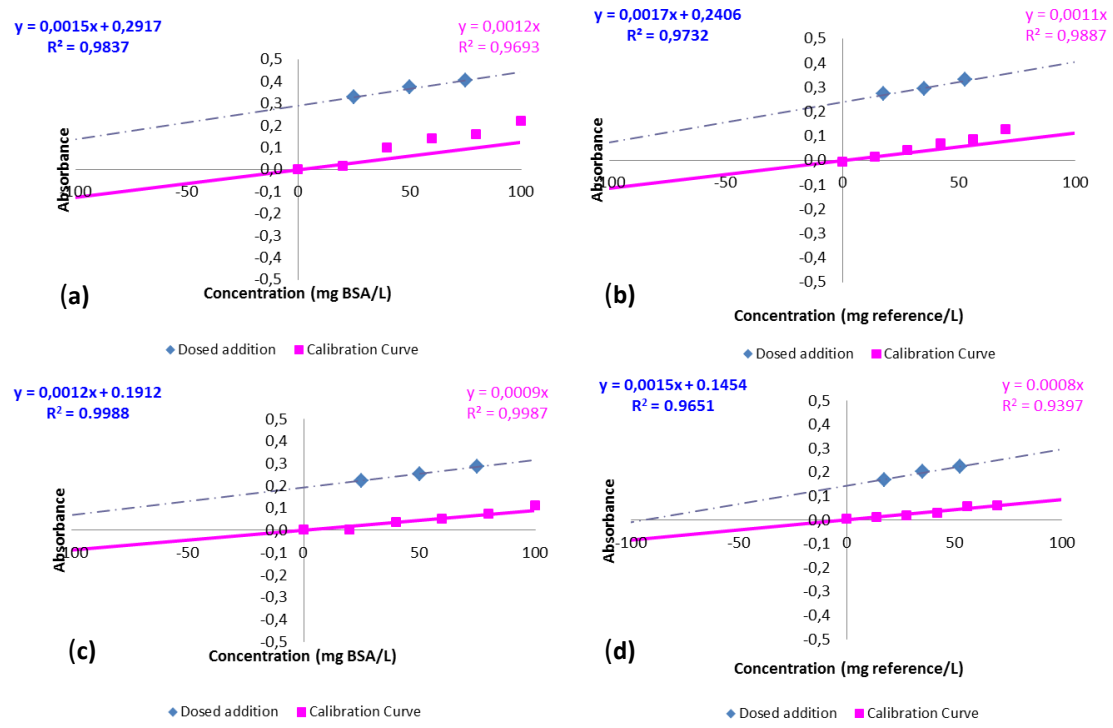

Figure 98 : Specificity test on protein determination: dosed addition and calibration curves regression model (a) Lowry method for BSA added (b) Lowry method for certified reference substrate added; (c) BCA method for BSA added; (d) BCA method for certified reference substrate added.

Concerning the specificity test on the methods for carbohydrates content determination, Figure 5 shows the results obtained after addition of glucose and cellulose in demineralised water (standard curve calibration) and digested sludge (dosed addition calibration curve) using the Dubois (Figures 5a and 5b) and the Anthrone method (Figures 5c and 5d). Table 6 summarizes the results obtained from the graphs in Figure 5. Due to the low concentrations, the relative errors are more important than in the case of protein content determination (ranged from 9 to 39%).

However, the concentrations of glucose and cellulose measured by the Anthrone method seem to show a better recovery of these components. It is important to notice that it was difficult to have a good homogeneous addition of cellulose in the sludge matrix.

Table 44 : Carbohydrates concentration of sludge sample obtained by two methods: calibration curve and dosed addition of glucose and cellulose regression model

Methodologies	**Dubois**		**Anthrone**	
Substrate Added	Glucose	Cellulose	Glucose	Cellulose
Calibration curve ($g.L^{-1}$)	3.8	3.1	1.8	1.6
Dosed addition ($g.L^{-1}$)	2.3	3.6	1.9	1,3
Relative error (%)	39	16	9	21

The obtained Fisher test results are reported in table 7. Variances from the Dubois method have no significant difference, whereas the Anthrone method failed the test for glucose addition. The Student test reveals that the Dubois method has no interference since the test passed for both glucose and cellulose. In the case of the Anthrone method, the assay was positive for cellulose.

Table 45 : Fisher and Student tests results for the comparison of carbohydrates determination methods: Anthrone and Dubois

Fisher		**F_{test}**	**$F_{table(\alpha=0.05)}$**	**Conclusion**	**Student**	**t_{test}**	**$t_{table(\alpha=0.05)}$**	**Conclusion**
Glucose	**Dubois**	4.87	7.71	$F_{test}<F_{table}$	**Dubois**	0.87	12.80	$-t_{table}<t_{test}<t_{table}$
	Anthrone	8.95	7.71	$F_{test}>F_{table}$	**Anthrone**			

As previously mentioned, the Anthrone method is the most sensitive and shows better recovery of carbohydrates during the dosed addition, but the Dubois method has a better rightness and specificity, therefore less interferences in the measurement. The Dubois method is therefore recommended for the considered sludge matrix.

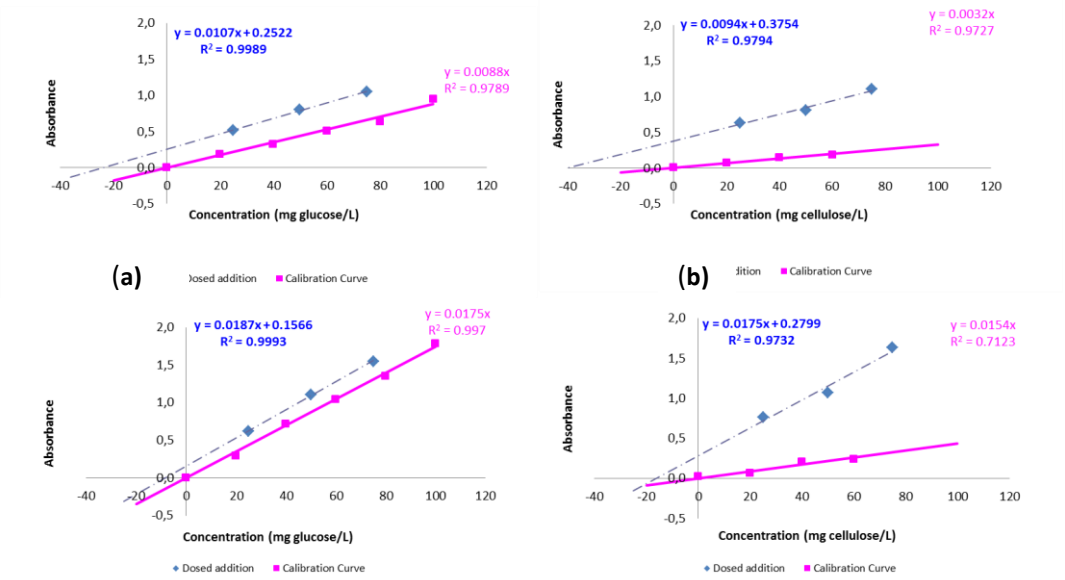

Figure 5 (c) ificity test on carbohydrates determination: (d) addition and calibration curves regression model (a) Dubois method for glucose addition; (b) Dubois method for cellulose addition; (c) Anthrone method for glucose addition; (d) Anthrone method for cellulose addition

2.4. Organic matter recovery

A validation of the selected characterisation methodologies (the Lowry and the Dubois methods) was carried out on several sludge samples obtained from different locations of the WWTP. The objective is to obtain the maximum organic matter recovery and its biochemical distribution for each kind of sludge.

Figure 6 presents the characterisation of the organic matter of the sludge samples based on the selected four biochemical families (proteins, carbohydrates, lipids and VFA) and express as percentage of volatile solids (VS). In average, these biochemical families represent 80 ± 7 % of the VS. The remaining non-characterized organic matter could be humic, fulvic and nucleic acid compounds, or detergents compounds as mentioned by Huang *et al.* (2010). Proteins and carbohydrates are the main components representing on average 69 ± 3% VS. As expected, primary sludge is mainly composed of carbohydrates (due to the presence of fibers). Biological sludge, SII and DS, are on average composed of 50% proteins and only 20% carbohydrates, which is coherent with the literature (Elefsionotis *et al.*, 1994, Mottet *et al.*, 2010). The mixed sludge, MS, of primary sludge and solid fraction of centrifuged sludge has similar percentages of proteins and carbohydrates. Therefore, the selected methods to characterise organic matter showed to be pertinent for sewage sludge analysis with a good recovery of the volatile matter.

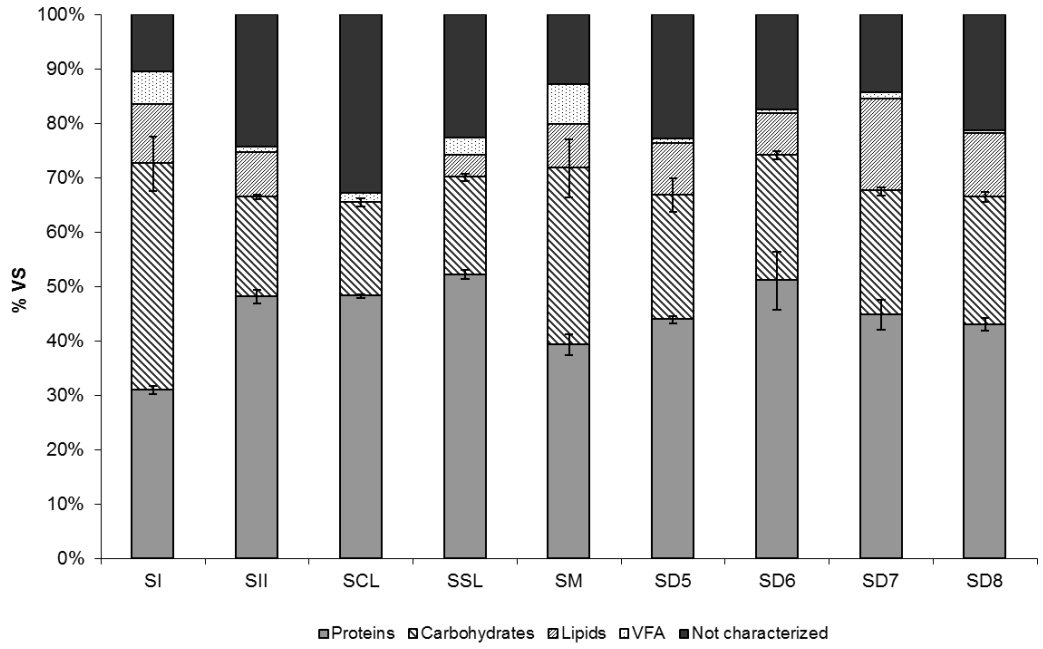

Figure 6 : Organic matter distribution as function of the volatile solid

3. Conclusions and guidelines

Table 8 summarizes the results obtained in the current study. Overall, taking into consideration all the statistical parameters, the Lowry and the Dubois methods are the best compromise to quantify proteins and carbohydrates respectively in sewage sludge samples.

The Lowry method showed better linearity, sensitivity and rightness than the BCA method and the others evaluated methods (modified Lowry and N-content methods). Moreover, the Lowry method has no interference with the considered matrix and in practical terms it is a good compromise between time consuming and reagents risk.

For carbohydrates, in the studied conditions, the Dubois method appears to be the most adequate. It shows better results in terms of rightness and specificity than the Anthrone method, although Anthrone method was more sensitive.

However, it is of key importance to point out that the statistical specificity comparison has been conducted in a specific sludge matrix. Therefore, in order to select the more adequate characterisation method for other type of substrates, the specificity test (dosed addition) should be conducted again on that matrix.

The colorimetric methods present the advantage of the easy application and facility of transport. But obviously they present limitations in terms of detailed characterisation compared to other technologies based

on molecular analysis. However their performance has been proved in the current study with a very good characterisation of 80% of the organic matter.

4. Acknowledgements

The authors wish to thank Faten BELHADJ-KAABI and David BENANOU from VEOLIA Environment Research and Innovation‘s analytical team for their support and their advice on this work.

Table 46 : Comparison summary of protein and carbohydrates dosage protocols

Methods	Reference sample				Dosed addition				Time/Practical character*	Dangerousness**
	Sensitivity and linearity, calibration regression model		Accuracy and rightness		Relative error compared with external calibration (%)		Specificity			
	Slope	R^2	Standard deviation (%)	Relative error / (%)	BSA/ Glucose	Reference/ Cellulose	BSA/ Glucose	Reference/ Cellulose		
Proteins										
Lowry	**0,0026**	**0,9929**	7	**3**	**5**	33	Positive test at 95%	Positive test at 95%	++	+
Modified Lowry	0,0026	0,9929	9	15					+	+
BCA	0,0010	0,9981	3	4	11	7	**Negative test at 95%**	Positive test at 95%	+++	+
TN content Shimazu®	*No calibration for these methods*		3	5					-	+
TN content Kjehdahl			2	15					--	-
Carbohydrates										
Dubois	0,0100	0,9989	4	**8**	39	16	Positive test at 95%	Positive test at 95%	+	--
Anthrone	**0,0187**	0,9984	2	26	**6**	**19**	**Negative test at 95%**	Positive test at 95%	+	--

*: qualitative comparison depending on time consuming and on practical character of the analysis: -- very negative, - negative, + positive, ++very positive, +++ extremely positive

**: qualitative comparison depending on reagent dangerousness: --: very dangerous, - dangerous, +: less dangerous

References

Angelidaki, I. and Sanders, W. (2004) Assessment of the anaerobic biodegradability of macropllutants. Reviews in Environmental Science and Bio/Technology 3, 117-129.

Batstone, D. J., Keller, J., Angelidaki, I., Kalyuzhnyi, S. V., Pavlostathis, S. G., Rozzi, A., Sanders, W. T. M., Siegrist, H., and Vavilin, V. A. (2002) Anaerobic Digestion Model No.1. (ADM1). IWA Scientific and Technical Report No. 13. IWA, ISBN:1-900222-78-7.

Bradford, M.M. (1976) A rapid and sensitive method for the quantitation of microgram quantities of protein utilizing the principle of protein-dye binding. *Analytical Biochemistry* **72** (1-2), 248-254.

Brown, L. and Lester, J. N. (1980) Comparison of bacterial extracellular polymer extraction methods. Applied and Environmental Microbiology 40[2], 179-185.

Comte, S., Guibaud, G., and Baudu, M. (2006) Relations between extraction protocols for activated sludge extracellular polymeric substances (EPS) and EPS complexation properties Part I. Comparison of the efficiency of eight EPS extraction methods. *Enzyme and Microbial Technology* **38** (1-2), 237-245.

D'Abzac, P., Bordas, F., Van Hullebusch, E., Lens, P.N.L., and Guibaud, G. (2010) Extraction of extracellular polymeric substances (EPS) from anaerobic granular sludges: comparison of chemical and physical extraction protocols. *Appl Microbiol Biotechnol* **85** (5), 1589-1599.

Dignac, M.F., Urbain, V., Rybacki, D., Bruchet, A., Snidaro, D., and Scribe, P. (1998) Chemical description of extracellular polymers: Implication on activated sludge floc structure. *Water Science and Technology* **38** (8-9 -9 pt 7), 45-53.

Dreywood, R. (1946) Qualitative Test for Carbohydrate Material. *Industrial & Engineering Chemistry Analytical Edition* **18** (8), 499.

Dubois, M., Gilles, K.A., Hamilton, J.K., Rebers, P.A., and Smith, F. (1956) Colorimetric method for determination of sugars and related substances. *Analytical Chemistry* **28** (3), 350-356.

Elefsiniotis, P. and Oldham, W.K. (1994) Influence of pH on the acid-phase anaerobic digestion of primary sludge. *Journal of Chemical Technology & Biotechnology* **60** (1), 89-96.

Elefsiniotis, P. and Oldham, W.K. (1994) Anaerobic acidogenesis of primary sludge: The role of solids retention time. *Biotechnology and Bioengineering* **44** (1), 7-13.

Feller, Christian, Jeanson, P., Giummelly, P., and Bonaly, P. (1991) Comparaison de différentes méthodes d'hydrolyse acide en vue du dosage des glucides totaux dans les sols.

Frölund, B., Palmgren, R., Keiding, K., and Nielsen, P.H. (1996) Extraction of extracellular polymers from activated sludge using a cation exchange resin. *Water Research* **30** (8), 1749-1758.

Greenfield, H., Southgate, D. A. T. (2003) Food composition data, Production, management and use. Second Edition. Food and Agriculture Organisation of United Nations, pp147.

Gornall, A. G., Bardawill, C. J., and David, M. M. (1949) Determination of serum proteins by means of the biuret reaction. Journal of Biochemical Chemistry 177, 751-766.

Huang,M.h., Li,Y.m., and Gu,G.w. (2010) Chemical composition of organic matters in domestic wastewater. *Desalination* **262** (1-3), 36-42.

Ji, Z., Chen, G., and Chen, Y. (2010) Effects of waste activated sludge and surfactant addition on primary sludge hydrolysis and short-chain fatty acids accumulation. *Bioresource Technology* **101** (10), 3457-3462.

Kjeldahl, J. (1883) A new method for the determination of nitrogen in organic matter. Z.Anal.Chem. 22-366.

Liu, H. and Fang, H.H.P. (2002) Extraction of extracellular polymeric substances (EPS) of sludges. *Journal of Biotechnology* **95** (3), 249-256.

Lesteur,M., Latrille,E., Maurel,V.B., Roger,J.M., Gonzalez,C., Junqua,G., and Steyer,J.P. (2011) First step towards a fast analytical method for the determination of Biochemical Methane Potential of solid wastes by near infrared spectroscopy. *Bioresource Technology* **102** (3), 2280-2288.

Lowry, O.H., Rosebrough, N.J., Farr, A.L., and Randall, R.J. (1951) Protein measurement with the Folin phenol reagent. *The Journal of biological chemistry* **193** (1), 265-275.

Malamis, S. and Andreadakis, A. (2009) Fractionation of proteins and carbohydrates of extracellular polymeric substances in a membrane bioreactor system. *Bioresource Technology* **100** (13), 3350-3357.

Massé, A. (2004) Immersed membrane bioreactor for the municipal wastewater treatment: biological environment physico-chemical specificities and fouling. PhD thesis LIPE.

Mottet, A., François, E., Latrille, E., Steyer, J.P., Déléris, S., Vedrenne, F., and Carrère, H. (2010) Estimating anaerobic biodegradability indicators for waste activated sludge. *Chemical Engineering Journal* **160** (2), 488-496.

Nielsen, P. H., Thomsen, T. R., and Nielsen, J. L. (2004) Bacterial composition of activated sludge-importance for floc and sludge properties. Water Science and Technology 49[10], 51-58.

Novak, J.T., Sadler, M.E., and Murthy, S.N. (2003) Mechanisms of floc destruction during anaerobic and aerobic digestion and the effect on conditioning and dewatering of biosolids. *Water Research* **37** (13), 3136-3144.

Piccolo,A., Zena,A., and Conte,P. (1996) A comparison of acid hydrolyses for the determination of carbohydrate content in soils. *Communications in Soil Science and Plant Analysis* **27** (15-17), 2909-2915.

Prahl, S. (2012) http://omlc.ogi.edu/spectra/PhotochemCAD/html/072.html

Ras, M., Girbal-Neuhauser, E., Paul, E., Sperandio, M., and Lefebvre, D. (2008) Protein extraction from activated sludge: An analytical approach. *Water Research* **42** (8-9), 1867-1878.

Raunkjaer, K., Hvitved-Jacobsen, T., and Nielsen, P.H. (1994) Measurement of pools of protein, carbohydrate and lipid in domestic wastewater. *Water Research* **28** (2), 251-262.

Smith, P.K., Krohn, R.I., Hermanson, G.T., Mallia, A.K., Gartner, F.H., Provenzano, M.D., Fujimoto, E.K., Goeke, N.M., Olson, B.J., and Klenk, D.C. (1985) Measurement of protein using bicinchoninic acid. *Analytical Biochemistry* **150** (1), 76-85.

Wang, Z., Wu, Z., and Tang, S. (2009) Characterization of dissolved organic matter in a submerged membrane bioreactor by using three-dimensional excitation and emission matrix fluorescence spectroscopy. *Water Research* **43** (6), 1533-1540.

Wang, Z., Tang, S., Zhu, Y., Wu, Z., Zhou, Q., and Yang, D. (2010) Fluorescent dissolved organic matter variations in a submerged membrane bioreactor under different sludge retention times. *Journal of Membrane Science* **355** (1-2), 151-157.

Wilson, C.A. and Novak, J.T. (2009) Hydrolysis of macromolecular components of primary and secondary wastewater sludge by thermal hydrolytic pretreatment. *Water Research* **43** (18), 4489-4498.

Annex 2: ADM1 and modified ADM1 (Mottet, 2009) Petersen matrix

- ADM1 (Batstone et al., 2002): Biochemical rate coefficients (ν_i) and kinetic rate equations (ρ_i) for soluble components (i=1-12, j=1-19)

Component → i		1	2	3	4	5	6	7	8	9	10	11	12	Rate (ρ_j, kg COD.m^{-3}.d^{-1})
j	Process ↓	S_{su}	S_{aa}	S_{fa}	S_{va}	S_{bu}	S_{pro}	S_{ac}	S_{h2}	S_{ch4}	S_{IC}	S_{IN}	S_I	
1	Disintegration												$f_{sI,xc}$	$k_{dis} \cdot X_c$
2	Hydrolysis Carbohydrates	1												$k_{hyd,ch} \cdot X_{ch}$
3	Hydrolysis of Proteins		1											$k_{hyd,pr} \cdot X_{pr}$
4	Hydrolysis of Lipids	$1-f_{fa,li}$		$f_{fa,li}$										$k_{hyd,li} \cdot X_{li}$
5	Uptake of Sugars	-1				$(1-Y_{su}) \cdot f_{bu,su}$	$(1-Y_{su}) \cdot f_{pro,su}$	$(1-Y_{su}) \cdot f_{ac,su}$	$(1-Y_{su}) \cdot f_{h2,su}$		$-\sum_{i=1-9,11-24} C_i \nu_{i,5}$	$-(Y_{su}) \cdot N_{bac}$		$k_{m,su} \cdot \frac{S_{su}}{K_S + S} \cdot X_{su} \cdot I_1$
6	Uptake of Amino Acids		-1		$(1-Y_{aa}) \cdot f_{va,aa}$	$(1-Y_{aa}) \cdot f_{bu,aa}$	$(1-Y_{aa}) \cdot f_{pro,aa}$	$(1-Y_{aa}) \cdot f_{ac,aa}$	$(1-Y_{aa}) \cdot f_{h2,aa}$		$-\sum_{i=1-9,11-24} C_i \nu_{i,6}$	$N_{aa} - (Y_{aa}) \cdot N_{bac}$		$k_{m,aa} \cdot \frac{S_{aa}}{K_S + S_{aa}} \cdot X_{aa} I_1$
7	Uptake of LCFA			-1				$(1-Y_{fa}) \cdot 0.7$	$(1-Y_{fa}) \cdot 0.3$			$-(Y_{fa}) \cdot N_{bac}$		$k_{m,fa} \cdot \frac{S_{fa}}{K_S + S_{fa}} \cdot X_{fa} \cdot I_2$
8	Uptake of Valerate				-1		$(1-Y_{c4}) \cdot 0.54$	$(1-Y_{c4}) \cdot 0.31$	$(1-Y_{c4}) \cdot 0.15$			$-(Y_{c4}) \cdot N_{bac}$		$k_{m,c4} \cdot \frac{S_{va}}{K_S + S_{va}} \cdot X_{c4} \cdot \frac{1}{1+S_{bu}/S_{va}} \cdot I_2$
9	Uptake of Butyrate					-1		$(1-Y_{c4}) \cdot 0.8$	$(1-Y_{c4}) \cdot 0.2$			$-(Y_{c4}) \cdot N_{bac}$		$k_{m,c4} \cdot \frac{S_{bu}}{K_S + S_{bu}} \cdot X_{c4} \cdot \frac{1}{1+S_{va}/S_{bu}} \cdot I_2$
10	Uptake of Propionate						-1	$(1-Y_{pro}) \cdot 0.57$	$(1-Y_{pro}) \cdot 0.43$		$-\sum_{i=1-9,11-24} C_i \nu_{i,10}$	$-(Y_{pro}) \cdot N_{bac}$		$k_{m,pr} \cdot \frac{S_{pro}}{K_S + S_{pro}} \cdot X_{pro} \cdot I_2$
11	Uptake of Acetate							-1		$(1-Y_{ac})$	$-\sum_{i=1-9,11-24} C_i \nu_{i,11}$	$-(Y_{ac}) \cdot N_{bac}$		$k_{m,ac} \cdot \frac{S_{ac}}{K_S + S_{ac}} \cdot X_{ac} \cdot I_3$
12	Uptake of Hydrogen								-1	$(1-Y_{h2})$	$-\sum_{i=1-9,11-24} C_i \nu_{i,12}$	$-(Y_{h2}) \cdot N_{bac}$		$k_{m,h2} \cdot \frac{S_{h2}}{K_S + S_{h2}} \cdot X_{h2} \cdot I_1$
13	Decay of X_{su}													$k_{dec,Xsu} \cdot X_{su}$
14	Decay of X_{aa}													$k_{dec,Xaa} \cdot X_{aa}$
15	Decay of X_{fa}													$k_{dec,Xfa} \cdot X_{fa}$
16	Decay of X_{C4}													$k_{dec,Xc4} \cdot X_{c4}$
17	Decay of X_{pro}													$k_{dec,Xpro} \cdot X_{pro}$
18	Decay of X_{ac}													$k_{dec,Xac} \cdot X_{ac}$
19	Decay of X_{h2}													$k_{dec,Xh2} \cdot X_{h2}$
		Monosaccharides (kg COD·m^{-3})	Amino Acids (kg COD·m^{-3})	Long chain fatty acids (kg COD·m^{-3})	Total valerate (kg COD·m^{-3})	Total butyrate (kg COD·m^{-3})	Total propionate (kg COD·m^{-3})	Total acetate (kg COD·m^{-3})	Hydrogen gas (kg COD·m^{-3})	Methane gas (kg COD·m^{-3})	Inorganic Carbon (kg-mole C·m^{-3})	Inorganic nitrogen (kg-mole N·m^{-3})	Soluble inerts (kg COD·m^{-3})	Inhibition factors (3.7): $I_1 = I_{pH} \cdot I_{IN,lim}$ $I_2 = I_{pH} \cdot I_{IN,lim} \cdot I_{h_2}$ $I_3 = I_{pH} \cdot I_{IN,lim} \cdot I_{NH3,Xac}$

- ADM1 (Batstone et al., 2002): Biochemical rate coefficients (ν_i) and kinetic rate equations (ρ_i) for particulate components (i=13-24, j=1-19)

Component → i		13	14	15	16	17	18	19	20	21	22	23	24	
j	Process ↓	X_c	X_{ch}	X_{pr}	X_{li}	X_{su}	X_{aa}	X_{fa}	X_{c4}	X_{pro}	X_{ac}	X_{h2}	X_I	Rate (ρ_j, kg COD.m^{-3}.d^{-1})
1	Disintegration	-1	$f_{ch,xc}$	$f_{pr,xc}$	$f_{li,xc}$								$f_{xI,xc}$	$k_{dis} \cdot X_c$
2	Hydrolysis Carbohydrates		-1											$k_{hyd,ch} \cdot X_{ch}$
3	Hydrolysis of Proteins			-1										$k_{hyd,pr} \cdot X_{pr}$
4	Hydrolysis of Lipids				-1									$k_{hyd,li} \cdot X_{li}$
5	Uptake of Sugars					Y_{su}								$k_{m,su} \cdot \frac{S_{su}}{K_S + S} \cdot X_{su} \cdot I_1$
6	Uptake of Amino Acids						Y_{aa}							$k_{m,aa} \cdot \frac{S_{aa}}{K_S + S_{aa}} \cdot X_{aa} I_1$
7	Uptake of LCFA							Y_{fa}						$k_{m,fa} \cdot \frac{S_{fa}}{K_S + S_{fa}} \cdot X_{fa} \cdot I_2$
8	Uptake of Valerate								Y_{c4}					$k_{m,c4} \cdot \frac{S_{va}}{K_S + S_{va}} \cdot X_{c4} \cdot \frac{1}{1+S_{bu}/S_{va}} \cdot I_2$
9	Uptake of Butyrate								Y_{c4}					$k_{m,c4} \cdot \frac{S_{bu}}{K_S + S_{bu}} \cdot X_{c4} \cdot \frac{1}{1+S_{va}/S_{bu}} \cdot I_2$
10	Uptake of Propionate									Y_{pro}				$k_{m,pr} \cdot \frac{S_{pro}}{K_S + S_{pro}} \cdot X_{pro} \cdot I_2$
11	Uptake of Acetate										Y_{ac}			$k_{m,ac} \cdot \frac{S_{ac}}{K_S + S_{ac}} \cdot X_{ac} \cdot I_3$
12	Uptake of Hydrogen											Y_{h2}		$k_{m,h2} \cdot \frac{S_{h2}}{K_S + S_{h2}} \cdot X_{h2} \cdot I_1$
13	Decay of X_{su}	1				-1								$k_{dec,Xsu} \cdot X_{su}$
14	Decay of X_{aa}	1					-1							$k_{dec,Xaa} \cdot X_{aa}$
15	Decay of X_{fa}	1						-1						$k_{dec,Xfa} \cdot X_{fa}$
16	Decay of X_{c4}	1							-1					$k_{dec,Xc4} \cdot X_{c4}$
17	Decay of X_{pro}	1								-1				$k_{dec,Xpro} \cdot X_{pro}$
18	Decay of X_{ac}	1									-1			$k_{dec,Xac} \cdot X_{ac}$
19	Decay of X_{h2}	1										-1		$k_{dec,Xh2} \cdot X_{h2}$
		Composites (kg COD·m^{-3})	Carbohydrates (kg COD·m^{-3})	Proteins (kg COD·m^{-3})	Lipids (kg COD·m^{-3})	Sugar degraders (kg COD·m^{-3})	Amino acid degraders (kg COD·m^{-3})	LCFA degraders k(g COD·m^{-3})	Valerate and butyrate degraders (kg COD·m^{-3})	Propionate degraders (kg COD·m^{-3})	Acetate degraders (kg COD·m^{-3})	Hydrogen degraders (kg COD·m^{-3})	Particulate inerts (kg COD·m^{-3})	Inhibition factors (3.7): $I_1 = I_{pH} \cdot I_{IN,lim}$ $I_2 = I_{pH} \cdot I_{IN,lim} \cdot I_{h_2}$ $I_3 = I_{pH} \cdot I_{IN,lim} \cdot I_{NH3,Xac}$

- Modified ADM1 model (Mottet, 2009): Petersen matrix modified for particulate compounds (i=13-17, 25-30, j=1-5, 21-25)

Component		i	1	2	3	12	Rate (ρ_j, $kg_{COD}.m^{-3}.d^{-1}$)
j	**Process**		Ssu	Saa	Sfa	S_I	
1	Disintegration of X_{cr}					$(1\text{-}Y_{Xcr})*f_{sI,Xcr}$	$k_{m,Xcr}\frac{X_{cr}}{K_{S,Xcr}X_{Xcr}+X_{cr}}X_{Xcr}$
2	Disintegration of X_{cs}					$(1\text{-}Y_{Xcs})*f_{sI,Xcs}$	$k_{m,Xcs}\frac{X_{cs}}{K_{S,Xcs}X_{Xcs}+X_{cs}}X_{Xcs}$
3	Hydrolysis Carbohydrates		$1\text{-}Y_{ch}$				$k_{m,ch}\frac{X_{ch}}{K_{S,ch}X_{Xch}+X_{ch}}X_{Xch}$
4	Hydrolysis of Proteins			$1\text{-}Y_{pr}$			$k_{m,pr}\frac{X_{pr}}{K_{S,pr}X_{Xpr}+X_{pr}}X_{Xpr}$
5	Hydrolysis of Lipids		$(1\text{-}Y_{li})*(1\text{-}f_{fa,li})$		$(1\text{-}Y_{li})*f_{fa,li}$		$k_{m,li}\frac{X_{li}}{K_{S,li}X_{Xli}+X_{li}}X_{Xli}$
			Monosaccharides ($kg_{COD}.m^{-3}$)	Amino acids ($kg_{COD}.m^{-3}$)	Long chain fatty acids ($kg_{COD}.m^{-3}$)	Soluble inerts ($kg_{COD}.m^{-3}$)	

- Modified ADM1 model (Mottet, 2009): Petersen matrix modified for particulate compounds (i=13-17, 25-30, j=1-5, 21-25)

Component i		**13**	**14**	**15**	**16**	**17**	**25**	**26**	**27**	**28**	**29**	**30**	**Rate (ρ_j, $kg_{COD}.m^{-3}.d^{-1}$)**
j	**Process**	X_{cr}	X_{cs}	X_{ch}	X_{pr}	X_{li}	X_{Xcr}	X_{Xcs}	X_{Xch}	X_{Xpr}	X_{Xli}	X_I	
1	Disintegration of X_{cr}	-1	-1	$(1-Y_{Xcr})*f_{ch,Xcr}$	$(1-Y_{Xcr})*f_{pr,Xcr}$	$(1-Y_{Xcr})*f_{li,Xcr}$	Y_{Xcr}					$(1-Y_{Xcr})*f_{xI,Xcr}$	$k_{m,Xcr}\frac{X_{cr}}{K_{S,Xcr}X_{Xcr}+X_{cr}}X_{Xcr}$
2	Disintegration of X_{cs}	-1	-1	$(1-Y_{Xcs})*f_{ch,Xcs}$	$(1-Y_{Xcs})*f_{pr,Xcs}$	$(1-Y_{Xcs})*f_{li,Xcs}$		Y_{Xcs}				$(1-Y_{Xcs})*f_{xI,Xcs}$	$k_{m,Xcs}\frac{X_{cs}}{K_{S,Xcs}X_{Xcs}+X_{cs}}X_{Xcs}$
3	Hydrolysis Carbohydrates		-1	-1					Y_{ch}				$k_{m,ch}\frac{X_{ch}}{K_{S,ch}X_{Xch}+X_{ch}}X_{Xch}$
4	Hydrolysis of Proteins				-1					Y_{pr}			$k_{m,pr}\frac{X_{pr}}{K_{S,pr}X_{Xpr}+X_{pr}}X_{Xpr}$
5	Hydrolysis of Lipids					-1					Y_{li}		$k_{m,li}\frac{X_{li}}{K_{S,li}X_{Xli}+X_{li}}X_{Xli}$
21	Decay of X_{Xcr}	1					-1						$k_{dec,Xcr}X_{Xcr}$
22	Decay of X_{Xcs}	1						-1					$k_{dec,Xcs}X_{Xcs}$
23	Decay of X_{Xch}	1							-1				$k_{dec,ch}X_{Xch}$
24	Decay of X_{Xpr}	1								-1			$k_{dec,pr}X_{Xpr}$
25	Decay of X_{Xli}	1									-1		$k_{dec,li}X_{Xli}$
		Readily hydrolysable composites ($kg_{COD}.m^{-3}$)	Slowly hydrolysable composites ($kg_{COD}.m^{-3}$)	Carbohydrates ($kg_{COD}.m^{-3}$)	Proteins ($kg_{COD}.m^{-3}$)	Lipids ($kg_{COD}.m^{-3}$)	X_{Xcr} degraders ($kg_{COD}.m^{-3}$)	X_{Xcs} degraders ($kg_{COD}.m^{-3}$)	Carbohydrate degraders ($kg_{COD}.m^{-3}$)	Protein degraders ($kg_{COD}.m^{-3}$)	Lipid degraders ($kg_{COD}.m^{-3}$)	Particulate inerts ($kg_{COD}.m^{-3}$)	

Annex 3: PLS regression results for BD prediction with X-variables containing VFA percent of total COD

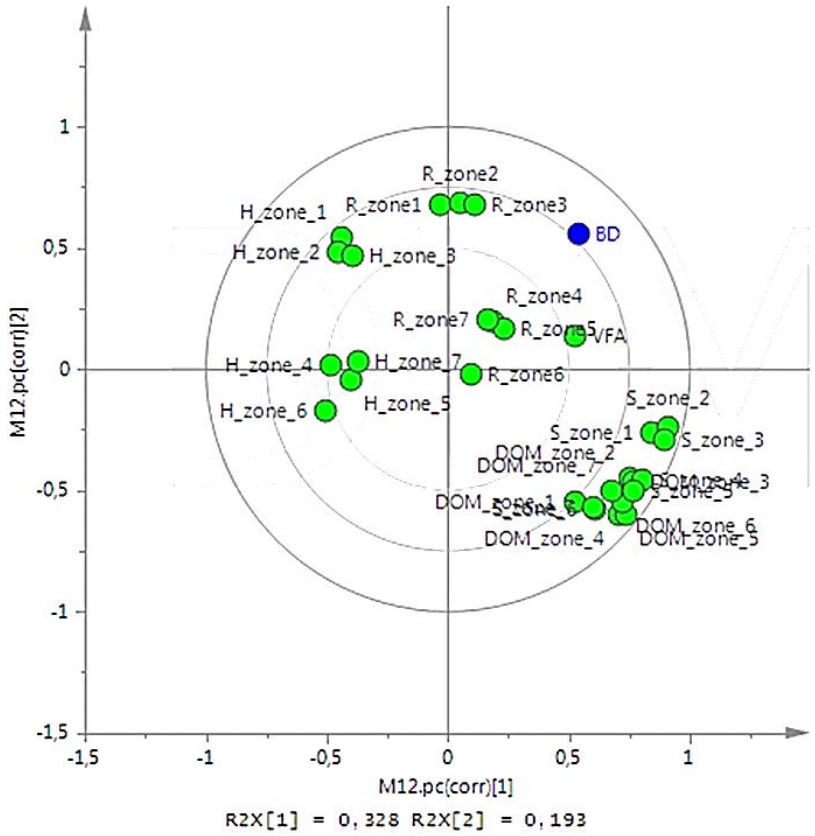

Figure A3.1 : Correlation circle obtained in the two first components in PLS regression of BD with VFA addition

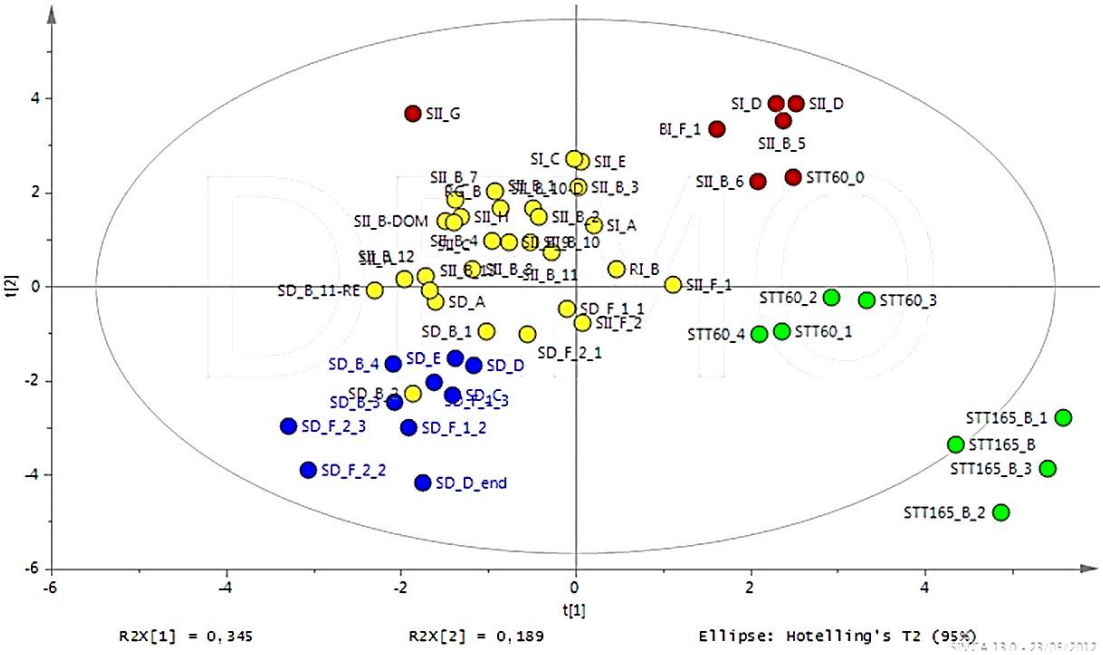

Figure A3.2 : Correlation circle for sludge sample obtained in PLS regression of BD with VFA addition for components 1 and 2

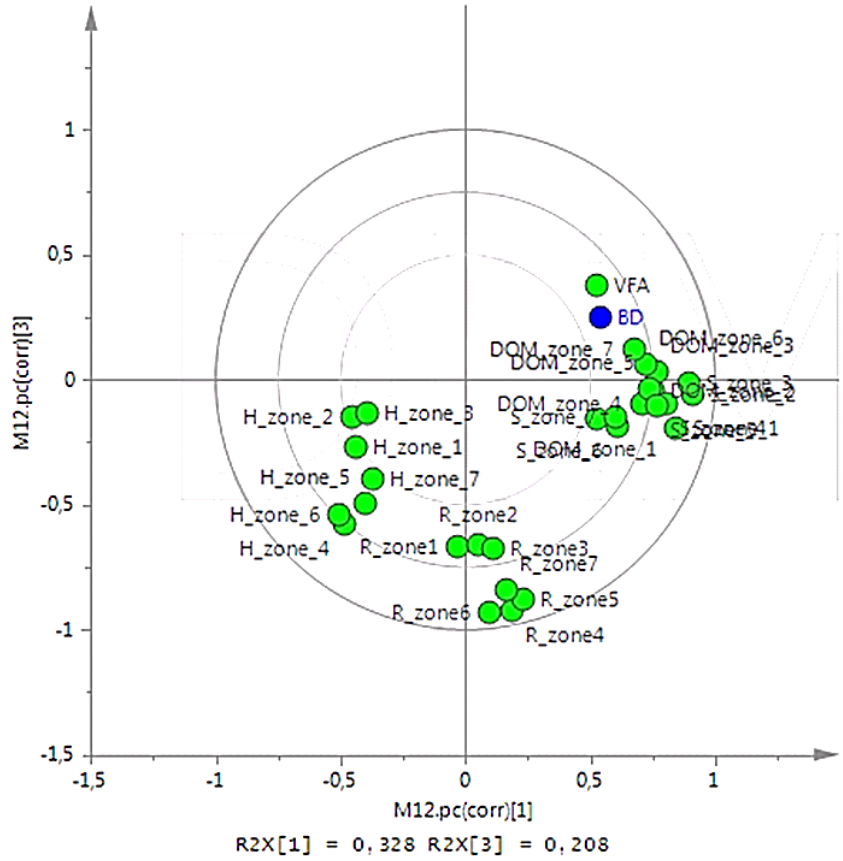

Figure A3.3 : Correlation circle obtained in the first and third components in PLS regression with VFA addition on BD prediction

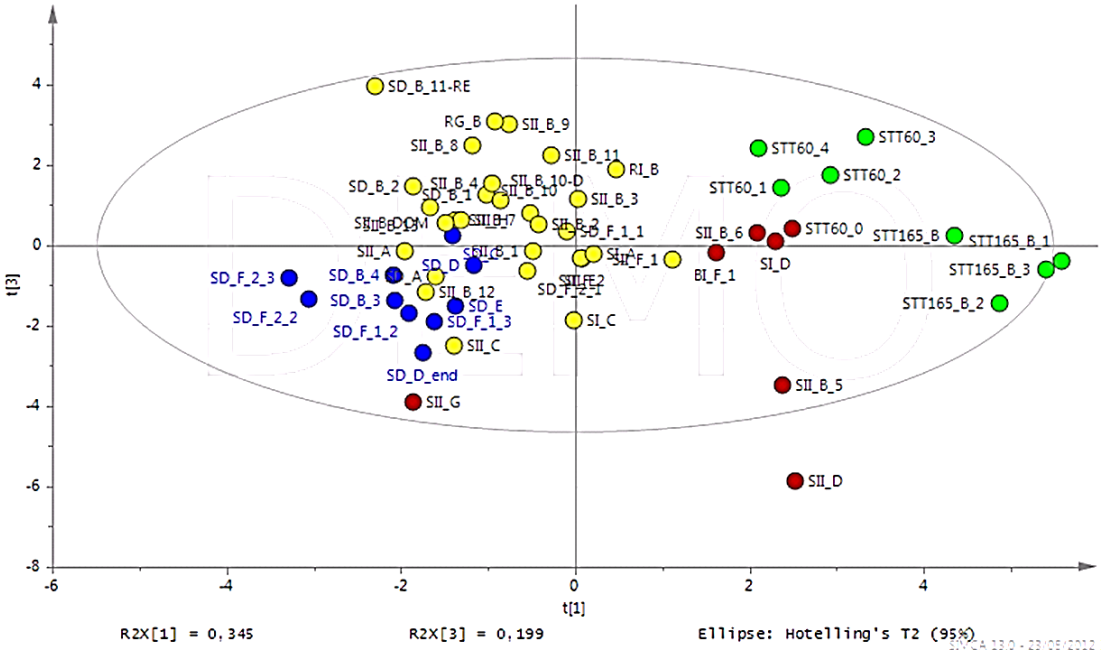

Figure A3.4 : Correlation circle for sludge sample obtained in PLS regression of BD with VFA addition for component 1 and 3

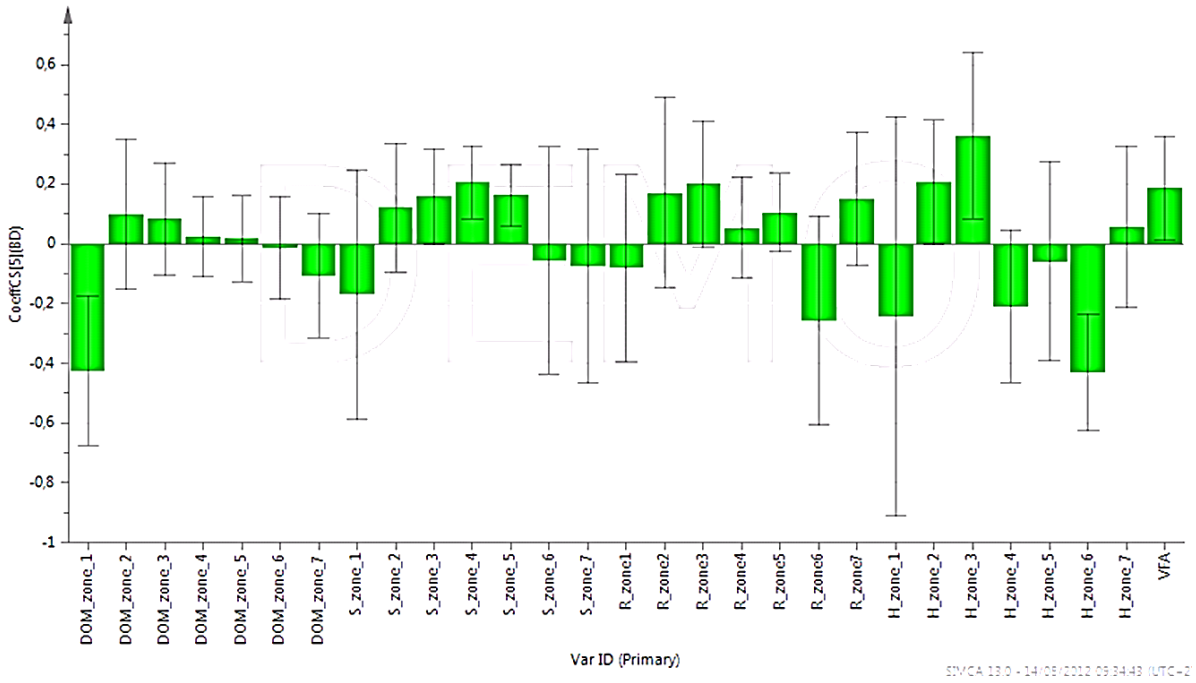

Figure A3.5 : Scaled and centered coefficients values obtained in PLS regression of BD with VFA addition, confidence interval of 95%

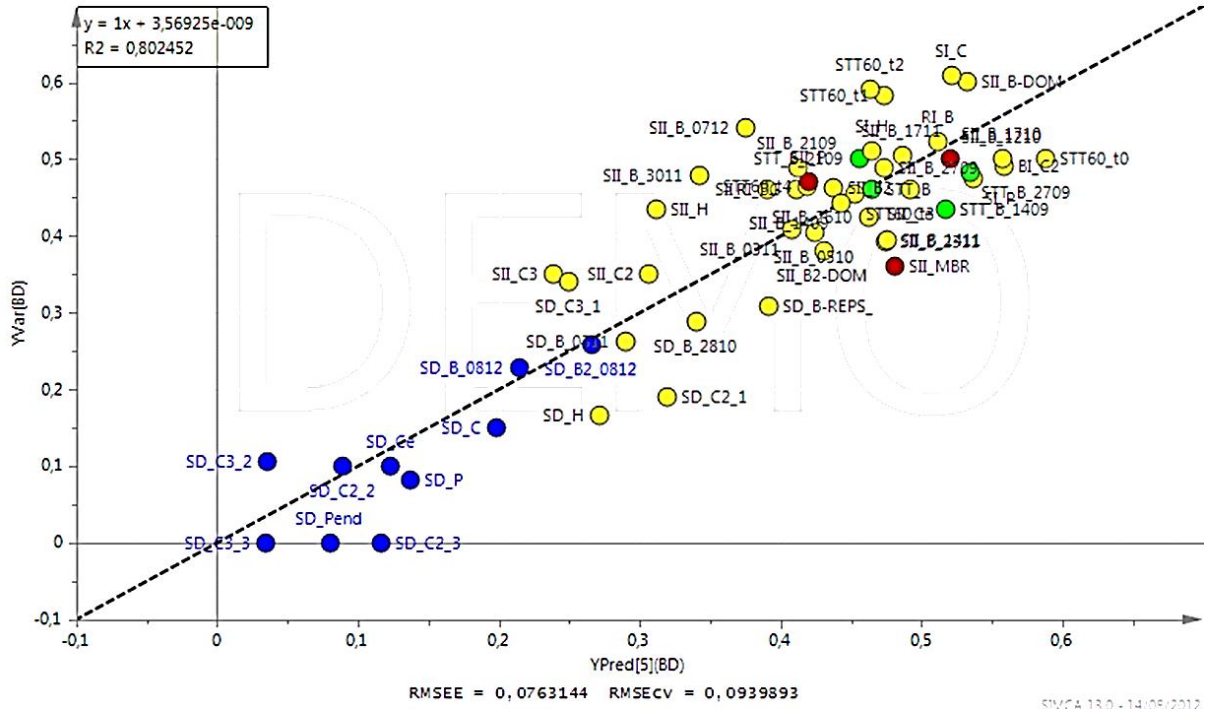

Figure A3.6 : Observed versus predicted BD obtained in PLS regression with VFA addition

Annex 4: Identification of fluorescence compounds in zones VI

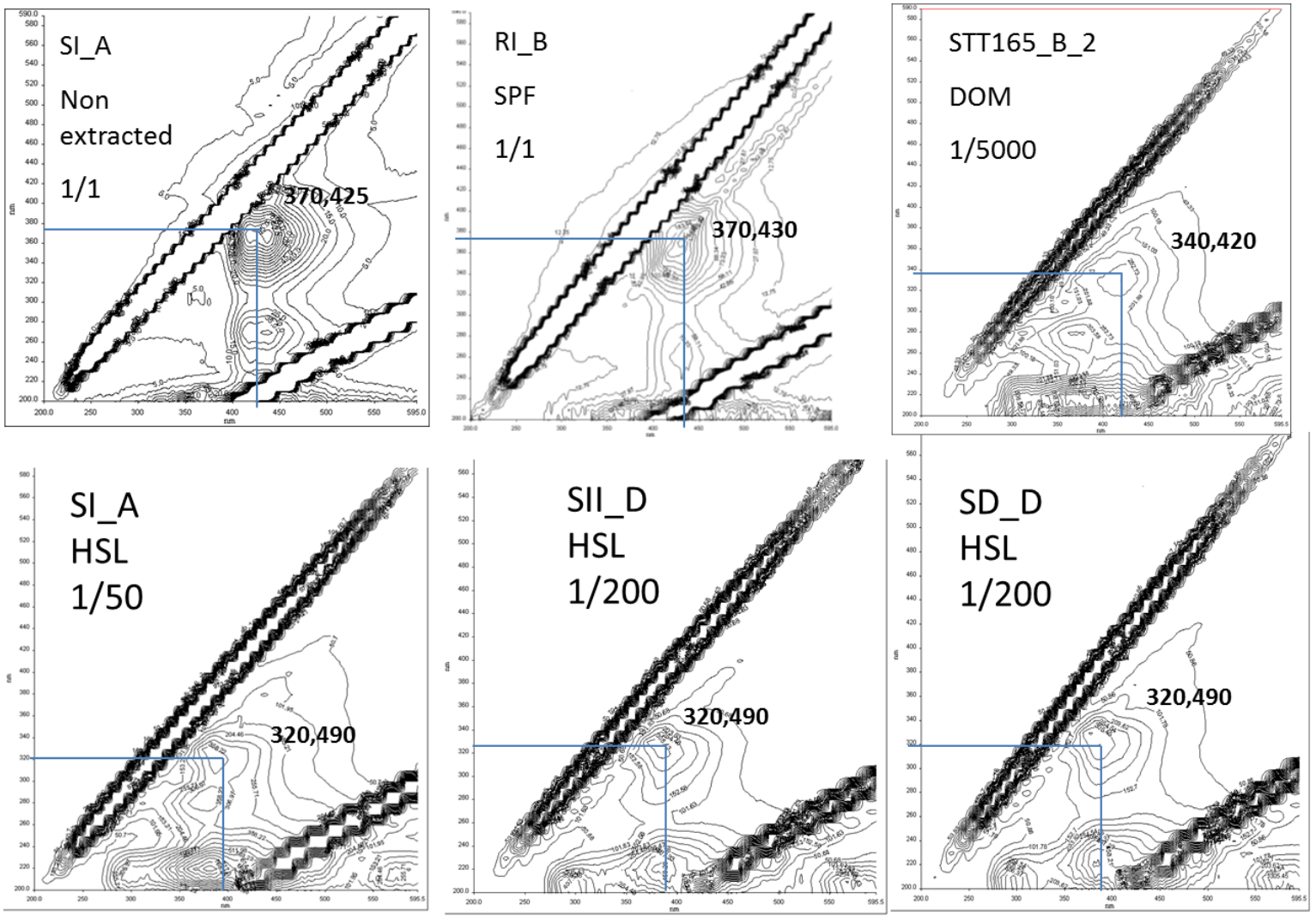

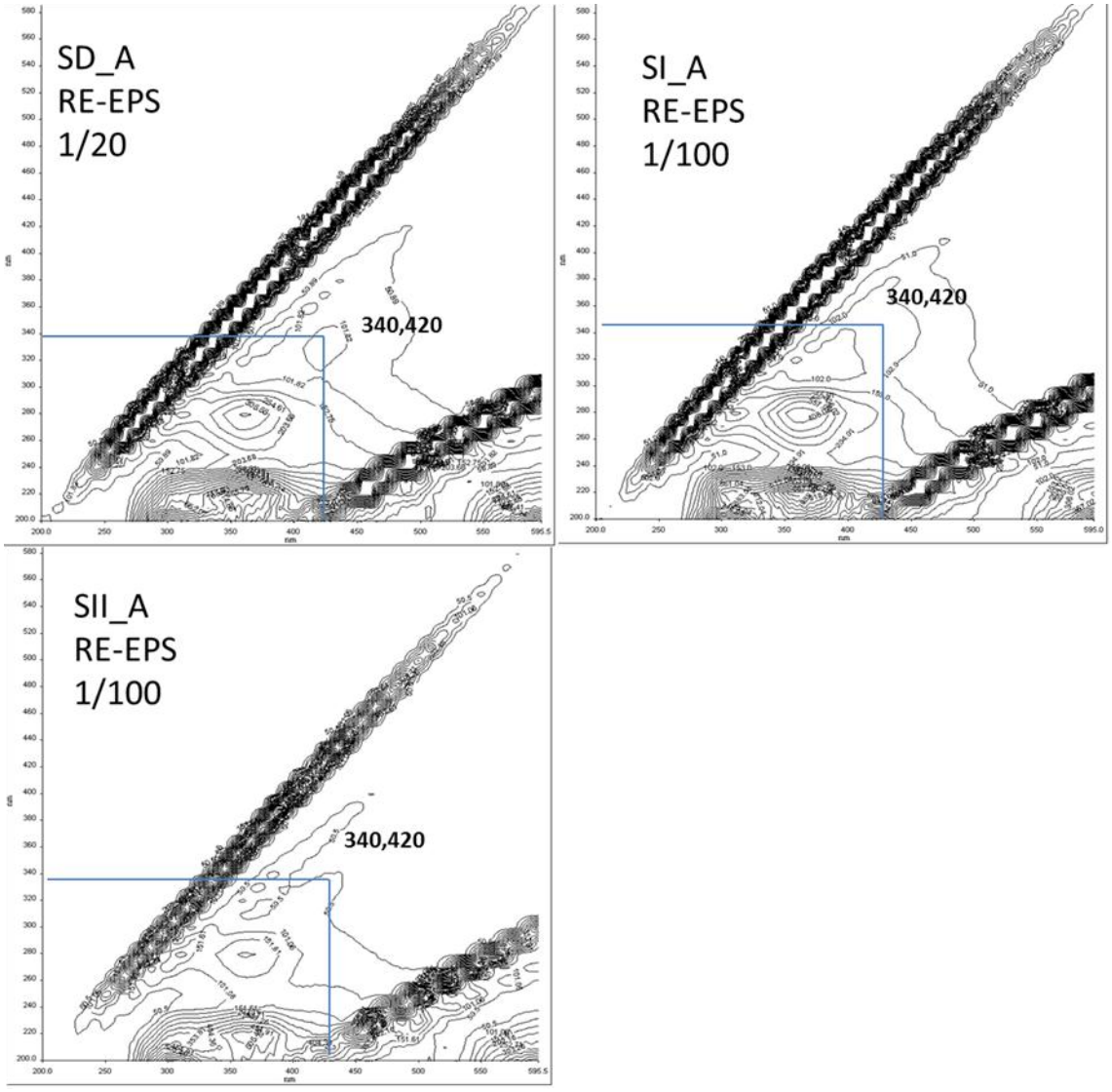
SD_A
RE-EPS
1/20
340,420
SI_A
RE-EPS
1/100
340,420
SII_A
RE-EPS
1/100
340,420

Annex 5: Simulation results obtained for reactors P1 and P2 for all data

- **REACTOR P2: DISTURBING REACTOR**

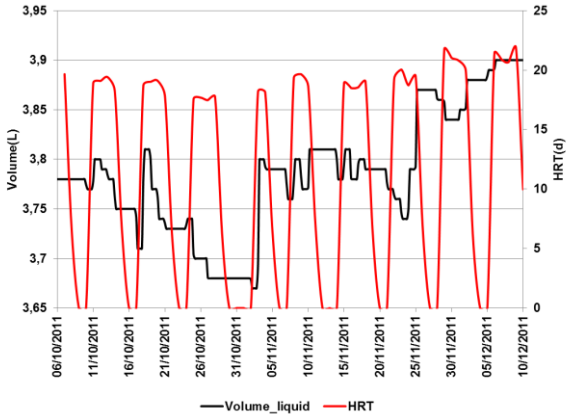

Figure A5.1: Reactor volume and hydraulic retention time applied to P2

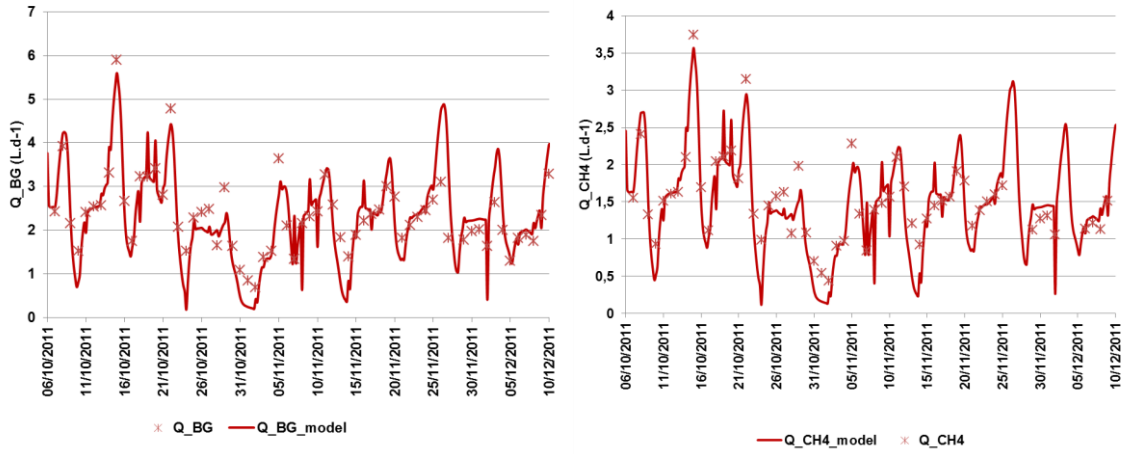

Figure A5.2: Total biogas flow rate (a) and Methane flow rate (b) simulated in P2

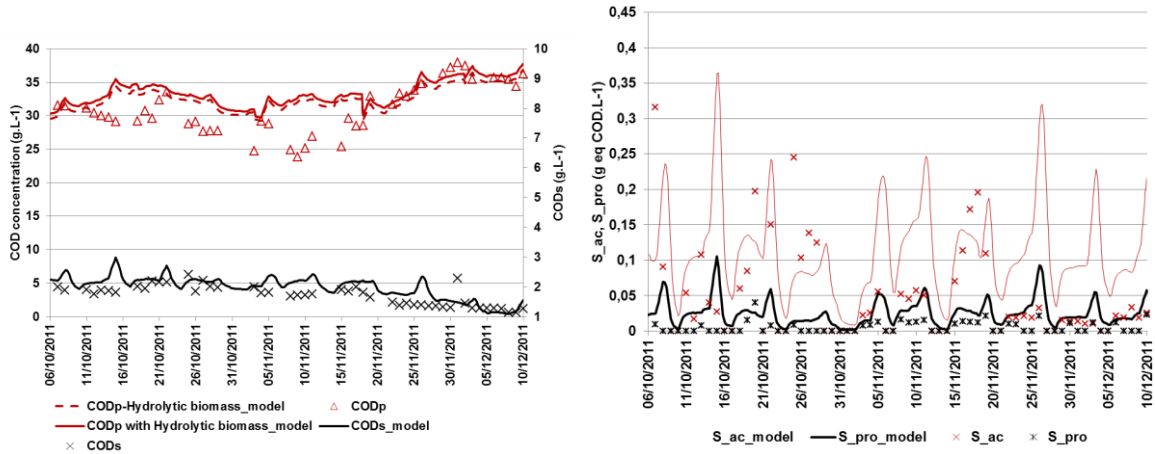

Figure A5. 3: Output reactor particulate and soluble COD (a) and VFA concentrations (b) simulated in P2

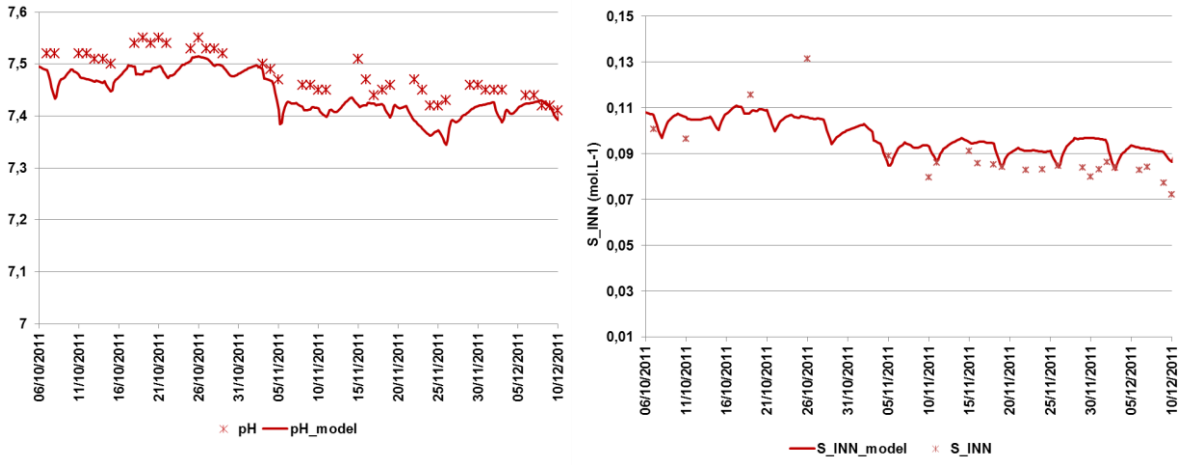

Figure A5.4: pH (a) and ammonium concentrations (b) simulated in P2

- **REACTOR P1: REFERENCE REACTOR**

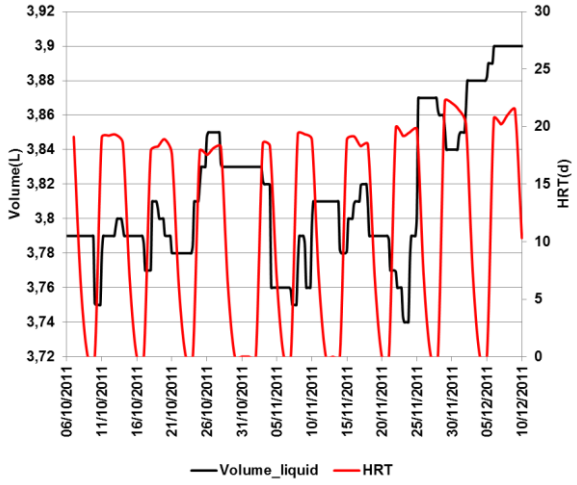

Figure A5.5: Reactor volume and hydraulic retention time applied to P1

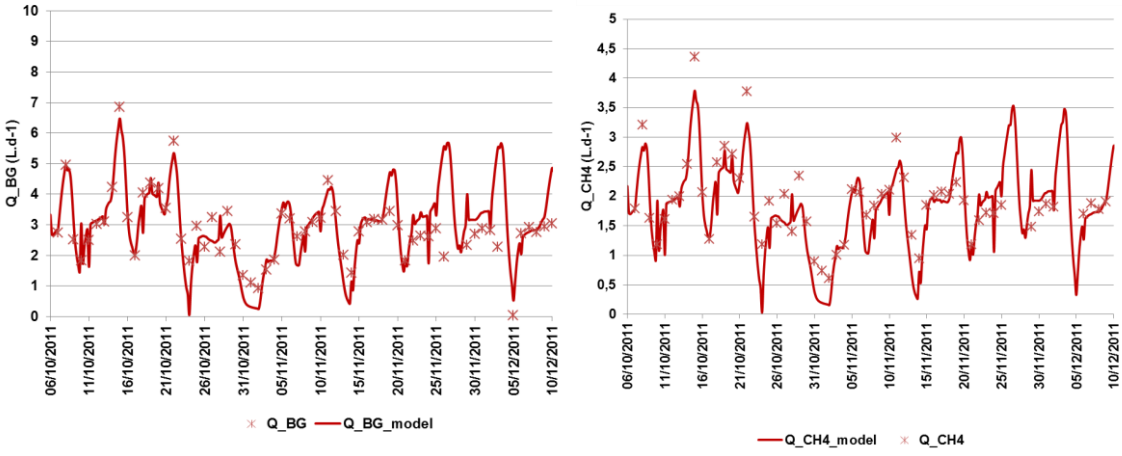

Figure A5. 6: Total biogas flow rate (a) and Methane flow rate (b) simulated in P1

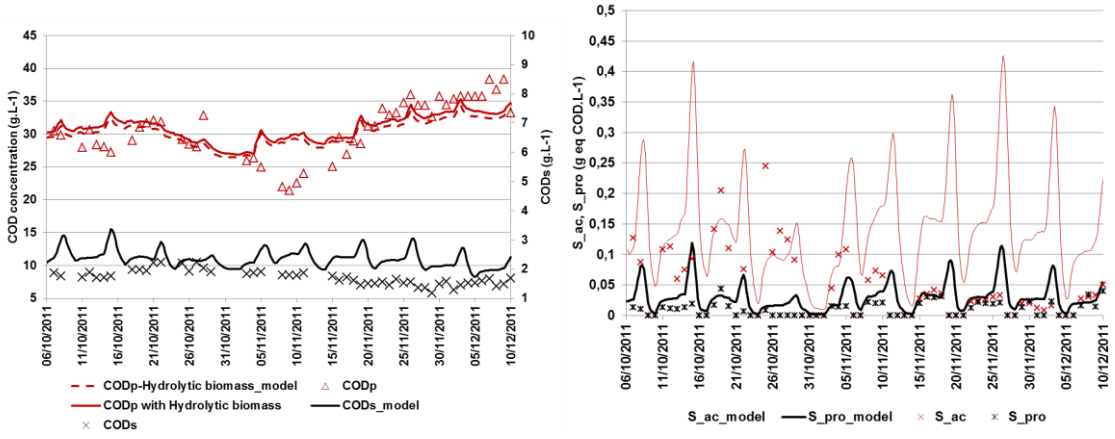

Figure A5.7: Output reactor particulate and soluble COD (a) and VFA concentrations (b) simulated in P1

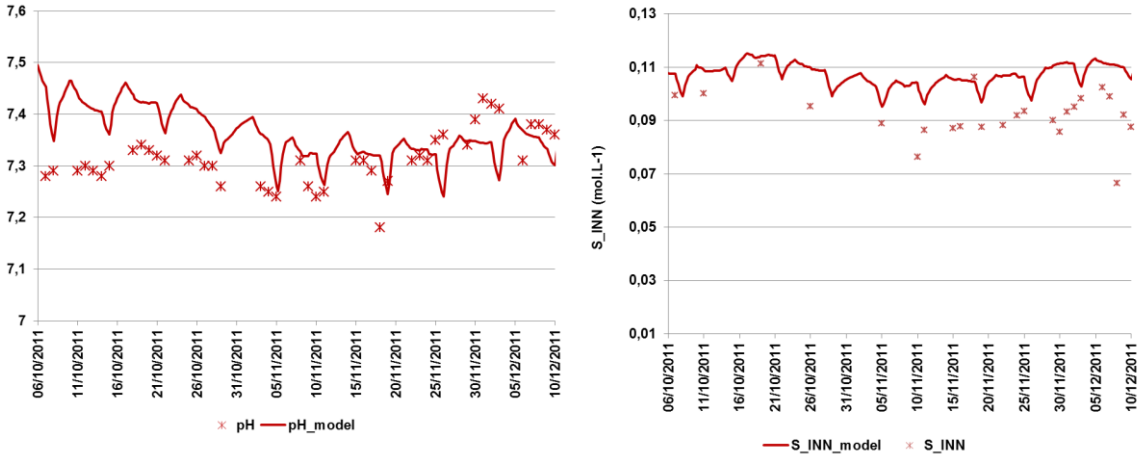

Figure A5.8: pH (a) and ammonium concentrations (b) simulated in P1

Abstract

In an energetic crisis context, alternative sources of energy and saving costs has become of first importance. From this observation, the wastewater treatment plants of the future aim at a positive energetic balance and worldwide research on sludge treatment today focuses on energetic and material valorization through the optimization of anaerobic digestion processes. To this end, knowledge of the input organic matter is crucial to avoid suffering from these disturbances and to control, predict or drive the process through modeling. In the present study, a methodology of sludge characterization is investigated to describe biodegradability and bioaccessibility variables used in anaerobic digestion models. This method is based on the three dimensional fluorescence spectroscopy measurement performed on the chemical extraction of sludge simulating accessibility. Results obtained in 52 sludge samples (primary, secondary digested and thermally treated) show that the method can be successfully correlated with the sludge biodegradability and bioaccessibility within 5 days instead of the 30 days usually needed for the biochemical methane potential tests. Based on these results, input variables of dynamic models of biological processes occurring in anaerobic digestion have been characterized as well as recalcitrant fluorescent compounds. Validation has been performed with modeling of experimental data obtained from two different laboratory scale reactors. Scenarios analysis with the calibrated model have shown that using the measurements of sludge bioaccessibility and biodegradability, a minimal hydraulic retention time could be calculated with a linear correlation leading to the improvement of digesters design. Moreover, this approach has a high potential for applications such as instrumentation or decision support systems to improve both control and optimization of anaerobic digestion processes.

(PhD thesis in English)

Defended on November 23rd, 2012 at : UNIVERSITÉ MONTPELLIER 2 SCIENCES ET TECHNIQUES

with the financial support of : VEOLIA ENVIRONNEMENT Recherche & Développement

INRA

INSTITUT NATIONAL DE LA RECHERCHE AGRONOMIQUE
Laboratoire de Biotechnologie de l'Environnement UR50
Avenue des Etangs F-11100 NARBONNE – France
Tel. +00 33 (0)468 425 151 · Fax +00 33 (0) 468 425 160 Email: lbe.contact@supagro.inra.fr
http://www.montpellier.inra.fr/narbonne/